

Monitoring and Modelling of Biological Aerosols

Thesis presented by
Jerry Hourihane Clancy, BSc

For the degree of
Doctor of Philosophy

Dublin City University
School of Chemistry

Supervisor: Dr David O'Connor

January 2024

Declaration

I hereby certify that this material, which I now submit for assessment on the programme of study leading to the award of Doctor of Philosophy is entirely my own work, and that I have exercised reasonable care to ensure that the work is original, and does not to the best of my knowledge breach any law of copyright, and has not been taken from the work of others save and to the extent that such work has been cited and acknowledged within the text of my work.

Signed: Jerry Clancy

ID No.: 22260445

Date: 08/01/2024

Acknowledgements

This thesis really was a team effort. I know people always talk about “standing on the shoulders of giants” when talking about academic progress, but the other phrase that comes to mind is “it takes a village”. There really is no scenario in which I completed even a fraction of this degree without the support and persistence of the people below. So, thanks so much all of you, because I did not complete a PhD, I’m just the lucky one who gets the fancy hat at the end.

David, an apology is almost more appropriate than a thank you, because I put you through the ringer and neither of us came out of it unscathed. To say you went above and beyond to ensure I could both grow as an academic, and get across that finish line, is putting it lightly. I still write like someone trying to capture the breadth of the world of science in one paragraph, or one sentence given my love of commas, but you have forced me to find a way out of the waffle and hoist those numbers onto the page. I’ve gone from someone who could take 4 months to write a page, and an hour to present it, to someone apparently good enough at public speaking for radio shows, and dangerously unsustainable writing speeds if under pressure. I have you to thank for that. Sincerely I either got the exact right supervisor for me, or you’re just that good. Sample size isn’t there yet, but we’ll see how you push on now. I won’t say it enough, thank you.

To the rest of the lab in DCU and TU Dublin, I’m sure a lot of different people’s sweat is on those glass slides and those lines of code. Moisés, you arrived at the worst possible time, and you still somehow turned a pile of cardboard boxes into the lab it is today. We tested each other beyond breaking point many times and I wouldn’t have it any other way. ¡Hasta luego y sláinte! José you kicked off the entire process and provided me with so much education in such a short time. Thank you for this. Cristina we still have all your drawings up in the lab and they are NEVER coming down! You were the best counter and the most genuine person. Thank you! To Gemma, Alex, and Rebecca, why are you even reading this get back to work!

I have to thank “Julnie”, “Jeph”, and Aoife, you made sure I always had something to do and something to drink whenever I did manage to join in, and don’t worry, it’ll be a lot more often now! Kale, ok I have some time off, so I’ll play you in FIFA or Madden finally. Shannon, can you make me a cool graduation sticker thanks bestie. Jemma you insisted against all reason to make sure I actually had a fun time all throughout my degree and I won’t forget that. Phill, I’ll always be on the other end of the line when you go through a drive-thru, and I don’t wanna incriminate myself, so I’ll just say we’re good to go.

Esha and Gavin, you’re welcome for getting the opportunity to grow and develop under my tutelage and guidance. I expect gifts. Mom and Dad, since I started you’ve moved house twice, got a bunch of different jobs, suffered through a shite pandemic, and had to watch me move away, changing colleges, cities, and housing so much that I count 17 different roommates and probably 30 hotel rooms since I started. Without a permanent place to call home, I never felt lost. I had you both throughout this journey, and the chance to call and talk and just understand that I had something concrete to go back to, was the drive I needed to keep going on days when I might otherwise have packed it all in. I can’t repay you your sacrifices and I owe you a lifetime debt that I hope is softened by my charismatic charm, my insatiable wit, and my soft, understated humility. I love you both, thanks for being there.

And I think that’s everyone importa----ahh Emma! Listen Emma, I legitimately can’t put it into words as no amount of thanks will do justice to everything you have done. Sooo.....I won’t. ☺

Be yourself.
If people aren't
taking you
seriously, then they
need to change, not
you.

-Lightning McQueen

Publications and Presentations

Publications

Hagan, R., Markey, E., **Clancy, J.H.**, Keating, M., Donnelly, A., O'Connor, D.J., Morrison, L., McGillicuddy, E.J., 2023. Non-Road Mobile Machinery Emissions and Regulations: A Review. *Air 1*, 14–36. <https://doi.org/10.3390/air1010002>

Markey, E., **Clancy, J.H.**, Martínez-Bracero, M., Maya-Manzano, J.M., Smith, M., Skjøth, C., Dowding, P., Sarda-Estève, R., Baisnée, D., Donnelly, A., McGillicuddy, E., Sewell, G., O'Connor, D.J., 2022a. A comprehensive aerobiological study of the airborne pollen in the Irish environment. *Aerobiologia* 38, 343–366. <https://doi.org/10.1007/s10453-022-09751-w>

Markey, E., **Clancy, J.H.**, Martínez-Bracero, M., Neeson, F., Sarda-Estève, R., Baisnée, D., McGillicuddy, E.J., Sewell, G., O'Connor, D.J., 2022b. A Modified Spectroscopic Approach for the Real-Time Detection of Pollen and Fungal Spores at a Semi-Urban Site Using the WBS-4+, Part I. *Sensors* 22, 8747. <https://doi.org/10.3390/s22228747>

Martinez-Bracero, M., Markey, E., **Clancy, J.H.**, McGillicuddy, E.J., Sewell, G., O'Connor, D.J., 2022. Airborne Fungal Spore Review, New Advances and Automatisation. *Atmosphere* 13, 308. <https://doi.org/10.3390/atmos13020308>

Martínez-Bracero, M., Markey, E., **Clancy, J.H.**, Sodeau, J., O'Connor, D.J., 2022. First Long-Time Airborne Fungal Spores Study in Dublin, Ireland (1978–1980). *Atmosphere* 13, 313. <https://doi.org/10.3390/atmos13020313>

Maya-Manzano, J.M., Smith, M., Markey, E., **Clancy, J.H.**, Sodeau, J., O'Connor, D.J., 2020. Recent developments in monitoring and modelling airborne pollen, a review. *Grana* 60, 1–19. <https://doi.org/10.1080/00173134.2020.1769176>

Presentations

“Sticky Tape, Lasers, and Chemical Tracers: Building a Bioaerosol Network”, DCU 8th Annual Chemical Research Symposium, May 2023. **Clancy, J.H.**

“Bioaerosol Identification and Monitoring in Ireland: Transition from Traditional Analysis, to Real-Time Sensors and Algorithms”, European Aerosol Conference 2023, Malaga, September 2023, **Clancy, J.H.**, Markey, E., Martinez-Bracero, M., O'Connor, D.J.

Table of Contents

Declaration.....	II
Acknowledgements.....	III
Publications and Presentations	V
Table of Contents	VI
Abbreviations	IX
Figures	X
Tables.....	XIII
Abstract	XIV
CHAPTER 1. INTRODUCTION	1
1.1. Airborne Fungal Spores	2
1.2. Size, shape, and morphology of fungal spores.....	3
1.3. Spore release mechanisms and transport.....	5
1.4. Impacts of Fungal Spores	6
1.5. Fungal Spore Sampling Methodologies.....	9
1.5.1. <i>Traditional Spore Sampling</i>	10
1.5.2. <i>Real Time Monitoring Techniques</i>	14
1.5.3. <i>Chemical or molecular based monitoring and recognition techniques</i>	25
1.5.4. <i>Fungal Spore Modelling and Forecasting Methods</i>	31
1.6. Summary and Conclusion	36
1.7. References	38
CHAPTER 2. MATERIALS AND METHODS	56
2.1. Location	57
2.2. Instrumentation	60
2.2.1. <i>Hirst-Lanzoni and SporeWatch</i>	60
2.2.2. <i>WIBS-NEO</i>	67
2.2.3. <i>IBAC</i>	72
2.3. Data Analysis and Protocol	74
2.4. Summary	76
2.5. References.....	78

CHAPTER 3. TRADITIONAL FUNGAL SPORE MONITORING	82
3.1. Background	83
3.2. Historical Monitoring Data.....	84
3.2.1. <i>Overview of Prevalent Fungal Types and Trends</i>	85
3.3. Contemporary Monitoring Sites	92
3.3.1. <i>Overview of Prevalent Fungal Types and Trends in Dublin</i>	95
3.4. Multi-site traditional monitoring campaign in Summer 2021.....	100
3.5. Conclusion.....	106
3.6. References.....	108
CHAPTER 4. REAL-TIME MONITORING	114
4.1. Introduction.....	115
4.2. Instrumentation.....	116
4.3. Materials and Methods	117
4.4. WIBS Real-Time Monitoring Campaign	119
4.4.1. <i>Campaign Overview</i>	119
4.4.2. <i>Fungal Monitoring Data</i>	119
4.4.3. <i>WIBS Monitoring Data</i>	121
4.4.4. <i>Comparison of Hirst and WIBS Fungal Data</i>	124
4.4.5. <i>Meteorological Influence on Fluorescent particles and Fungal Spores</i>	128
4.4.6. <i>Diurnal Comparisons</i>	134
4.4.7. <i>WIBS Channel potential Bimodal distribution</i>	140
4.5. IBAC-2 Real-Time Monitoring Campaign	141
4.5.1. <i>Campaign Overview</i>	141
4.5.2. <i>IBAC-2 Monitoring Results</i>	142
4.6. Comparison Between Real Time Devices.....	146
4.6.1. <i>Comparison of IBAC and WIBS with pollutant interferents</i>	148
4.7. Conclusion.....	151
4.8. References	153
CHAPTER 5. DATA ANALYSIS OF MODELLING AND FORECASTING OF FUNGAL SPORES	161
5.1. Introduction.....	162
5.2. Modelling and Forecasting Developments as they Relate to Bioaerosols.....	162

5.3. Model Parameters.....	164
5.3.1. Parameter Sourcing Methods.....	164
5.3.2. Bioaerosol Instrumentation.....	164
5.3.3. Geographical origin of ambient bioaerosol and FAP (Fluorescent Aerosol Particle) concentrations	165
5.3.4. Anthropogenic Pollutants.....	172
5.3.5. Meteorological parameters.....	175
5.4. Real-Time Campaign Investigations.....	178
5.4.1. Multiple Linear Regression.....	178
5.4.2. Other investigated methods.....	181
5.5. Development of an Irish Fungal Spore Model.....	181
5.5.1. Forecast Input Variables.....	182
5.5.2. Cladosporium forecasting.....	183
5.5.3. Alternaria Forecasting.....	187
5.6. Conclusion.....	191
5.7. References.....	193
CHAPTER 6. FUTURE WORK AND RECOMMENDATIONS.....	204
6.1. Traditional Monitoring.....	205
6.2. Real-time monitoring.....	206
6.3. IBAC.....	207
6.4. Forecasts.....	208

Abbreviations

<i>Abbreviation</i>	<i>Term</i>
PBAP	Primary Biological Aerosol Particles
CCN	Cloud Condensation Nuclei
IN	Ice Nuclei
UV-APS	Ultraviolet Aerodynamic Particle Sizer
WIBS	Wideband Integrated Bioaerosol Sensor
IBAC	Instantaneous Bioaerosol Analysis and Collection
Nd: YAG	Neodymium: Yttrium Aluminium Garnet
Da	Aerodynamic Diameter
UV-LED	Ultraviolet Light-Emitting Diode
Vcl	Volumes of Collecting Liquids
RH	Relative Humidity
FBAP	Fluorescent Biological Aerosol Particles
FAP	Fluorescent Aerosol Particles
FL	Fluorescence
(HA-CA)	Hierarchical Agglomerative Cluster Analysis
MTIST	Microtiter Immunospore Trapping Device
ELISA	Enzyme-Linked Immunosorbent Assay
PCR	Polymerase Chain Reaction
ARIMA	Autoregressive Integrated Moving Average
ANN	Artificial Neural Networks
MRT	Multiple Regression Trees
RF	Random Forest
LIF	Laser Induced Fluorescence
PMT	Photomultiplier Tube
AF	Asphericity Factor
NWR	Non-parametric Wind Regression
POMMEL	Pollen Monitoring and Modelling
FONTANA	Fungal Monitoring Network And Algorithm
SSIn	Seasonal Spore Integral
LOESS	Locally Weighted Scatterplot Smoothing
EAN	European Aeroallergen Network
EAS	European Aeroallergen Society
EPA	Environmental Protection Agency
AQI	Air Quality Index
PAH	Polycyclic aromatic hydrocarbon
SOA	Secondary Organic Aerosol
PPE	Personal Protective Equipment
MLA	Machine Learning Algorithms
HULIS	Humic-Like Substances
MLR	Multiple Linear Regression
SVMR	Support Vector Machine Regression
KNN	K-Nearest Neighbour
RMSE	Root Mean Square Error
GAM	Generalised Additive Model

Figures

Figure 1.1: An Assortment of Different Fungal Spore Shapes and Sizes, Photographed Under a Scanning Electron Microscope (Crandall et al., 2020)	4
Figure 2.1: Fungal spore sampling sites, both historical and contemporary. Dublin was used for both studies, while Cork, Carlow, and Sligo were in operation for the contemporary study.....	58
Figure 2.2: The set up of one of the Hirst volumetric sampling devices. This device was located on the rooftop of the TU Dublin Kevin Street building (has since been demolished).	59
Figure 2.3: A. The Hirst-type volumetric sampler, with the wind vane and vacuum pump visible (Hirst, 1952); B. The interior of the Hirst, showing the impact unit, with the drum, inlet, and clock mechanisms all visible (Galán et al., 2007).....	61
Figure 2.4: Alignment of the drum with the lid of the Hirst along the red line of the drum (Levetin)	62
Figure 2.5: Alignment of start and end of the week on a Hirst drum along the green line (Levetin)	63
Figure 2.6: A pair of images showing the samples before and after the process of cutting and separating each week of collected sample, into 7 glass slides each representing 24 hours of sampling.....	64
Figure 2.7: A pair of images showing: 1. The sample adhesive still mounted on the Hirst metal drum. 2. The still wet mounting medium immediately after being placed on the sample slide, prior to placement of the cover slip.	65
Figure 2.8: Diagram of Melinex tape placed upon a Perspex ruler, with grooves marked for each hour of the day, as well as daily grooves along the ruler (Galán et al., 2007)	65
Figure 2.9: Fungal spore data collection form for one spore type on one day. There are two rows of cells, to account for the two passes that are made across the length of each slide under the microscope.....	66
Figure 2.10: WIBS-NEO Flow System Diagram showing the flow of air throughout the device (“Wideband Integrated Bioaerosol Sensor – Droplet Measurement Technologies”)	68
Figure 2.11: WIBS-NEO measurement cycle, showing the process by which each individual particle is analysed (“Wideband Integrated Bioaerosol Sensor – Droplet Measurement Technologies”)	69
Figure 2.12: WIBS-NEO Derivation of particle asphericity factor and measuring azimuthal variation in particle forward scattering. Particles scatter light based on their size and shape (“Wideband Integrated Bioaerosol Sensor – Droplet Measurement Technologies”). This represents the “Laser beam” portion of Figure 2.11.	70
Figure 2.13: Particle fluorescence definitions outlining the different categorisations, based off a diagram from (Savage et al., 2017).....	72
Figure 2.14: constituent parts in Line Power Configuration (left), and Battery Power Configuration (right), and with extension stack installed (right), (“FLIR IBAC 2 Bio-Threat Detection & Collection Teledyne FLIR,” 2021).....	74
Figure 3.1: Donut chart of fungal spore composition of each year, showing that basidiospore values were proportionally highest in 1980, and <i>Cladosporium</i> was proportionally highest in 1978.....	86

Figure 3.2: Stacked bar graph showing the contribution of each year to the total concentration of each spore type. Of note is the fact that in 1978, <i>Tilletiopsis</i> concentrations were high enough to be counted, unlike the other years studied.	87
Figure 3.3: Monthly fungal spore concentration box plots for each year of the 1978-1980 study period. July is the overall peak month studied.	88
Figure 3.4: Fungal spore seasonal peak periods and fructification periods of allergenic spores from 1978-1980.	89
Figure 3.5: Sampling sites used in the contemporary fungal spore study.	94
Figure 3.6: Clustered bar charts showing the percentage makeup of the four major fungal spore types from 2017 to 2020.	95
Figure 3.7: Time series chart of contemporary fungal spore concentrations in Dublin from 2017 to 2020 inclusive.	96
Figure 3.8: Start and end date box plots of major spore types in Dublin collected by the Hirst during the campaign.	98
Figure 3.9: CORINE landcover maps of the four locations where fungal spore sampling occurred.	101
Figure 3.10: Spider Plot showing the compositional distribution of the major fungal spore types (less <i>Cladosporium</i>) at all four locations where sampling took place (Summer 2021).	102
Figure 3.11: Fungal spore concentration and proportional density for Dublin, Carlow, Cork, and Sligo (Summer 2021).	103
Figure 3.12: Correlation plot comparing fungal spore concentrations at each sampling site, with local meteorological conditions.	104
Figure 4.1: Real time monitoring sample site location in Dublin city centre, on the roof of the TU Dublin Kevin Street building.	118
Figure 4.2: Daily concentrations of each major fungal spore identified during the study period, along with “other” fungal spores. Hourly measured Hirst data was used.	120
Figure 4.3: Concentrations of the WIBS fluorescent particle types at 3, 6, and 9 sigma during the real-time study period.	124
Figure 4.4: (A) Time series of Hirst fungal spore counts and BC WIBS particles (daily), with (B) linear scatterplot ($R^2 = 0.29$), and (C) logarithmic scatterplot of daily values ($R^2 = 0.058$). (All WIBS channels were analysed, BC was the most promising).	126
Figure 4.5: (A) Time series of Hirst basidiospore counts and BC WIBS particles (daily), with (B) linear scatterplot ($R^2 = 0.44$), and (C) logarithmic scatterplot of daily values ($R^2 = 0.25$).	127
Figure 4.6: Fluorescent aerosols particles concentrations vs pressure (grey), ground minimum temperature (green), minimum temperature (red) and wind speed (blue).	129
Figure 4.7: (A) Time series of Hirst ascospore counts and rainfall (daily), with (B) linear scatterplot ($R^2 = 0.011$), and (C) cross correlation lag regression plot.	131
Figure 4.8: Grid of scatterplots of increasing rain data lag.	132
Figure 4.9: (A) Time series of Hirst ascospores counts and AC WIBS particles (days with 1mm of rainfall or less), with (B) linear scatterplot ($R^2 = 0.87$), and (C) logarithmic scatterplot of daily values.	133

Figure 4.10: Log of diurnal WIBS particle distributions.	134
Figure 4.11: 9 Sigma, Log10 size distributions of WIBS particles.	135
Figure 4.12: WIBS-NEO diurnal charts of each band (>2 μm , 3-Sigma). Each graph highlights one of the bands, with the remaining 6 in the background, to better highlight how each individual and fits within the overall fluorescent particle trend diurnally.	137
Figure 4.13: Diurnal charts of major fungal spore types, similar to the previous WIBS diurnal chart for direct comparison.	138
Figure 4.14: Combined normalized diurnal concentrations of A and AB WIBS bands, and ascospores. This is to highlight the correlation diurnally between WIBS particles and fungal spores.	139
Figure 4.15: Graph showing the level of FII intensity expressed by every ABC particle. This shows a clear bimodality between the more and less intense particles.	140
Figure 4.16: Corrplot highlighting the difference in correlative characteristics of the two ABC modes.	141
Figure 4.17: Daily boxplots of all small (0.7-1.5 μm) and large (1.5-10 μm) IBAC particles.	144
Figure 4.18: Daily boxplots of biological small (0.7-1.5 μm) and large (1.5-10 μm) IBAC particles.	144
Figure 4.19: Comparison between the WIBS NEO, and the IBAC particle sensor for all particle type and size ranges, highlighting the points of agreement between the two devices (0.7-10 μm).	147
Figure 4.20: Comparison between IBAC particles and PM ₁₀ emissions during the monitoring campaign.	149
Figure 4.21: Normalised direct comparison of particles observed by the WIBS vs PM ₁₀	150
Figure 5.1: NWR generated wind rose for WIBS sampling period. White circles represent a wind speed scale in kilometres per hour. The colour grid represents the estimated concentration (Particles/m ³) at each wind speed and wind direction.	166
Figure 5.2: Origin of (A) Urticaceae and (B) Poaceae pollen, and (C) Cladosporium, (D) Basidiospore, (E) Ascospore, and (F) Alternaria fungal spores at Dublin. The colour grid represents the estimated concentration (Particles/m ³) at each wind speed and wind direction.	167
Figure 5.3: Map of 5km radius from the sampling point in Dublin city, with “green areas” of interest marked in red.	170
Figure 5.4: Origin of WIBS Particles at Dublin. The colour grid represents the estimated concentration (Particles/m ³) for any wind speed and wind direction.	171
Figure 5.5: Comparison between WIBS fluorescent particles and PM ₁₀ particles.	174
Figure 5.6: Comparison between IBAC fluorescent particles and PM ₁₀ particles.	174
Figure 5.7: Multiple Linear Regression plot of fungal spores for the real-time monitoring campaign.	179
Figure 5.8: Multiple Linear Regression plot of Basidiospores for the real-time monitoring campaign.	180
Figure 5.9: Comparison of selected regression forecast models based on previous studies, contrasted with observed <i>Cladosporium</i> concentrations.	185

Figure 5.10: A: Time series comparison of counted 2020 Cladosporium fungal concentrations with forecast support vector machine regression values. B: Logarithmic regression line of the data.....	186
Figure 5.11: Comparison of selected regression forecast models with observed Alternaria concentrations.....	188
Figure 5.12: Comparison of counted 2020 Alternaria fungal concentrations with forecast support vector machine regression values.....	189

Tables

Table 1: Table outlining the different instrument properties and limitations associated with the sampling type, with regards to their bioaerosol monitoring capabilities specifically.	9
Table 2: WIBS-NEO particle fluorescence classification the different FI results are representative of the channels in which particles are detected, as a result of their fluorescence excitation and emission wavelengths ("WIBS-NEO-Toolkit.pdf") ...	71
Table 3: Pearson correlation table of IBAC particles and fungal spores	143
Table 4: Pearson correlation table of IBAC particles and WIBS-Neo particles.	146
Table 5: Spearman’s rank correlation coefficients between daily hourly Dublin WIBS channel data and meteorological parameters.	176
Table 6: Input variable characteristics, for Cladosporium and Alternaria regression models. Two variables with data quality issues had to be removed due to the quantity of missing data.....	182

Abstract

Monitoring and Modelling of Biological Aerosols

Jerry Hourihane Clancy

The work completed had the primary aim of providing fungal spore monitoring capabilities to the previously established Irish Pollen Network. This in turn led to the creation of the first Irish Bioaerosol Network for the simultaneous measurement of both pollen and fungal spores. The network was established by traditional and real-time monitoring methods into the previously disparate traditional sampling network (Dublin and Carlow). Full integration of sites in Cork and Sligo, and the collected fungal spore data from all sites are being utilized to create an Irish fungal spore network.

This work primarily focused on the fungal spores in the ambient air, which have human health and agricultural implications, with information on this being of great help to allergy sufferers as well as the farming community, which is particularly susceptible to changes in fungal spore concentrations, as they can damage crops.

The work involved a set of traditional device campaigns, from the analysis of old data collected decades ago, to the collection of our own data at various sites nationwide. After this, several novel spectroscopic techniques such as the WBS-NEO and IBAC were implemented in a test centre in Dublin as part of a real-time monitoring campaign for detection of ambient fungal spores, to determine the suitability of these instruments for deployment in a wider multi-site sampling network. Finally, data generated via both traditional and novel methods along with collected meteorological and pollution data was combined, and the process of developing and refining a set of forecasting algorithms was carried out, with a view to have full forecasting and predictive models in operation in the near future.

Chapter 1. Introduction

1.1. Airborne Fungal Spores

The composition of the atmosphere includes a variety of particles that can be characterised as having biological properties. Such particles are commonly referred to as Primary Biological Aerosol Particles (PBAPs). They have a size range spanning from a few nanometres, comparable to the dimensions of individual virus or bacterial cells, to several hundred micrometres, resembling small insects or insect fragments (Després et al., 2012; Idalia Kasprzyk, 2008) The fungal spore is a widely distributed PBAB that's been observed throughout various regions, temperatures, and seasons worldwide. The fungal spore kingdom can be characterised as comprising exclusively eukaryotic, heterotrophic organisms. There are both single-cellular and multi-cellular forms in the kingdom. Fungi have a characteristic organisation known as hyphae, which are filamentous structures. These hyphae further aggregate to form a larger structure called a mycelium. These organisms lack chlorophyll, are immobile, and possess chitin in their cell walls. According to Simon-Nobbe et al. (Simon-Nobbe et al., 2008), fungi can exhibit several ecological relationships, including parasitism, mutualism, and commensalism with other creatures. Additionally, McLaughlin and Spatafora (McLaughlin and Spatafora, 2014) suggest that there may be up to 5 million different species of fungi now known to exist. According to the study conducted by Simon-Nobbe et al. in 2008 (Simon-Nobbe et al., 2008), fungi exhibit a variety of cell architectures, encompassing yeasts as single-celled fungus, cross-walled fungi with a single nucleus, and coenocytic fungi characterised by many nuclei.

The focal point of this study revolves around the fungal spore. Fungal spores are a subject of great scientific interest owing to their widespread occurrence and significant influence on various aspects of the biosphere. Fungal spores are ubiquitously present in the atmosphere, soil, and aquatic environments. Proliferation can occur through the growth of fungus on decomposing or deceased plant and animal matter, as well as in soils that are abundant in nutrients. Certain species of fungi have been observed to proliferate on both living plants and animals (Köhler et al., 2017). Various environments, including agricultural lands, woodlands, urban green spaces, and moist habitats, offer favourable circumstances for the growth and spread of fungi.

The optical identification and discrimination of spores is facilitated by their diverse range of colours/pigments, shapes, and sizes (Dijksterhuis, 2019; Dilcher and Sheffy, 1971). Fungal spores are dispersed through both passive means, such as wind or rain, and active mechanisms, including sporangium explosions or bursts, by the fungus. Airborne spores have a tendency to remain suspended in the atmosphere for extended periods, allowing them to be transported by air currents over national borders and bodies of water before eventually

settling. An illustration of this phenomenon is evident in the extensive migration of *Cladosporium* clouds, spanning a distance of about 1,000km across the North Sea, from England to Denmark (M. J. Carlile et al., 2001). The impact of rainfall on fungal spores frequently leads to the aerosolization of specific types of fungal spores, such as ascospores, which were previously deposited on the ground. Consequently, rain events can contribute to the further dissemination of spores, akin to the dispersal caused by high wind events. Spores frequently disperse not solely in the form of dry clouds, but rather as constituents of larger aerosols, capable of travelling distances spanning hundreds or even thousands of kilometres. The dissemination of spores facilitates the colonisation of new places, enabling the fungi to continue their growth cycle (M. J. Carlile et al., 2001; Grinn-Gofroń et al., 2018; Ingold, 1971, 1999; I. Kasprzyk, 2008; Pringle et al., 2005; Smith, 1984, 1986).

1.2. Size, shape, and morphology of fungal spores

Fungal spore size, shape and morphology varies by a greater degree compared to other types of PBAPs, such as pollen grains or plant materials. The pigmentation of fungal spores plays a significant role in their identification, as it can range from nearly colourless (hyaline) to nearly black. The morphologies of many spores are determined by their respective growth strategies throughout their life cycles (Lacey and West, 2006). Ascospores, characterised by their elliptical morphology, are generated within a specialised structure called an ascus and can exist as either single-celled or multi-celled entities. Basidiospores are characterised by the presence of a discernible scar, facilitating their identification, as they originate from a basidium. Asexually generated spores, known as conidia, may appear larger compared to Basidiospores or Ascospores. However, it is important to note that there is no definitive standard for size and form classification of fungal spores, and numerous deviations exist within this categorization (Lacey and West, 2006).

Due to the significant variation in spore sizes, optical microscopy is a suitable method for analysing bigger fungal spore species. However, certain forms of fungal spores, such as aspergillus and penicillium, are too small for manual optical analysis (Quintero et al., 2013). In a recent study conducted by Crandall et al. (Crandall et al., 2020), significant variations in the diameters of the fungal spores under investigation were observed. The researchers observed a significant disparity in spore sizes within their samples. Specifically, the smallest spores exhibited a “spore perimeter” that was 23.5 times smaller than that of the largest spores. The measurements revealed that the smallest spores had a perimeter of 7.8µm, while the largest spores had a perimeter of 183.8µm. Additionally, the width of the spores varied considerably, with certain spores being up to 26.5 times wider than others. The width

measurements ranged from 2.2 μm to 58.3 μm . Crandall et al. (Crandall et al., 2020) observed various surface smoothness and sphericity characteristics, ranging from nearly spherical to highly oblong shapes, and exhibiting smooth, spiny, or ridged surfaces.

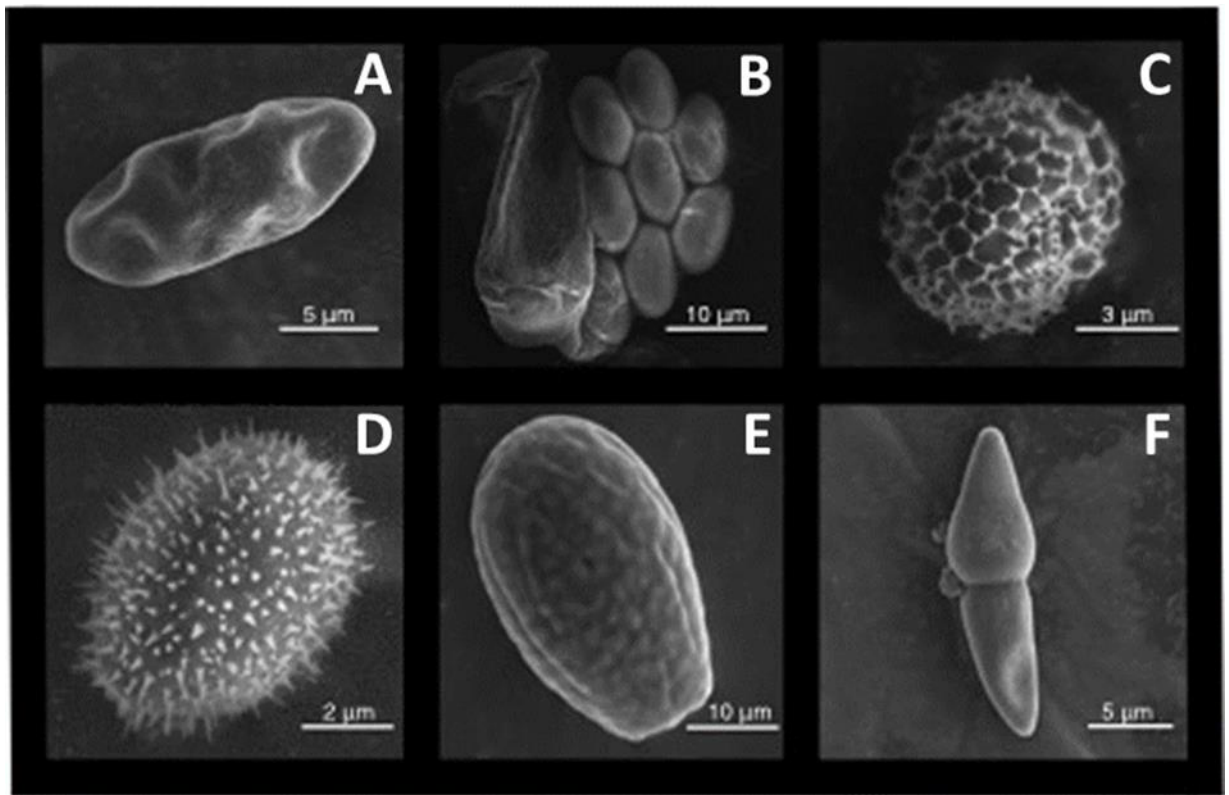


Figure 1.1: An Assortment of Different Fungal Spore Shapes and Sizes, Photographed Under a Scanning Electron Microscope (Crandall et al., 2020)

Figure 1.1 displays a range of fungal spore sizes and morphologies, illustrating their significant variations. For example, spore C exhibits a high degree of sphericity, while spore F has the lowest sphericity and bears resemblance to a rod-like structure. Spores D and E exhibit comparable morphological structures, although they possess distinct surface characteristics. Specifically, spore D is characterised by a spiky surface, while spore E exhibits a surface that is slightly bumpy. Upon examination of the dimensions of the two spores, it becomes evident that spore E has a size that is five times more than that of spore D.

There exists considerable variability in the size of spores, which can manifest as differences between individual spores as well as between distinct spore species. *Cladosporium*, a frequently encountered spore type, possesses a size distribution spanning from 3 to 20 μm . The spores with the smallest average size, such as aspergillus and penicillium, have a diameter of about 1 or 2 μm . Conversely, certain elongated spores can reach lengths of several hundred microns.

The characteristics of fungal spores can be influenced by differences in their size or shape. A study investigating the virulence of a pathogenic fungal spore revealed a significant positive correlation between the size of the fungal spore and the percentage change in patients' survival. The results of the study indicate that there is a strong relationship between the size of fungal spores belonging to the same or nearly related species and their virulence. Specifically, it was shown that larger spores exhibited higher levels of virulence and lower rates of survival ($p=0.0021$). Research such as the one conducted by (Li et al., 2011) emphasises that variations in size and shape of spores have implications beyond just aesthetic preferences, as they also impact the inherent features of the spores.

1.3. Spore release mechanisms and transport

When examining the techniques by which spores are released, they can be classified into two distinct categories: survival spores and dispersal spores (M. Carlile et al., 2001). Survival spores exhibit a characteristic wherein they do not necessitate quick liberation or growth, since their inherent design enables them to remain in a dormant state for prolonged durations subsequent to their release. According to Carlile et al. (M. Carlile et al., 2001), the main purpose of dispersal spores is to establish new spore colonies. Therefore, it is necessary for these spores to be quickly released from the fungi upon their creation.

Fungi can be released by either active or passive mechanisms. Passive methods require the reliance on the external environment for the liberation of spores from the fruiting body or fungi, while active means entail the utilisation of energy by the fungi itself to detach the spores from the fungus. Various mechanisms are employed for the release of spores. These include the disintegration of the fruiting structure, facilitating wind dispersal, the explosive ejection of spores from the fruiting body, the propulsion of spores through a catapult-like mechanism, and the release of motile spores into aquatic environments, where they can actively swim away using flagella. Certain species of fungi exhibit explosive release behaviour in response to specific environmental cues, such as the presence of advantageous conditions like rainfall (Money, 2016).

The primary mechanisms of fungal spore dispersal encompass passive transportation through air and water, whereby spores or clusters of spores are carried along by wind or water currents. The primary focus of this study pertains to spores that exhibit airborne dispersal, commonly referred to as air spora. These spores have been selected as the subject of investigation due to their ability to be captured by the various equipment and instruments employed in this research endeavour. Spores have the potential to undergo displacement due to convection currents generated by solar radiation impacting the Earth's surface, irrespective

of the presence of air currents, atmospheric pressure, or winds. On days characterised by low wind levels, the phenomenon of re-suspension occurs, enabling dry spores that had previously settled to become airborne once again and disperse over greater distances from their original source (M. Carlile et al., 2001; Money, 2016).

1.4. Impacts of Fungal Spores

PBAPs such as fungal spores, have been observed to exert an influence on climatic conditions and weather patterns. One significant mechanism via which they might exert effect on the climate in a given region is by directly impacting the processes of precipitation development and cloud formation. In sufficiently humid conditions, water condensation can occur on the surface of soluble particles, such as the coatings of various PBAPs. The saturation threshold leads to the aggregation of particles, resulting in the mass condensation and subsequent production of clouds facilitated by PBAP particles. The cloud formation event can be attributed to particles referred to as Cloud Condensation Nuclei (CCN) (Conen et al., 2017). This phenomenon can only occur at temperatures equal to or beyond 0°C, although it does demonstrate the direct climatic effects induced by fungal spores and other primary biological aerosol particles (PBAPs).

The cloud formation process below 0°C, reaching temperatures as low as -36°C, is primarily influenced by Ice Nuclei (IN) rather than Cloud Condensation Nuclei (CCN). This process entails the solidification of droplets by their interaction with aerosols that exhibit insolubility or are coated with insoluble substances. PBAPs, such as fungal spores, typically exhibit soluble coatings that are well-suited for the formation of CCN clouds. However, it is worth noting that IN processes can also occur, since PBAPs may contain certain insoluble components (Mohler et al., 2007; Phillips et al., 2009). The study of atmospheric aerosols that have a significant impact on cloud formation, including smoke particles, sea salt, sulphates, and dust, has received more attention and extensive research compared to primary biological aerosol particles (PBAPs) in this context. However, there has been a recent surge in interest regarding the role of bioaerosols in contributing to the overall formation of cloud condensation nuclei (CCN) and ice nuclei (IN) in clouds, although this topic remains controversial (Bieber et al., 2020).

Since their original discovery in the 1970s, several instances of biological sources of Ice Nuclei (IN) and Cloud Condensation Nuclei (CCN) have been identified over the years (Bauer et al., 2002; Christner et al., 2008; Maki et al., 1974; Pratt et al., 2009; Prenni et al., 2009; Schnell and Vali, 1972). The study of Ice Nuclei (IN) in the context of bioaerosols is of considerable

importance since, at relatively higher temperatures around -20°C , the principal agents responsible for IN production, namely mineral dusts and combustion aerosols, become ineffective in facilitating cloud formation through IN. Multiple studies have shown evidence for the existence of IN formed clouds within the temperature range of -20°C to -1°C . It has been established that only particles of biological origin possess the necessary properties to serve as ice nuclei at these specific temperatures (DeMott et al., 2010; Després et al., 2012; Murray et al., 2012).

The comprehensive understanding of the influence of biological aerosols and primary biological aerosol particles (PBAPs) on the development of ice nuclei (IN) and cloud condensation nuclei (CCN), as well as the magnitude of their contribution to these processes, remains incomplete. Nevertheless, prior research has conducted estimations indicating that the influence, specifically with regards to Ice Nuclei, is substantial. According to a study conducted by Pratt et al. (Pratt et al., 2009), it was discovered that a significant proportion, up to 33%, of ice-crystal residues created during cloud formation can be attributed to the presence of biological particles. Studies have also investigated the possible effects of bioaerosols and primary biological aerosol particles (PBAPs) on ice nucleation cloud formation in areas devoid of human-induced influences. In the Amazon basin, a large climatic region characterised by limited human impact over extensive areas and frequent rainfall, scientific research has observed that the hydrological cycle remains in equilibrium through the influence of primary biological aerosol particles (PBAPs) and biogenic (Andreae et al., 2004; Després et al., 2012; Pöschl et al., 2010; Prenni et al., 2009; Whitehead et al., 2016). Fungal spores, in particular, exhibited a high prevalence in the Amazon Basin region, as evidenced by studies that measured ambient fluorescent particle concentrations. These investigations revealed that fungal spores accounted for 70% of all identified luminous particles (Whitehead et al., 2016).

Although research conducted on specific regions or small-scale models suggests that fungal spores and primary biological aerosol particles (PBAPs) play a significant role in the creation of ice nuclei (IN) and cloud condensation nuclei (CCN) for cloud (Phillips et al., 2009), findings from worldwide studies, large-scale studies, and models present a contrasting viewpoint. Numerous extensive investigations conducted on a wide geographical scale have established that, according to simulations, fungal spores and primary biological aerosol particles (PBAPs) are incapable of exerting a global influence on the overall composition of ice nuclei (IN) exceeding 1% of the total, even under ideal simulated conditions for PBAP-induced IN formation. According to several studies (Haga et al., 2014; Hoose et al., 2010;

Hummel et al., 2018; Sesartic et al., 2013; Spracklen and Heald, 2014), simulations have indicated that around 93% of global information on IN (ice-nucleating) particles can be attributed to commonly understood particles, such as mineral dusts, whereas the contribution of biological particles is considered minimal. The aforementioned studies indicate that fungal spore derived ice nucleation (IN) formation may not have a substantial impact on a global scale. However, the localised impact of fungal spores as carriers of IN and contributors to cloud formation, particularly in regions characterised by warmer temperatures, lower altitudes, and other conditions that inhibit conventional IN processes, remains a topic of considerable interest and merits additional investigation. The presence of varying outcomes across different studies and study methodologies suggests that there remains a significant knowledge gap regarding the role of fungal spores and other primary biological aerosol particles (PBAPs) in the formation of ice nuclei (IN) and cloud condensation nuclei (CCN). This observation is supported by previous studies (Haga et al., 2014; Hoose et al., 2010; Hummel et al., 2018; Sesartic et al., 2013; Spracklen and Heald, 2014). In a laboratory experiment conducted by Pouleur et al. (Pouleur et al., 1992), the ice nucleating activities of 20 different fungal spore types were investigated at elevated temperatures. The results indicated that only two spore types, namely *Fusarium acuminatum* and *Fusarium avenaceum*, exhibited discernible ice nucleating activities above -5°C . According to Morris et al, among the fungi that have been shown to have IN (ice nucleation) capabilities at comparatively higher temperatures (-10°C), only certain rust fungus, specifically Uredospores, have been identified as relatively prevalent (Morris et al., 2013). Fungi have significantly influenced human history, particularly in their role in agricultural crop systems, as humanity has advanced in farming techniques and embraced monoculture. Fungal organisms, specifically *Phytophthora infestans* (commonly referred to as potato blight) in Ireland and *Daktulosphaira vitifoliae* (*phylloxera*) in vineyards, have had significant economic and societal impacts. These effects have resulted in profound transformations in the fates of entire cultures and civilizations, primarily through the occurrence of famines (Banerjee et al., 2007; Ristaino, 2002). Several prevalent fungal spore species in Ireland, including *Alternaria*, *Aspergillus*, and *Cladosporium*, have been observed to cause food contamination during storage (Vagelas et al., 2011). In addition to the matter of food and crop contamination and destruction, fungal spores have the potential to directly affect animals and the human population. Frequently, asthma attacks and seasonal respiratory allergy syndromes are frequently attributed to the presence of airborne fungal spores, leading to the introduction of the term “sick-building syndrome” to describe respiratory ailments associated with fungal spores and PBAPs within building stock.

These PBAPs can be found within residential or occupational environments, significantly affecting the daily lives of individuals residing or working in these spaces. In recent times, there has been a notable occurrence of individuals experiencing symptoms resembling those of SARS-CoV-2 (COVID-19), which has led to confusion. It has been observed that these symptoms could potentially be caused by airborne fungus spores, and conversely, symptoms attributable to fungal spores may be mistaken for COVID-19 symptoms (D’Amato et al., 1997; Gostic et al., 2020; Rapiejko et al., 2007). The profound and consequential effects of fungus on human existence, whether through direct or indirect means, underscore the imperative for additional investigation and examination in the field of aerobiology.

1.5. Fungal Spore Sampling Methodologies

The understanding of seasonal and temporal patterns in fungal spore concentrations, along with knowledge about several principal ambient species present in the environment, holds significance due to the value of fungal spores. To effectively study these factors, it is imperative to thoroughly examine and explore all potential methodologies that have been employed in the past, are already being utilised, and could perhaps be applicable in the foreseeable future. This section is organised into three primary fungal spore sampling approaches that are examined or used in various ways during the duration of this study. The techniques employed encompass conventional monitoring methods, exemplified by the Hirst PBAP sampler, contemporaneous monitoring methods, exemplified by the WIBS-NEO, and approaches based on chemical and molecular analysis, exemplified by the utilisation of chemical tracers.

Table 1: Table outlining the different instrument properties and limitations associated with the sampling type, with regards to their bioaerosol monitoring capabilities specifically.

Sampler Name/ Type of Sampler	Monitoring Type	Initial Device Output	Raw	Lab Processing Required?	Particle Type Obtained	Lower Size Limit
Hirst	Traditional	Adhesive tapes		Yes	Fungal Spores	~2µm
PVAS	Traditional	Adhesive tapes		Yes	Fungal Spores	~2µm
UV-APS	Real-Time	Particle Data		No	Fluorescent particles	0.7µm
WIBS	Real-Time	Particle Data		No	Fluorescent particles	0.7µm
BioScout	Real-Time	Particle Data		No	Fluorescent particles	0.7µm
IBAC	Real-Time	Particle Data		No	Fluorescent particles	0.7µm
Chemical Tracers	Chemical/DNA	Filter papers		Yes	Fungal Tracers	None
Molecular/DNA	Chemical/DNA	Liquid well		Yes	DNA Sample	None

1.5.1. Traditional Spore Sampling

1.5.1.1. Hirst Volumetric Sampler

The Hirst 7-day sampling device consists of an electrically operated motor that draws air into the device at a rate of 10 litres per minute. This airflow carries particulate matter, which is then directed onto an adhesive surface located within the device. The purpose of this arrangement is to facilitate the impaction of bioaerosols onto the medium, enabling their collection. The sticky surface has the capability to be detached and transported to a laboratory where a comprehensive manual analysis of the sample can be conducted using optical microscopy. The bioaerosol sampler discussed below is widely employed due to its established protocols for operation, maintenance, and analysis of results.

The operation of the device's suction mechanism necessitates a consistent and dependable electrical power source, which is facilitated by a motor. The primary limitation of this device is in its inability to facilitate the sampling of fungal spores in distant areas without necessitating modifications to its performance. Essentially, the device needs to be connected to mains electrical supply at all times, and needs weekly collection of samples by a trained professional. Given its widespread usage and the availability of a consistent and dependable mains electricity supply throughout all sampling sites, the utilisation of this particular sampler was deemed the most suitable choice for the project. Prior research utilising this apparatus has explicitly documented the temporal variations in fungal spore densities, their potential as allergenic particles, and their potential adverse effects on crop yield. The studies conducted by Grinn-Gofroń et al., M Martínez-Bracero et al., and O'Connor et al. (Grinn-Gofroń et al., 2018; Martínez-Bracero et al., 2019a; O'Connor et al., 2014a) provide noteworthy findings regarding the device's capacity to effectively monitor fungal spore concentrations with a high level of temporal precision, specifically on an hourly basis. Furthermore, these studies demonstrate the device's ability to integrate this data with publicly accessible datasets, such as meteorological information, to identify diurnal and seasonal patterns. Additionally, the device can construct predictive models for fungal spore levels without requiring any supplementary equipment, instrumentation, or academic resources.

To mitigate the constraints observed in the Hirst sampling device, alternative versions were developed. The primary issues that these devices aim to address are the considerable size and weight, which hinder their usability in confined spaces with limited surrounding area, as well as the need on a mains electrical power source. The primary focus of the Personal Volumetric Air Sampler is to overcome the challenge of mains electrical sampling. This requirement can

be bypassed by utilising battery power, while ensuring that the air suction rate, drum rotation speed, and other relevant parameters remain unchanged. Consequently, the data obtained from this device should exhibit an indistinguishable resemblance to that obtained from a conventional Hirst device. (Feliziani and Marfisi, 1992; García-Mozo et al., 2014) have been cited in the present study.

The Rotorod air sampler is an example of a device that deviates from the original Hirst design. The device described is a bioaerosol impaction sampler that utilises the motion of an adhesive rod to enhance the airflow towards its adhesive surface. The adhesive-coated rod undergoes rapid circular motion in the air, resulting in the impaction of particles onto its surface. The utilisation of battery power in the sampler facilitates its deployment in remote areas, offering a more convenient alternative to the conventional Hirst device. Although several studies have utilised this sampler, its usage is significantly overshadowed by the extensive and enduring fungal spore surveys conducted by Hirst, with ongoing efforts to standardise Rotorod results. The Hirst is often regarded as the preferred sampling device due to several factors, as supported by multiple studies (Anderson et al., 2020; Hollins et al., 2004; Kapadi and Patel, 2019).

1.5.1.2. Personal Volumetric Air Sampler

The Personal Volumetric Air Sampler (PVAS) is a portable air sampling equipment produced by Burkard Manufacturing Co Ltd. It operates without reliance on electrical mains power and is designed for short-term monitoring of particulate matter in the atmosphere (“Personal volumetric air sampler – Burkard Manufacturing Co Ltd,” 2021) The device operates on same principles to the Hirst 7 Day Volumetric Sampler and employs comparable techniques for sample collection. The suction of air via a 2 mm slit is facilitated by an electrically powered motor, operating at a rate of 10L/min. The air sample is then directed towards an adhesive surface, enabling its subsequent removal for further analysis. In designing the PVAS, the primary goal was to enhance the portability of this device and improve its functionality in situations when access to a main power supply is limited (“Personal volumetric air sampler – Burkard Manufacturing Co Ltd,” 2021). The aforementioned objectives were successfully accomplished due to the device's light weight of 590g, together with its compact dimensions of 115 mm in height and 88 mm in diameter. These specifications facilitate convenient transportation and positioning of the device in distant environments. The device has the capability to be powered by a mains energy source. However, in contrast to the conventional Hirst sampler, it also has the option of being powered by 700 ma.h-1 NiCad batteries.

Although Burkard Manufacturing does not offer specific predictions regarding battery performance or the duration of optimal flow rates before electrical power depletion, several research have been conducted to investigate these aspects.

A comparative analysis was conducted to assess the performance of the PVAS in relation to a conventional Hirst 7-day volumetric spore sampler (Feliziani and Marfisi, 1992). One aspect of the research entailed evaluating the effectiveness of aspiration and battery functionality by utilising a flow metre. The study revealed that when the device was fully charged, it exhibited an aspiration flow rate of 10 L/min. The rate of flow exhibited a decline concurrent with the depletion of the battery. The study revealed that the maintenance of the ideal flow was limited to a duration of 30 minutes. Following an hour of exposure to mild environmental circumstances characterised by a temperature of 18°C and a humidity level of 62%, the device's flow rate exhibited a decrease to 7.5 L/min. Similarly, when subjected to colder and more humid conditions with a temperature of 7°C and a humidity level of 75%, the flow rate saw a further reduction to 2.5 L/min. Regardless of the circumstances, the device exhibited an inability to operate solely on battery power for a duration exceeding 2 hours. In most instances, it ceased functioning after around 1.5 hours (Feliziani and Marfisi, 1992).

The conventional Hirst device employs a drum that is enveloped in tape coated with adhesive, facilitating subsequent removal and analysis in a controlled laboratory setting. In contrast, the PVAS method entails the direct deposition of particulate matter onto the glass slide itself. One notable advantage of this alternative to the conventional Hirst device is the elimination of a processing step in the collection of samples. Specifically, there is no longer a requirement to remove samples from a drum and subsequently divide them into 24-hour segments before adhering them to a glass slide.

To assess the dependability of samples acquired from the battery-powered device, the researchers conducted a comparative analysis between a conventional Hirst Volumetric Sampler and a Personal Volumetric Air Sampler. The two devices were operated simultaneously for a duration of 30 minutes to evaluate the collection of particulate matter. Due to the relatively slow rotation rate of 2mm per hour exhibited by the Hirst device, and the limited operational duration of the PVAS, which successfully functioned for only thirty minutes before experiencing a decline in flow rate, the task of comparing spore concentrations between these two devices proved to be highly challenging. Additional efforts were made to extend the duration of the Hirst device's operation and to synchronise the timing of both devices. However, these attempts encountered difficulties in directly comparing particle counts. Comparable values were only achieved after applying correction factors for the Hirst device. Specifically, during a 30-minute period, particles deposited

during the rotation of the drum necessitated the counting of a 2mm section, along with half of a 1mm section on each side of the 2mm point. It should be noted that only a fraction of the particles present on these "edge" sections of the tape would have been deposited within the 30-minute window.

During the period under investigation, the state of battery technology was comparatively less sophisticated than its present state. The device in question had a limited operational duration of merely thirty minutes, coupled with a protracted charge period of twelve hours. Consequently, the device was deemed impractical and not yet suitable for routine utilisation. On the contrary, its use is limited to highly particular and temporary remote scenarios. Furthermore, substantial data correction is necessary to establish a correlation between particle values obtained from this device and those obtained from the conventional Hirst device. Given the rapid advancements in battery technology since the time of the initial examination, it is justifiable to conduct a contemporary evaluation of an upgraded system.

A study was conducted by Aizenberg et al. (Aizenberg et al., 2000) to evaluate the performance of the PVAS device with the Air-O-Cell Sampler and the Button Aerosol Sampler device in terms of their capabilities for collecting fungal spores using portable devices. The three sample instruments serve a common purpose but employ distinct methods, with the Air-O-Cell operating at a flow rate of 15 L/min, the PVAS at 10 L/min, and the Button Sampler at 5 L/min. Both the Air-O-Cell and the PVAS employ glass slide impaction as their sampling method, while the Button Sampler utilises a filter sampler approach, employing 37-mm closed-face two-piece filter cassettes for particle collection.

When comparing the PVAS to other glass slide impaction samplers, it was found that the PVAS exhibited a comparable particle size cut-off, about. The collecting efficiencies of particles with a diameter of 2.3µm and particles of similar size, such as PSL particles, are comparable. A notable disparity was seen in the collection efficiencies pertaining to fungal spores, whereby the PVAS exhibited a substantially superior fungal spore collection efficiency compared to the Air-O-Cell. The Button Aerosol Sampler demonstrated a high particle collection efficiency, close to 100%, for fungal spores within the size range under investigation. This remarkable performance can be attributed to the inherent design characteristics of the device as well as the careful selection of an appropriate filter size. After excluding the smallest sampled microorganism type (*B. subtilis*) from the dataset, the results of the two-way ANOVA indicated that there was no significant difference in the collection efficiency between the PVAS and the Button sampler. This suggests that as long as the fungal spores being sampled fall within the PVAS's operating parameters, it exhibits a sufficiently high collection efficiency. Furthermore, the collection efficiency of the PVAS was found to be

significantly higher than that of the Air-O-Cell glass slide impaction sampler (Aizenberg et al., 2000).

Research conducted on the Personal Volumetric Air Sampler has indicated that its initial design allows for effective sampling periods of approximately 30 minutes in situations where a mains power supply is unavailable. In comparison to other portable air sampling devices, it demonstrates relatively satisfactory performance. However, it is not a viable substitute for the Hirst 7-Day Volumetric Sampler. To enable extended sampling durations of several hours or an entire day in remote areas, improved battery technology is necessary for the Personal Volumetric Air Sampler to be deemed practical. Although the device possesses a specific application and can be advantageous under appropriate circumstances, it generally necessitates extensive data processing and sample quality testing to ensure accurate flow speed and adherence to the high standards set by traditional fixed samplers commonly employed.

1.5.2. Real Time Monitoring Techniques

1.5.2.1. Ultraviolet aerodynamic particle sizer (UV-APS)

Throughout the literature on the real-time characterization of Primary Biological Aerosol Particles (PBAPs), the Ultraviolet Aerodynamic Particle Sizer (UV-APS) has emerged as the predominant commercially accessible real-time ambient fluorescence spectrometer. The UV-APS instrument employs a combination of particle fluorescence and aerodynamic size measurements to classify ambient aerosol particles as potentially of biological origin. The method has been widely employed in prior research endeavours to discern and describe fungal matter, and is rooted in a prototype devised by Hairston, Po, and Quant (Hairston et al., 1997). The operational procedures of the UV-APS have been extensively examined by multiple authors and will therefore be summarised concisely in the next section (Agranovski et al., 2003; Brosseau et al., 2000; Huffman et al., 2012, 2010).

The UV-APS device collects samples of ambient air at a flow rate of 5 litres per minute. The airflow is subsequently divided, with a flow rate of 1 L min⁻¹ allocated for the purpose of analysis. The 4 L min⁻¹ of the air sample that remains is employed as a sheath flow in order to facilitate the movement of the particle stream, which flows at a rate of 1 L min⁻¹, towards the centre flow. The measurement of fluorescent particles is conducted using a diode-pumped, frequency-tripled Neodymium: Yttrium Aluminium Garnet (Nd: YAG) laser with a wavelength of 355 nm. This laser is capable of determining both the fluorescence intensity

and quantity of these particles. Fluorescent emission intensities are detected from excited particles by employing an elliptical mirror, while filters at 410 nm and 630 nm are employed to distinguish between emission and scattered light. Subsequently, the fluorescence intensity of the particles, the quantity of particles, and the aerodynamic size of the particles are measured and documented. The initial investigations enhanced the capability of the instruments and replaced the continuous wave laser with a pulsed stimulated laser. In this study, a diode-pumped Nd: YAG UV laser with a wavelength of 355 nm is employed to stimulate particles in order to facilitate fluorescence detection. A suitable apparatus is employed to capture the dispersed light for the purpose of ascertaining the dimensions of the particles, and these measurements are subsequently compared with a database containing particle size information (Després et al., 2012; Fennelly et al., 2018).

The UV-APS exhibits a distinctive approach in determining the size distribution of particles. The majority of technologies utilised in the realm of real-time bioaerosol detection employ the Mie scattering technique to determine the optical size of particles. The UV-APS is capable of determining the aerodynamic diameter (Da) of a particle in an alternate manner. The Ultraviolet Aerodynamic Particle Sizer (UV-APS) is employed to determine the aerodynamic diameter (Da) of particles. This is achieved by analysing the correlation between the velocity of particles and the velocity of air in an accelerating airflow. The measurement of particle time of flight is conducted using two successive laser beams with a wavelength of 680 nm. This allows for the assessment of the time it takes for particles to travel through the space between each laser beam. Therefore, the determination of the aerodynamic diameter and side scatter parameter of particles involves the calculation of the time it takes for each particle to traverse between two lasers within the apparatus (Després et al., 2012; Fennelly et al., 2018). The UV-APS device provides measurements of total and fluorescent particle concentrations aggregated over a specific time interval, as opposed to providing information on individual particles, which distinguishes it from many contemporary Laser-Induced Fluorescence (LIF) instruments. Additionally, it should be acknowledged that the fluorescence intensity may be significantly affected by the lack of regular monitoring and correction of the detector response to the fluorescence background, which is not typically done in comparison to other similar instruments. Consequently, this has the potential to impact the subsequent analysis and understanding of the data (Huffman et al., 2020).

1.5.2.1.1. Laboratory and Field Campaigns

Despite its discontinuation in the commercial market, the UV-APS continues to be extensively employed in various geographical areas and for diverse research purposes. These

settings encompass both indoor laboratory environments and ambient sample sites, primarily utilised for the purpose of bioaerosol analysis (Bhangar et al., 2014; Shen et al., 2019; Vélez-Pereira et al., 2019; Wei et al., 2016).

Experiments involving the UV-APS have primarily concentrated on comprehending its efficacy inside a controlled laboratory environment. Specifically, these studies have aimed to investigate its capabilities in assessing various particle volumes, types, and distributions (Agranovski et al., 2003; Kaliszewski et al., 2013).

A laboratory investigation conducted by Kanaani et al. (Kanaani et al., 2007) examined the performance of the UV-APS in detecting and measuring the concentration of fungal spores, specifically *Aspergillus niger* and *Penicillium*. One noteworthy observation derived from this study was the decline in fluorescence percentage of fungal spores as they aged. In the present investigation, the samples were subjected to analysis at predetermined intervals, specifically at 2-day and 4-day time points following the first culture. In a comparable manner, the fluorescence intensity of *Penicillium* exhibited a lesser magnitude compared to that of *Aspergillus*, provided that both spores were collected within the same time interval. Therefore, within the confines of a controlled laboratory environment, the UV-APS exhibited the capability to discern distinct fungal spore species. However, the applicability of this scenario to real-world environments is limited, as it is likely that several spores of different ages would coexist in the same site. The study revealed that after a period of 4 days, the fluorescence % of *Aspergillus* was comparable to that of *Penicillium* after 14 days. Additionally, there were instances of overlapping fluorescence percentages at various stages of the culturing process.

The UV-APS has been employed in several indoor settings, including expansive public areas characterised by numerous potential particle emission sources, such as hospitals, as well as enclosed locations where substantial crowds congregate, such as lecture halls. The primary focus of the research conducted by Huffman et al. (Huffman et al., 2010) and Pereira et al. (Pereira et al., 2017) were around the release and dispersal path of particles, as well as their potential impact. Pereira et al. (Pereira et al., 2017) have provided a description of the UV-APS device, which is utilised for the purpose of identifying the source activities responsible for elevated levels of fluorescent particles in the air, as well as the daily temporal fluctuations in their concentrations within an indoor hospital environment. The researchers established that the size range of fungus spores most likely falls between 2.0 and 5.0 μm . Upon the removal of particles smaller than 1 μm , it was observed that the UV-APS inlet transmission efficiency experienced a rapid decrease to below 0.8 μm (Huffman et al., 2013). The distribution of fluorescent particles displayed a bimodal pattern, characterised by one mode

located at or near the 1 μm threshold, and a second mode that varied between 2 and 9 μm , contingent upon the surveyed location. There is a significant degree of overlap between the size range estimated for fungal spores, which is 2 to 5 μm , as previously mentioned in the research. The study additionally determined that the daily rise in particulate matter might, to some extent, be ascribed to individuals traversing carpeted surfaces, which leads to the release of particles like fungal spores into the atmosphere. This phenomenon occurs due to the tendency of carpets to absorb and accumulate airborne particles. Research findings indicate that individuals who received medical treatment in rooms with carpeted flooring exhibited the presence of fungal spores and other microorganisms that were also found in the carpet (Anderson et al., 1982).

Previous research has conducted investigations utilising the UV-APS in indoor settings, albeit to a lesser extent and with fewer studies compared to those centred on outdoor surroundings. Consequently, the efficacy of the gathered data has been constrained. Limited long-term research has been conducted thus far, resulting in an insufficient database to discern trends or characteristics pertaining to the association between indoor environments, the proliferation and diffusion of bioaerosols, and their influence on the population. In stark contrast, the UV-APS has been employed in numerous field experiments. The UV-APS instrument has been utilised in several environmental contexts, encompassing urban and rural areas, industrial sites, woodlands, and dry (Shen et al., 2019; Valsan et al., 2016).

A primary area of investigation in previous research is the comparative analysis of rural and urban habitats under comparable temporal frameworks or under analogous circumstances. In their study, Shen et al. (Shen et al., 2019) provided a description of the use of the UV-APS instrument in outdoor environments, encompassing both rural and urban areas. The UV-APS instrument was employed to discern disparities in biological particulate matter (PM) between the urban region of Beijing and the rural region of Wangdu. The findings revealed that rural areas exhibited elevated levels of biological PM in comparison to urban areas. The study observed that the average concentration of biological particulate matter (PM) in the urban region ranged from 83 to 20166 $\mu\text{g}/\text{m}^3$, whereas in rural areas, the concentration varied between 1366 and approximately 1,100,000 $\mu\text{g}/\text{m}^3$. The device demonstrated the ability to detect distinct diurnal patterns in the concentrations, with elevated levels observed between the time intervals of 18:00 to 00:00 and 04:00 to 08:00 under conditions of clean air.

The device has also been utilised as a standard/control apparatus for the purpose of comparing results with those obtained from untested, freshly produced, or less commonly used equipment (Kesavan et al., 2019; Zheng and Yao, 2017).

In the investigation conducted by Kesavan et al., a comparison was made between the UV-APS and a 275 nm UV-LED continuous ambient air monitoring device known as the TAC-BIO® bioaerosol detector. The development of the technology was undertaken by the United States. The research paper delineates the TAC-BIO as a possibly more cost-effective substitute for the UV-APS under certain circumstances, albeit accompanied by various trade-offs. According to the study, the TAC-BIO device is capable of detecting particles with a size greater than 1.5 μm , whereas the UV-APS device has a lower detection limit of 0.5 μm . The TAC-BIO is characterised by its operational similarity to the BioScout, an optical LIF real-time bioaerosol detector. The latter is further elaborated upon below, as it employs the identical methodology of capturing scattered light and fluorescence. A correlation analysis was conducted between the two devices for particles with sizes over 1.5 μm , as the TAC-BIO is unable to identify particles below this threshold. The Pearson correlation coefficient obtained from the 6-hour continuous in-clinic test was found to be $r = 0.485$. Additionally, the linear regression analysis yielded an R^2 value of 0.209, with a p-value of less than 0.00001.

The UV-APS was employed in another instance to aid in the testing of a different device, namely the SKC BioSampler. This particular device is designed to collect bioaerosols, including fungal spores and bacteria, and preserve them in a liquid medium, such as water, to ensure the viability of the collected samples. The collection efficiency of the BioSampler were assessed at three different flow rates (5, 12.5, and 20 L/min) and three distinct amounts of collection liquid (5, 10, and 20 mL). The UV-APS was employed at a flow rate of 12.5 L/min to investigate the relationship between collection efficiency and collection liquid volume. The results indicated that as the amount of the collection liquid rose, the collection efficiency also increased. Specifically, a collection liquid volume of 5 ml resulted in a collection efficiency of 25%, while a volume of 10 ml yielded a collection efficiency of 41%. Furthermore, a collection liquid volume of 20 ml exhibited the highest collection efficiency of 83%. In conclusion, it was found that around 20% of the sample was lost despite the utilisation of the most optimal collection liquid volume. The conducted experiments on various sampling rates revealed a positive correlation between higher sampling rates and improved collection efficiency. However, it is worth mentioning that prior research has indicated that elevated sampling rates may lead to a decline in sample viability. This correlation was also observed in connection to the amounts of liquid collected. The researchers reached the conclusion that the optimal collection conditions, including both the total sample taken and the viable sample, were a sampling rate of 12.5 L/min and a collection liquid volume of 20 mL. The adaptability of the UV-APS instrument is demonstrated by its capability to assess sample

collection efficiency, indicating its potential for applications outside its intended purpose (“BioSampler, 20 ml, 3 Pieces | Order High-Quality BioSampler, 20 ml, 3 Pieces Products at SKC, Inc.,” 2021; Zheng and Yao, 2017).

Another example in which the UV-APS was used to assist in testing another device was in the study involving the SKC BioSampler, a device that collects bioaerosols such as fungal spores and bacteria and stores them in a liquid such as water to maintain sample viability. The test for bioaerosols encompasses bacterial species that have been aerosolized, as well as those originating from interior air. In order to achieve the most efficient results, several flow rates (Q_{sampl}) of 5, 12.5, and 20 L/min, as well as varied volumes of collecting liquids (V_{cl}) of 5, 10, and 20 mL, were examined for the purpose of analysing bioaerosol particles ranging from 0.5 to 10 μm . Furthermore, the viability of bioaerosol collecting efficiencies of the BioSampler was confirmed using the DNA stain method, specifically the LIVE/DEAD BacLight dye and culture techniques. The experimental results indicated that the collection efficiency of the BioSampler declined from 82.7% (at a volumetric collection rate of 20 mL) to 24.8% (at a volumetric collection rate of 5 mL) when sampling aerosolized *Bacillus subtilis* at a flow rate of 12.5 L/min. The findings obtained from the utilisation of BacLight dye and culturing techniques for the samples collected by the BioSampler yielded comparable outcomes. The collecting efficiency of viable biological particles in indoor air were determined through sampling. The efficiencies were found to be 95.3%, 87.7%, and 65.5% for $V_{\text{cl}}=20\text{mL}$, 10mL, and 5mL, respectively, at a flow rate of 12.5L/min. When the flow rate of Q_{sampl} was 20 litres per minute, the performance of the BioSampler was seen to be superior when the collection volume (V_{cl}) was set at 5 millilitres compared to other values. The findings of this study indicate that the sampling flow rate significantly influences the total physical collection efficiency, while the collection volume is essential for maintaining the viability of bioaerosol particles. In contrast to conventional practise, it is necessary to appropriately modify the operating settings of the BioSampler for the specific types of viral, bacterial, and fungal aerosol particles being targeted (McLaughlin and Spatafora, 2014; Simon-Nobbe et al., 2008).

1.5.2.2. Wideband integrated bioaerosol sensor (WIBS)

The WIBS-NEO played a significant role in this study, and a comprehensive account of its design, functioning, and techniques for collecting samples may be found in the material and methods portion of this report.

In summary, the device under consideration is a real-time continuous monitoring apparatus that employs UV-LIF technology. It distinguishes itself by utilising Zenon flashlamp sources instead of the relatively pricier solid-state UV lasers commonly employed in similar applications. This substitution facilitates the creation of a cost-effective and readily available bioaerosol monitoring device referred to as "WIBS sensors."

1.5.2.2.1. Previous campaigns using the WIBS technology.

The following section presents a compilation of applications and historical implementations of the WIBS technology. In a study conducted by Perring et al. (Perring et al., 2015), a WIBS-4 instrument was deployed on an airship to investigate the correlation between fungal distribution and the distribution of other airborne particles in the southern region of the United States of America. The airship embarked on a journey originating in central Florida, traversing a path that encompassed the states of Alabama, Louisiana, Texas, New Mexico, and Arizona, ultimately culminating in its arrival on the Western Coast of California. Throughout the duration of the campaign, a prevailing pattern was observed that related fluorescent particles to fungal spores. Specifically, fluorescent particles detected in the eastern region of the United States exhibited attributes indicative of fungal spores. In contrast, as the airship advanced westward, the levels of modelled fungal particulate matter diminished and were overtaken by other forms of biological particulate matter. Estimates from Spracklen and Heald (Spracklen and Heald, 2014) have the super micron concentration of fungal spores to be approx. 0.4m^3 at the Florida Panhandle, decreasing to approx. 0.1m^3 once one reaches the Arizona/California desert.

Although the WIBS apparatus has predominantly been employed in outdoor research, a few investigations have been conducted in inside settings. The primary focus of these assessments involves conducting laboratory evaluations to determine the testing capabilities and limitations of the WIBS system, as documented by Healy et al. (Healy et al., 2012a, 2012b). One notable study conducted by Xie et al. (Xie et al., 2017) examined the influence of outside particles on indoor environments using a WIBS-4A instrument. During a continuous 6-day period, a WIBS-4A instrument was used to sample both interior and outdoor air. The sampling process involved alternating between indoor and outdoor sampling at 5-minute intervals. The correlation coefficient for linear regression analysis between interior and outside air samples was approximately averaged to. The coefficient of determination (R^2) was found to be 0.8 for the various particle sizes, indicating a strong positive correlation. Notably, smaller particles exhibited steeper slopes in comparison. The authors propose that this phenomenon could be attributed to the enhanced mobility of tiny particles, facilitating their

infiltration from the external environment into the interior of the building. The author also observed a notable decrease in concentration across all particle sizes, along with a delay in the transition from outside to indoor measurements. This study examined airborne particles in a comprehensive manner, with a specific focus on the linear regression analysis of particles within the fungal spore size range, which exhibited more gradual slopes.

The majority of experiments conducted using WIBS instrumentation are conducted in outdoor settings, such as the examination of agricultural emissions sources and the assessment of the potential impact of different meteorological conditions on Fluorescent Biological Aerosol Particles (FBAP) (Daly et al., 2019; O'Connor et al., 2013). Cheng et al. (Cheng et al., 2020) conducted an outdoor investigation utilising WIBS to monitor bioaerosols, specifically fungal spores. The researchers conducted a characterization of the fluorescent aerosol particles (FAPs) found in the urban area of Tianjin throughout the summer season. The WIBS-4A instrument successfully detected what they determined to be “likely” fungal spores, which were found to constitute a significant fraction of the diurnal peaks observed during sunrise and in the evening. The concentration of fungal aerosol particles (FAPs) in the FLI channel exhibited a statistically significant increase ($p < 0.05$) when the relative humidity exceeded 65%, compared to instances when the relative humidity was below this threshold. This observation suggests that humidity may potentially influence the process of particle aerosolization, particularly in the case of fungal spores. The relative humidity (RH) similarly exhibits an increase from midnight to morning, mirroring the diurnal pattern observed in the levels of FAP. This suggests that relative humidity may play a role in driving the observed diurnal trend.

A research site in the United States was selected for a study that utilised the WIBS-3 and WIBS-4 instruments. The study area was set outdoors, namely in a forested region. The two instruments were positioned around 300 metres apart, with the WIBS-3 placed at ground level and the WIBS-4 put on a platform that could be controlled by a winch. The height of the platform varied between 5 metres and 20 metres. Both methods, together with hierarchical agglomerative cluster analysis (HA-CA), were employed for the quantification of ambient bioaerosol emissions. The WIBS instruments detected what the researchers determined to be multiple fluorescent clusters of biological particles, and characteristics of both fungal clusters and bacterial clusters were observable with a HA-CA used for the statistical separation of particle types that are physically distinct from each other. Consequently, the identification of both fungal and bacterial clusters was achieved. There is a positive correlation between the presence of fungal clusters and higher levels of relative humidity and damp environmental conditions. Under conditions of high relative humidity

(RH), fungal clusters constituted 20% of the total count of fluorescent particles. This percentage increased to 60% when the RH exceeded 90% in wet conditions. According to Crawford et al. (Crawford et al., 2014), when the relative humidity (RH) falls below 40%, the proportion of fungal clusters in the entire population of fluorescent particles is less than 10%.

1.5.2.3. BioScout

The BioScout instrument was developed at Tampere University of Technology and shares similarities in design and function with the UV-APS, serving as an optical LIF real-time bioaerosol device. Following its development, the product was subsequently brought to market by Environics Ltd, a company based in Finland. Numerous comparative studies have been conducted to explore the parallels between the two instruments, which are further elaborated upon in the subsequent discussion. The BioScout utilises a 405 nm continuous wave laser diode operating at an optical power of 200 mW to achieve autofluorescence of individual biological particles. The elliptical mirror is employed to catch scattered light and autofluorescence emitted by particles that have been stimulated, similar to the UV-APS instrument. Subsequently, the two beams are directed onto two photomultiplier tubes (PMTs) by means of a beam splitter in order to achieve focused alignment. In order to facilitate optical particle size estimation, a pass filter with a wavelength of 442 nm is employed to selectively separate the autofluorescence while disregarding the scattered light. The fluorescence intensity is distributed among sixteen distinct intensity channels. The data can be accurately collected with a temporal precision of 1 millisecond, while the optimal particle size range for effective operation falls within the range of 0.3 to 5 micrometres. The UV-APS has been employed as a benchmark tool in the BioScout particle size calibration in prior studies, as outlined in the works of Fennelly et al. (Fennelly et al., 2018) and Saari et al. (Saari et al., 2015).

1.5.2.3.1. Field and laboratory campaigns

The BioScout has been employed in various diverse settings. Extensive investigations have been conducted to thoroughly examine the comparative performance of the BioScout and the UV-APS under various environmental and laboratory circumstances.

In a laboratory environment, Saari, Reponen, and Keskinen (Saari et al., 2014) conducted a comparative study between the BioScout device and the UV-APS. The objective of their research was to assess the efficacy of a 405 nm diode laser for real-time fluorescence detection. The primary objective of this study was to investigate the identification of aerosolized fungus spores and bacteria. The BioScout device exhibited superior detection capabilities for fluorescent particles compared to the UV-APS device. The study ascribes the

higher values of Fluorescent Particle Fraction (FPF) to the laser employed in the BioScout, which exhibits greater power compared to the UV-APS laser. Fluorescent Particle Fraction (FPF) is a measure of the proportion of particles in an aerosol that are fluorescent.

Another proposed distinguishing factor is the utilisation of distinct wavelengths by each device. The BioScout device use a 405nm wavelength, while the UV-APS utilises a 355nm wavelength. The plausibility of this assertion is substantiated by empirical evidence indicating that the UV-APS exhibited greater fluorescence than the BioScout alone in instances when NADH, a biological compound characterised by an excitation spectrum spanning from 340 to 366nm, was aerosolized (Agranovski et al., 2003).

The research findings indicate that fungal spores exhibit a fluorescence rate of 50%. It is important to note that the fluorescence of these spores can be influenced by various circumstances, including humidity and development conditions. According to the author, the determination of ambient fungal spore concentrations using the BioScout is contingent upon the availability of BioScout FPF values specific to prevalent fungal spores in the local environment. The concentration of fluorescent particles is divided by the FPF value in order to determine the concentration of ambient fungal spores. Despite the availability of this information, the produced result cannot be guaranteed to possess a high level of accuracy. The determination of the FPF was conducted inside a controlled laboratory environment in the present investigation. In a practical context, various external elements, such as ambient conditions and the life cycle of fungal spores, can exert an influence on the fluorescence properties of these spores.

Previous laboratory-based investigations have examined the impact of nutritional composition on fungal growth and subsequent fungal spore production. Saari et al. (Saari et al., 2015) conducted a study utilising the BioScout and UV-APS instruments to assess the potential effects and significance of the aforementioned external influences. One of the observed results indicated a decline in FPF values in the presence of inadequate nutrient conditions during the cultivation of fungal spores. Additionally, a negative relationship was observed between the advancing age of fungal spores and a drop in FPF values, except for *Penicillium brevicompactum*, which exhibited an increase in FPF values with time. Additionally, it has been shown that fluorescence-based equipment may potentially underestimate the concentration of *Cladosporium Cladosporioides* spores due to their tendency to produce significantly lower FPF values in comparison to other types of fungal spores. This observation is particularly noteworthy as *Cladosporium* spores have been identified as the prevailing fungal spore type in the ambient air of Ireland. The observed

connection between decreased air velocity and elevated FPF readings suggests the potential underestimation of prematurely aerosolized immature spores (Saari et al., 2015).

The initial field investigation conducted by Saari et al., (2014) involved a comparative analysis of the BioScout and UV-APS instruments in urban and suburban regions of Helsinki. This study aimed to assess the fluorescent biological aerosol particles FBAPs and their size distributions during both winter and summer seasons, employing two different measurement devices. During the summer measuring campaign, the FBAPs were categorised based on their size into two distinct groups: tiny particles, which ranged from 0.5 to 1.5 μm , and coarse particles, which ranged from 1.5 to 5 μm . The study yielded findings indicating a strong positive correlation between the results obtained from the UV-APS and the BioScout instruments. Specifically, the correlation coefficients for coarse and fine particles were determined to be $R=0.83$ and $R=0.92$, respectively. This investigation provided the initial confirmation of the BioScout's capability to function at a comparable level to the commonly employed UV-LIF sensors under ambient circumstances.

An additional instance of the utilisation of the BioScout device in a controlled environment is demonstrated in the study conducted by Wu et al. (Wu et al., 2018). In this study, the BioScout device was transported on a trolley in close proximity to a mechanical crawling infant, with the aim of quantifying the concentration of biological particulate matter that becomes airborne and potentially inhaled when an infant crawls on a carpeted surface. The investigation additionally encompassed the replication of an adult's movement on a carpet through the utilisation of a volunteer equipped with a comparable device configuration. The utilisation of the BioScout in research endeavours of this nature underscores the device's adaptability, as it may be employed not only for the monitoring of ambient air, but also for investigations pertaining to particular circumstances that lead to the dispersion of potentially hazardous fungal spores and other FBAPs.

1.5.2.4. Instantaneous biological analyser and collector (IBAC)

The IBAC-2 plays a significant role in this study and report. Consequently, a more comprehensive explanation of its functioning, protocols, and structure may be found in the material and methods section. The IBAC device is infrequently utilised, leading to a scarcity of published articles and studies examining its operational mechanisms and functionalities. Santarpia et al. (Santarpia et al., 2013) conducted a 10-day outdoor ambient air research utilising the IBAC device. The researchers graphed the data collected from meteorological

conditions assessed using a Transportable Automated Meteorological Station at the identical site. The IBAC was employed to facilitate the identification of both biological and non-biological particles, which were classified into two distinct size ranges: 0.5-1.7 microns and 1.7-10 microns. A positive association was observed between tiny particle biological particles and relative humidity. A correlation coefficient of $R > 0.7$ was observed between the two measures. The researchers reached the conclusion that the robust correlation can be attributed to the phenomenon wherein biological particles absorb water, hence increasing their detectability by the IBAC equipment. This observation suggests that the IBAC has a higher probability of detecting a particle with hygroscopic properties and water content compared to a particle that is devoid of moisture.

The IBAC device has been utilised in several studies as a means of controlling the experimentation process when evaluating innovative approaches to particle analysis. The FIDO B2 IBAC was employed in a study conducted by Choi et al. (Choi et al., 2018) to compare its performance with a suggested correlation value for the analysis of airborne particles through the utilisation of light scattering signals.

Pazienza et al. (Pazienza, 2013) conducted a controlled laboratory investigation including the discharge of a simulated aerosol composed of a solution containing *Saccharomyces Cerevisiae* at a concentration of 7 g/L. Using the IBAC, they were able to calculate overall particle counts, as well as particle counts specifically for fluorescent/biological particles, and separate these into two size categories: big (more than 0.7 microns) and tiny (less than 0.7 microns) (less than or equal to 0.7 microns). This information was then utilised to examine particle counts vs time via nebulisation utilising a pre-compression pump and an automated atomizer operating at varying temperatures. They determined that standard approaches for biothreat detection and sampling are too time-consuming and insufficiently sensitive. In a military and civilian setting, they thought that a single instrument like the IBAC would not be adequate for identifying required biological agents and possible poisons, and that the ideal configuration is now a mix of devices and methodologies.

1.5.3. Chemical or molecular based monitoring and recognition techniques

1.5.3.1. Chemical Tracer molecules

The utilisation of tracer molecules in the measurement and monitoring of aerosols and bioaerosols has been a subject of investigation for a considerable period of time (Simoneit

and Mazurek, 1989). In recent times, the utilisation of tracer molecules has emerged as a viable approach for the measurement and quantification of PBAP. Arabitol, mannitol, and ergosterol have emerged as the most often employed molecular tracers in various scholarly works. Additional compounds, including (1→3)-β-d-glucan, potassium, and endotoxins, have also been employed as tracer molecules. Arabitol and mannitol are effective tracer molecules for fungal spores due to their role as energy reserves for these spores, which are afterwards discharged in conjunction with the spores. Ergosterol, on the other hand, is considered a good tracer molecule as it is naturally present in the cell membranes of fungal spores. Analysis of such tracers has been conducted using Ion and Gas Chromatography techniques (Gosselin et al., 2016).

Additional investigations have been conducted in the field of fungal spore research, wherein alternative tracers, such as (1→3)-β-d-glucan, have been employed. This particular tracer is of interest due to its presence in the fungal cell wall. The study conducted by Wang et al. (Wang et al., 2013) focused on the use of (1→3)-β-d-glucan as a tracer for fungal spores. This research stands out as one of the limited numbers of indoor studies that explore the application of tracer molecules in quantifying and analysing fungal spores. The present investigation involved the collection of air samples via Button Personal Inhalable Samplers. Two sampling devices were operated concurrently for a duration of 24 hours at each respective location. The presence of spores was determined to account for a mere 0.21% of the organic carbon content detected in indoor particulate matter.

Several research investigations have been conducted to quantify the total quantity of fungal spores in the air utilising arabitol and mannitol as tracers (Bauer et al., 2008; Burshtein et al., 2011; Di Filippo et al., 2013; Gosselin et al., 2016; Verma et al., 2018). According to Carlile and Watkinson (M. J. Carlile et al., 2001), a significant proportion of the dry weight of fungal spores consists of these two tracer molecules, which explains their suitability for this particular application.

The majority of investigations utilising arabitol and mannitol as fungal proxies frequently observe positive relationships between these tracers. Burshtein et al. (Burshtein et al., 2011) also observed this phenomenon, wherein arabitol and mannitol had a strong positive correlation, whereas ergosterol did not exhibit a significant correlation with either compound throughout specific periods of the year. A positive association between ergosterol and the other two tracers was observed exclusively during the spring and autumn seasons. The study's findings suggest that arabitol and mannitol may not be optimal indicators for specifically identifying fungus. The authors hypothesised that the observed elevations in arabitol and mannitol throughout the spring and fall seasons may be attributed to the discharge of plant

debris resulting from heightened spring flowering events and autumn breakdown, rather than indicating an actual rise in fungal spore concentrations during these periods.

A study conducted by Di Filippo et al. (Di Filippo et al., 2013) arrived at a comparable finding to that of Burshtein et al. (Burshtein et al., 2011), even providing a word of warning to anyone contemplating the use of arabitol and mannitol as molecular tracers for fungal spores. The research area's primary contributors of arabitol and mannitol were determined to be biomass burning and sea spray, rather than fungal spores. It has been observed that ergosterol does not encounter the same limitation, making it a more dependable molecular tracer, especially in situations where fungal spore levels are minimal.

Despite the additional time required for the utilisation of ergosterol as a tracer, due to the necessity of chemical derivatization through silylation prior to conducting gas chromatography analysis, its perceived dependability as a technique for fungal tracing is a potential advantage that may outweigh the labour-intensive quantification procedure. Several studies have indicated a decrease in ergosterol concentrations following the death of fungal spores. However, investigations into the duration of ergosterol persistence within fungal spore cells before its decline have not been conducted due to the high cost and specialised nature of such research (Burshtein et al., 2011; Gosselin et al., 2016; Gutarowska and Piotrowska, 2007; Mensah-Attipoe and Täubel, 2017; Verma et al., 2018).

The utilisation of tracer molecules is commonly employed in research pertaining to outdoor habitats, particularly in the context of identifying sources of biomass burning. In a study conducted in 2020, Xu et al. (Xu et al., 2020) employed various tracer molecules to quantify PBAPs and to determine their temporal distribution in Beijing. The study involved the identification of tracer compounds that were initially found in fungal spores and afterwards emitted due to the combustion of biomass.

Typically, investigations examining the correlation between biomass burning and the prevalence of fungal spores in the atmosphere primarily aim to identify the origins of biomass burning. However, a notable long-term study spanning 13 years conducted on Chichi Jima Island, Japan, diverged from this convention by exploring the potential impact of biomass burning on ambient fungal spore levels. The researchers discovered that the majority (97%) of sugar compounds, such as mannitol, arabitol, and trehalose, originated from sources such as plants, pollen, and microbiological processes. In contrast, a minor proportion (3%) of these compounds was attributed to biomass burning. This observation indicates that the influence of biomass burning on arabitol and mannitol values as fungal tracers is typically minimal and does not significantly affect them (Verma et al., 2018).

The utilisation of molecular tracers has been implemented in conjunction with additional bioaerosol sensors. In their study, Gosselin et al. (Gosselin et al., 2016) conducted a comparison between the use of tracers in conjunction with both wideband integrated bioaerosol sensors (WIBs) and ultraviolet aerodynamic particle sizers (UV-APS). The study aimed to ascertain the correlation between the use of fungal tracers arabitol and mannitol. A stronger connection than anticipated was observed between the tracers and the instruments in estimating fungal spores, encompassing both temporal and quantitative outcomes. This finding is particularly noteworthy considering the differences in methodologies employed by the devices and tracers to obtain their respective results. The comparison was made between the correlation of the fungal tracers and the WIBS device, and the clusters established by Crawford et al (Crawford et al., 2014). The hierarchical agglomerative clusters utilised in this study are derived from the WIBS-3 data. The fluorescent particles were categorised into four distinct groups, namely CII (cluster 1) through CI4 (cluster 4). Cluster 1 exhibits a correlation with, and is specifically characterised by, fungal spores, while the following clusters exhibit correlations with bacterial spores. The present investigation observed a correlation of about $R^2 = 0.8$ between fungal tracers and the output of the WIBS device. This correlation was seen for CII, specifically for arabitol in all situations and for mannitol in dry conditions. The lower correlation for mannitol in dry conditions can be attributed to the presence of mannitol from sources other than fungal spores. The correlation between the CII fluorescence channel and other WIBS fluorescence channels was not as strong. The UV-APS instrument, employed in this investigation, exhibited a strong positive correlation (often $R^2 > 0.7$) with mannitol and arabitol under wet conditions. However, this connection was considerably weaker (about $R^2 = 0.15$) in drier settings. The authors ascribed this phenomenon to the observation that fungal spores associated with arabitol and mannitol are exclusively released by moist discharge mechanisms.

1.5.3.2. Molecular and DNA methodologies for spore determination

The research community has consistently shown interest in and focused on methods that eliminate the time-consuming and labour-intensive procedure of manually counting fungal spores using optical microscopy (Suchorab et al., 2019). Due to the considerable diversity in the morphology, dimensions, and colour of fungal spores, the effort of memorising or cataloguing the extensive array of spores is inherently challenging. One of the indirect approaches to identification does not focus exclusively on the identification of fungal spores,

but rather aims to locate and distinguish the key characteristic of fungal spores that directly relates to their influence on human health (West and Kimber, 2015a). The assessment of the quantities of allergenic proteins and DNA in fungal spores has gained significant traction in recent times. There exist various methodologies and approaches aimed at accomplishing this objective, such as the Microtiter Immunospore Trapping Device (MTIST device) and Enzyme-linked immunosorbent assay (ELISA), which will be elaborated upon in the subsequent sections (Musgrave and Fletcher, 1986, 1984).

The Microtiter Immunospore Trapping Device (MTIST) is an air sampling instrument that functions as a modified version of the Personal Volumetric Air Sampler, developed by Burkard Manufacturing Co Ltd. The device employs a suction mechanism to collect air samples, with air being pulled into the apparatus at a rate of 20 litres per minute. The airflow is directed through a trumpet nozzle, subsequently traversing a collection of 32 microtiter wells arranged in a configuration of 4 rows containing 8 wells each. Since it is a modified version of the PVAS, it has the capability to be powered by batteries. According to Kennedy et al. (Kennedy et al., 2000), this particular device is equipped with rechargeable 6-V batteries, enabling prolonged operation for a duration of at least 3 hours before necessitating battery replacement or recharging. The collecting wells are equipped with an adhesive covering, such as albumin, which serves to enhance the efficiency of the collection process. The rationale behind the division of the samples into 32 distinct wells is to facilitate the implementation of diverse testing and sampling methodologies for each well. This approach enables the execution of various tests on the same air sample, taken at the same time and day. The MTIST device and spore/PBAP collecting methods were developed with the intention of facilitating further analysis using techniques like the enzyme-linked immunosorbent assay (ELISA), as outlined by West and Kimber (West and Kimber, 2015).

The ELISA was first devised to quantify fungal allergens present in the air, namely those captured in liquid impingers like those found in the MTIST device. The ELISA was specifically developed to target *Cladosporium* and *Alternaria* spores, as highlighted by Flückiger et al. (Flückiger et al., 2000). The ELISA is a widely used technique in biomedical research for detecting the presence of a specific protein in a liquid sample. This method involves the employment of antibodies to mark the protein of interest, allowing for its quantification. The antibodies exhibit affinity towards the protein under investigation, and the quantification of protein concentration is accomplished using an enzyme-based assay, which induces a colour change in the sample solution. The ELISA technique has predominantly been employed for the purpose of identifying fungal spores since its inception. However, recent advancements have enabled the identification and quantification of specific allergens present in known

fungal spores. These developments have sparked significant interest in disciplines pertaining to human health and exposure to ambient air (Musgrave and Fletcher, 1986, 1984).

DNA analysis has emerged as an additional approach for the detection and quantification of fungal spores or fungal spore densities. Various fungal spore samplers and impactors have been modified or redesigned to facilitate the incorporation of DNA analysis methodologies (West and Kimber, 2015). There are two main types of samplers that can be utilised for DNA analysis or can be modified for DNA analysis: dry or wet wall cyclones, which encompass small cyclones and multi vial cyclones. All cyclone-based collection devices operate by generating a swirling motion above the chamber where collection takes place. Particles are influenced or adhered to a surface, whether it is dry or moist, upon their egress from the vortex or "cyclone". This phenomenon arises as a result of the centrifugal force exerted. One notable advantage of cyclone-based samplers is their capacity to gather substantial quantities of physical material, hence enabling much prolonged collection durations. Additionally, these devices can be built in a compact manner, enabling their utilisation as portable or personal sample instruments. Several drawbacks are associated with the device, including the inconsistent collection efficiency, the tendency for foggy conditions to cause all sample tubes to fill with water instead of obtaining usable samples, and the gradual accumulation of particles in the cyclone over time (Carisse et al., 2008; Lindsley et al., 2006).

The data obtained from this cyclone-based apparatus is utilised for the purpose of DNA analysis. Polymerase Chain Reaction (PCR) is a frequently employed method for DNA analysis (Carisse et al., 2009). Through this particular procedure, DNA strands are elongated by use of DNA polymerase. The mechanism under consideration is an enzymatic one, which necessitates the presence of specific primers and the denaturation of DNA in order to facilitate the identification of the targeted DNA segment for replication (Di Pinto et al., 2005; Zhou et al., 2000). The utilisation of DNA analysis offers an alternative approach for the identification of fungal spores, emphasising the extensive variability among different types of fungal spores. However, the considerable duration needed to complete the entire process of cyclone collection and PCR analysis raises concerns about its suitability as a measurement tool for continuous sampling or long-term studies. Instead, it is appropriate for the objective of acquiring a comprehensive overview of the distribution of fungal spore diversity within a specific geographical region at a specific point in time. The rapid and efficient implantation of the device and subsequent analysis is hindered by the limited availability of specialised knowledge pertaining to fungal spores and their DNA profiles (Dodge and Wackett, 2005).

1.5.4. Fungal Spore Modelling and Forecasting Methods

Various modelling strategies have been utilised to provide predictions and projections for ambient bioaerosol concentrations (Maya-Manzano et al., 2021; Vélez-Pereira et al., 2021). The prevailing focus in literature studies has primarily been on the forecasting of ambient pollen concentrations, rather than the forecasting of ambient fungal spore concentrations. This emphasis persists, despite the fact that fungal spores pose a higher risk to human and plant health and are more abundant in the atmosphere (Damialis and Gioulekas, 2006). With that being stated, there is a growing focus and heightened attention on fungal spore modelling research due to the aforementioned health problems and their capacity to efficiently spread plant infections. In contemporary times, a diverse range of modelling techniques has been employed to analyse fungal spore densities, encompassing observational, process-based, and source-oriented models.

1.5.4.1. Observational Based Models

Observational models are employed in order to make predictions about the behaviour of a dependent variable by utilising data pertaining to associated independent variables. The independent variables, which serve as the inputs for the model, and the model outputs typically exhibit site-specific characteristics, hence rendering these models predominantly constrained to certain locations and not readily adaptable to other sites. The dissemination, dispersion, and transportation of fungal spores are heavily influenced by several environmental elements, such as meteorological conditions, geographical characteristics, and phenological parameters. Consequently, fungal spore prediction models commonly incorporate climatic and phenological characteristics as independent variables. Nevertheless, the importance of various parameters appears to change based on the specific fungal species and the method of release. The literature extensively documents the relationship and influence of diverse meteorological variables on several types of fungal spores (Damialis and Gioulekas, 2006; Filali Ben Sidel et al., 2015; Grinn-Gofroń and Bosiacka, 2015; Grinn-Gofroń and Mika, 2008; Ianovici, 2016; Jones and Harrison, 2004; Li and Kendrick, 1995; Lyon et al., 1984; Sadyś et al., 2018). Through the examination of this correlation, approximate calculations can be derived on the circumstances that lead to the emission of particular spores. Consequently, certain spore species, such as *Cladosporium* and *Alternaria*, have been classified as "dry spore types," indicating their notable correlation with arid, dry climatic

conditions (Grinn-Gofroń and Mika, 2008; Ianovici, 2016; Sady et al., 2014; Stępańska and Wołek, 2012). Conversely, it has been shown that other forms of spores, namely *Leptosphaeria* and Ascospores, exhibit a comparable relationship with relative humidity and rainfall (Li and Kendrick, 1995; Lyon et al., 1984). As a result, they have been classified as "wet spore types".

Regression analysis is a widely utilised method for predicting aerobiological phenomena. The simplest strategy is linear regression. This method uses a linear model to establish the correlation between a single dependent variable and a single independent variable. In the context of intricate systems, such as the dissemination and dispersion of fungal spores, it is frequently necessary to incorporate multiple independent variables in order to comprehensively elucidate the dynamics of the dependent variable. Many regression analyses involve the use of many independent variables in order to predict concentrations of a dependent variable. Various regression models have been employed in previous studies to forecast the quantities of fungal spores. The models employed in this study encompass various regression techniques, such as simple linear regression models (Mediavilla Molina et al., 1998; Rodríguez-Rajo et al., 2005), multiple regression models (Aira et al., 2008; Burch and Levetin, 2002; Fernández-González et al., 2013; Grinn-Gofroń and Mika, 2008; Hollins et al., 2004; Rodríguez et al., 2020; Stępańska and Wołek, 2005), as well as other multiple regression techniques including step-wise multiple regression (Burch and Levetin, 2002; Filali Ben Sidel et al., 2015; Recio et al., 2012) backwards elimination regression (Lyon et al., 1984) and logistic regression (De Linares et al., 2010; Vélez-Pereira et al., 2019).

Various models have been employed to forecast a variety of outcomes, such as daily (Mediavilla Molina et al., 1998; Rodríguez et al., 2020; Vélez-Pereira et al., 2019), weekly (Filali Ben Sidel et al., 2015) and annual (De Linares et al., 2010) fungal spore concentrations. The primary emphasis of these models has been on the prediction of concentrations of well-documented allergenic and pathogenic fungal spores, such as *Alternaria* (Aira et al., 2008; Burch and Levetin, 2002; De Linares et al., 2010; Filali Ben Sidel et al., 2015; Recio et al., 2012; Rodríguez-Rajo et al., 2005; Stępańska and Wołek, 2005), *Cladosporium* (Aira et al., 2008; Burch and Levetin, 2002; Hollins et al., 2004; Lyon et al., 1984; Mediavilla Molina et al., 1998; Recio et al., 2012; Rodríguez-Rajo et al., 2005; Vélez-Pereira et al., 2019), *Epicoccum* (Burch and Levetin, 2002; Ščevková et al., 2019; Stępańska and Wołek, 2005), *Ganoderma*, *Leptosphaeria*, *Didymella* (Stępańska and Wołek, 2005) and *Botrytis* (Rodríguez et al., 2020; Stępańska and Wołek, 2005) amongst other fungal types.

These models can be developed with computational ease, rendering them a widely favoured option. Nevertheless, it is worth noting that these models frequently fall short in accurately reflecting the complete seasonal patterns observed in aerobiological data, hence potentially impacting the overall accuracy of the models (Astray et al., 2010). Time-series analysis is a viable alternative method for identifying seasonal or underlying trends, as it does not rely on assumptions of normalcy or linearity. Time-series models aim to forecast future values by analysing historical values and identifying underlying patterns, including both general trends and seasonal variation (Maya-Manzano et al., 2021). The autoregressive integrated moving average (ARIMA) model is widely employed in the field of time-series analysis for the prediction of fungal spore concentrations. The aforementioned technique has been employed for the purpose of forecasting atmospheric levels of other fungal spore categories, including *Alternaria* (Damialis and Gioulekas, 2006; Escuredo et al., 2011), *Cladosporium* (Damialis and Gioulekas, 2006; Stephen et al., 1990), *Botrytis* (Rajo and Jato, 2009; Rodríguez-Rajo et al., 2010)], as well as other phytopathogenic taxa such as *Erysiphe* and *Plasmopara* (Fernández-González et al., 2016).

The aforementioned conventional observational techniques may not consistently provide accurate representations of the intricate dynamics of biological systems, such as the interplay between fungal spores and environmental factors. In recent times, there has been a notable inclination towards employing more intricate machine learning methodologies in order to address these aforementioned constraints. Artificial neural networks (ANN) have emerged as the predominant forecasting method employed in the analysis of fungal spore data. The present methodology is specifically engineered to replicate the functioning of biological processing systems and has demonstrated notable efficacy in handling aerobiological data. Artificial neural networks (ANNs) have been employed to simulate various fungal spore concentrations at hourly (Grinn-Gofroń and Strzelczak, 2009) and daily fungal spore concentrations, including *Alternaria* (Astray et al., 2010; Bruno et al., 2007; Grinn-Gofroń and Strzelczak, 2009, 2008; Tomassetti et al., 2013, 2009), *Cladosporium* (Grinn-Gofroń et al., 2011; Grinn-Gofroń and Strzelczak, 2013, 2009; Grinn-Gofroń and Strzelczak, 2008; O'Connor et al., 2014b) *Ganoderma* (Jedryczka et al., 2015; Kasprzyk et al., 2011; Kumar et al., 2013; O'Connor et al., 2014b; Sadyś et al., 2016) and *Pleospora* (Bruno et al., 2007; Tomassetti et al., 2013, 2009) among others (Sadyś et al., 2018; Verma and Pathak, 2009).

Furthermore, in the field of fungal spore forecasting, decision trees have been commonly employed as advanced techniques with artificial neural networks (ANNs). Several research have utilised multiple regression trees (MRTs) in the modelling of fungal spores, with many of these studies also using artificial neural networks (ANNs). The approach utilised in this

study involves the iterative clustering of data and the subsequent graphical representation of the data as decision trees (De'ath, 2002). MRTs have been applied to forecasting *Alternaria*, *Cladosporium* (Grinn-Gofroń and Strzelczak, 2009; O'Connor et al., 2014b), *Didymella* (O'Connor et al., 2014b) and *Ganoderma* (Kasprzyk et al., 2011; Sadyś et al., 2016), concentrations. Random forest (RF), a type of multiple decision tree approach, has been utilised in the analysis of various aerobiological datasets (Maya-Manzano et al., 2021). The application of Random Forest (RF) to fungal spore data in academic literature has not been extensively explored, despite its utilisation in predicting concentrations of *Alternaria* and *Cladosporium* previously (Grinn-Gofroń et al., 2019). More recently RF models have been employed for the purpose of predicting *Ganoderma*. This is achieved by utilising conventional observational data in conjunction with back trajectory analysis and land cover data (Grinn-Gofroń et al., 2021).

While these methods present an advancement compared to simpler strategies, new research indicates that these advanced methods may exhibit lower accuracy in forecasting precise exposure risks for individuals with allergies (Jedryczka et al., 2015). However, this could also show a need for more street-level sampling hence enhancing the accuracy of these projections.

1.5.4.2. Process and source-based modelling

Phenological observations have been commonly employed to identify key stages in plant growth and have been consistently utilised in the determination of flowering periods for the purpose of predicting pollen levels (Grundström et al., 2019; Tormo et al., 2011). In the context of fungal spore modelling, phenological investigations can be employed to assess the primary phenophases of the plant species that serve as hosts for numerous fungal spores, which function as plant diseases. The aforementioned information might be combined with meteorological parameters in order to predict the occurrence of fungal diseases on plants (Fernández-González et al., 2013). This method is widely utilised in the prediction of crop disease periods, with the primary objective of facilitating the application of precise chemical treatments. The approach in question has been extensively reported in the literature for many vineyard diseases, including *Uncinula neactor* (Fernández-González et al., 2013; Martínez-Bracero et al., 2019b), *Botrytis cinereal* (Fernández-gonzález et al., 2012; Martínez-Bracero et al., 2019b; Rodríguez-Rajo et al., 2010), *Plasmopara viticola* (Martínez-Bracero et al., 2019b) and *Erysiphe necator* (González-Fernández et al., 2019).

The primary cause of fungal spore emissions is derived from plants that are sick and organic matter that is decaying. Consequently, the analysis of land use can also assist in forecasting the concentration of spores released into the air (Ansari et al., 2015; Apangu et al., 2020;

Crandall and Gilbert, 2017; Kallawicha et al., 2015; Qi et al., 2020). The composition of ambient fungal spores is ultimately influenced by the geographical location and, in certain instances, by the type of plant present (Redondo et al., 2020). The examination of land cover can be useful in identifying primary origins of potentially pathogenic and allergic fungal spores (Apangu et al., 2020) as well as in forecasting the ambient levels of these spores in the surrounding environment.

According to the literature, source oriented models have the ability to forecast the dispersion pattern of fungal spores with a reduced reliance on large monitoring (Ansari et al., 2015). The models included in this study utilise modified chemical transport models that were originally designed for the purpose of simulating the spread of bioaerosols. The application of this method was first limited to the analysis of ambient pollen data, but in more recent times, it has also been extended to the analysis of fungal spore data. Various transport models have been utilised in the field of fungal spore modelling, such as the COSMO-ART and WRF-Chem models (Ansari et al., 2015; Hummel et al., 2015). In recent studies, the ZeFir source-receptor model and other transportation models have been utilised to examine the source of ambient fungal spores (Sarda-Estève et al., 2019). Previous studies have utilised these models to provide predictions for the concentrations of *Alternaria* (Apangu et al., 2020; Sadyś et al., 2015; Sarda-Estève et al., 2019; Skjøth et al., 2012), *Ganoderma* (Sarda-Estève et al., 2019; Skjøth and Kennedy, 2014) and *Cladosporium* (Sarda-Estève et al., 2019).

In regions where there is a significant occurrence of long-distance transport of fungal spores, the use of transport data/models can enhance the predictive capacity compared to solely relying on local meteorological data (Grinn-Gofroń et al., 2021).

1.6. Summary and Conclusion

The atmosphere contains primary biological aerosol particles (PBAPs), which vary in size from nanometers to several hundred micrometres. Fungal spores are ubiquitous in the environment, present in diverse habitats including agricultural lands, woodlands, urban green spaces, and moist environments. Spores can be categorised as survival spores, which remain inactive as a protection method, and dispersal spores, which establish new colonies. Spores can be discharged through either active or passive mechanisms, with the main emphasis of this work being on dispersal through the air. Fungal spores have a direct impact on climatic conditions and weather patterns by influencing the development of precipitation and the formation of clouds. Cloud condensation nuclei (CCN) form at temperatures at or above 0°C, whereas ice nuclei (IN) impact cloud formation at temperatures below 0°C. Biological sources of Ice Nuclei (IN) and Cloud Condensation Nuclei (CCN) have been recognised since the 1970s. The investigation of ice nucleation (IN) in the context of bioaerosols is essential because the primary agents that generate IN, such as mineral dusts and combustion aerosols, lose their effectiveness at elevated temperatures. Only particles that are biological possess the characteristics necessary to act as ice nuclei at these higher temperatures.

This study primarily investigates various techniques for sampling fungal spores, including traditional methods such as the Hirst sampler, modern methods like the WIBS-NEO, and approaches involving chemical and DNA analysis. The Hirst sampler is a commonly used instrument for monitoring fungal spore concentrations. However, it has limitations, such as its lack of flexibility in working in remote or unpopulated areas spores. Modifications to the technology, like the Personal Volumetric Air Sampler (PVAS), have tried to overcome these limitations through use of battery power, ensuring consistency of data without mainline electricity connection. Aside from traditional monitoring, there is real-time sampling also. The Ultraviolet Aerodynamic Particle Sizer (UV-APS) is a commercially available instrument that can quickly and accurately identify ambient aerosol particles that may have come from biological sources. It has been widely used in different geographical regions and for various research objectives, with a focus on detecting and quantifying the concentration of fungal spores. The WIBS device is also often used to observe bioaerosols, specifically fungal spores. Previous studies of the WIBS have discovered that humidity can affect the aerosolization especially of fungal spores, and there's been positive correlation between the occurrence of fungal clusters and elevated levels of relative humidity and moist environmental conditions in multiple different campaigns. Another device, The BioScout, created at Tampere

University of Technology, resembles the UV-APS device and employs a 405 nm continuous wave laser diode to induce autofluorescence in individual biological particles. The IBAC-2 device has been also employed in numerous studies to regulate experimentation and assess novel methodologies for particle analysis, acting as a control or comparative device.

Arabitol, mannitol, and ergosterol are frequently employed as tracer molecules to quantify and track bioaerosols. The utilisation of molecular tracers in combination with bioaerosol sensors has demonstrated high correlation, in estimating fungal spore concentrations, compared to the Hirst. DNA analysis is another technique employed to identify and measure fungal spores. It uses modified samplers and impactors that incorporate DNA analysis methodologies. Several regression models have been employed to predict fungal spore concentrations, yet they frequently fail to accurately track seasonal patterns. Time-series analysis is often used to attempt to predict future values by examining past values and identifying underlying patterns. Traditional methods of observation may not provide an accurate depiction of the behaviour of the complex and still understudied ecological and biological systems. As a result, artificial neural networks (ANN) have become a primary method for predicting and analysing fungal spore data. Phenological observations and source models are examples of process and source-based modelling techniques that can be used to forecast fungal spore concentrations.

The study of fungal spores and their impact on the atmosphere is crucial for understanding climatic conditions and weather patterns. Fungal spores play a role in the formation of clouds and precipitation, and their ability to act as ice nuclei at higher temperatures makes them unique compared to other particles. Various techniques for sampling fungal spores have been developed, including traditional methods like the Hirst sampler, and modern approaches involving chemical and DNA analysis. Real-time sampling devices like the UV-APS and WIBS have also been used to detect and quantify fungal spores. Molecular tracers and DNA analysis are employed to track and measure fungal spore concentrations. However, traditional methods and regression models often fail to accurately predict seasonal patterns. The study of fungal spores and their behaviour in the atmosphere is a complex and ongoing field of research that requires innovative ideas and approaches to fully understand their ecological, human health, and biological impact. That is the purpose of this thesis; to analyse and compare all methods and techniques, past and present, and design and develop the best approach for Ireland today and for the future.

1.7. References

- Agranovski, V., Ristovski, Z., Hargreaves, M., Blackall, Patrick.J., Morawska, L., 2003. Real-time measurement of bacterial aerosols with the UVAPS: performance evaluation. *J. Aerosol Sci.* 34, 301–317. [https://doi.org/10.1016/S0021-8502\(02\)00181-7](https://doi.org/10.1016/S0021-8502(02)00181-7)
- Aira, M.J., Rodríguez-rajo, F.J., Jato, V., 2008. ANNUAL RECORDS OF ALLERGENIC FUNGI SPORE: PREDICTIVE MODELS FROM THE NW IBERIAN PENINSULA. *Ann. Agric. Environ. Med.* 15, 91–98.
- Aizenberg, V., Reponen, T., Grinshpun, S.A., Willeke, K., 2000. Performance of Air-O-Cell, Burkard, and Button Samplers for Total Enumeration of Airborne Spores. *AIHAJ - Am. Ind. Hyg. Assoc.* 61, 855–864. <https://doi.org/10.1080/15298660008984598>
- Anderson, J., Pityn, P., Kelly, M., 2020. Pollen Count Standardization for Burkard & Rotorod Samplers. *J. Allergy Clin. Immunol.* 145, AB37. <https://doi.org/10.1016/j.jaci.2019.12.741>
- Anderson, R.L., Mackel, D.C., Stoler, B.S., Mallison, G.F., 1982. Carpeting in hospitals: an epidemiological evaluation. *J. Clin. Microbiol.* 15, 408–415. <https://doi.org/10.1128/jcm.15.3.408-415.1982>
- Andreae, M.O., Rosenfeld, D., Artaxo, P., Costa, A.A., Frank, G.P., Longo, K.M., Silva-Dias, M.A.F., 2004. Smoking Rain Clouds over the Amazon. *Science* 303, 1337–1342. <https://doi.org/10.1126/science.1092779>
- Ansari, T.U., Valsan, A.E., Ojha, N., Ravikrishna, R., Narasimhan, B., Gunthe, S.S., 2015. Model simulations of fungal spore distribution over the Indian region. *Atmos. Environ.* 122, 552–560. <https://doi.org/10.1016/j.atmosenv.2015.10.020>
- Apangu, G.P., Frisk, C.A., Adams-Groom, B., Satchwell, J., Pashley, C.H., Skjøth, C.A., 2020. Air mass trajectories and land cover map reveal cereals and oilseed rape as major local sources of *Alternaria* spores in the Midlands, UK. *Atmospheric Pollut. Res.* 11, 1668–1679. <https://doi.org/10.1016/j.apr.2020.06.026>
- Astray, G., Rodríguez-Rajo, F.J., Ferreira-Lage, J.A., Fernández-González, M., Jato, V., Mejuto, J.C., 2010. The use of artificial neural networks to forecast biological atmospheric allergens or pathogens only as *Alternaria* spores. *J. Environ. Monit.* 12, 2145–2152. <https://doi.org/10.1039/c0em00248h>
- Banerjee, A., Duflo, E., Postel-Vinay, G., Watts, T.M., 2007. Long Run Health Impacts of Income Shocks: Wine and Phylloxera in 19th Century France (Working Paper No. 12895), Working Paper Series. National Bureau of Economic Research. <https://doi.org/10.3386/w12895>

- Bauer, H., Claeys, M., Vermeylen, R., Schueller, E., Weinke, G., Berger, A., Puxbaum, H., 2008. Arabitol and mannitol as tracers for the quantification of airborne fungal spores. *Atmos. Environ.* 42, 588–593. <https://doi.org/10.1016/j.atmosenv.2007.10.013>
- Bauer, H., Kasper-Giebl, A., Löflund, M., Giebl, H., Hitzenberger, R., Zibuschka, F., Puxbaum, H., 2002. The contribution of bacteria and fungal spores to the organic carbon content of cloud water, precipitation and aerosols. *Atmospheric Res.* 64, 109–119. [https://doi.org/10.1016/S0169-8095\(02\)00084-4](https://doi.org/10.1016/S0169-8095(02)00084-4)
- Bhangar, S., Huffman, J.A., Nazaroff, W.W., 2014. Size-resolved fluorescent biological aerosol particle concentrations and occupant emissions in a university classroom. *Indoor Air* 24, 604–617. <https://doi.org/10.1111/ina.12111>
- Bieber, P., Seifried, T.M., Burkart, J., Gratzl, J., Kasper-Giebl, A., Schmale, D.G., Grothe, H., 2020. A drone-based bioaerosol sampling system to monitor ice nucleation particles in the lower atmosphere. *Remote Sens.* 12. <https://doi.org/10.3390/rs12030552>
- BioSampler, 20 ml, 3 Pieces | Order High-Quality BioSampler, 20 ml, 3 Pieces Products at SKC, Inc. [WWW Document], 2021. URL <https://www.skinc.com/products/biosampler-20-ml-3-pieces> (accessed 7.22.21).
- Brosseau, L.M., Vesley, D., Rice, N., Goodell, K., Nellis, M., Hairston, P., 2000. Differences in Detected Fluorescence Among Several Bacterial Species Measured with a Direct-Reading Particle Sizer and Fluorescence Detector. *Aerosol Sci. Technol.* 32, 545–558. <https://doi.org/10.1080/027868200303461>
- Bruno, A.A., Pace, L., Tomassetti, B., Coppola, E., Verdecchia, M., Pacioni, G., Visconti, G., 2007. Estimation of fungal spore concentrations associated to meteorological variables. *Aerobiologia* 23, 221–228. <https://doi.org/10.1007/s10453-007-9066-y>
- Burch, M., Levetin, E., 2002. Effects of meteorological conditions on spore plumes. *Int. J. Biometeorol.* 46, 107–117. <https://doi.org/10.1007/s00484-002-0127-1>
- Burshtein, N., Lang-Yona, N., Rudich, Y., 2011. Ergosterol, arabitol and mannitol as tracers for biogenic aerosols in the eastern Mediterranean. *Atmospheric Chem. Phys.* 11, 829–839. <https://doi.org/10.5194/acp-11-829-2011>
- Carisse, O., Savary, S., Willocquet, L., 2008. Spatiotemporal Relationships Between Disease Development and Airborne Inoculum in Unmanaged and Managed Botrytis Leaf Blight Epidemics. *Phytopathology*® 98, 38–44. <https://doi.org/10.1094/PHYTO-98-1-0038>
- Carisse, O., Tremblay, D.M., Lévesque, C.A., Gindro, K., Ward, P., Houde, A., 2009. Development of a TaqMan Real-Time PCR Assay for Quantification of Airborne

- Conidia of *Botrytis squamosa* and Management of *Botrytis* Leaf Blight of Onion. *Phytopathology*® 99, 1273–1280. <https://doi.org/10.1094/PHYTO-99-11-1273>
- Carlile, M., Watkinson, S., Gooday, G., 2001. *The Fungi* 2nd Edition Academic Press.
- Carlile, M.J., Watkinson, S.C., Gooday, G.W., 2001. *The Fungi*. Gulf Professional Publishing.
- Cheng, B., Yue, S., Hu, W., Ren, L., Deng, J., Wu, L., Fu, P., 2020. Summertime fluorescent bioaerosol particles in the coastal megacity Tianjin, North China. *Sci. Total Environ.* 723, 137966. <https://doi.org/10.1016/j.scitotenv.2020.137966>
- Choi, K., Koh, Y.J., Jeong, Y.-S., Chong, E., 2018. Experimental Studies on the Classification of Airborne Particles Based on Their Optical Properties. *Bull. Korean Chem. Soc.* 39, 369–374. <https://doi.org/10.1002/bkcs.11396>
- Christner, B.C., Morris, C.E., Foreman, C.M., Cai, R., Sands, D.C., 2008. Ubiquity of biological ice nucleators in snowfall. *Science* 319, 1214. <https://doi.org/10.1126/science.1149757>
- Conen, F., Yakutin, M., Yttri, K., Hüglin, C., 2017. Ice Nucleating Particle Concentrations Increase When Leaves Fall in Autumn. *Atmosphere* 8, 202. <https://doi.org/10.3390/atmos8100202>
- Crandall, S.G., Gilbert, G.S., 2017. Meteorological factors associated with abundance of airborne fungal spores over natural vegetation. *Atmos. Environ.* 162, 87–99. <https://doi.org/10.1016/j.atmosenv.2017.05.018>
- Crandall, S.G., Saarman, N., Gilbert, G.S., 2020. Fungal spore diversity, community structure, and traits across a vegetation mosaic. *Fungal Ecol.* 45, 100920. <https://doi.org/10.1016/j.funeco.2020.100920>
- Crawford, I., Robinson, N.H., Flynn, M.J., Foot, V.E., Gallagher, M.W., Huffman, J.A., Stanley, W.R., Kaye, P.H., 2014. Characterisation of bioaerosol emissions from a Colorado pine forest: results from the BEACHON-RoMBAS experiment. *Atmospheric Chem. Phys.* 14, 8559–8578. <https://doi.org/10.5194/acp-14-8559-2014>
- Daly, S.M., O'Connor, D.J., Healy, D.A., Hellebust, S., Arndt, J., McGillicuddy, E.J., Feeney, P., Quirke, M., Wenger, J.C., Sodeau, J.R., 2019. Investigation of coastal sea-fog formation using the WIBS (wideband integrated bioaerosol sensor) technique. *Atmospheric Chem. Phys.* 19, 5737–5751. <https://doi.org/10.5194/acp-19-5737-2019>
- D'Amato, G., Chatzigeorgiou, G., Corsico, R., Gioulekas, D., Jäger, L., Jäger, S., Kontou-Fili, K., Kouridakis, S., Liccardi, G., Meriggi, A., Palma-Carlos, A., Palma-Carlos, M.L., Aleman, A.P., Parmiani, S., Puccinelli, P., Russo, M., Spieksma, F.Th.M., Torricelli, R., Wuthrich, B., 1997. Evaluation of the prevalence of skin prick test positivity to *Alternaria* and *Cladosporium* in patients with suspected respiratory allergy.: A European multicenter study promoted by the Subcommittee on Aerobiology and

- Environmental Aspects of Inhalant Allergens of the European Academy of Allergology and Clinical Immunology. *Allergy* 52, 711–716. <https://doi.org/10.1111/j.1398-9995.1997.tb01227.x>
- Damialis, A., Gioulekas, D., 2006. Airborne allergenic fungal spores and meteorological factors in Greece: Forecasting possibilities. *Grana* 45, 122–129. <https://doi.org/10.1080/00173130600601005>
- De Linares, C., Belmonte, J., Canela, M., de la Guardia, C.D., Alba-Sanchez, F., Sabariego, S., Alonso-Pérez, S., 2010. Dispersal patterns of *Alternaria* conidia in Spain. *Agric. For. Meteorol.* 150, 1491–1500. <https://doi.org/10.1016/j.agrformet.2010.07.004>
- De'ath, G., 2002. Multivariate regression trees: A new technique for modeling species-environment relationships. *Ecology* 83, 1105–1117. [https://doi.org/10.1890/0012-9658\(2002\)083\[1105:MRTANT\]2.0.CO;2](https://doi.org/10.1890/0012-9658(2002)083[1105:MRTANT]2.0.CO;2)
- DeMott, P.J., Prenni, A.J., Liu, X., Kreidenweis, S.M., Petters, M.D., Twohy, C.H., Richardson, M.S., Eidhammer, T., Rogers, D.C., 2010. Predicting global atmospheric ice nuclei distributions and their impacts on climate. *Proc. Natl. Acad. Sci.* 107, 11217–11222. <https://doi.org/10.1073/pnas.0910818107>
- Després, V., Huffman, J.A., Burrows, S.M., Hoose, C., Safatov, A., Buryak, G., Fröhlich-Nowoisky, J., Elbert, W., Andreae, M., Pöschl, U., Jaenicke, R., 2012. Primary biological aerosol particles in the atmosphere: a review. *Tellus B Chem. Phys. Meteorol.* 64, 15598. <https://doi.org/10.3402/tellusb.v64i0.15598>
- Di Filippo, P., Pomata, D., Riccardi, C., Buiarelli, F., Perrino, C., 2013. Fungal contribution to size-segregated aerosol measured through biomarkers. *Atmos. Environ.* 64, 132–140. <https://doi.org/10.1016/j.atmosenv.2012.10.010>
- Di Pinto, A., Ciccarese, G., Tantillo, G., Catalano, D., Forte, V.T., 2005. A Collagenase-Targeted Multiplex PCR Assay for Identification of *Vibrio alginolyticus*, *Vibrio cholerae*, and *Vibrio parahaemolyticus*. *J. Food Prot.* 68, 150–153. <https://doi.org/10.4315/0362-028X-68.1.150>
- Dijksterhuis, J., 2019. Fungal spores: Highly variable and stress-resistant vehicles for distribution and spoilage. *Food Microbiol.* 81, 2–11. <https://doi.org/10.1016/j.fm.2018.11.006>
- Dilcher, D.L., Sheffy, M.V., 1971. Morphology and Taxonomy of Fungal Spores. *Palaeontogr. Abt. B* 133, 34–51.
- Dodge, A.G., Wackett, L.P., 2005. Metabolism of Bismuth Subsalicylate and Intracellular Accumulation of Bismuth by *Fusarium* sp. Strain BI. *Appl. Environ. Microbiol.* 71, 876–882. <https://doi.org/10.1128/AEM.71.2.876-882.2005>

- Escuredo, O., Seijo, M.C., Fernández-González, M., Iglesias, I., 2011. Effects of meteorological factors on the levels of *Alternaria* spores on a potato crop. *Int. J. Biometeorol.* 55, 243–252. <https://doi.org/10.1007/s00484-010-0330-4>
- Feliziani, V., Marfisi, R.M., 1992. Pollen Aerobiological Monitoring with the personal volumetric air sampler (PVAS). Correlation with a fixed Hirst type sampling station. *Aerobiologia* 8, 471–477. <https://doi.org/10.1007/BF02272918>
- Fennelly, M.J., Sewell, G., Prentice, M.B., O'Connor, D.J., Sodeau, J.R., 2018. Review: The Use of Real-Time Fluorescence Instrumentation to Monitor Ambient Primary Biological Aerosol Particles (PBAP). *Atmosphere* 9, 1. <https://doi.org/10.3390/atmos9010001>
- Fernández-González, M., Ramos-Valcárcel, D., Aira, M.J., Rodríguez-Rajo, F.J., 2016. Prediction of biological sensors appearance with ARIMA models as a tool for integrated pest management protocols. *Ann. Agric. Environ. Med.* 23, 129–137. <https://doi.org/10.5604/12321966.1196868>
- Fernández-González, M., Rodríguez-Rajo, F.J., Escuredo, O., Aira, M.J., 2013. Optimization of integrated pest management for powdery mildew (*Uninula necator*) control in a vineyard based on a combination of phenological, meteorological and aerobiological data. *J. Agric. Sci.* 151, 648–658. <https://doi.org/10.1017/S0021859612000743>
- Fernández-gonzález, M., Rodríguez-rajo, F.J., Jato, V., Aira, M.J., Ribeiro, H., Oliveira, M., Abreu, I., 2012. Forecasting ARIMA models for atmospheric vineyard pathogens in Galicia and Northern Portugal : *Botrytis cinerea* spores 19, 255–262.
- Filali Ben Sidel, F., Bouziane, H., del Mar Trigo, M., El Haskouri, F., Bardei, F., Redouane, A., Kadiri, M., Riadi, H., Kazzaz, M., 2015. Airborne fungal spores of *Alternaria*, meteorological parameters and predicting variables. *Int. J. Biometeorol.* 59, 339–346. <https://doi.org/10.1007/s00484-014-0845-1>
- Flückiger, B., Koller, T., Monn, C., n.d. Comparison of airborne spore concentrations and fungal allergen content 4.
- García-Mozo, H., Yaezel, L., Oteros, J., Galán, C., 2014. Statistical approach to the analysis of olive long-term pollen season trends in southern Spain. *Sci. Total Environ.* 473–474, 103–109. <https://doi.org/10.1016/j.scitotenv.2013.11.142>
- González-Fernández, E., Piña-Rey, A., Fernández-González, M., Rodríguez-Rajo, F.J., 2019. Effect of environmental conditions and phenology in the dispersal of secondary *Erysiphe necator* conidia in a vineyard. *Vitis - J. Grapevine Res.* 58, 49–58. <https://doi.org/10.5073/vitis.2019.58.special-issue.49-58>
- Gosselin, M.I., Rathnayake, C.M., Crawford, I., Pöhlker, C., Fröhlich-Nowoisky, J., Schmer, B., Després, V.R., Engling, G., Gallagher, M., Stone, E., Pöschl, U., Huffman, J.A., 2016.

- Fluorescent bioaerosol particle, molecular tracer, and fungal spore concentrations during dry and rainy periods in a semi-arid forest. *Atmospheric Chem. Phys.* 16, 15165–15184. <https://doi.org/10.5194/acp-16-15165-2016>
- Gostic, K., Gomez, A.C., Mummah, R.O., Kucharski, A.J., Lloyd-Smith, J.O., 2020. Estimated effectiveness of symptom and risk screening to prevent the spread of COVID-19. *eLife* 9, e55570. <https://doi.org/10.7554/eLife.55570>
- Grinn-Gofroń, A., Bogawski, P., Bosiacka, B., Nowosad, J., Camacho, I., Sadyś, M., Skjøth, C.A., Pashley, C.H., Rodinkova, V., Çeter, T., Traidl-Hoffmann, C., Damialis, A., 2021. Abundance of *Ganoderma* sp. in Europe and SW Asia: modelling the pathogen infection levels in local trees using the proxy of airborne fungal spore concentrations. *Sci. Total Environ.* 793. <https://doi.org/10.1016/j.scitotenv.2021.148509>
- Grinn-Gofroń, A., Bosiacka, B., 2015. Effects of meteorological factors on the composition of selected fungal spores in the air. *Aerobiologia* 31, 63–72. <https://doi.org/10.1007/s10453-014-9347-1>
- Grinn-Gofroń, A., Bosiacka, B., Bednarz, A., Wolski, T., 2018. A comparative study of hourly and daily relationships between selected meteorological parameters and airborne fungal spore composition. *Aerobiologia* 34, 45–54. <https://doi.org/10.1007/s10453-017-9493-3>
- Grinn-Gofroń, A., Mika, A., 2008. Selected airborne allergenic fungal spores and meteorological factors in Szczecin, Poland, 2004–2006. *Aerobiologia* 24, 89–97. <https://doi.org/10.1007/s10453-008-9088-0>
- Grinn-Gofroń, A., Nowosad, J., Bosiacka, B., Camacho, I., Pashley, C., Belmonte, J., De Linares, C., Ianovici, N., Manzano, J.M.M., Sadyś, M., Skjøth, C., Rodinkova, V., Tormo-Molina, R., Vokou, D., Fernández-Rodríguez, S., Damialis, A., 2019. Airborne *Alternaria* and *Cladosporium* fungal spores in Europe: Forecasting possibilities and relationships with meteorological parameters. *Sci. Total Environ.* 653, 938–946. <https://doi.org/10.1016/j.scitotenv.2018.10.419>
- Grinn-Gofroń, A., Strzelczak, A., 2013. Changes in concentration of *Alternaria* and *Cladosporium* spores during summer storms. *Int. J. Biometeorol.* 57, 759–768. <https://doi.org/10.1007/s00484-012-0604-0>
- Grinn-Gofroń, A., Strzelczak, A., 2009. Hourly predictive artificial neural network and multivariate regression tree models of *Alternaria* and *Cladosporium* spore concentrations in Szczecin (Poland). *Int. J. Biometeorol.* 53, 555–562. <https://doi.org/10.1007/s00484-009-0243-2>

- Grinn-Gofroń, A., Strzelczak, A., 2008. Artificial neural network models of relationships between *Alternaria* spores and meteorological factors in Szczecin (Poland). *Int. J. Biometeorol.* 52, 859–868. <https://doi.org/10.1007/s00484-008-0182-3>
- Grinn-Gofroń, A., Strzelczak, A., 2008. Artificial neural network models of relationships between *Cladosporium* spores and meteorological factors in Szczecin (Poland). *Grana* 47, 305–315. <https://doi.org/10.1080/00173130802513784>
- Grinn-Gofroń, A., Strzelczak, A., Wolski, T., 2011. The relationships between air pollutants, meteorological parameters and concentration of airborne fungal spores. *Environ. Pollut.* 159, 602–608. <https://doi.org/10.1016/j.envpol.2010.10.002>
- Grundström, M., Adams-Groom, B., Pashley, C.H., Dahl, Å., Rasmussen, K., de Weger, L.A., Thibaudon, M., Fernández-Rodríguez, S., Silva-Palacios, I., Skjøth, C.A., 2019. Oak pollen seasonality and severity across Europe and modelling the season start using a generalized phenological model. *Sci. Total Environ.* 663, 527–536. <https://doi.org/10.1016/j.scitotenv.2019.01.212>
- Gutarowska, B., Piotrowska, M., 2007. Methods of mycological analysis in buildings. *Build. Environ.* 42, 1843–1850. <https://doi.org/10.1016/j.buildenv.2006.02.015>
- Haga, D.I., Burrows, S.M., Iannone, R., Wheeler, M.J., Mason, R.H., Chen, J., Polishchuk, E.A., Pöschl, U., Bertram, A.K., 2014. Ice nucleation by fungal spores from the classes *Agaricomycetes*, *Ustilaginomycetes*, and *Eurotiomycetes*, and the effect on the atmospheric transport of these spores. *Atmospheric Chem. Phys.* 14, 8611–8630. <https://doi.org/10.5194/acp-14-8611-2014>
- Hairston, P.P., Ho, J., Quant, F.R., 1997. Design of an instrument for real-time detection of bioaerosols using simultaneous measurement of particle aerodynamic size and intrinsic fluorescence. *J. Aerosol Sci.* 28, 471–482. [https://doi.org/10.1016/s0021-8502\(96\)00448-x](https://doi.org/10.1016/s0021-8502(96)00448-x)
- Healy, D.A., O'Connor, D.J., Burke, A.M., Sodeau, J.R., 2012a. A laboratory assessment of the Waveband Integrated Bioaerosol Sensor (WIBS-4) using individual samples of pollen and fungal spore material. *Atmos. Environ.* 60, 534–543. <https://doi.org/10.1016/j.atmosenv.2012.06.052>
- Healy, D.A., O'Connor, D.J., Sodeau, J.R., 2012b. Measurement of the particle counting efficiency of the “Waveband Integrated Bioaerosol Sensor” model number 4 (WIBS-4). *J. Aerosol Sci.* 47, 94–99. <https://doi.org/10.1016/j.jaerosci.2012.01.003>
- Hollins, P.D., Kettlewell, P.S., Atkinson, M.D., Stephenson, D.B., Corden, J.M., Millington, W.M., Mullins, J., 2004. Relationships between airborne fungal spore concentration

- of *Cladosporium* and the summer climate at two sites in Britain. *Int. J. Biometeorol.* 48, 137–141. <https://doi.org/10.1007/s00484-003-0188-9>
- Hoose, C., Kristjánsson, J.E., Burrows, S.M., 2010. How important is biological ice nucleation in clouds on a global scale? *Environ. Res. Lett.* 5, 024009. <https://doi.org/10.1088/1748-9326/5/2/024009>
- Huffman, J.A., Perring, A.E., Savage, N.J., Clot, B., Crouzy, B., Tummon, F., Shoshanim, O., Damit, B., Schneider, J., Sivaprakasam, V., Zawadowicz, M.A., Crawford, I., Gallagher, M., Topping, D., Doughty, D.C., Hill, S.C., Pan, Y., 2020. Real-time sensing of bioaerosols: Review and current perspectives. *Aerosol Sci. Technol.* 54, 465–495. <https://doi.org/10.1080/02786826.2019.1664724>
- Huffman, J.A., Prenni, A.J., DeMott, P.J., Pöhlker, C., Mason, R.H., Robinson, N.H., Fröhlich-Nowoisky, J., Tobo, Y., Després, V.R., Garcia, E., Gochis, D.J., Harris, E., Müller-Germann, I., Ruzene, C., Schmer, B., Sinha, B., Day, D.A., Andreae, M.O., Jimenez, J.L., Gallagher, M., Kreidenweis, S.M., Bertram, A.K., Pöschl, U., 2013. High concentrations of biological aerosol particles and ice nuclei during and after rain. *Atmospheric Chem. Phys.* 13, 6151–6164. <https://doi.org/10.5194/acp-13-6151-2013>
- Huffman, J.A., Sinha, B., Garland, R.M., Snee-Pollmann, A., Gunthe, S.S., Artaxo, P., Martin, S.T., Andreae, M.O., Pöschl, U., 2012. Size distributions and temporal variations of biological aerosol particles in the Amazon rainforest characterized by microscopy and real-time UV-APS fluorescence techniques during AMAZE-08. *Atmospheric Chem. Phys.* 12, 11997–12019. <https://doi.org/10.5194/acp-12-11997-2012>
- Huffman, J.A., Treutlein, B., Pöschl, U., 2010. Fluorescent biological aerosol particle concentrations and size distributions measured with an Ultraviolet Aerodynamic Particle Sizer (UV-APS) in Central Europe. *Atmospheric Chem. Phys.* 10, 3215–3233. <https://doi.org/10.5194/acp-10-3215-2010>
- Hummel, M., Hoose, C., Gallagher, M., Healy, D.A., Huffman, J.A., O'Connor, D., Pöschl, U., Pöhlker, C., Robinson, N.H., Schnaiter, M., Sodeau, J.R., Stengel, M., Toprak, E., Vogel, H., 2015. Regional-scale simulations of fungal spore aerosols using an emission parameterization adapted to local measurements of fluorescent biological aerosol particles. *Atmospheric Chem. Phys.* 15, 6127–6146. <https://doi.org/10.5194/acp-15-6127-2015>
- Hummel, M., Hoose, C., Pummer, B., Schaupp, C., Fröhlich-Nowoisky, J., Möhler, O., 2018. Simulating the influence of primary biological aerosol particles on clouds by heterogeneous ice nucleation. *Atmospheric Chem. Phys.* 18, 15437–15450. <https://doi.org/10.5194/acp-18-15437-2018>

- Ianovici, N., 2016. Atmospheric concentrations of selected allergenic fungal spores in relation to some meteorological factors, in Timișoara (Romania). *Aerobiologia* 32, 139–156. <https://doi.org/10.1007/s10453-016-9427-5>
- Ingold, C.T., 1999. Active liberation of reproductive units in terrestrial fungi. *Mycologist* 13, 113–116. [https://doi.org/10.1016/S0269-915X\(99\)80040-8](https://doi.org/10.1016/S0269-915X(99)80040-8)
- Ingold, C.T., 1971. *Fungal spores: their liberation and dispersal*. Clarendon Press, Oxford.
- Jedryczka, M., Strzelczak, A., Grinn-Gofron, A., Nowak, M., Wolski, T., Siwulski, M., Sobieralski, K., Kaczmarek, J., 2015. Advanced statistical models commonly applied in aerobiology cannot accurately predict the exposure of people to *Ganoderma* spore-related allergies. *Agric. For. Meteorol.* 201, 209–217. <https://doi.org/10.1016/j.agrformet.2014.11.015>
- Jones, A.M., Harrison, R.M., 2004. The effects of meteorological factors on atmospheric bioaerosol concentrations - A review. *Sci. Total Environ.* 326, 151–180. <https://doi.org/10.1016/j.scitotenv.2003.11.021>
- Kaliszewski, M., Trafny, E.A., Lewandowski, R., Włodarski, M., Bombalska, A., Kopczyński, K., Antos-Bielska, M., Szpakowska, M., Młyńczak, J., Mularczyk-Oliwa, M., Kwaśny, M., 2013. A new approach to UVAPS data analysis towards detection of biological aerosol. *J. Aerosol Sci.* 58, 148–157. <https://doi.org/10.1016/j.jaerosci.2013.01.007>
- Kallawicha, K., Tsai, Y.J., Chuang, Y.C., Lung, S.C.C., Wu, C. Da, Chen, T.H., Chen, P.C., Chompuchan, C., Chao, H.J., 2015. The spatiotemporal distributions and determinants of ambient fungal spores in the Greater Taipei area. *Environ. Pollut.* 204, 173–180. <https://doi.org/10.1016/j.envpol.2015.04.020>
- Kanaani, H., Hargreaves, M., Ristovski, Z., Morawska, L., 2007. Performance assessment of UVAPS: Influence of fungal spore age and air exposure. *J. Aerosol Sci.* 38, 83–96. <https://doi.org/10.1016/j.jaerosci.2006.10.003>
- Kapadi, M.R., Patel, S.I., 2019. Aeromycological approach of some fungal diseases on Tomato Crop (*Lycopersicon esculentum* Mill.) at Nashik, India 422007. *J. Drug Deliv. Ther.* 9, 329–331. <https://doi.org/10.22270/jddt.v9i3.2666>
- Kasprzyk, Idalia, 2008. Aeromycology–main research fields of interest during the last 25 years. *Ann Agric Env. Med* 15, 1–7.
- Kasprzyk, I., 2008. Aeromycology - Main research fields of interest during the last 25 years. *Ann. Agric. Environ. Med. AAEM* 15, 1–7.
- Kasprzyk, I., Grinn-Gofroń, A., Strzelczak, A., Wolski, T., 2011. Hourly predictive artificial neural network and multivariate regression trees models of *Ganoderma* spore

- concentrations in Rzeszów and Szczecin (Poland). *Sci. Total Environ.* 409, 949–956.
<https://doi.org/10.1016/j.scitotenv.2010.12.002>
- Kennedy, R., Wakeham, A.J., Byrne, K.G., Meyer, U.M., Dewey, F.M., 2000. A New Method To Monitor Airborne Inoculum of the Fungal Plant Pathogens *Mycosphaerella brassicicola* and *Botrytis cinerea*. *Appl. Environ. Microbiol.* 66, 2996–3003.
<https://doi.org/10.1128/AEM.66.7.2996-3003.2000>
- Kesavan, J., Kilper, G., Williamson, M., Alstadt, V., Dimmock, A., Bascom, R., 2019. Laboratory validation and initial field testing of an unobtrusive bioaerosol detector for health care settings. *Aerosol Air Qual. Res.* 19, 331–344.
<https://doi.org/10.4209/aaqr.2017.10.0371>
- Köhler, J.R., Hube, B., Puccia, R., Casadevall, A., Perfect, J.R., 2017. Fungi that Infect Humans. *Microbiol. Spectr.* 5. <https://doi.org/10.1128/microbiolspec.FUNK-0014-2016>
- Kumar, A., Agrawal, R., Chattopadhyay, C., 2013. Weather based forecast models for diseases in mustard crop. *MAUSAM* 64, 663–670.
- Lacey, M.E., West, J.S., 2006. *The Air Spora: A manual for catching and identifying airborne biological particles.* Springer US. <https://doi.org/10.1007/978-0-387-30253-9>
- Li, C.H., Cervantes, M., Springer, D.J., Boekhout, T., Ruiz-Vazquez, R.M., Torres-Martinez, S.R., Heitman, J., Lee, S.C., 2011. Sporangiospore Size Dimorphism Is Linked to Virulence of *Mucor circinelloides*. *PLoS Pathog.* 7, e1002086.
<https://doi.org/10.1371/journal.ppat.1002086>
- Li, D.W., Kendrick, B., 1995. A year-round study on functional relationships of airborne fungi with meteorological factors. *Int. J. Biometeorol.* 39, 74–80.
<https://doi.org/10.1007/BF01212584>
- Lindsley, W.G., Schmechel, D., Chen, B.T., 2006. A two-stage cyclone using microcentrifuge tubes for personal bioaerosol sampling. *J. Environ. Monit.* 8, 1136–1142.
<https://doi.org/10.1039/B609083D>
- Lyon, F.L., Kramer, C.L., Eversmeyer, M.G., 1984. Variation of airspora in the atmosphere due to weather conditions. *Grana* 23, 177–181. <https://doi.org/10.1080/00173138409427713>
- Maki, L.R., Galyan, E.L., Chang-Chien, M.M., Caldwell, D.R., 1974. Ice nucleation induced by *Pseudomonas syringae*. *Appl. Microbiol.* 28, 456–459.
<https://doi.org/10.1128/aem.28.3.456-459.1974>
- Martínez-Bracero, M., Alcázar, P., Velasco-Jiménez, M.J., Galán, C., 2019a. Fungal spores affecting vineyards in Montilla-Moriles Southern Spain. *Eur. J. Plant Pathol.* 153, 1–13.
<https://doi.org/10.1007/s10658-018-1532-6>

- Martínez-Bracero, M., Alcázar, P., Velasco-Jiménez, M.J., Galán, C., 2019b. Fungal spores affecting vineyards in Montilla-Moriles Southern Spain. *Eur. J. Plant Pathol.* 153, 1–13. <https://doi.org/10.1007/s10658-018-1532-6>
- Maya-Manzano, J.M., Smith, M., Markey, E., Hourihane Clancy, J., Sodeau, J., O'Connor, D.J., 2021. Recent developments in monitoring and modelling airborne pollen, a review. *Grana* 60, 1–19. <https://doi.org/10.1080/00173134.2020.1769176>
- McLaughlin, D.J., Spatafora, J.W. (Eds.), 2014. *The Mycota: A comprehensive treatise on fungi as experimental systems for basic and applied research.* Springer Berlin Heidelberg, Berlin, Heidelberg. <https://doi.org/10.1007/978-3-642-55318-9>
- Mediavilla Molina, A., Angulo Romero, J., Infante García-Pantaleón, F., Comtois, P., Domínguez Vilches, E., 1998. Preliminary statistical modeling of the presence of two conidial types of *Cladosporium* in the atmosphere of Córdoba, Spain. *Aerobiologia* 14, 229–234. <https://doi.org/10.1007/bf02694211>
- Mensah-Attipoe, J., Täubel, M., 2017. Analysis Approaches for Fungi in Indoor Environmental Assessments, in: Viegas, C., Viegas, S., Gomes, A., Täubel, M., Sabino, R. (Eds.), *Exposure to Microbiological Agents in Indoor and Occupational Environments.* Springer International Publishing, Cham, pp. 109–127. https://doi.org/10.1007/978-3-319-61688-9_6
- Mohler, O., DeMott, P.J., Vali, G., Levin, Z., 2007. Microbiology and atmospheric processes: the role of biological particles in cloud physics 13.
- Money, N.P., 2016. Chapter 3 - Spore Production, Discharge, and Dispersal, in: Watkinson, S.C., Boddy, L., Money, N.P. (Eds.), *The Fungi (Third Edition).* Academic Press, Boston, pp. 67–97. <https://doi.org/10.1016/B978-0-12-382034-1.00003-7>
- Morris, C.E., Sands, D.C., Glaux, C., Samsatly, J., Asaad, S., Moukahel, A.R., Gonçalves, F.L.T., Bigg, E.K., 2013. Urediospores of rust fungi are ice nucleation active at > -10 °C and harbor ice nucleation active bacteria. *Atmospheric Chem. Phys.* 13, 4223–4233. <https://doi.org/10.5194/acp-13-4223-2013>
- Murray, B.J., O'sullivan, D., Atkinson, J.D., Webb, M.E., 2012. Ice nucleation by particles immersed in supercooled cloud droplets. *Chem. Soc. Rev.* 41, 6519–6554. <https://doi.org/10.1039/c2cs35200a>
- Musgrave, D.R., Fletcher, L.R., 1986. Optimisation and characterisation of enzyme-linked immunosorbent assay (ELISA) for the detection of the *Acremonium loliae* endophyte in *Lolium perenne*. *N. Z. J. Agric. Res.* 29, 117–120. <https://doi.org/10.1080/00288233.1986.10417983>

- Musgrave, D.R., Fletcher, L.R., 1984. The development and application of ELISA detection of *Lolium* endophyte in ryegrass staggers research.
- O'Connor, D.J., Healy, D.A., Sodeau, J.R., 2013. The on-line detection of biological particle emissions from selected agricultural materials using the WIBS-4 (Waveband Integrated Bioaerosol Sensor) technique. *Atmos. Environ.* 80, 415–425. <https://doi.org/10.1016/j.atmosenv.2013.07.051>
- O'Connor, D.J., Lovera, P., Iacopino, D., O'Riordan, A., A. Healy, D., R. Sodeau, J., 2014a. Using spectral analysis and fluorescence lifetimes to discriminate between grass and tree pollen for aerobiological applications. *Anal. Methods* 6, 1633–1639. <https://doi.org/10.1039/C3AY41093E>
- O'Connor, D.J., Sadyś, M., Skjøth, C.A., Healy, D.A., Kennedy, R., Sodeau, J.R., 2014b. Atmospheric concentrations of *Alternaria*, *Cladosporium*, *Ganoderma* and *Didymella* spores monitored in Cork (Ireland) and Worcester (England) during the summer of 2010. *Aerobiologia* 30, 397–411. <https://doi.org/10.1007/s10453-014-9337-3>
- Pazienza, M., 2013. Use of Particle Counter System for the Optimization of Sampling, Identification and Decontamination Procedures for Biological Aerosols Dispersion in Confined Environment. *J. Microb. Biochem. Technol.* 06. <https://doi.org/10.4172/1948-5948.1000120>
- Pereira, M.L., Knibbs, L.D., He, C., Grzybowski, P., Johnson, G.R., Huffman, J.A., Bell, S.C., Wainwright, C.E., Matte, D.L., Dominski, F.H., Andrade, A., Morawska, L., 2017. Sources and dynamics of fluorescent particles in hospitals. *Indoor Air* 27, 988–1000. <https://doi.org/10.1111/ina.12380>
- Perring, A.E., Schwarz, J.P., Baumgardner, D., Hernandez, M.T., Spracklen, D.V., Heald, C.L., Gao, R.S., Kok, G., McMeeking, G.R., McQuaid, J.B., Fahey, D.W., 2015. Airborne observations of regional variation in fluorescent aerosol across the United States. *J. Geophys. Res. Atmospheres* 120, 1153–1170. <https://doi.org/10.1002/2014JD022495>
- Personal volumetric air sampler – Burkard Manufacturing Co Ltd, 2021. URL <http://burkard.co.uk/product/personal-volumetric-air-sampler/> (accessed 8.5.21).
- Phillips, V.T.J., Andronache, C., Christner, B., Morris, C.E., Sands, D.C., Bansemmer, A., Lauer, A., McNaughton, C., Seman, C., 2009. Potential impacts from biological aerosols on ensembles of continental clouds simulated numerically. *Biogeosciences* 6, 987–1014. <https://doi.org/10.5194/bg-6-987-2009>
- Pöschl, U., Martin, S.T., Sinha, B., Chen, Q., Gunthe, S.S., Huffman, J.A., Borrmann, S., Farmer, D.K., Garland, R.M., Helas, G., Jimenez, J.L., King, S.M., Manzi, A., Mikhailov, E., Pauliquevis, T., Petters, M.D., Prenni, A.J., Roldin, P., Rose, D., Schneider, J., Su,

- H., Zorn, S.R., Artaxo, P., Andreae, M.O., 2010. Rainforest aerosols as biogenic nuclei of clouds and precipitation in the Amazon. *Science* 329, 1513–1516. <https://doi.org/10.1126/science.1191056>
- Pouleur, S., Richard, C., Martin, J.-G., Antoun, H., 1992. Ice Nucleation Activity in *Fusarium acuminatum* and *Fusarium avenaceum*†. *Appl. Environ. Microbiol.* 58, 2960–2964. <https://doi.org/10.1128/aem.58.9.2960-2964.1992>
- Pratt, K.A., DeMott, P.J., French, J.R., Wang, Z., Westphal, D.L., Heymsfield, A.J., Twohy, C.H., Prenni, A.J., Prather, K.A., 2009. In situ detection of biological particles in cloud ice-crystals. *Nat. Geosci.* 2, 398–401. <https://doi.org/10.1038/ngeo521>
- Prenni, A.J., Petters, M.D., Kreidenweis, S.M., Heald, C.L., Martin, S.T., Artaxo, P., Garland, R.M., Wollny, A.G., Pöschl, U., 2009. Relative roles of biogenic emissions and saharan dust as ice nuclei in the amazon basin. *Nat. Geosci.* 2, 402–405. <https://doi.org/10.1038/ngeo517>
- Pringle, A., Patek, S.N., Fischer, M., Stolze, J., Money, N.P., 2005. The captured launch of a ballistospore. *Mycologia* 97, 866–871. <https://doi.org/10.1080/15572536.2006.11832777>
- Qi, Y., Li, Y., Xie, W., Lu, R., Mu, F., Bai, W., Du, S., 2020. Temporal-spatial variations of fungal composition in PM_{2.5} and source tracking of airborne fungi in mountainous and urban regions. *Sci. Total Environ.* 708, 135027. <https://doi.org/10.1016/j.scitotenv.2019.135027>
- Quintero, E., Bolaños, B., Cantrell, S., 2013. Molecular Identification of Airborne Fungal Spores from Caguas and San Juan, Puerto Rico 9.
- Rajo, F.J.R., Jato, V., 2009. Incidence of fungals in a vineyard of the denomination of origin ribeiro (Ourense - North-Western Spain).
- Rapiejko, P., Stanlaewicz, W., Szczygielski, K., Jurkiewicz, D., 2007. [Threshold pollen count necessary to evoke allergic symptoms]. *Otolaryngol. Pol. Pol. Otolaryngol.* 61, 591–594. [https://doi.org/10.1016/s0030-6657\(07\)70491-2](https://doi.org/10.1016/s0030-6657(07)70491-2)
- Recio, M., del Mar Trigo, M., Docampo, S., Melgar, M., García-Sánchez, J., Bootello, L., Cabezudo, B., 2012. Analysis of the predicting variables for daily and weekly fluctuations of two airborne fungal spores: *Alternaria* and *Cladosporium*. *Int. J. Biometeorol.* 56, 983–991. <https://doi.org/10.1007/s00484-011-0509-3>
- Redondo, M.A., Berlin, A., Boberg, J., Oliva, J., 2020. Vegetation type determines spore deposition within a forest-agricultural mosaic landscape. *FEMS Microbiol. Ecol.* 96, 1–12. <https://doi.org/10.1093/femsec/fiaa082>

- Ristaino, J.B., 2002. Tracking historic migrations of the Irish potato famine pathogen, *Phytophthora infestans*. *Microbes Infect.* 4, 1369–1377. [https://doi.org/10.1016/S1286-4579\(02\)00010-2](https://doi.org/10.1016/S1286-4579(02)00010-2)
- Rodríguez, J.A.C., Fernández-González, E., Fernández-González, M., Vázquez-Ruiz, R.A., Aira, M.J., 2020. Fungal diseases in two north-west Spain vineyards: Relationship with meteorological conditions and predictive aerobiological model. *Agronomy* 10. <https://doi.org/10.3390/agronomy10020219>
- Rodríguez-Rajo, F.J., Iglesias, I., Jato, V., 2005. Variation assessment of airborne *Alternaria* and *Cladosporium* spores at different bioclimatical conditions. *Mycol. Res.* 109, 497–507. <https://doi.org/10.1017/S0953756204001777>
- Rodríguez-Rajo, F.J., Jato, V., Fernández-González, M., Aira, M.J., 2010. The use of aerobiological methods for forecasting *Botrytis* spore concentrations in a vineyard. *Grana* 49, 56–65. <https://doi.org/10.1080/00173130903472393>
- Saari, S., Niemi, J., Roñkko, T., Kuuluvainen, H., Järvinen, A., Pirjola, L., Aurela, M., Hillamo, R., Keskinen, J., 2015. Seasonal and Diurnal Variations of Fluorescent Bioaerosol Concentration and Size Distribution in the Urban Environment. *Aerosol Air Qual. Res.* 15, 572–581. <https://doi.org/10.4209/aaqr.2014.10.0258>
- Saari, S., Reponen, T., Keskinen, J., 2014. Performance of Two Fluorescence-Based Real-Time Bioaerosol Detectors: BioScout vs. UVAPS. *Aerosol Sci. Technol.* 48, 371–378. <https://doi.org/10.1080/02786826.2013.877579>
- Sady, M., Strzelczak, A., Grinn-gofro, A., Kennedy, R., 2014. Application of redundancy analysis for aerobiological data. <https://doi.org/10.1007/s00484-014-0818-4>
- Sadyś, M., Kaczmarek, J., Grinn-Gofron, A., Rodinkova, V., Prikhodko, A., Bilous, E., Strzelczak, A., Herbert, R.J., Jedryczka, M., 2018. Dew point temperature affects ascospore release of allergenic genus *Leptosphaeria*. *Int. J. Biometeorol.* 62, 979–990. <https://doi.org/10.1007/s00484-018-1500-z>
- Sadyś, M., Skjøth, C.A., Kennedy, R., 2016. Forecasting methodologies for *Ganoderma* spore concentration using combined statistical approaches and model evaluations. *Int. J. Biometeorol.* 60, 489–498. <https://doi.org/10.1007/s00484-015-1045-3>
- Sadyś, M., Skjøth, C.A., Kennedy, R., 2015. Determination of *Alternaria* spp. habitats using 7-day volumetric spore trap, Hybrid Single Particle Lagrangian Integrated Trajectory model and geographic information system. *Urban Clim.* 14, 429–440. <https://doi.org/10.1016/j.uclim.2014.08.005>

- Santarpia, J.L., Ratnesar-Shumate, S., Gilberry, J.U., Quizon, J.J., 2013. Relationship Between Biologically Fluorescent Aerosol and Local Meteorological Conditions. *Aerosol Sci. Technol.* 47, 655–661. <https://doi.org/10.1080/02786826.2013.781263>
- Sarda-Estève, R., Baisnée, D., Guinot, B., Sodeau, J., O'Connor, D., Belmonte, J., Besancenot, J.-P., Petit, J.-E., Thibaudon, M., Oliver, G., Sindt, C., Gros, V., 2019. Variability and Geographical Origin of Five Years Airborne Fungal Spore Concentrations Measured at Saclay, France from 2014 to 2018. *Remote Sens.* 11, 1671. <https://doi.org/10.3390/rs11141671>
- Ščevková, J., Hrabovsky, M., Kováč, J., Rosa, S., 2019. Intradiurnal variation of predominant airborne fungal spore biopollutants in the Central European urban environment 34603–34612.
- Schnell, R.C., Vali, G., 1972. Atmospheric Ice Nuclei from Decomposing Vegetation. *Nature* 236, 163–165. <https://doi.org/10.1038/236163a0>
- Sesartic, A., Lohmann, U., Storelvmo, T., 2013. Modelling the impact of fungal spore ice nuclei on clouds and precipitation. *Environ. Res. Lett.* 8. <https://doi.org/10.1088/1748-9326/8/1/014029>
- Shen, F., Zheng, Y., Niu, M., Zhou, F., Wu, Yan, Wang, J., Zhu, Tong, Wu, Yusheng, Wu, Z., Hu, M., Zhu, Tianle, 2019. Characteristics of biological particulate matters at urban and rural sites in the North China Plain. *Environ. Pollut. Barking Essex* 253, 569–577. <https://doi.org/10.1016/j.envpol.2019.07.033>
- Simoneit, B.R.T., Mazurek, M.A., 1989. Organic Tracers in Ambient Aerosols and Rain. *Aerosol Sci. Technol.* 10, 267–291. <https://doi.org/10.1080/02786828908959264>
- Simon-Nobbe, B., Denk, U., Pöll, V., Rid, R., Breitenbach, M., 2008. The spectrum of fungal allergy. *Int. Arch. Allergy Immunol.* 145, 58–86.
- Skjøth, C.A., Kennedy, R., 2014. Back-trajectories show export of airborne fungal spores (*Ganoderma* sp.) from forests to agricultural and urban areas in England 84, 88–99. <https://doi.org/10.1016/j.atmosenv.2013.11.015>
- Skjøth, C.A., Sommer, J., Frederiksen, L., Gosewinkel Karlson, U., 2012. Crop harvest in Denmark and Central Europe contributes to the local load of airborne *Alternaria* spore concentrations in Copenhagen. *Atmospheric Chem. Phys.* 12, 11107–11123. <https://doi.org/10.5194/acp-12-11107-2012>
- Smith, E.G., 1986. Sampling and identifying allergenic pollens and molds Vol. II, Vol. II., Blewstone Press, San Antonio, Tex.
- Smith, E.G., 1984. Sampling and identifying allergenic pollens and molds [I]. Blewstone, San Antonio, Tex.

- Spracklen, D.V., Heald, C.L., 2014. The contribution of fungal spores and bacteria to regional and global aerosol number and ice nucleation immersion freezing rates. *Atmospheric Chem. Phys.* 14, 9051–9059. <https://doi.org/10.5194/acp-14-9051-2014>
- Stępańska, D., Wołek, J., 2012. The estimation of fungal spore concentrations using two counting methods. *Acta Agrobot.* 62, 117–123. <https://doi.org/10.5586/aa.2009.033>
- Stępańska, D., Wołek, J., 2005. Variation in fungal spore concentrations of selected taxa associated to weather conditions in Cracow, Poland, in 1997. *Aerobiologia* 21, 43–52. <https://doi.org/10.1007/s10453-004-5877-2>
- Stephen, E., Raffery, A.E., Dowding, P., 1990. Forecasting spore concentrations: A time series approach. *Int. J. Biometeorol.* 34, 87–89. <https://doi.org/10.1007/BF01093452>
- Suchorab, Z., Frąć, M., Guz, Ł., Oszust, K., Łagód, G., Gryta, A., Bilińska-Wielgus, N., Czerwiński, J., 2019. A method for early detection and identification of fungal contamination of building materials using e-nose. *PLOS ONE* 14, e0215179. <https://doi.org/10.1371/journal.pone.0215179>
- Tomassetti, B., Angelosante Bruno, A., Pace, L., Verdecchia, M., Visconti, G., 2009. Prediction of *Alternaria* and Pleospora concentrations from the meteorological forecast and artificial neural network in L'Aquila, Abruzzo (Central Italy). *Aerobiologia* 25, 127–136. <https://doi.org/10.1007/s10453-009-9117-7>
- Tomassetti, B., Lombardi, A., Cerasani, E., Di Sabatino, A., Pace, L., Ammazalorso, D., Verdecchia, M., 2013. Mapping of *Alternaria* and pleospora concentrations in central Italy using meteorological forecast and neural network estimator. *Aerobiologia* 29, 55–70. <https://doi.org/10.1007/s10453-012-9262-2>
- Tormo, R., Silva, I., Gonzalo, Á., Moreno, A., Pérez, R., Fernández, S., 2011. Phenological records as a complement to aerobiological data. *Int. J. Biometeorol.* 55, 51–65. <https://doi.org/10.1007/s00484-010-0308-2>
- Vagelas, I., Gougoulis, N., Nedesca, E.-D., Liviu, 2011. Bread contamination with fungus. *Carpathian J. Food Sci. Technol.* 3, 1–6.
- Valsan, A.E., Ravikrishna, R., Biju, C.V., Pöhlker, C., Després, V.R., Huffman, J.A., Pöschl, U., Gunthe, S.S., 2016. Fluorescent biological aerosol particle measurements at a tropical high-altitude site in southern India during the southwest monsoon season. *Atmospheric Chem. Phys.* 16, 9805–9830. <https://doi.org/10.5194/acp-16-9805-2016>
- Vélez-Pereira, A.M., De Linares, C., Belmonte, J., 2021. Aerobiological modeling I: A review of predictive models: Aerobiological predictive models, a review. *Sci. Total Environ.* 795. <https://doi.org/10.1016/j.scitotenv.2021.148783>

- Vélez-Pereira, A.M., De Linares, C., Canela, M.-A., Belmonte, J., 2019. Logistic regression models for predicting daily airborne *Alternaria* and *Cladosporium* concentration levels in Catalonia (NE Spain). *Int. J. Biometeorol.* 63, 1541–1553. <https://doi.org/10.1007/s00484-019-01767-1>
- Verma, K.S., Pathak, A.K., 2009. A Comparative Analysis of Forecasting Methods for Aerobiological Studies. *Asian J Exp Sci* 23, 193–198.
- Verma, S.K., Kawamura, K., Chen, J., Fu, P., 2018. Thirteen years of observations on primary sugars and sugar alcohols over remote Chichijima Island in the western North Pacific. *Atmospheric Chem. Phys.* 18, 81–101. <https://doi.org/10.5194/acp-18-81-2018>
- Wang, H., Reponen, T., Adhikari, A., Grinshpun, S.A., 2013. Contribution of Fungal Spores to Organic Carbon Aerosol in Indoor and Outdoor Environments in the Greater Cincinnati Area. *Aerosol Air Qual. Res.* 13, 1348–1355. <https://doi.org/10.4209/aaqr.2012.10.0291>
- Wei, K., Zou, Z., Zheng, Y., Li, J., Shen, F., Wu, C.-Y., Wu, Y., Hu, M., Yao, M., 2016. Ambient bioaerosol particle dynamics observed during haze and sunny days in Beijing. *Sci. Total Environ.* 550, 751–759. <https://doi.org/10.1016/j.scitotenv.2016.01.137>
- West, J.S., Kimber, R.B.E., 2015. Innovations in air sampling to detect plant pathogens. *Ann. Appl. Biol.* 166, 4–17. <https://doi.org/10.1111/aab.12191>
- Whitehead, J.D., Darbyshire, E., Brito, J., Barbosa, H.M.J., Crawford, I., Stern, R., Gallagher, M.W., Kaye, P.H., Allan, J.D., Coe, H., Artaxo, P., McFiggans, G., 2016. Biogenic cloud nuclei in the central Amazon during the transition from wet to dry season. *Atmospheric Chem. Phys.* 16, 9727–9743. <https://doi.org/10.5194/acp-16-9727-2016>
- Wu, T., Täubel, M., Holopainen, R., Viitanen, A.-K., Vainiotalo, S., Tuomi, T., Keskinen, J., Hyvärinen, A., Hämeri, K., Saari, S.E., Boor, B.E., 2018. Infant and Adult Inhalation Exposure to Resuspended Biological Particulate Matter. *Environ. Sci. Technol.* 52, 237–247. <https://doi.org/10.1021/acs.est.7b04183>
- Xie, Y., Fajardo, O.A., Yan, W., Zhao, B., Jiang, J., 2017. Six-day measurement of size-resolved indoor fluorescent bioaerosols of outdoor origin in an office. *Particuology* 31, 161–169. <https://doi.org/10.1016/j.partic.2016.09.004>
- Xu, S., Ren, L., Lang, Y., Hou, S., Ren, H., Wei, L., Wu, L., Deng, J., Hu, W., Pan, X., Sun, Y., Wang, Z., Su, H., Cheng, Y., Fu, P., 2020. Molecular markers of biomass burning and primary biological aerosols in urban Beijing: size distribution and seasonal variation. *Atmospheric Chem. Phys.* 20, 3623–3644. <https://doi.org/10.5194/acp-20-3623-2020>

- Zheng, Y., Yao, M., 2017. Liquid impinger BioSampler's performance for size-resolved viable bioaerosol particles. *J. Aerosol Sci.* 106, 34–42. <https://doi.org/10.1016/j.jaerosci.2017.01.003>
- Zhou, G., Whong, W.-Z., Ong, T., Chen, B., 2000. Development of a fungus-specific PCR assay for detecting low-level fungi in an indoor environment. *Mol. Cell. Probes* 14, 339–348. <https://doi.org/10.1006/mcpr.2000.0324>

Chapter 2. Materials and Methods

This section breaks down the locations where the different sampling campaigns took place, along with all of the instruments used during the project. A description of the operation and design differences between each instrument is also described, better clarifying the differences in how each device samples and categorises particles. A description of the data analysis process, along with an explanation on the ZeFir wind rose software are also provided.

2.1. Location

Historical fungal spore sampling was carried out at Trinity College Dublin from 1978-1980. In 1978, sampling took place from April 27th to September 29th, in 1979 fungal spore sampling occurred between the dates of March 7th and September 5th, and in 1980, sampling took place between the 23rd of April and the 31st of July, with some individual sampling days taking place intermittently from March 15th onwards. In 1978, fungal spore counts were taken at three-hour intervals, and in 1979 and 1980, hourly intervals were taken. Fungal spore sampling occurred on the grounds of Trinity College Dublin, at a site 1.1km northeast of the contemporary TU Dublin site.

Contemporary traditional fungal sampling was carried out across Ireland, using data collected from four sites, two rural (Carlow and Sligo), and two urban (Dublin and Cork) (Figure 2.). The surveyed region possesses a cool temperate oceanic climate. The sites were chosen to allow a maximum possible range in population density and anthropological setting, with an even spread throughout, as far as was practicable.

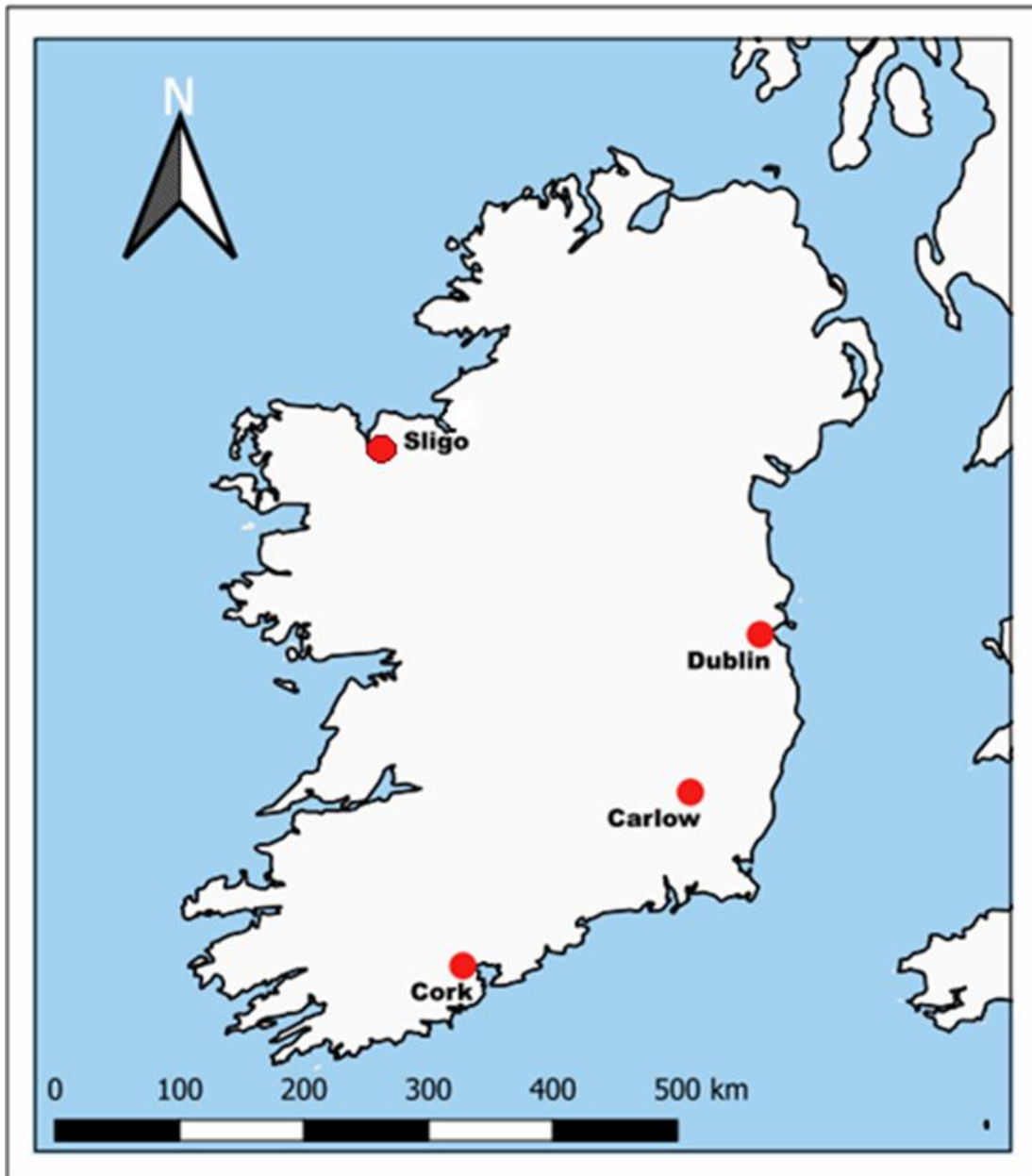


Figure 2.1: Fungal spore sampling sites, both historical and contemporary. Dublin was used for both studies, while Cork, Carlow, and Sligo were in operation for the contemporary study.

The contemporary Dublin site (2017-2021) has a mean annual temperature of 9.8°C, and a mean annual total rainfall of 758mm. (“Dublin 1981–2010 averages,” 2021) It is an urban site, with instrumentation being placed on the rooftop of the TU Dublin Kevin Street building, which is five stories tall (approx. 20m high). It is the centre of a coastal metropolitan region that encompasses around 318 km² and has a population density of 4,811/km² (“Population Distribution - CSO - Central Statistics Office,” 2021).

The WIBS-NEO was operational at the Dublin site for a total of six weeks, beginning on August 7 and ending on September 16, 2019. During this time, sampling was also performed

at the Dublin site using the Hirst, as it had been for the two years previous. The IBAC-2 was operational at the Dublin location for a total of twelve weeks, beginning on June 26, 2019, and ending on September 16, 2019.



Figure 2.2: The set up of one of the Hirst volumetric sampling devices. This device was located on the rooftop of the TU Dublin Kevin Street building (has since been demolished).

The Carlow site (2021) has a mean annual temperature of 9.9°C, and a mean annual total rainfall of 868mm (“Historical Data - Met Éireann - The Irish Meteorological Service,”). It is a rural, agricultural, inland area with a population density of 63/km² (“Population

Distribution - CSO - Central Statistics Office,” 2021). Its spore trap is located in a field that is part of a farm. Both sites have lower rainfall than the national average, which is approximately 1200mm annually (“Historical Data - Met Éireann - The Irish Meteorological Service,”) The Carlow site completed all monitoring with the Hirst-Lanzoni 7-day volumetric sampler, running continuously for the project duration.

The Cork site (2021) has a mean annual temperature of 10°C, and a mean annual total rainfall of 1,239mm (“Cork Airport 1991–2020 averages,” 2023). This is considerably higher than the rainfall levels found in the east of the country. The sampler is at the edge of a major metropolitan, coastal centre, with Cork City being the second largest city in the nation. The sampler is located on the roof of the Environmental Research Centre (University College Cork), on the banks of the river Lee. In Cork, the sampler used was a SporeWatch device, which is a modernized traditional sampler with electronic control capabilities, based upon the original Hirst design, and with setting set to ensure it is operationally and performatively identical (Burkard, 2023).

The Sligo site (2021) has a mean annual temperature of 9.3°C, and a mean annual total rainfall of 1,244mm, similar to the concentrations seen in Cork (“Historical Data - Met Éireann - The Irish Meteorological Service,” 2022). The sampler was placed in a rural, coastal site near the small village of Enniscrone, in the west of the county, near the Mayo border.

2.2. Instrumentation

2.2.1. Hirst-Lanzoni and SporeWatch

The instrumentation used in all sites will be described in this section, including their design, operation, and sample collection methods.

Three of the four sampling sites (Dublin, Carlow, and Sligo) use the Lanzoni brand of Hirst 7-day volumetric spore-trap as the means of traditional, impact-based suction flow onto an adhesive surface. They are capable of providing data at both a daily and hourly temporal resolution. In Cork, the Spore Watch was used, which contains all the same instrumentation and apparatus within, rendering it identical for the purposes of this project.

The Hirst device has long been used as a basic tool for primary biological aerosol particles, with approximately 637 samplers of this type in operation around the world (Buters et al., 2018), and with more than 73% of them utilised for fungal spores monitoring. Hirst-type volumetric spore traps consist of 3 parts; the impact unit, the wind-vane, and the vacuum

pump (Galán et al., 2007). The impact unit (Figure 4 (B)) includes an inlet of 14x2mm, through which particles pass at the inhalation rate of the human lung, a rate of 10 litres/minute, as controlled by the vacuum pump. The particles impact upon a layer of Melinex tape that is coated with an adhesive substance. The tape is wound around the drum, which has a circumference of 336mm and rotates at a rate of 2mm/h thanks to a clock mechanism, thus completing one full rotation in exactly 7 days. In order to ensure that the inlet always faces the prevailing wind, a vane (Figure 2.3 (A)) is attached to the top of the impact unit (Hirst, 1952).

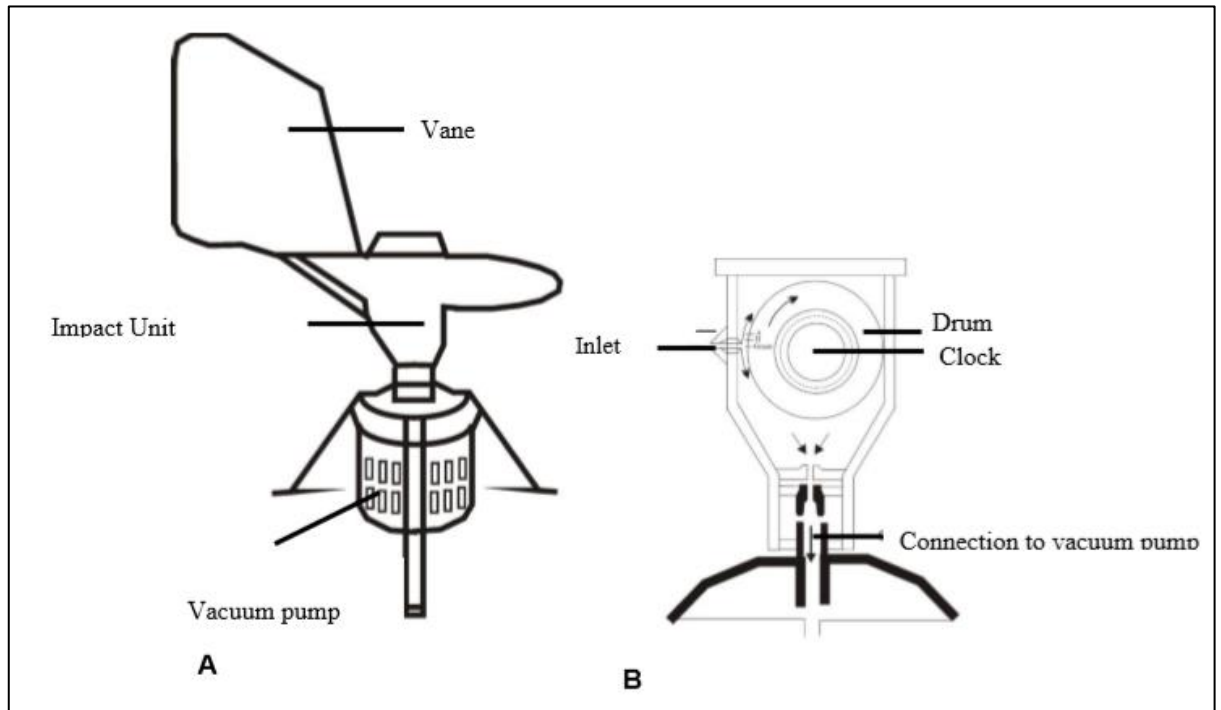


Figure 2.3: A. The Hirst-type volumetric sampler, with the wind vane and vacuum pump visible (Hirst, 1952); B. The interior of the Hirst, showing the impact unit, with the drum, inlet, and clock mechanisms all visible (Galán et al., 2007).

After 7 days, the entire drum and attached tape are removed and replaced together, being replaced with another pre-prepared drum and tape. The drum, still with the spore sample-coated tape attached, is securely stored in a hermetically sealed metal drum-carrier, to avoid potential contamination during transportation to the laboratory for sample preparation. The fresh drum and tape are also transported from the laboratory to the Hirst in a hermetically sealed metal drum-carrier, for the same purpose. As the fresh drum is placed into the Hirst device, the clock mechanism is rewound to allow 7 full days of rotation. The red line on the drum, and the arrow within the Hirst must be aligned, as seen in Figure 2.4. When the device is closed, the start and end point of the new drum is marked by scratching a line along the tape with a needle, via the 14x2mm inlet opening.

After a period of 7 days, the complete drum and attached tape are removed and replaced simultaneously. In their place, a new drum and tape that have been prepared in advance are installed. The drum, which still has the spore sample-coated tape attached to its outer surface, is safely placed in a metal drum-carrier that is hermetically sealed. This is done to prevent the drum from becoming contaminated in any way while it is being transported to the laboratory for sample preparation. For the same reason, a hermetically sealed metal drum-carrier is used to bring the fresh drum and tape from the laboratory to the Hirst. The clock mechanism is rewound when the new drum is inserted into the Hirst device, which enables the device to rotate for a full seven days. As can be seen in Figure 2.5, it is imperative that the red line on the drum and the arrow included within the Hirst be aligned. When the sampler is mounted and shut, the beginning and ending points of the new tape are identified by using a needle to scratch a line along the tape, via inserting it into the 14x2mm inlet opening.

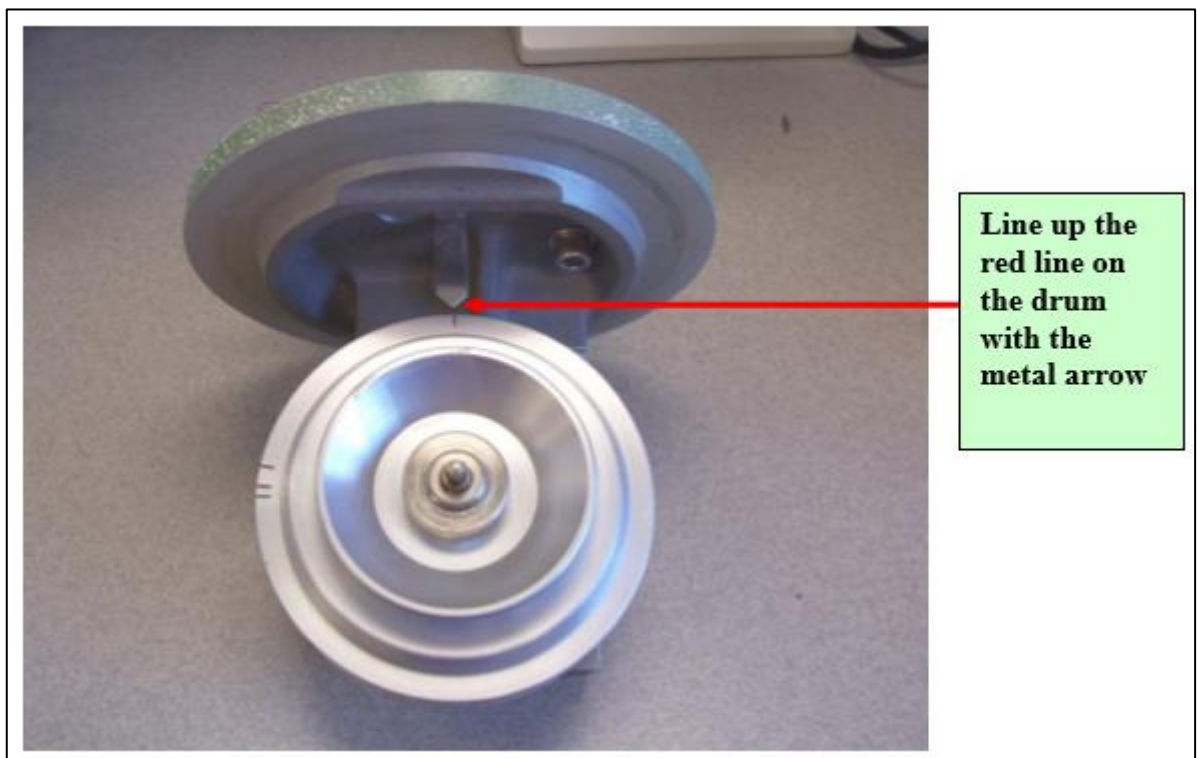


Figure 2.4: Alignment of the drum with the lid of the Hirst along the red line of the drum (Levetin)

In the lab, the drum carrier is opened, and the starting scratch is located inside. It ought to be aligned along the green line as shown in Figure 2.5. With the drum placed on a surface so that the “handle”, or smaller, textured edge rim is facing upwards, the start point is at the needle scratch/green line and represents time and day at which the drum was inserted into the Hirst. The tape continues to wrap around the drum in an anti-clockwise orientation until

336 millimetres have been reached, where there is a visible black line engraved into the drum. The tape is removed gently using a scalpel and tweezers, and then is positioned such that the outer side (the sample side) of the tape surface is facing upward, with the start point on the left side of the Perspex ruler, as shown in Figure 2.8. This ruler has been sprayed with an ethanol-water mixture to prevent the tape from sticking to it and preventing it from moving about on the ruler. As one moves from left to right along the ruler, a scalpel is used to cut along each of the deep grooves which denote 24-hour segments. This results in the creation of seven distinct segments of tape, each of which represents one day.

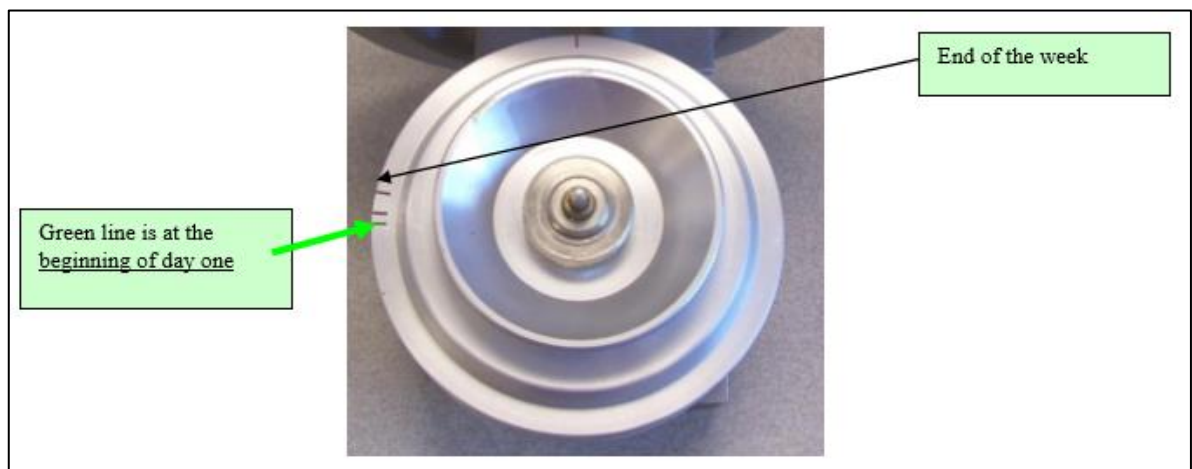


Figure 2.5: Alignment of start and end of the week on a Hirst drum along the green line (Levetin)

Each portion of tape is then transferred onto a glass microscope slide that has been labelled with the date, location, and time, with the start of each day at the “top” or label end of each slide. A pre-prepared slide mounting medium is heated and placed on coverslips, which are then placed on to the tape and slide, for the purpose of sealing the sample for long term storage.

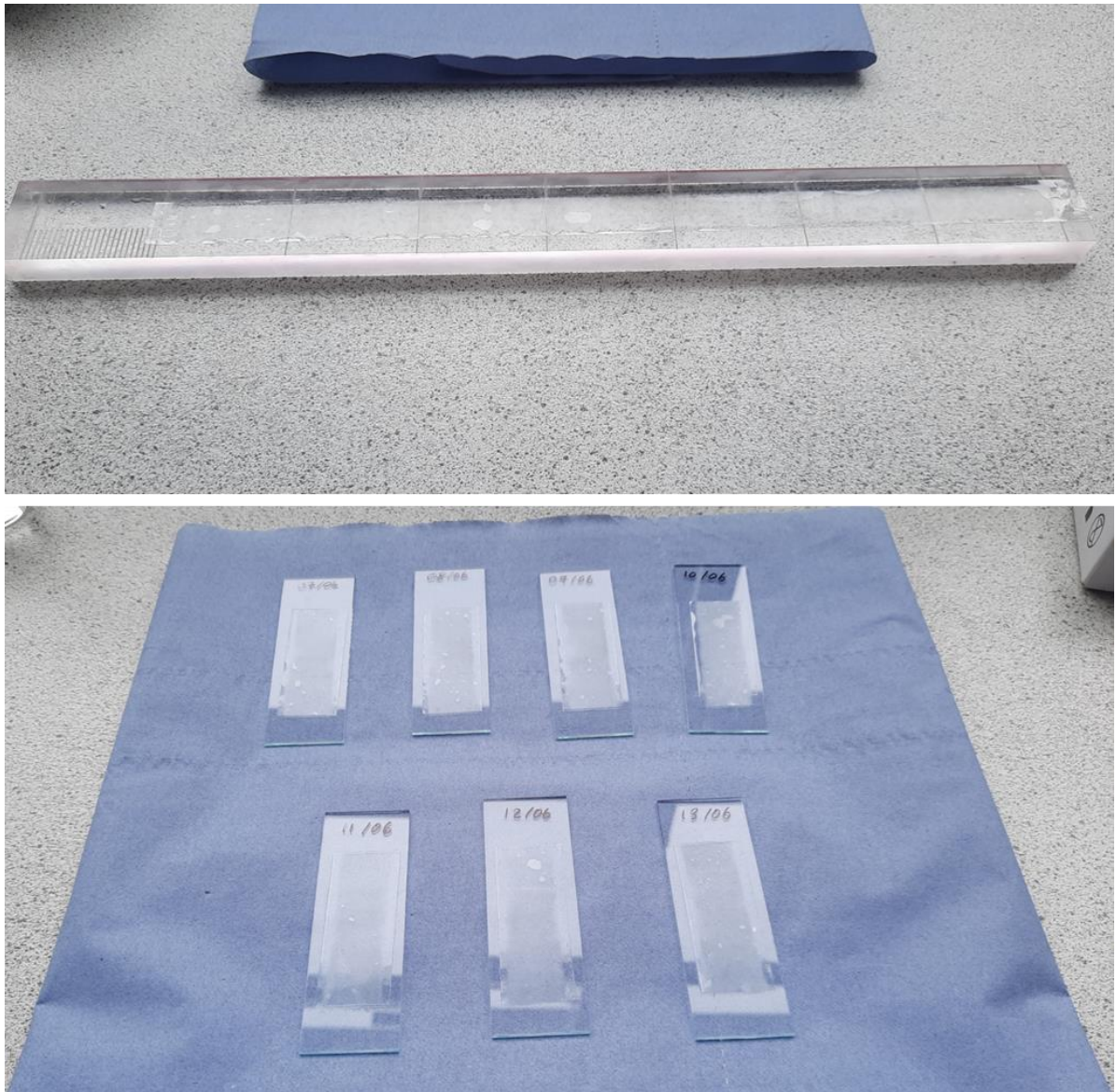


Figure 2.6: A pair of images showing the samples before and after the process of cutting and separating each week of collected sample, into 7 glass slides each representing 24 hours of sampling.

The composition of the mounting medium is 50 ml glycerin, 7 grams gelatin, 1 gram of phenol and a small amount of basic fuchsin, diluted in 42 ml distilled water. This is a bright pink mixture that is liquid when heated but solid at room temperature, allowing for easy application and rapid preservation. The basic fuchsin also acts as a colourant, and stains the vegetal walls of pollen grains, but does not have the same effect on fungal spores, which can be recognised by their own colour. As both pollen grains and fungal spores are present in the same sample, the basic fuchsin is still a necessary ingredient for the mounting medium, even though it has no effect on fungal spore recognition.

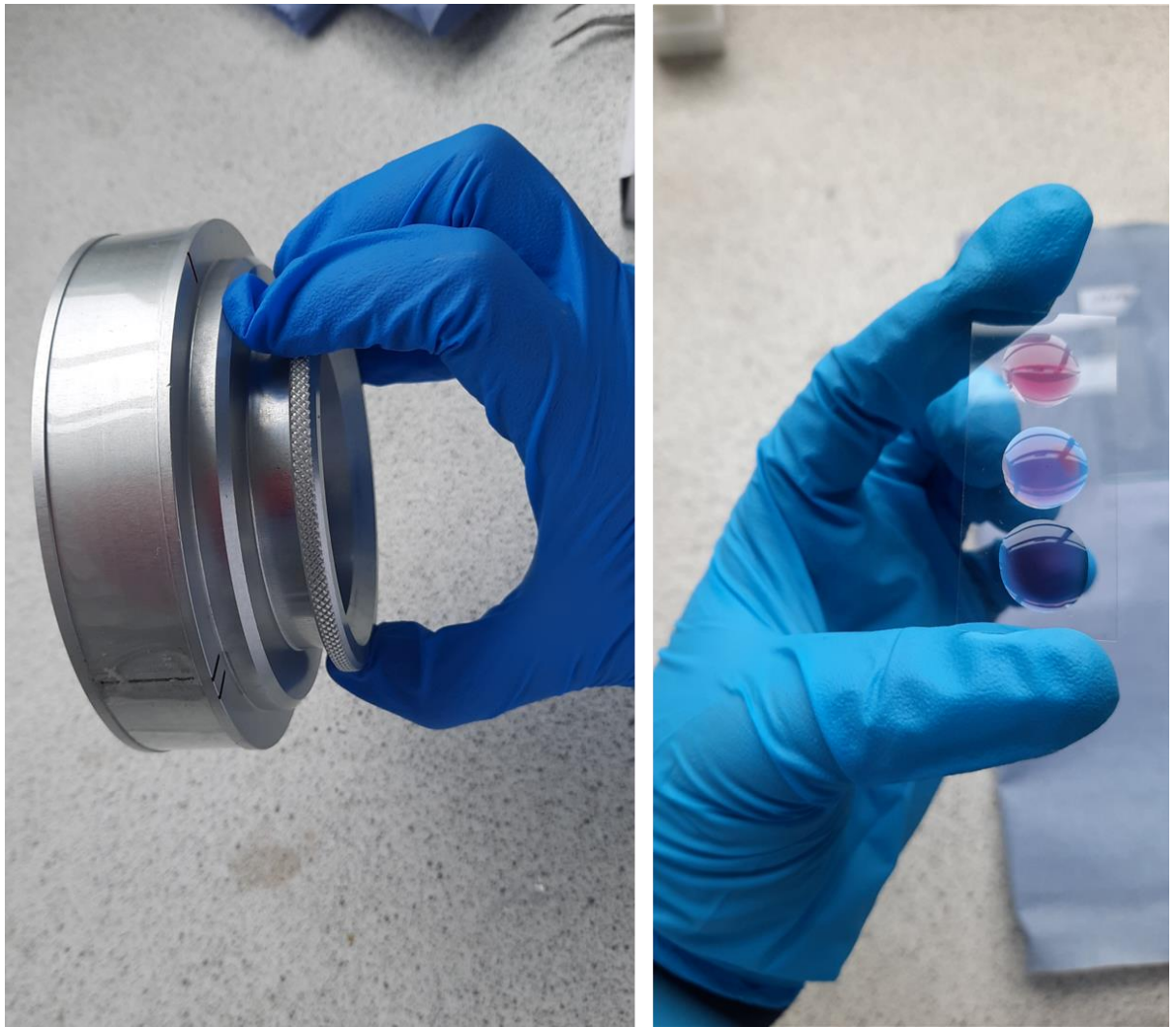


Figure 2.7: A pair of images showing: 1. The sample adhesive still mounted on the Hirst metal drum. 2. The still wet mounting medium immediately after being placed on the sample slide, prior to placement of the cover slip.



Figure 2.8: Diagram of Melinex tape placed upon a Perspex ruler, with grooves marked for each hour of the day, as well as daily grooves along the ruler (Galán et al., 2007)

After preparation, analysis of the slide-mounted tapes by light microscopy is carried out. A magnification of 40x10 is used, to keep a balance between maintaining a large visual field, while still enabling identification of most spore types. For counting of fungal spores, 2 horizontal lines along the length of the slide are counted at this magnification. Both of these

decisions are made to align with the standardized methods for airborne fungal spore monitoring counting and analysis suggested by the Spanish Aerobiology Network (REA), the minimum requirements and the fungal spore monitoring of the European Aerobiological Society. (Galán et al., 2021; Galán et al., 2014, 2007; Molina et al., 1996) The tape is 48mm long, so the slide is divided into 24, 2mm sections, each representing one hour, with each section composing the entire width of the slide horizontally. Looking at a slide, the first hour of the day is the first 2mm segment at the top of the slide, next to the date, location, and time label. This is the hour at which the Hirst device began counting, and the end of the tape or bottom of the slide section marks exactly 24 hours later. Data collected is added to the fungal collection database, with one table representing a single spore type on a single day. In the example below, the drum was switched at 10am. The table often has room for the data of 4 horizontal lines, as is required for the counting of pollen grains in the same manner. But a two lined counting table is also appropriate, to help in differentiation from pollen counting datasheets, which can appear similar at first glance.

10	11	12	13	14	15	16	17	18	19	20	21	22	23	24	1	2	3	4	5	6	7	8	9

Figure 2.9: Fungal spore data collection form for one spore type on one day. There are two rows of cells, to account for the two passes that are made across the length of each slide under the microscope.

This requires a high level of skill to accurately count and properly identify the particles collected. This is a slow process and, as a result, only a small sub-sample of individual microscope slides are examined and the overall count is an extrapolation (Comtois et al., 1999; Šikoparija et al., 2011). The data also relies on the skill of the operator and so there have been concerted efforts of late to evaluate data quality (Galán et al., 2014; Šikoparija et al., 2011; Smith et al., 2019) and standardise methods. (Galán et al., 2021, 2014) Hirst-type samplers are the most commonly used samplers in Europe that meet the minimum requirements of the European Aerobiology Society. (Galán et al., 2014)

Calculation of the correction factor, which accounts for both the field of view of the microscope and the proportion of the slide that has been sampled, to determine the amount of spores per slide, and resultantly, amount of spores per cubic metre of air, according to the Spanish Aerobiology Network, can be outlined as follows:

The Air Sampling rate is 10 litres per minute, or 14400 litres per day, or 14.4 m³.

The Field of View is 0.49 mm

The area of a horizontal sweep is 0.49 mm x 48 mm = 23.52 mm²

The surfaced analysed for fungal spores is 23.52 x 2 sweeps = 47.04 mm²

Total sampled surface = 48 mm (length) x 14 mm (width) = 672 mm²

Particles per m³ of air is (672 mm² / 47.04 mm²) x (1 / 14.4) x N

(N = total number of fungal spores on 2 sweeps of a slide)

Particles per m³ of air is N x 0.992

2.2.2. WIBS-NEO

The WIBS-NEO real-time air sampler, or simply WIBS, was used in only Dublin as part of the shorter real-time monitoring campaign. It is a three-channel single aerosol particle fluorescence monitor. It detects Fluorescent Biological Aerosol Particles (FBAP) in real time using Laser-induced fluorescence (LIF). It was invented for the purpose of detecting airborne particles in a defensive setting at the University of Hertfordshire by Professor Paul Kaye. (Fennelly et al., 2018) It has become one of the most common real-time Primary Biological Aerosol Particle (PBAP) monitoring devices commercially available (commercialised by Droplet Measurement Technologies (DMT)). A diagram of the flow system of the WIBS NEO can be seen below in Figure 2.10.

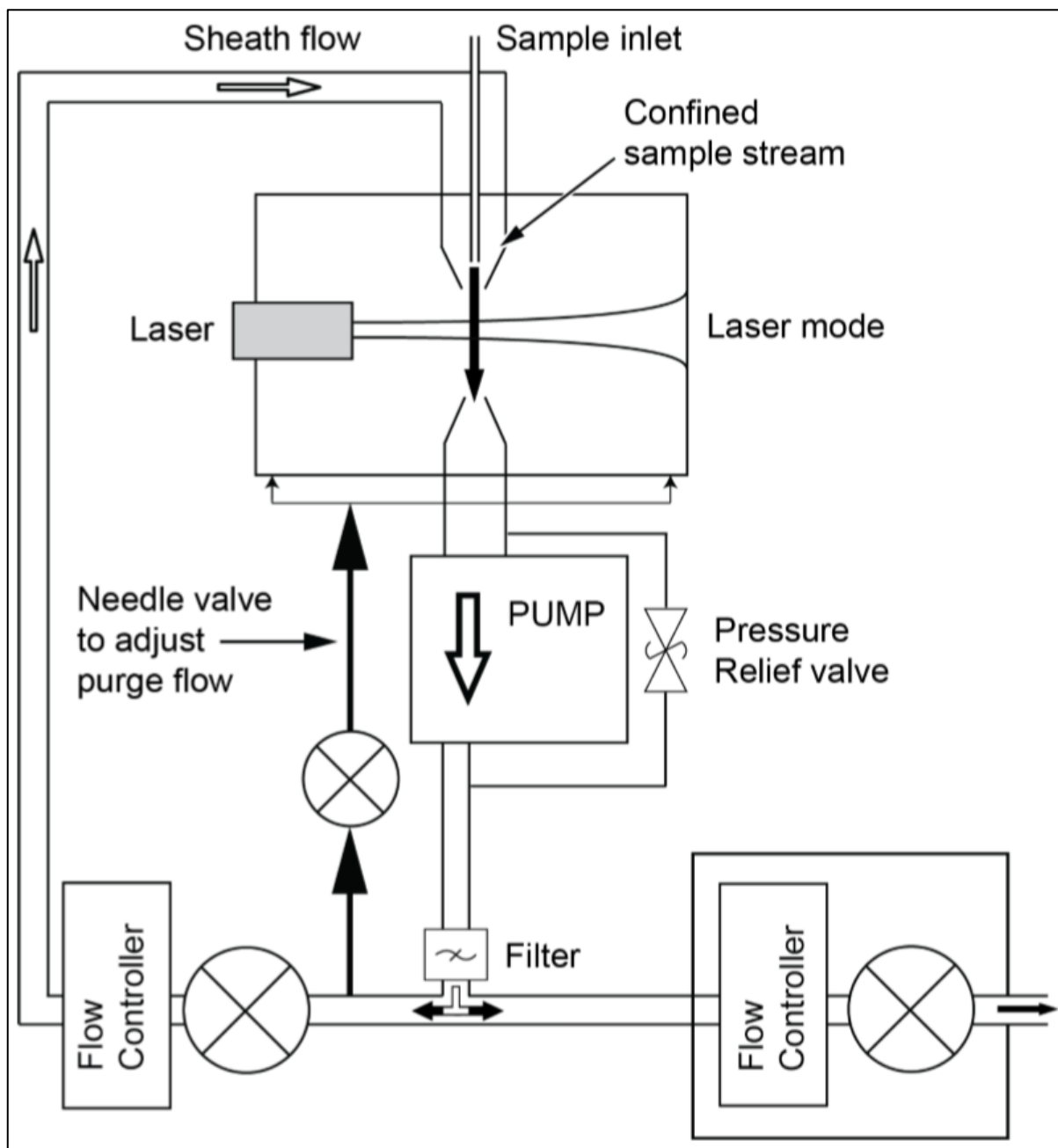


Figure 2.10: WIBS-NEO Flow System Diagram showing the flow of air throughout the device (“Wideband Integrated Bioaerosol Sensor – Droplet Measurement Technologies”)

The individual shape and size of both fluorescent and non-fluorescent particles are obtained by measuring the forward and side optical scatter, and the spectrally unresolved fluorescent intensity of individual particles at a time resolution of one millisecond. Several versions of the WIBS instrument have been used throughout the literature. Such, versions include Model 3 and 4 (prototype instruments) and the WIBS 4A and WIBS NEO which are commercially available models. (Fennelly et al., 2018)

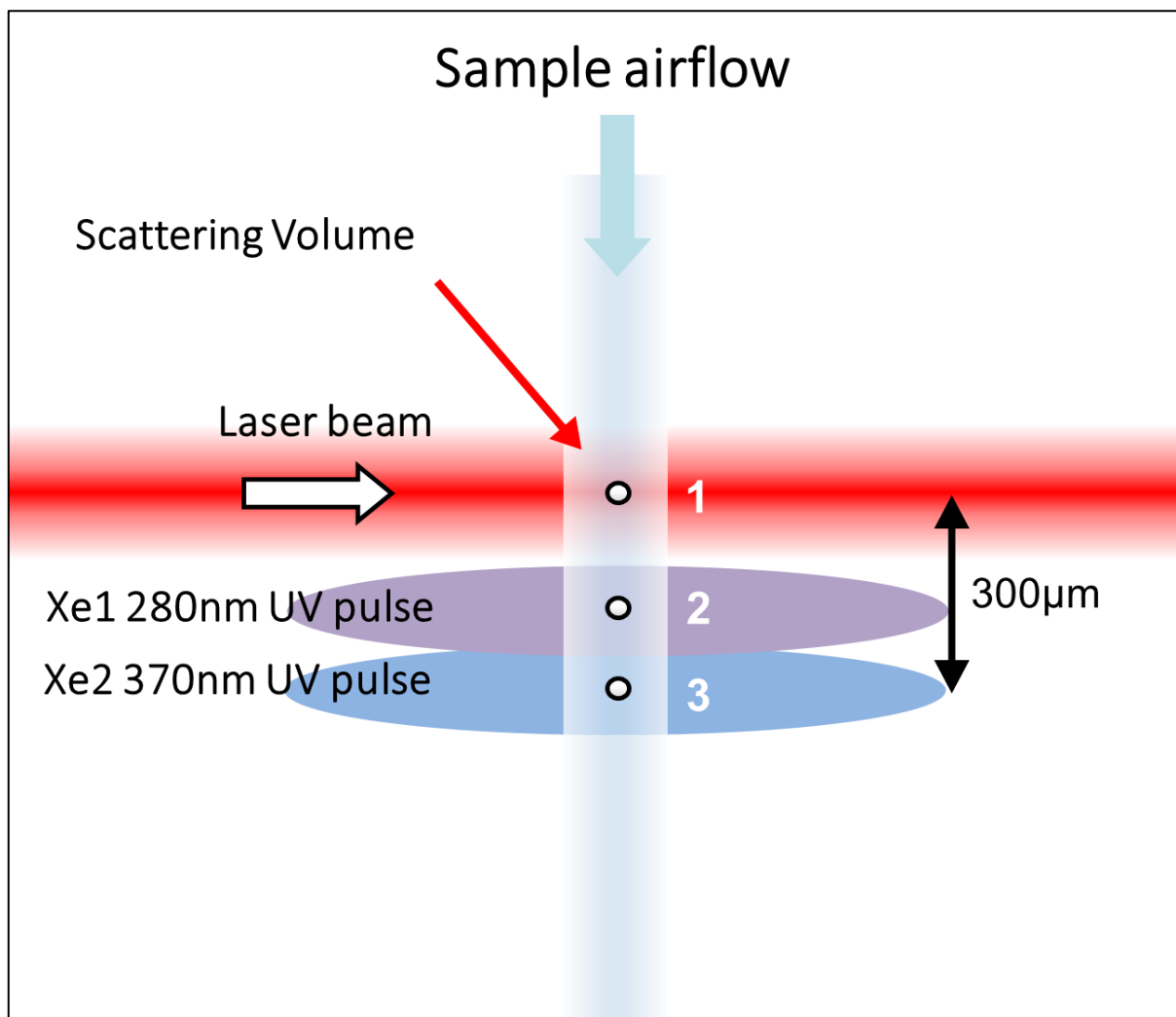


Figure 2.11: WIBS-NEO measurement cycle, showing the process by which each individual particle is analysed (“Wideband Integrated Bioaerosol Sensor – Droplet Measurement Technologies”)

All WIBS models operate slightly differently, but only with regard to the exact volumes of air used in the sampling of ambient air. The WIBS-NEO operates as follows; ambient air is drawn into the main optical chamber at 2.4 L min⁻¹. Next, 0.3 L min⁻¹ of this air is separated for use as the sample flow, which will be measured by the device. Fibrous particles tend to align lengthwise in flow direction, in a single file stream. The rest of the air (2.1 L min⁻¹) is then filtered and holds and confines the sample flow in a vertical column of air by forming a sheath flow. This sheath flow, along with a small bleed flow are used for the purging of irrelevant particulate matter from the optical chamber. A continuous wave diode laser of 635 nm (seen in Figure 2.11) encounters the particles as they pass through the optical chamber. The scattering volume of the device is the intersection between the airflow and the laser beam. It measures approximately 0.7mm diameter, and 60µm deep.

Light from each particle is scattered and is collected by the fluorescence collection mirrors (Figure 2.12) and passed into the dichroic beam splitter, before subsequent FL2 channel detection. From here, the light is converted to an electrical signal for the purpose of particle sizing and triggering of the (Xenon) Xe1 280nm flash lamp, followed by the Xe2 370nm xenon flash lamp. Detector wavelength bands of 310-400 nm and 420-650 nm are then used to detect the fluorescence emission that result from the interaction with the two flash lamps. Fluorescence signals are divided into three detector channels, namely FL1 (excitation at 280nm detection between 310-400 nm), FL2, and FL3 (excitation at 280 and 370 nm respectively and detection between 420-650 nm). (Després et al., 2012; Fennelly et al., 2018; Huffman et al., 2020; O'Connor et al., 2014)

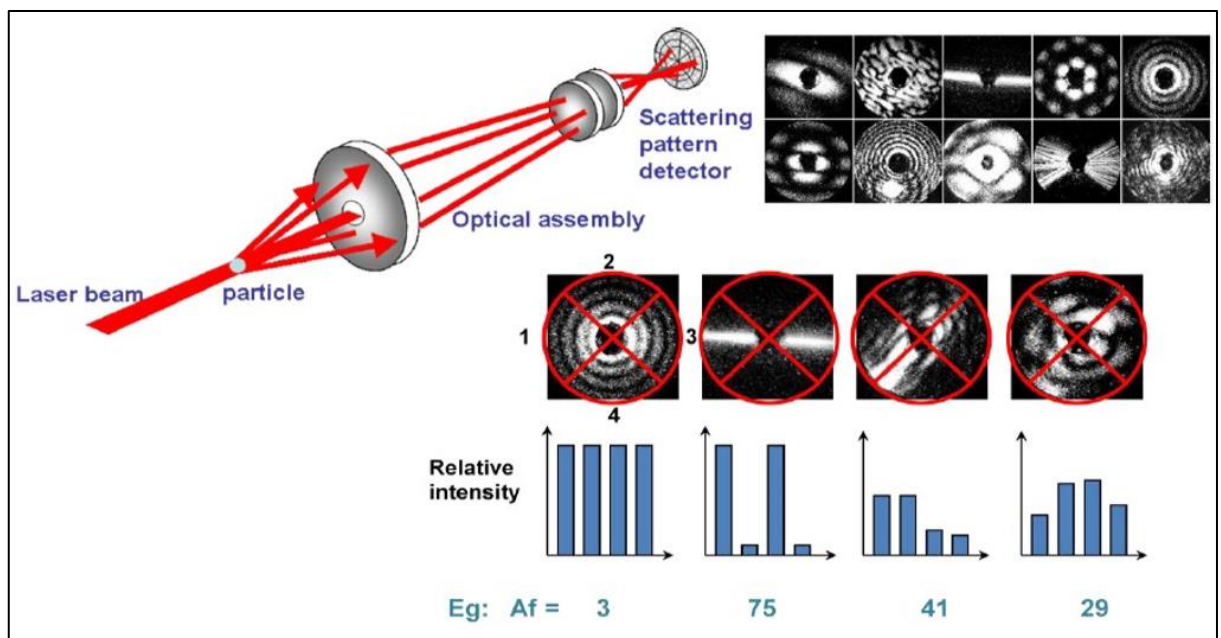


Figure 2.12: WIBS-NEO Derivation of particle asphericity factor and measuring azimuthal variation in particle forward scattering. Particles scatter light based on their size and shape (“Wideband Integrated Bioaerosol Sensor – Droplet Measurement Technologies”). This represents the “Laser beam” portion of Figure 2.11.

Mie theory calculation is used to get particle size. This is a calculation used to describe the scattering of particles, assuming all are spherical and homogeneous. It is important in describing the light scatter within clouds of particles and is described in detail by Hergert and Wriedt, (2012). MIE theory works better for particles such as pollen grains, and Mie theory assumes that particles are spherical and uniformly illuminated. Because of these assumptions, the shape/asymmetry should also be taken into account to improve validity of the data somewhat. The Multi Element Forward Scattering Detector (Figure 2.12) is used to calculate this asymmetry factor. There is a quadrant photomultiplier tube (PMT) that receives

the forward scattered light from the particle, and the scatter intensity of each of the 4 quadrants is recorded, and the root-mean-square variation around the mean is calculated to result in the Asphericity Factor (AF) or “shape”. The “shape” output is given as a value between 0 and 100 where a value of zero is a perfect sphere and a value closer to 100 shaped like a rod. (Fennelly et al., 2018)

Perring et al., (2015) introduced the lettering system for differentiating fluorescence channels. They are divided as follows; Channel A are emissions from particles excited at 280nm and emission between 310-400nm, Channel B is excitation at 280 nm and emission between 420-650 nm and Channel C is excitation at 370 nm and emission between 420nm and 650 nm. Particles that fluoresce in only one of the three channels are described as A, B, or C particles. Particles outputting a signal in two channels are AB, AC, or BC particles, whereas a particle labelled ABC would exhibit a signal in all channels.

Table 2: WIBS-NEO particle fluorescence classification the different FI results are representative of the channels in which particles are detected, as a result of their fluorescence excitation and emission wavelengths ("WIBS-NEO-Toolkit.pdf")

Name	Fluorescence must be above background for:
All	All particles
Excited	Particles excited by the flash lamp
Fluorescent	Fluorescent particles detected in any channel
FL1	Fluorescent particles detected in channel FL1 (excitation at 280 nm, emission 310-400 nm)
FL2	Fluorescent particles detected in channel FL2 (excitation at 280 nm, emission 420-650 nm)
FL3	Fluorescent particles detected in channel FL3 (excitation at 370 nm, emission 420-650 nm)
A	Fluorescent particles detected in channel FL1 only
B	Fluorescent particles detected in channel FL2 only
C	Fluorescent particles detected in channel FL3 only
AB	Fluorescent particles detected in channels FL1 and FL2 only
AC	Fluorescent particles detected in channels FL1 and FL3 only
BC	Fluorescent particles detected in channels FL2 and FL3 only
ABC	Fluorescent particles detected in channels FL1, FL2, and FL3

For example, a particle that is detected in channel FL2 could be a B, AB, BC, or ABC particle depending on which other FL channels are also excited. It is noted that even though there is a combination of Xenon flash lamp excitation (Xe2, at 370nm) and fluorescence detection channel (FL1, emission 310-400nm) that has not been mentioned, it is not possible for this theoretical “FL4” to be of any use. There is an overlap in wavelengths that results on saturation if this combination of FL channel and xenon flash lamp are used. Resultantly, the outputs are unreadable and without use.

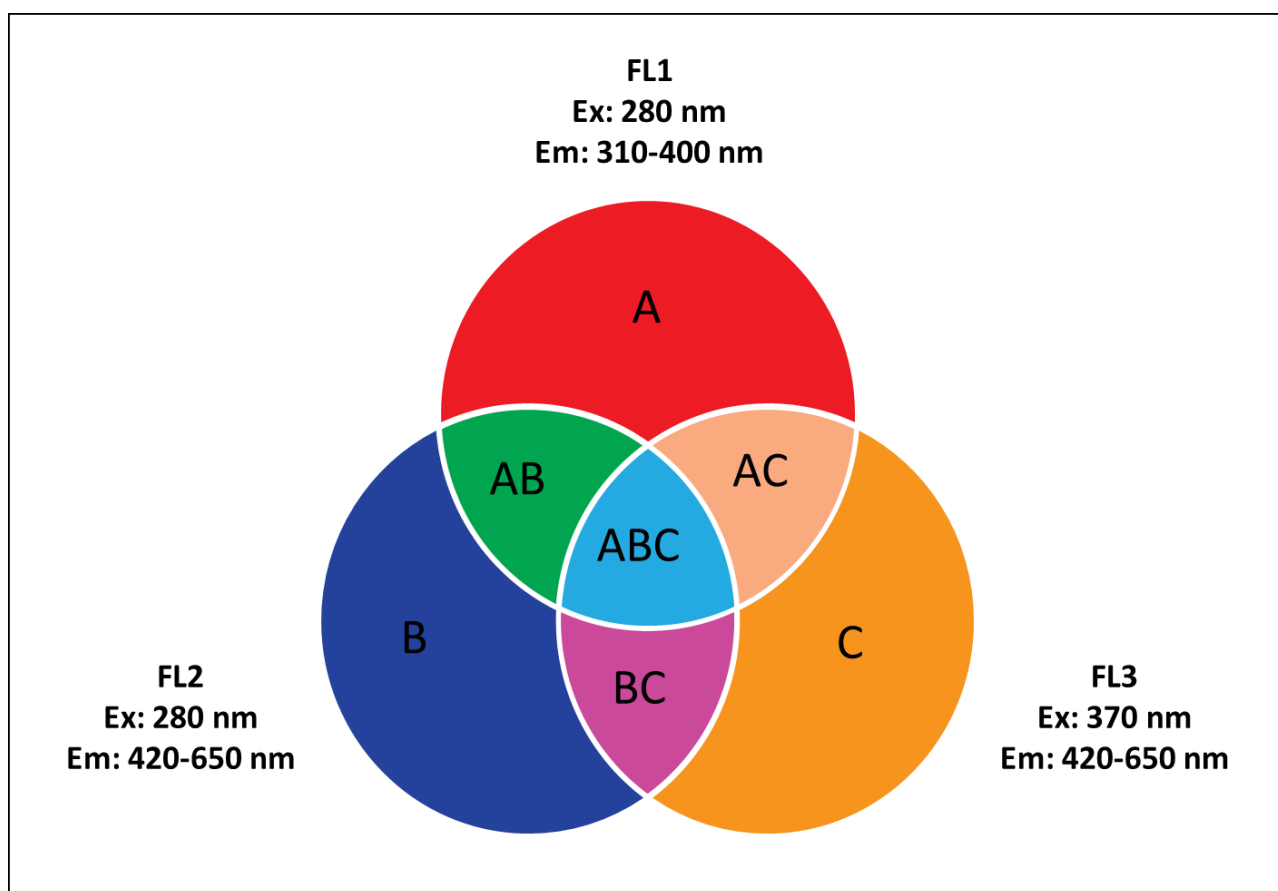


Figure 2.13: Particle fluorescence definitions outlining the different categorisations, based off a diagram from (Savage et al., 2017)

2.2.3. IBAC

The Instantaneous Bioaerosol Analysis and Collection (IBAC) device was also only implemented in the Dublin sampling site, as part of the Real-time monitoring campaign.

This device was being tested both as a comparative tool as part of the wider campaign, but also to test for suitability as part of future aerosol and bioaerosol projects itself. The IBAC (previously known as the FIDO B2, and the Instantaneous Biological Analyzer and Collector (IBAC)) is a UV-LIF continuous air monitor initially developed by ICx Biodefense for the

purpose of detecting potential threats related to biological aerosols and acting as an early warning system. It is commercialized by FLIR Systems (“FLIR IBAC 2 Bio-Threat Detection & Collection | Teledyne FLIR,” 2021). Similar to UV-APS it can differentiate between biological and non-biological particles via elastic scattering (photomultiplier tubes) and particle fluorescence utilizing a 405nm laser as an excitation source. Particles are drawn into the device at a rate of 3.8 litres per minute. They pass through an optical illumination region, where the 405nm laser excites the particles. Size and concentration of particles are measured from the light scatter. If the integrated fluorescence emitted by a particle falls between 450-600nm, and exceeds a pre-set threshold, it is determined to be fluorescent/biological. Individual particles analysis is capable at up to 500,000 particles per litre, allowing 1,500,000 particles per minute to be individually interrogated, as the count rate has a maximum of 25,000 particles per second.

The device also distinguishes between small (less than 1.5 μm), and large (greater than or equal to 1.5 μm) particle sizes. As a result, there are four distinct groupings determined by both size and fluorescence. It has dual sampling capabilities and when set to function as an early warning system, it can commence sample collection after detection of potential bio threats, while also continuously monitoring via its UV-LIF technology. The sample collector includes a high-flow air sampling pump that can be equipped to collect either dry or wet samples via one of either a DFU polyester filter (dry sample) or a C100 Collector (wet sample). The IBAC is capable of detecting particles ≥ 0.7 microns, and possesses a response time of between 30s and 1 min. Thus, the device can detect spores, and bacteria, among others. It was designed to be modular so that extra functions and capabilities such as aerosol samplers could later be integrated into the system. Primary customers of the first IBAC have been described as homeland security and defence customers. (Anchlia, 2015; DeFreez, 2009; Jonsson and Kullander, 2014; Pazienza, 2013; Santarpia et al., 2013)



Figure 2.14: constituent parts in Line Power Configuration (left), and Battery Power Configuration (right), and with extension stack installed (right), (“FLIR IBAC 2 Bio-Threat Detection & Collection | Teledyne FLIR,” 2021)

Advantages of the IBAC over other biological particle sensors and detectors include its ability to work more efficiently. The IBAC is designed with threat detection and warning in mind. The filter sampler within the IBAC only commences sample collection upon detection of a possible bio threat, allowing analysis of the most important desired air samples in great detail. As a result, less maintenance than a continuous manual sampler is required. A disadvantage that the IBAC possesses is possible confusion when detecting particles from anthropogenic sources, with the device occasionally struggling to correctly identify whether some particles from these sources are biological in origin. (“FLIR IBAC 2 Bio-Threat Detection & Collection | Teledyne FLIR,” 2021)

2.3. Data Analysis and Protocol

Along with carrying out a contemporary study, previously unpublished historical fungal spore data from 1978-1980 was processed and collated to output a first calendar of fungal spore fructification in Ireland. The production of the calendar was undertaken using the below described protocol.

The data for this calendar was obtained from Trinity College, Dublin, another urban site situated 1.1km northeast of the contemporary Hirst sampling site on the roof of TU Dublin. The mean daily spore values for all years were calculated for the 15 most abundant spore

types. These included *Scopulariopsis*, *Ganoderma*, yeasts, *Venturia*, *Ascospores*, *Cladosporium*, *Basidiospores*, Rusts, downy mildew, *Botrytis*, *Erysiphe*, *Epicoccum*, *Alternaria*, *Tilletiopsis*, and *Polythrincium*. Daily values for each month were further divided into 5 sections per month, containing 6 days each. The mean value for each section was then calculated. This was repeated for each spore type. The main fructification period was calculated (10-90%) as beginning once 10% of the total annual fungal spore concentration had been reached and ended once 90% was reached. Early and late fructification periods, outside the main fructification periods, were determined similarly. The early period was defined as greater than 0.5% of the total annual concentration but less than 10%. The late fructification period corresponded to greater than 90% of the total annual concentration but less than 99.5%. Finally, possible occurrence times were determined as any time outside of the 0.5-99.5% range, where some (greater than or equal to one) fungal spores were observed. The fungal spore calendar was then constructed and coloured according to the level of allergenicity posed by each type, and shaded according to possible, early/late, and main fructification periods.

In addition to the fungal spore fructification calendar, a series of wind models, created of the determination of geographical source of fungal spores, and a set of regression and forecasting models were constructed. Full descriptions of these processes will be described in the appropriate chapter on modelling of biological aerosol.

All statistical analysis was carried out using R software. Packages used include *nortest*, *dplyr*, *lubridate*, *ggplot2*, *tidyverse*, *plyr*, *viridis*, *tidyr*, *reshape2*, and *corrplot*. (Gross and Ligges, 2015; Spinu, 2016; Wei et al., 2016; Wickham et al., 2019; Wickham and Wickham, 2020, 2007)

Additionally, the geographical origin of airborne pollen grains and fungal spores collected at the Dublin Hirst sampling location was examined by combining the daily spore concentrations counted as part of the study, with the publicly available wind speed and directional data available from Met Éireann. (The Irish National Meteorological Service, 2020).

The two-dimension Non-parametric Wind Regression (NWR) was used to assess the geographical origin of atmospheric spores. This method has been used in multiple studies for geographical wind origin analysis, as well as for air quality analysis (Donnelly et al., 2015; Han et al., 2017; Wang et al., 2013).

These calculations can be completed using the ZeFir wind modelling package, which can then be used to create wind origin plots for each pollen or spore type.

2.4. Summary

This section provided a comprehensive account of the geographical locations and scientific equipment employed in both past and present fungal spore sampling campaigns conducted in Ireland. Trinity College, Dublin was the site for historical sampling between 1978 and 1980, while contemporary sampling was carried out at four locations in Ireland: Dublin, Carlow, Cork, and Sligo. The Hirst-Lanzoni 7-day volumetric spore-trap was employed at three out of the four locations, whereas the SporeWatch device was utilised in Cork. There is no notable difference between these models scientifically. The Hirst device is currently being used in as many as 637 locations across the globe. In addition, the data analysis process and the ZeFir wind rose software were described in this chapter.

The Hirst process involves a monitoring period of 7 days, after which the sampling portion of the device, the drum and tape are removed and replaced. Subsequently, the tape is transferred onto a glass microscope slide and labelled with the date, location, and time. A pre-made slide mounting medium is utilised to seal the sample for extended storage and ease of optical recognition. Basic fuchsin dye is an essential component of the mounting medium, but it does not have any impact on the identification of fungal spores and primarily assists in pollen identification. The tape can be considered 24 segments, with each segment corresponding to a single hour. Counted data is added to a database for fungal analysis. The process necessitates a high level of expertise to precisely quantify and classify the gathered bioaerosols, leading to an estimation of the total concentration of spores in the air.

The WIBS-NEO device utilises Laser-induced fluorescence (LIF) to instantly detect Fluorescent Biological Aerosol Particles (FBAP). The device monitors the fluorescence of individual aerosol particles in three different channels. It is specifically designed for real-time monitoring campaigns. It works by taking air into an optical chamber. A diode laser emitting a continuous wave interacts with particles as they pass through the chamber. The collection mirrors gather light emitted by each particle, which is then directed into a dichroic beam splitter for size and shape detection. Then the Xenon flash lamps are activated, and the fluorescence emission is detected using detector wavelength bands ranging from 310 to 400 nm and from 420 to 650 nm. Fluorescence channels are differentiated using a system based on letters. The results indicate the channels in which particles are identified by their fluorescence excitation and emission wavelengths.

The Dublin sampling site also incorporated the IBAC device as a part of the real-time monitoring campaign. The UV-LIF continuous air monitor was designed as a detection tool

for identifying potential hazards associated with biological aerosols. By identifying particle fluorescence with a 405nm laser as an excitation source, it distinguishes between biological and non-biological particles. The IBAC has the ability to detect particles that are equal to or greater than 0.7 microns in size, and it's equipped with dual sampling capabilities.

Additionally, an initial fungal spore fructification chart for Ireland was compiled utilising archival data spanning from 1978 to 1980. The calendar was color-coded based on allergenicity and phytopathogenicity, and shaded to highlight the possible, early/late, and main fructification periods. The Dublin Hirst sampling location was used to analyse the geographical source of airborne pollen grains and fungal spores. This was done using the two-dimensional Non-parametric Wind Regression (NWR) method. The campaigns associated with the instruments, methodologies, locations, and research, are outlined in the subsequent chapters, along with the results of said campaigns.

2.5. References

- Anchlia, P. 1987-, 2015. *Aerosol Data Modeling & Similarity Assessment – a Probabilistic Approach* (Thesis).
- Burkard, n.d. *SporeWatch Brochure*.
- Buters, J.T.M., Antunes, C., Galveias, A., Bergmann, K.C., Thibaudon, M., Galán, C., Schmidt-Weber, C., Oteros, J., 2018. Pollen and spore monitoring in the world. *Clin. Transl. Allergy* 8, 9. <https://doi.org/10.1186/s13601-018-0197-8>
- Comtois, P., Alcázar, P., Néron, D., 1999. Pollen counts statistics and its relevance to precision. *Aerobiologia* 15, 19–28. <https://doi.org/10.1023/A:1007501017470>
- Cork Airport 1991–2020 averages [WWW Document], n.d. URL https://www.met.ie/cms/assets/uploads/2023/09/www_met_ie_cork_9120.htm (accessed 10.7.23).
- DeFreez, R., 2009. LIF Bio-Aerosol Threat Triggers: then and now. *Proc. SPIE - Int. Soc. Opt. Eng.* 7484. <https://doi.org/10.1117/12.835088>
- Després, V., Huffman, J.A., Burrows, S.M., Hoose, C., Safatov, A., Buryak, G., Fröhlich-Nowoisky, J., Elbert, W., Andreae, M., Pöschl, U., Jaenicke, R., 2012. Primary biological aerosol particles in the atmosphere: a review. *Tellus B Chem. Phys. Meteorol.* 64, 15598. <https://doi.org/10.3402/tellusb.v64i0.15598>
- Dublin 1981–2010 averages [WWW Document], 2021. URL <https://www.met.ie/climate-ireland/1981-2010/dublin.html> (accessed 7.22.21).
- Fennelly, M.J., Sewell, G., Prentice, M.B., O'Connor, D.J., Sodeau, J.R., 2018. Review: The Use of Real-Time Fluorescence Instrumentation to Monitor Ambient Primary Biological Aerosol Particles (PBAP). *Atmosphere* 9, 1. <https://doi.org/10.3390/atmos9010001>
- FLIR IBAC 2 Bio-Threat Detection & Collection | Teledyne FLIR [WWW Document], 2021. URL <https://www.flir.com/products/ibac-2/> (accessed 7.22.21).
- Galán, C., Cariñanos, P., Alcázar, P., Domínguez Vilches, E., Aira-Rodríguez, M., Sánchez, A., Belmonte Soler, J., Ramos, B., Artero, C., Fernández, C., González, C., de la Guardia Guerrero, D., Rendueles, E., González, F., Minero, G., Bustillo, G., Álvarez, I., Rodríguez, J., García, L., Andrés, M.M., Grau, M., Badía, P., Criado, R., Rajó, R., Javier, Francisco, Valenzuela, R., Pérez, S., Javier, F., Tormo-Molina, R., Pérez, Tortajada, Pérez, Trigo, del Mar, M., Barrera, V., Ma,

- R., Maray, V., Ma, A., Blanco, V., 2007. Spanish Aerobiology Network (REA): Management and Quality Manual (REA).
- Galán, C., Smith, M., Damialis, A., Frenguelli, G., Gehrig, R., Grinn-Gofroń, A., Kasprzyk, I., Magyar, D., Oteros, J., Šaulienė, I., Thibaudon, M., Sikoparija, B., EAS QC, W.G., 2021. Airborne fungal spore monitoring: between analyst proficiency testing. *Aerobiologia*. <https://doi.org/10.1007/s10453-021-09698-4>
- Galán, C., Smith, M., Thibaudon, M., Frenguelli, G., Oteros, J., Gehrig, R., Berger, U., Clot, B., Brandao, R., EAS QC Working Group, 2014. Pollen monitoring: minimum requirements and reproducibility of analysis. *Aerobiologia* 30, 385–395. <https://doi.org/10.1007/s10453-014-9335-5>
- Gross, J., Ligges, U., 2015. nortest: Tests for Normality. R package version 1.0-4. URL [HttpCRAN R-Proj. Orgpackage Nortest](http://CRAN.R-project.org/package=Nortest).
- Hergert, W., Wriedt, T., 2012. *The Mie Theory: Basics and Applications*. Springer.
- Hirst, J.M., 1952. An Automatic Volumetric Spore Trap. *Ann. Appl. Biol.* 39, 257–265. <https://doi.org/10.1111/j.1744-7348.1952.tb00904.x>
- Historical Data - Met Éireann - The Irish Meteorological Service [WWW Document], 2022. URL [//climate/available-data/historical-data](http://climate/available-data/historical-data) (accessed 11.22.21).
- Huffman, J.A., Perring, A.E., Savage, N.J., Clot, B., Crouzy, B., Tummon, F., Shoshanim, O., Damit, B., Schneider, J., Sivaprakasam, V., Zawadowicz, M.A., Crawford, I., Gallagher, M., Topping, D., Doughty, D.C., Hill, S.C., Pan, Y., 2020. Real-time sensing of bioaerosols: Review and current perspectives. *Aerosol Sci. Technol.* 54, 465–495. <https://doi.org/10.1080/02786826.2019.1664724>
- Jonsson, P., Kullander, F., 2014. Bioaerosol Detection with Fluorescence Spectroscopy, in: Jonsson, P., Olofsson, G., Tjärnhage, T. (Eds.), *Bioaerosol Detection Technologies, Integrated Analytical Systems*. Springer New York, New York, NY, pp. 111–141. https://doi.org/10.1007/978-1-4419-5582-1_7
- Levetin, E., n.d. USE OF THE BURKARD SPORE TRAP 14.
- Molina, R.T., Rodríguez, A.M., Palacios, I.S., 1996. Sampling in aerobiology. Differences between traverses along the length of the slide in Hirst sporetraps. *Aerobiologia* 12, 161–166. <https://doi.org/10.1007/BF02447407>

O'Connor, D.J., Lovera, P., Iacopino, D., O'Riordan, A., A. Healy, D., R. Sodeau, J., 2014. Using spectral analysis and fluorescence lifetimes to discriminate between grass and tree pollen for aerobiological applications. *Anal. Methods* 6, 1633–1639. <https://doi.org/10.1039/C3AY41093E>

Pazienza, M., 2013. Use of Particle Counter System for the Optimization of Sampling, Identification and Decontamination Procedures for Biological Aerosols Dispersion in Confined Environment. *J. Microb. Biochem. Technol.* 06. <https://doi.org/10.4172/1948-5948.1000120>

Perring, A.E., Schwarz, J.P., Baumgardner, D., Hernandez, M.T., Spracklen, D.V., Heald, C.L., Gao, R.S., Kok, G., McMeeking, G.R., McQuaid, J.B., Fahey, D.W., 2015. Airborne observations of regional variation in fluorescent aerosol across the United States. *J. Geophys. Res. Atmospheres* 120, 1153–1170. <https://doi.org/10.1002/2014JD022495>

Population Distribution - CSO - Central Statistics Office [WWW Document], 2021. URL <https://www.cso.ie/en/releasesandpublications/ep/p-cp2tc/cp2pdm/pd/> (accessed 7.22.21).

Santarpia, J.L., Ratnesar-Shumate, S., Gilberry, J.U., Quizon, J.J., 2013. Relationship Between Biologically Fluorescent Aerosol and Local Meteorological Conditions. *Aerosol Sci. Technol.* 47, 655–661. <https://doi.org/10.1080/02786826.2013.781263>

Savage, N.J., Krentz, C.E., Könemann, T., Han, T.T., Mainelis, G., Pöhlker, C., Huffman, J.A., 2017. Systematic characterization and fluorescence threshold strategies for the wideband integrated bioaerosol sensor (WIBS) using size-resolved biological and interfering particles. *Atmospheric Meas. Tech.* 10, 4279–4302. <https://doi.org/10.5194/amt-10-4279-2017>

Šikoparija, B., Pejak-Šikoparija, T., Radišić, P., Smith, M., Soldevilla, C.G., 2011. The effect of changes to the method of estimating the pollen count from aerobiological samples. *J. Env. Monit* 13, 384–390. <https://doi.org/10.1039/C0EM00335B>

Smith, M., Oteros, J., Schmidt-Weber, C., Buters, J.T.M., 2019. An abbreviated method for the quality control of pollen counters. *Grana* 58, 185–190. <https://doi.org/10.1080/00173134.2019.1570327>

Soldevilla, C.G., González, P.C., Teno, P.A., Vilches, E.D., Rodríguez, A., Jesús, M., Sánchez, A., Soler, B., Ramos, B., Artero, C., Fernández, C., González, C., González, F., Minero, G., Álvarez, I., Rodríguez, J., García, L., Andrés, M., Grau, M., Badía, P., Criado, R., Rajo, R., Javier, Francisco, Valenzuela, R., Pérez, S., Javier, F, Molina, T., Pérez, Tortajada, Pérez, Trigo, 2007. SPANISH AEROBIOLOGY NETWORK (REA): MANAGEMENT AND QUALITY MANUAL 36.

Spinu, M.V., 2016. Package 'lubridate.'

Wei, K., Zou, Z., Zheng, Y., Li, J., Shen, F., Wu, C., Wu, Y., Hu, M., Yao, M., 2016. Ambient bioaerosol particle dynamics observed during haze and sunny days in Beijing. *Sci. Total Environ.* 550, 751–759. <https://doi.org/10.1016/j.scitotenv.2016.01.137>

WIBS-NEO-Toolkit.pdf, n.d.

Wickham, H., Averick, M., Bryan, J., Chang, W., McGowan, L.D., François, R., Grolemund, G., Hayes, A., Henry, L., Hester, J., 2019. Welcome to the Tidyverse. *J. Open Source Softw.* 4, 1686.

Wickham, H., Wickham, M.H., 2020. Package 'plyr.' *Gramm. Data Manip. R Package Version 8.*

Wickham, H., Wickham, M.H., 2007. The ggplot package. Google Sch. [Httpftp Uni-Bayreuth DemathstatlibRCRAN/doc/packages/ggplot Pdf.](http://ftp.uni-bayreuth.de/mathstatlib/RCRAN/doc/packages/ggplot)

Wideband Integrated Bioaerosol Sensor – Droplet Measurement Technologies [WWW Document], n.d. URL <https://www.dropletmeasurement.com/product/wideband-integrated-bioaerosol-sensor/> (accessed 7.13.21).

Chapter 3. Traditional Fungal Spore Monitoring

3.1. Background

Biological aerosols are endemic to the air we breathe. For as long as life has existed, there have been biological aerosols. They can be living biological organisms like bacteria, or they can be materials and byproducts of living things such as pollen, fungal spores, and insect and plant matter. Across Europe and the world, there is a long history of traditional monitoring of bioaerosols, with the majority of that focus being the collection, monitoring, and analysis of pollen taxa (Buters et al., 2018; Maya-Manzano et al., 2021). Less commonly, fungal spore concentrations have also been tracked over the years, often as part of larger pollen monitoring campaigns (Galán et al., 2021; Gregory, 1978; Markey et al., 2022).

The kind of work being carried out with regards to fungal spore analysis have tended to focus on one or two species specifically, and not on fungal spore concentrations as a whole. The construction of fungal spore calendars, following the process commonly used to develop pollen calendars, is an area even less developed, as monitoring campaigns tend to be too short term and focused upon specific goals and objectives unrelated to researching annual and seasonal distribution patterns. The long term studies that do exist, often pick two specific fungal spores, *Cladosporium* and *Alternaria*, for their studies (Grinn-Gofroń et al., 2019; O'Connor et al., 2014; Rodríguez-Rajo et al., 2005; Sindt et al., 2016).

From an Irish context, almost no research at all has been carried out previously. The only previous study that involved seasonal monitoring of fungal spores was in the Summer of 1978 (McDonald and O'Driscoll, 1980). This study looked at changes in allergic reaction incidence in Galway. They attributed it to a change in meteorological conditions, which in turn influenced the fungal spore fructification periods, leading to reduced reactivity compared to the average year.

Since this study, no work in Ireland has been carried out on fungal spore seasonal distribution analysis, or traditional fungal spore monitoring in any form. Resultantly, the aim of this chapter is to update the knowledge on fungal spore seasonality and distribution in Ireland, by analysing and describing the data collected as part of this project. This includes our own daily collected and processed fungal spores' samples from the seasons of 2017 to 2020, as well as recently unearthed daily fungal spore monitoring data from Trinity College, Dublin that was never previously processed or published. This data, from the summers of 1978-1980, is an invaluable addition, and when combined with the contemporary monitoring Dublin data, changes between the time periods can be observed. Additionally, these extra years bring the number of monitored years at one location over the threshold required for construction of a

seasonal fungal spore fructification calendar, which was carried out and is described in this chapter.

3.2. Historical Monitoring Data

From May to September 1978, from March to September 1979, and from March to July 1980, the ambient concentrations of fungal spores on the grounds of Trinity College Dublin were measured. Trinity College is located in the heart of Dublin City, which is situated on the east coast of the island of Ireland. The city is distinguished by a big central river that flows east into the adjacent Irish Sea. The Dublin mountains lie to the south, while a large international airport is to the north. The city and the country to the west are composed of level, low-lying ground. The local climate is cool, temperate, and oceanic. The average monthly temperature fluctuates between 2.6 and 19.3 degrees Celsius (“Historical Data - Met Éireann - The Irish Meteorological Service,” 2022). The yearly precipitation is approximately 735 millimetres, with no seasonal fluctuation. Winter has both the driest and wettest typical months, with average precipitation of 51 mm in February and 77 mm in December.

Using the conventional volumetric-microscopic device, the 7-day Hirst volumetric spore sampler, a combination of hourly and bihourly quantities of main fungal spores were collected (Hirst, 1952). The device operates as follows. At a rate of 10 L/min, airborne particles are drawn into the Hirst device, where they pass through a 2 mm slit and impact upon an adhesive-coated tape. The tape is wound around a metal cylinder that rotates at a rate of 2 millimetres per hour and has a circumference of 336 millimetres. This results in one full revolution taking precisely seven days. As the aperture size and the rotating speed both equal 2 mm, every section of the tape is exposed to the air for precisely one hour. Every week, after a complete rotation, the tape is removed and replaced, and the mechanism that drives the rotation is rewound for another sampling session. The full sample is then processed in the bioaerosol laboratory by trained personnel. This entails slicing the 336-millimeter-long tape into seven 48-millimeter-long pieces, each of which represents a 24-hour period. Each "day" of tape is then transferred to a glass slide and coated with a preservation mixture including a staining agent for easier optical identification of bioaerosols.

During our campaign, these prepared samples were analysed by a trained technician using an optical microscope at 250× magnification. Two longitudinal transect lines, divided into 24 one-hour sections each, were tallied for each slide, as recommended by the REA handbook (Galan et al., 2007). Using these raw fungal counts, the percentage of the slide covered, the flow rate, and the rotational speed, the total number of fungal spores or other bioaerosols per

cubic metre of air could be calculated. This results in hourly and daily total fungal spore concentrations. The 15 most prevalent spore types categorised or named in the historical study were, in alphabetical order: *Alternaria*, Ascospores, Basidiospores, Botrytis, *Cladosporium*, Downy Mildew, *Epicoccum*, *Erysiphe*, *Ganoderma*, *Polythrincium*, Rusts, *Scopulariopsis*, *Tilletiopsis*, *Venturia* and yeasts.

While much work was completed in the collection of bioaerosols, counting and categorising spores and pollen grains, none of this data was ever published, or used for academic or educational purposes until it was rediscovered at the start of the EPA funded “POMMEL” and “FONTANA” Projects. The daily slides had been counted by hand but were never aggregated into seasonal or monthly concentrations or indices, and no known data processing or analysis or the bioaerosol tallies exist. Upon their discovery, each handwritten sheet was painstakingly digitised to preserve the data, and the freshly digitised datasets were processed and analysed, so that they could be used as a historical baseline against which the newly formed network could be compared. Possessing a complete multiyear dataset also provided the project with a head start on the possible creation of a Dublin bioaerosol calendar, as the majority of the scientific literature agrees that a minimum of five seasons of collected data is required for a dataset to be robust enough to be considered a calendar, as the effect of interannual variation diminished by the additional data (Bednarz and Pawłowska, 2016; Galan et al., 2007; Reyes et al., 2016).

3.2.1. Overview of Prevalent Fungal Types and Trends

Over the course of the 1978-1980 seasons, 10 different fungal spore types were sampled and categorised in all three study years. In total, 23 unique fungal spore types were categorised during at least one of the seasons of the sampling campaign. The spore types identified for each of the three years are seen below in Figure 3.1. This includes any spore type that made up at least 0.5% of the total concentration of all spores for any one year of the study, resulting in 8 spore types being included.

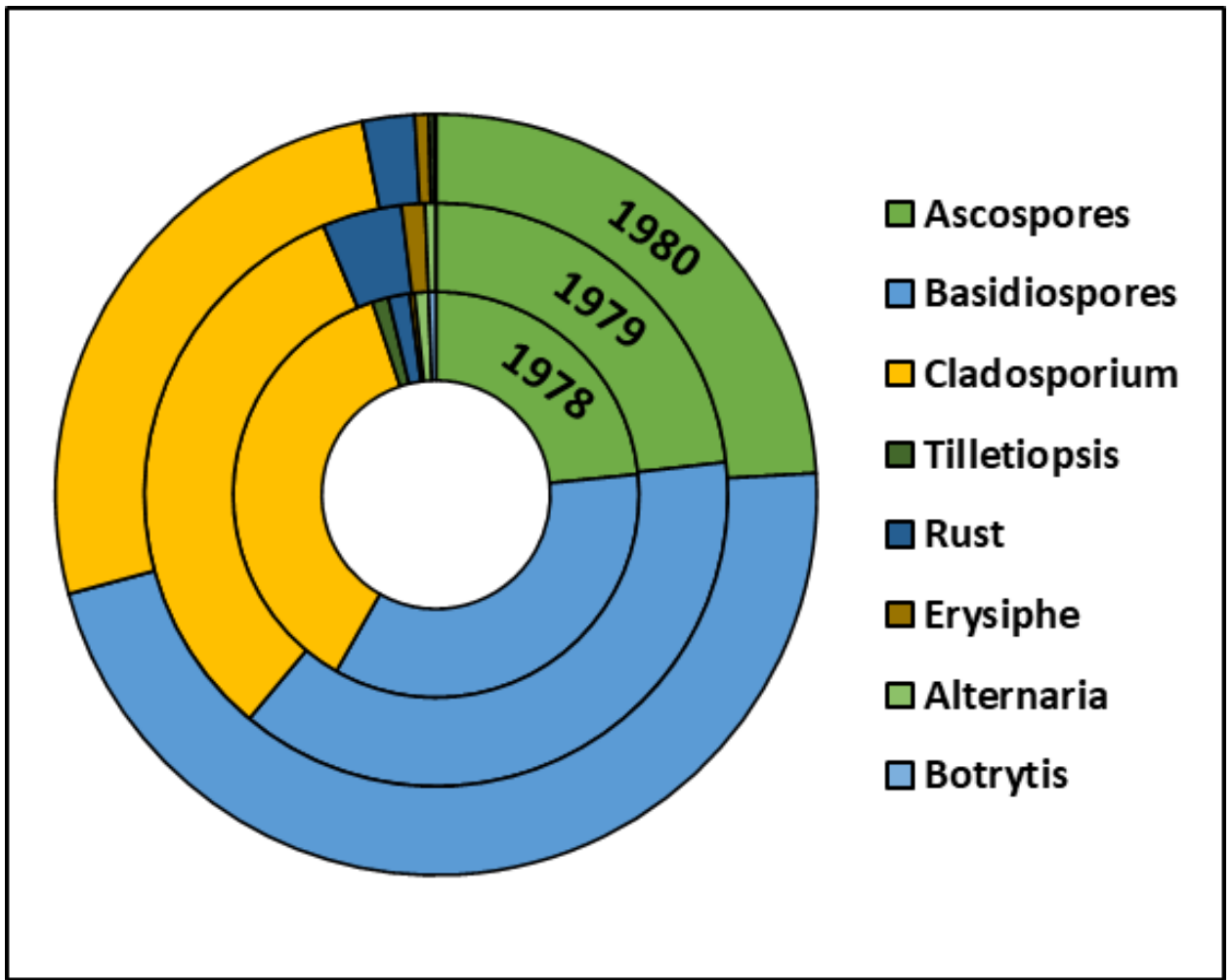


Figure 3.1: Donut chart of fungal spore composition of each year, showing that basidiospore values were proportionally highest in 1980, and *Cladosporium* was proportionally highest in 1978.

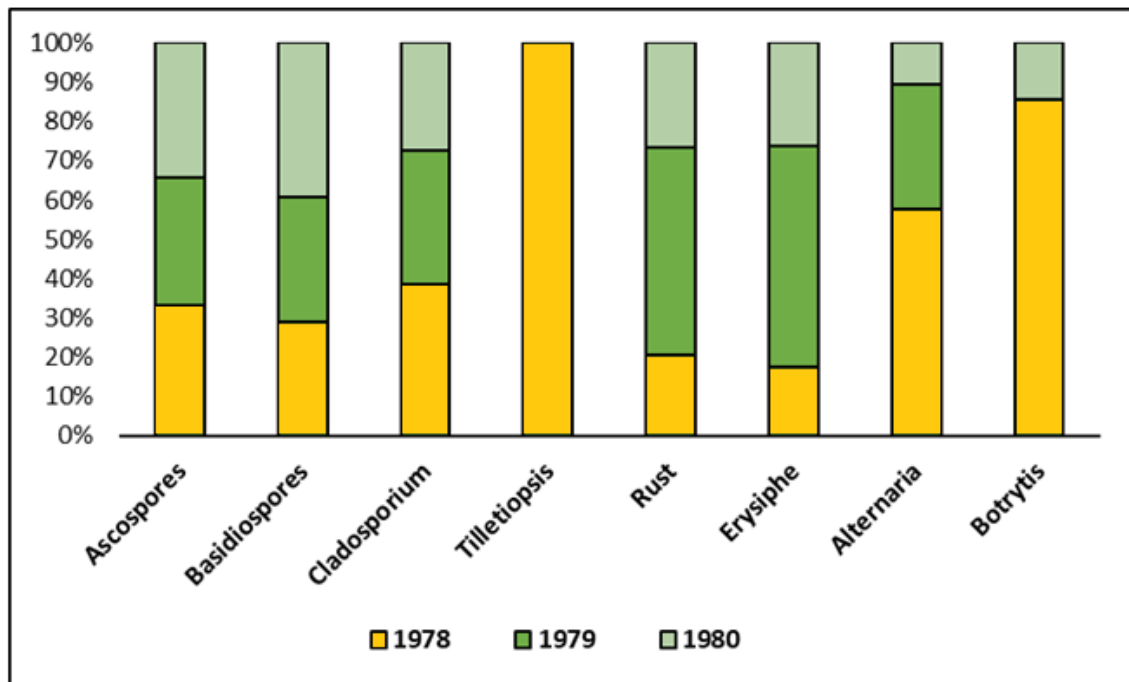


Figure 3.2: Stacked bar graph showing the contribution of each year to the total concentration of each spore type. Of note is the fact that in 1978, *Tilletiopsis* concentrations were high enough to be counted, unlike the other years studied.

When all years are aggregated into one study period, the predominant fungal spore types throughout the entire study period were identified as Basidiospores (40%), *Cladosporium* (32%), Ascospores (24%), and Rusts (3%), which represented 99% of fungal spores identified. Other fungal spores that were present in any concentration in all three years of the study period included *Tilletiopsis*, *Erysiphe*, Downy Mildew, *Epicoccum*, *Alternaria*, and *Botrytis*. The concentrations of Downy Mildew and *Epicoccum* were extremely low in all three years.

Figures 3.1 and 3.2 show the differences between the spore concentrations in each year, and how the makeup of each spore type varied throughout the years studied. The spores of highest concentration, Ascospores, Basidiospore, and *Cladosporium*, showed little variance year on year, but some spores had a significant proportion of their total concentration isolated to one study year, with *Tilletiopsis* being the standout figure. Over 99.8% of all *Tilletiopsis* concentrations were observed and counted in the 1978 season, with extremely small concentrations of spores identified in the subsequent years. 1978 also sees significantly larger concentrations of spores identified in the subsequent years. 1978 also sees significantly larger concentrations of *Botrytis* and *Alternaria* spores, as well as relatively lower concentrations of Rusts and *Erysiphe*, respectively, indicating that this year had differing climactic and meteorological conditions to the two subsequent years studied, as outlined in chapter 1.

Figure 3.3 shows a set of box and whisker plots for each month of each year throughout the study period. This gives a clear view of possible differences in seasonal trends of each year and

helps us to directly compare the rise and fall of the respective seasons. All fungal spore concentrations were low in the Spring, (March and April), before beginning to rise in May, with the median fungal concentration value for all three months increasing by 100% or more between the months of April and May. All years see significantly higher values in June, with concentrations rising into the summer months. Data for 1979 continues to rise, before its peak in August, while 1978 data has relatively similar values for both July and August. September shows the first sign of a marked decrease in concentrations for all months studied, signifying the end of the peak fungal fructification period. The lower peak values for the 1978 season, relative to the other two seasons studied, gives further credence to the idea that this season had a markedly different meteorological identity.

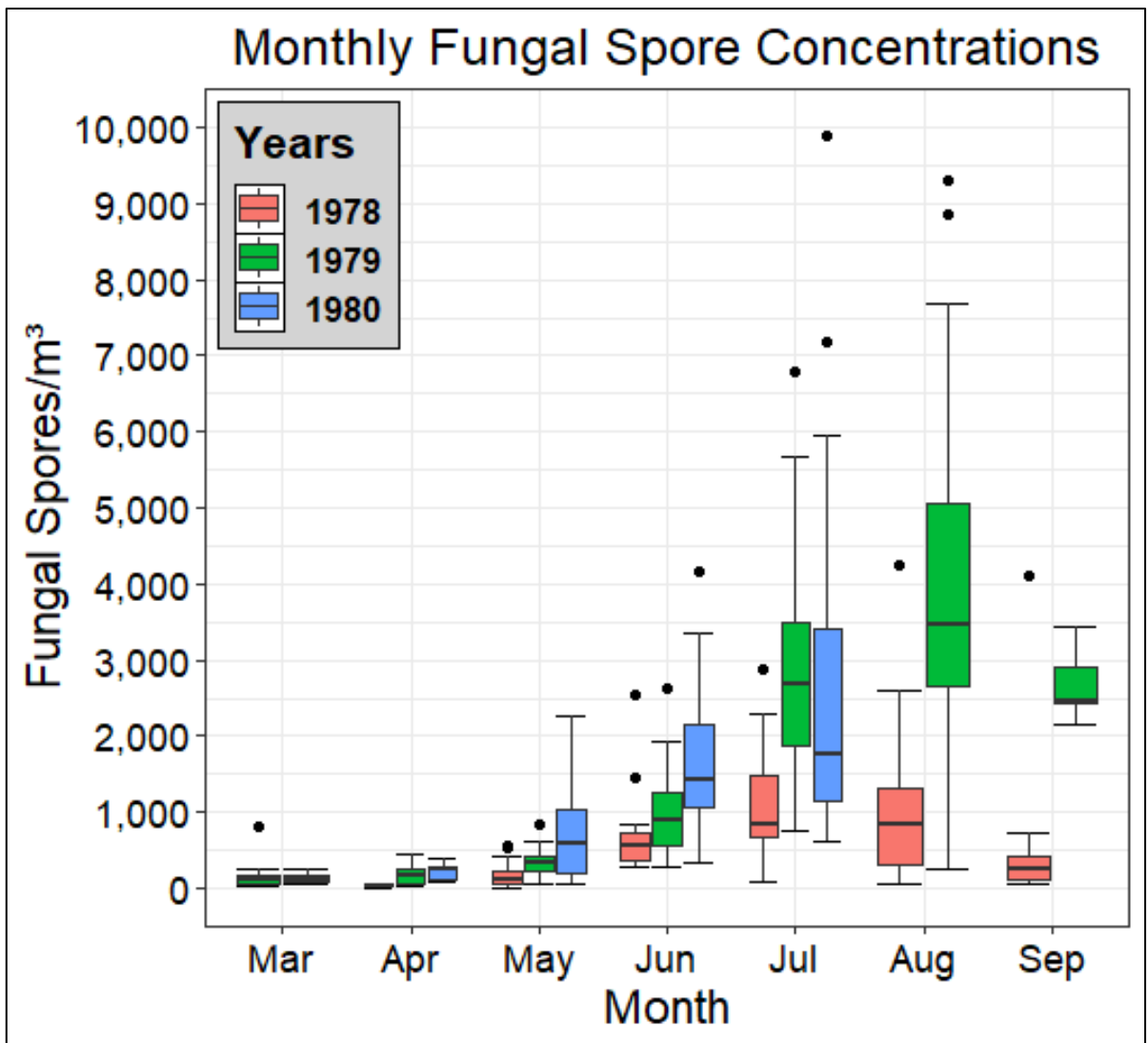


Figure 3.3: Monthly fungal spore concentration box plots for each year of the 1978-1980 study period. July is the overall peak month studied.

When the three years are merged into a “seasonal distribution” showing the average daily concentration of each fungal spore over the 1978-1980 period, the mean Basidiospores peak date fell on the 30th of July. On this date, an average of 6,650 spores/m³ was determined. On three instances, *Cladosporium* averages exceeded this value, with the highest being an average value of 8,931 fungal spores/m³, on July 29th. Ascospores appeared to have a less well-defined “peak” than Basidiospores, with average quantity of fungal spore in the lead up to the peak fructification period being of a similar concentration to those found throughout the rest of the season. During the anticipated “peak period” for Ascospores, there were several days with extremely low spore counts, such as July 16th, which had an average peak of only 269 spores/m³. This indicates that while seasonality does play a role for all three major spore types, a second factor also has a strong influence on ascospore concentrations, allowing for significant concentration changes from one day to the next. Consequently, looking solely at seasonality for ascospores will not be as useful as it will be for other spore types when attempting to determine possible fungal spore expected concentrations at certain times of the year.

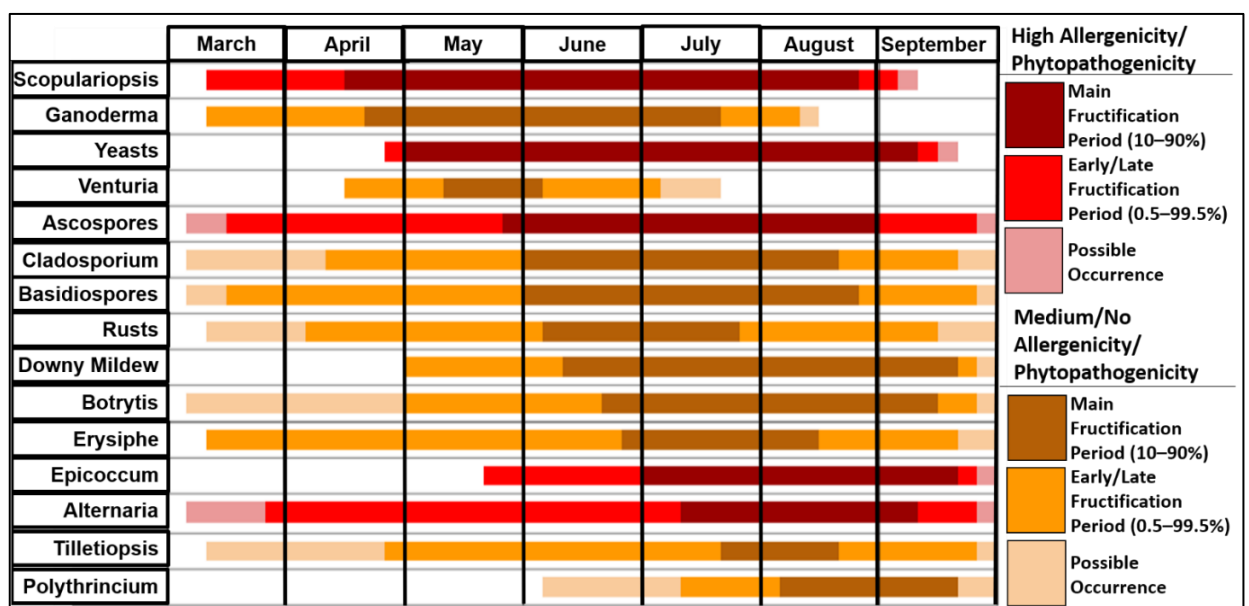


Figure 3.4: Fungal spore seasonal peak periods and fructification periods of allergenic spores from 1978-1980.

Figure 3.4 is a fungal spore seasonal distribution chart, constructed using all the available historical data. It was created in order to determine the peak fructification periods of fungal spores identified during this study period. The Peak Fructification periods for *Scopulariopsis* and yeasts were both longer than four months, lasting from the beginning of May to the middle of September for yeasts and from the beginning of April to the beginning of September for

Scopulariopsis, respectively. *Venturia* had the shortest Peak Fructification period, peaking in sections of May and June for less than four weeks. With only *Scopulariopsis* and *Ganoderma* having discharged at least 10% of their annual totals before May, *Scopulariopsis* was the spore type to have achieved its peak date first. At the other end of the calendar was *Polythrincium*, which did not attain peak fructification until August, making it highly likely that the absence of sampling beyond September may have had an impact on the overall spore values measured.

Basidiospores had the highest seasonal spore integral, followed by *Cladosporium*, and Ascospores. The reason for the concentrations of this spore type being so high could be indicated by the similar results obtained by McDonald and O'Driscoll, (McDonald and O'Driscoll, 1980), in which the definition of basidiospores was very broad, encompassing all micro - organisms of a darker pigmentation and all without identifying features such as containment within an ascus being. There simply is no description of how basidiospores were identified during either campaign beyond this. *Cladosporium* was the spore with the highest daily peak concentrations, despite having the second highest "seasonal spore integral" concentrations.

The majority of studies using the Hirst volumetric sampler during this time period, in the 1970s and 1980s, concentrated on pollen grains, which are larger and easier to distinguish (Gregory, 1978; Mandrioli et al., 1982; Mullins et al., 1977; Viander and Koivikko, 1978). While many studies on fungal spores were conducted at this time, a significant majority of them had an instrumental evaluation as their primary focus. Regarding fungal spore counting and analysis, as well as comparison with other instrumentation, the usefulness and practicability of the Hirst device, as well as its potential applications, were still frequently investigated (Burge et al., 1977; Käpylä and Penttinen, 1981; Lyon et al., 1984; Perrin, 1977). In other cases, investigations on the seasonality of particular spore types, or comparisons between regions in particular countries were completed. One such study looked at the amount of precipitation and humidity needed to trigger ascospore discharge (Johnson, 1979).

In one long-term investigation, Hirst volumetric samplers were operated at four different places around Finland in the mid-1970s (1974–1976) (Rantio-Lehtimäki, 1977). Two of the Finnish sites have "Boreal" climatic classifications and are located at latitudes substantially higher than Ireland (Beck et al., 2018). Both of the southern sampling locations are coastal and fall under the "Humid Continental" climate classification (Beck et al., 2018). These two sites can be compared to the 1979–1980 data acquired in Dublin, with monthly mean temperatures varying from a low of -3.8°C to a high of 18.1°C throughout the year ("Etusivu - Ilmatieteen laitos," 2022).

Similar to what was noted in the Dublin dataset, this Finnish study discovered an initial peak in spore densities in mid-July for both locations. It's interesting to note that a second, greater fungal spore peak was also found in Finland in late August. This once again demonstrates that it may have been premature to stop measuring fungal spores in Dublin in the late summer of each research year. Particularly so, as when counting in Dublin had stopped, the majority of fungal spore species had not yet dropped significantly below their "peak" values.

With 53% of all spores discovered being *Cladosporium* spores, they were by far the most prevalent spore type in southern Finland. As latitude increased, *Cladosporium*'s share of total spores decreased, falling to 16%, and then 4% as one travels north, and away from the continent. Previous work has been published exhibiting an in-depth examination of this monitored data. (Martínez-Bracero et al., 2022)

The calculation method used to construct the above chart (Figure 3.4) was the percentage technique, which has been applied in the past to describe pollen seasonality across multiple years (Adams-Groom et al., 2020; Bednarz and Pawłowska, 2016; Martínez-Bracero et al., 2015). In this instance, the 90% method was chosen, in which the main fructification period starts on the day that 10% of the total fungal spores for the year have been counted. It similarly comes to an end on the day when 90% of the spores for the entire year have been counted. The terms "early fructification period" and "late fructification period" refer to periods outside the main fructification period where at least 0.5 percent of the total fungal spore concentration of the year has already been accounted for (for the early period) and where at most 0.5 percent of fungal spores were remaining after this point (for the late period). Each month was broken into six 5-day segments, with months of 31-days having six days in their final segment, and the final portion of February having just three days.

The next value required was the arithmetic mean of each segment. To determine the arithmetic mean, the five daily values were put together and divided by 5. (Or divided by 6 or 3 accordingly). Then, using a 3-digit code that included the month's abbreviation and the segment's number, each section was classified. For instance, Ja1 to Ja6 stands for the six periods of January and Jn1 to Jn6 for the six periods of June. Many earlier works, mostly pertaining to pollen calendars and their development, have employed this method we used for creation of our fungal spore fructification period charts. Usually, methods such as these have been used to create historical bioaerosol calendars, with the vast majority specifically in relation to pollen calendars and their methodology (Ajouray et al., 2016; Lo et al., 2019; Pecero-Casimiro et al., 2020; Ščevková and Kováč, 2019).

It should be noted that this should be viewed as more of a historical fungal spore database than a calendar, as a sufficiently long, continuous monitoring programme was not in place at the time of this initial study. Generally, a pollen or fungal spore calendar requires at least 5 years' worth of data to reliably identify trends and normalize the impacts of major weather events (Martínez-Bracero et al., 2015).

3.3. Contemporary Monitoring Sites

While the ultimate aim for this project is the forecasting of future fungal spore values, the first step along that path was the commencement of traditional bioaerosol sampling. This was to establish a baseline of fungal and pollen concentration, and to build a robust database for future model and forecast development. Because of this, in 2017, the first contemporary traditional bioaerosol sampler was installed in Dublin, when the Hirst-Lanzoni 7-day sampler was installed on the roof of the TU Dublin Kevin Street building.

The modern fungal spore monitoring campaign was undertaken as a part of this doctoral thesis between 2017-2020. This long-term monitoring campaign had been running for 4 years at the time of data collection and analysis for this project. The Dublin monitoring campaign was the first campaign carried out whose aim involved analysing the resulting data and discovering the fungal spore dispersal character of Dublin, and subsequently all of Ireland. Three locations, Cork, Carlow, and Sligo were monitored as part of a comparative campaign, and one location Dublin, was continuously monitored for 4-years, and is still in operation today. All fungal spores identified were included in time series analysis of total fungal spores, and only fungal spores of national and international interest, were included for the species distribution investigations. In some instances, many fungal spore types were only categorised or identified for one of, or some of the years studied. Ten fungal spore types were counted consistently every year in Dublin from 2017-2020, with the five most common, and the five included in this chapter being Ascospores, Basidiospores, *Alternaria*, and the two *Cladosporium* species, *Cladosporium Cladosporioides*, and *Cladosporium Herbarum*, which were combined under the one name, "*Cladosporium*" for this study. The main fungal spore types varied slightly in each location. The predominant fungal spore types in Dublin were identified as *Cladosporium* (50.8%), Ascospores (35.6%), and Basidiospores (7.2 %). These three spores combined represented 93.6% of all major fungal spore types identified during the sampling period.

As counting occurred over a four-year period in Dublin, differences in spore concentrations can be identified and noted. Overall spore numbers were far lower in 2018 than in the other three years. Investigation into potential reasons behind this was carried out further in this

chapter by comparing fungal spore concentrations to meteorological conditions. The country-wide multisite comparison campaign used data from all four locations, Carlow, Dublin, Sligo, and Cork, while a longer-term contemporary conventional fungal sampling was conducted just in Dublin (Figure 3.5). The Dublin site was chosen because of the significance of the city, which is also one of only 15 primate cities (A city that's at least twice as large than the next largest city in that country, with regards to population or contribution to the economy etc.)(Jefferson, 1989) in the European Union and has the fifth-highest relative primacy of any city in the EU (Relative primacy of 4.8 over the next largest city, Cork). Dublin is also significant as the capital of Ireland, and long-term sampling here was easily facilitated as the university is in Dublin, meaning no long commute was required between the sampling site and the laboratory.

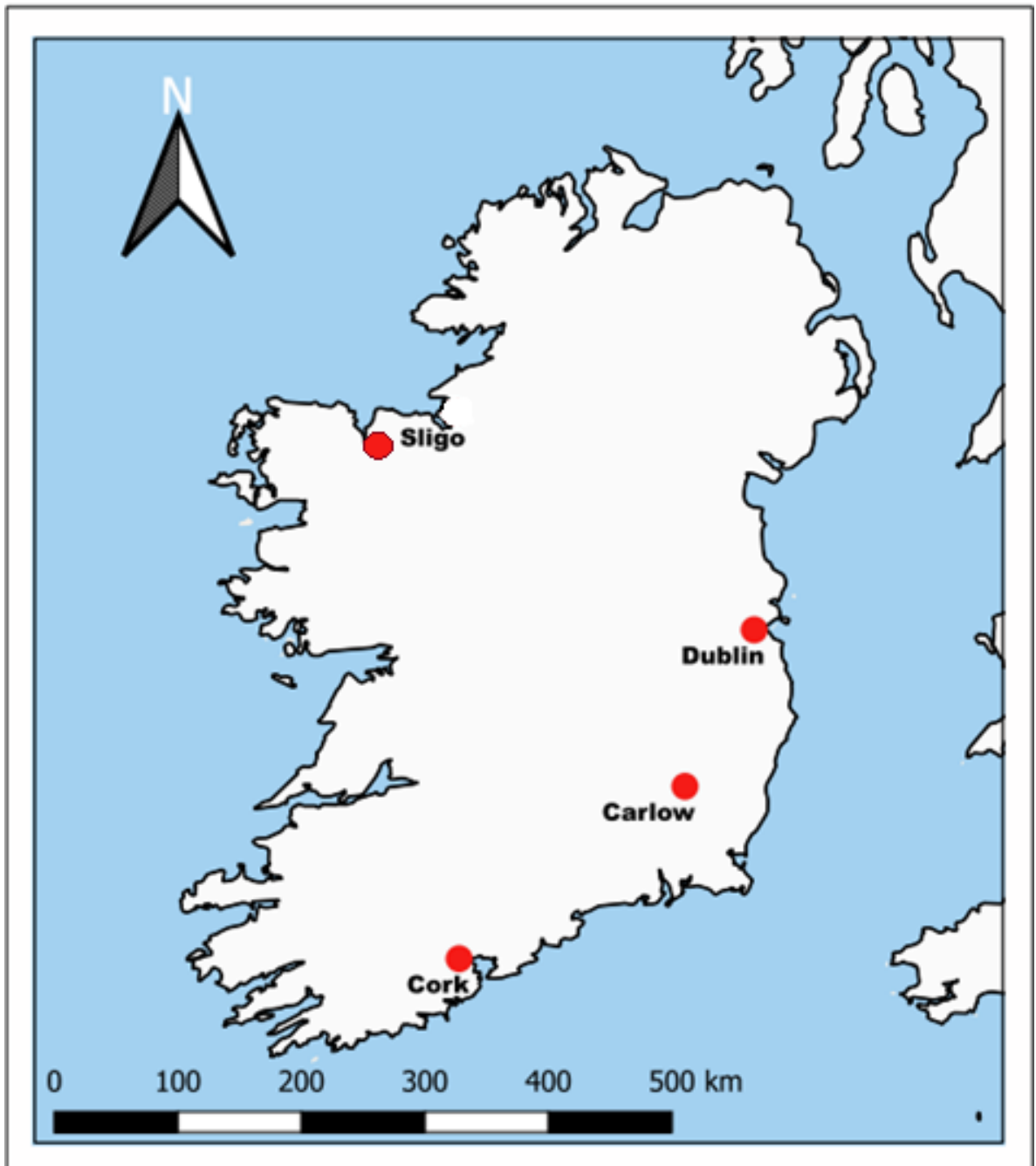


Figure 3.5: Sampling sites used in the contemporary fungal spore study.

The Dublin sampling location for the long-term dataset had instrumentation installed on the rooftop of the five-story TU Dublin Kevin Street building (53° 20' 12.4"N, 6° 16' 4.25"W) from 2017 to 2020. (approx. 20m high). The location has average annual temperatures of 9.9°C and lower annual rainfall (758mm) than the national average (1200mm) (“Historical Data - Met Éireann - The Irish Meteorological Service,” 2022). The Cork, Carlow, and Sligo locations both operated sporadically over the project's duration. During the busiest time of the year for fungi in 2021, all four locations were open. The results of both the long-term Dublin study, and the multi-location comparison are discussed below.

3.3.1. Overview of Prevalent Fungal Types and Trends in Dublin

For Dublin, 26 different fungal spore types were identified over the full campaign. The predominant fungal spore types were identified as *Cladosporium*, *Alternaria*, Ascospores, and Basidiospores. These three spore types combined represented 93.6% of all major fungal spore types classified during the sampling period.

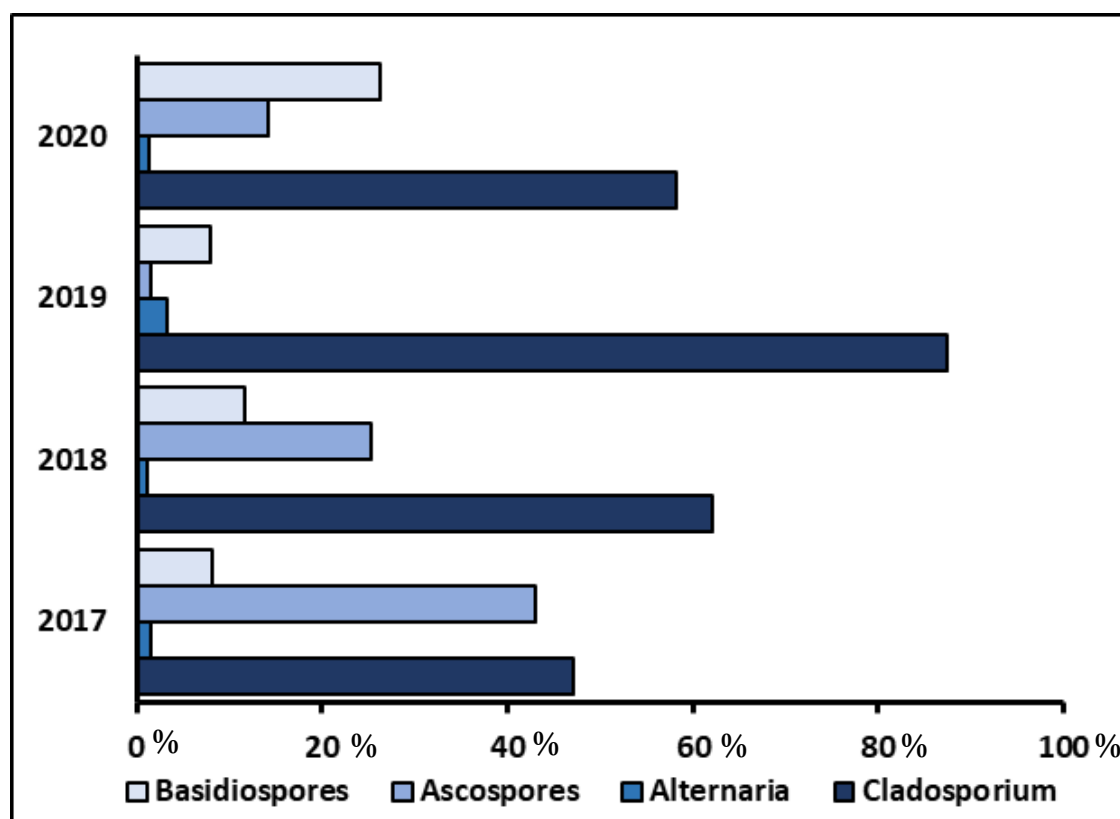


Figure 3.6: Clustered bar charts showing the percentage makeup of the four major fungal spore types from 2017 to 2020.

In Figure 3.6, above, a set of clustered bar charts is shown, with each bar representing a year studied, and the segments of each bar representing the four major spores analysed during the campaign. The change in spore type distribution in 2019 is of note, with *Cladosporium* comprising almost 90% of all spores counted during the year. Conversely, in 2017 less than half of all fungal spores counted were *Cladosporium*, due mostly in part to the large proportion of Ascospores which comprised the spore totals. In all 4 years studies, *Cladosporium* was the dominant fungal spore type. The second most frequently encountered fungal spore type was Ascospores in 2017 and 2018, but relative concentrations decreased to the point that

Basidiospores were the spore type of second highest concentration in 2019 and 2020. Studies have found that the ratio of Basidiospores to Ascospores can vary greatly by region and by year, depending on changes in regional climates and local agricultural factors (Rivera-Mariani and Bolaños-Rosero, 2012).

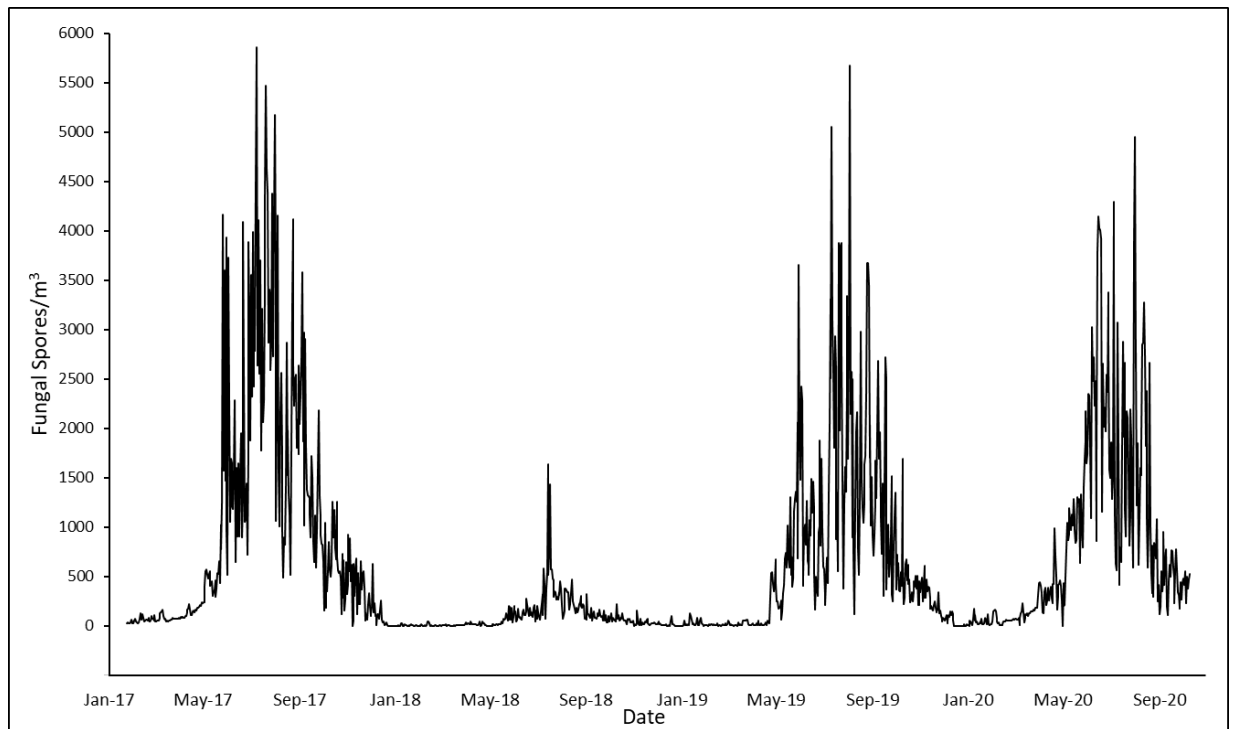


Figure 3.7: Time series chart of contemporary fungal spore concentrations in Dublin from 2017 to 2020 inclusive.

Above (Figure 3.7) is a time series of the fungal spore concentrations from 2017, 2018, 2019, and 2020. Not every single day was sampled, as at various points, events such as the Coronavirus pandemic, electrical faults, or staff illness resulted in some gaps in the dataset. In order to repair these gaps, an interpolation was carried out. The STL filtering procedure was used, in which the existing data in the database was used, and a seasonal trend composition based on the LOESS smoother is carried out (Cleveland et al., 1990). This is a recommended interpolation methods for bioaerosol time series repair and is the most appropriate method for datasets of at least three years in length, when there are no nearby traditional monitoring bioaerosol stations. This method is included in, and was executed as a part of the AeRobiology R package (Rojo et al., 2019). While the time series graph was made using this interpolation data, any other statistical analysis was carried out without the interpolated data, using only the days actually measured. This includes calculations of season start date, end date, and season length, peak fructification periods and peak dates, and all comparative research, be it

between years, between instrumentation, or between spore types. Based on the time series analysis presented in Figure 3.7, the years 2017, 2019, and 2020 all exhibited fungal spore concentrations that were comparable to one another throughout the year, as well as relatively comparable peak fructification date concentrations. The peak date occurred a little bit earlier in 2017 than it did in any of the other years that were examined. 2017 concentrations starting to rise rapidly at the end of June, reaching their highest point on July 8th. In 2018, the peak date was on July 14th, one week later. In 2019, a rise in concentrations of the same kind was not seen until the middle of the month of July, with the peak date arriving on August 3rd. The peak did not occur until July 31st in 2020, similar to what was seen in 2019. Additionally, total concentrations grew to a greater level during the peak season in 2017, as compared to 2019 and 2020.

In contrast, the levels of fungal spores were extremely low in 2018, reducing by roughly a factor of 4 when compared to the levels recorded in the surrounding three years. This was initially a surprising finding, until external factors were considered. 2018 was a highly unusual year, meteorologically in Ireland, during crucial periods in both the initial propagation and subsequent dispersal phases of the fungal spore season (Falzoi et al., 2019). The Winter and Spring were dominated with multiple stormfronts that brought record snowfall across the region from Storm Eleanor and Storm Emma. This hampered the growth of many fungi and plant species, with low concentrations seen in pollen grain analyses also (Markey et al., 2022). Following this, high pressure systems sat on top of the island throughout the summer, resulting in up to 40 days without any rainfall, and very low windspeeds, resulting in drought like conditions that impacted the phenological cycle across much of Europe, and had an effect on many aspects of the Irish ecosystem (Caloiero et al., 2018; O'Dwyer et al., 2020).

Studies comparing drought years to normal years, as it related to fungal spore concentrations, have been carried out in the past. Researchers in Turkey discovered significant reductions in the predicted spore concentration whenever there was drought or protracted heatwaves (Arslan, 2017; Çeter et al., 2020). In a study, which charted the fungal spore concentration of Nide, Turkey in 2014, researchers saw a 50 percent decrease in fungal spore concentrations during drought associated with low rainfall. For context and comparison, during the summer of 2018, Ireland had a drought that by some calculations lasted as long as 53 days in total (Moore, 2020). As a result, while the start and end dates, and ratios of different spores in 2018 can be compared and analysed against the other years in the study, the actual concentrations are just not comparable due to the dramatically unique meteorological conditions.

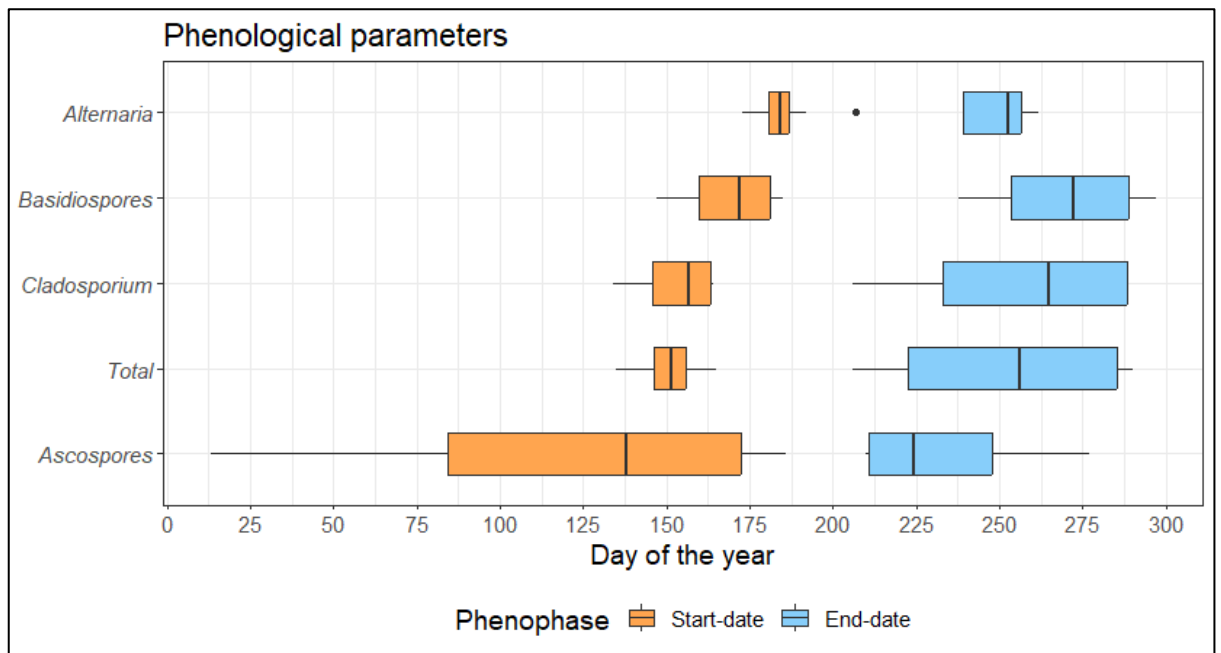


Figure 3.8: Start and end date box plots of major spore types in Dublin collected by the Hirst during the campaign.

A collection of boxplots depicting the average beginning and ending dates of the phenophase of each major fungal spore is presented in Figure 3.8, along with an aggregated "Total" plot representing all spores studied. It is clear from the graph that the *Alternaria* phenological season was the shortest of all major spore types. The beginning of the *Alternaria* season occurred later than the beginning of any of the other shown spore type. The conclusion of the *Alternaria* season occurred at an earlier date than all other spore types as well. On the other hand, ascospores had the longest phenological season, starting the season the earliest date by a large margin. While they were the spore that reached the end of their season earliest, it is not enough to outweigh the extremely early start date.

The extent of the variance in the beginning and ending dates of each spore type between each of the examined years is represented by the width of each boxplot. This provides us with more information again. The "start date" boxplot for Ascospores has an IQR (interquartile range) that spans nearly 100-days, highlighting the impact that external variable factors can have upon initial ascospore fructification. This high level of interannual variation has been seen in other studies, with conclusions being that as there is no "optimal" date of release, local conditions have a stronger impact than they would on other spore types (Marçais et al., 2009). The season of *Alternaria* was the most well defined, with the end date IQR spanning only 15 days, and the start date spanning just one week. With the Exception of Ascospores, all spore types had a narrower start date window, than their end date. Studies have found that the start

dates across the fungal kingdom are more location and weather specific, and that end dates tend to be more unpredictable and variable from year to year (Anees-Hill et al., 2022).

The phenological season for total spores appears influenced more strongly by the extremely high proportion of spores that are *Cladosporium*. The very narrow start date is of interest, as it has been seen that the start date of many spore types is a critical predictor of their survival rate, so timing that accurately is far more important for fungal spores than when the end date occurs (Lagomarsino Oneto et al., 2020). Direct comparisons may be made between related research as this method of establishing the start and end dates is the accepted and most extensively utilized in the aerobiology field. According to a study conducted in France, the length of the *Cladosporium* season shrinks as sampling distance from the equator increases (Sindt et al., 2016). In southern France, the season lasted 220 days, whereas it lasted 160 days in central France. Our Dublin study, which was conducted at a higher latitude, had a season length of between 100 and 115 days for each of the years examined, which is consistent with this trend. A future objective would be to replicate this study at the higher latitudes in Ireland, as the existing samplers in Cork, Dublin, and Sligo are each roughly one degree apart in latitude.

Alternaria had the shortest season of any spore in our study, lasting only 8 weeks on average from the 9th of July to the 7th of September. Once more, this is shorter than the seasons of other continental studies and aligns once again with expected variances due to change in latitude. According to research conducted in Kraków, Poland, the season begins three weeks sooner and ends one week later than it does in Ireland, however *Alternaria* has the same peak duration there as it does in Ireland (Stępalska and Wołek, 2005). Although Ireland is on the fringe of Europe and extends into the Atlantic Ocean, other spores in the Kraków study also show this trend, demonstrating that the seasonal pattern of fungal spores is substantially tied to and reflective of the European continental season as a whole.

The data presented here outlines the current state of the fungal spore season in Ireland; however, information for the entire calendar year is only available for a single 4-year period. As a consequence, the data does not yet demonstrate any potential long-term trends in the beginning, ending, peak dates, or duration of the season. Multiple research studies conducted in the UK have come to the conclusion that the lengths of distinct spores, as well as their beginning and ending dates, are subject to gradual change over the course of time and must be continuously checked to prevent data obsolescence (Andrew et al., 2018; Corden and Millington, 2001). An investigation that spanned 25-years into the start date of the *Alternaria*

season in Derby, United Kingdom, found that the start date had moved forward year after year to an earlier date in the season over the 25-year study. The start date, which was at the very end of June in 1972, had shifted all the way to the very beginning of June by 1997. (Corden and Millington, 2001). The most important factor in this season-shifting in fungal spores is climate change, and it is quite probable that this trend will grow more prominent with time. Because of this, it is highly unlikely that actual physical monitoring of bioaerosols will ever be completely replaced by advanced computer models and forecasts. This is because the degree of impact that climate change is having on bioaerosol seasons, diversity of species, and allergenicity cannot ever be guaranteed or accounted for in its entirety without real-world sampling.

3.4. Multi-site traditional monitoring campaign in Summer 2021

The CORINE land cover maps show the sampling locations used in the project (Figure 2.9). From the start of June to about the middle of August 2021, these sites operated simultaneously. There is a substantial disparity between the rural sites (Carlow and Sligo) and urban sites (Cork and Dublin), as can be seen in the image. The land surrounding the urban sites is predominantly used for commercial, industrial, and residential purposes (Purple). Conversely, the rural sites feature a greater concentration of pastures, agriculture, and non-irrigated arable land, with some peat bogs close by.

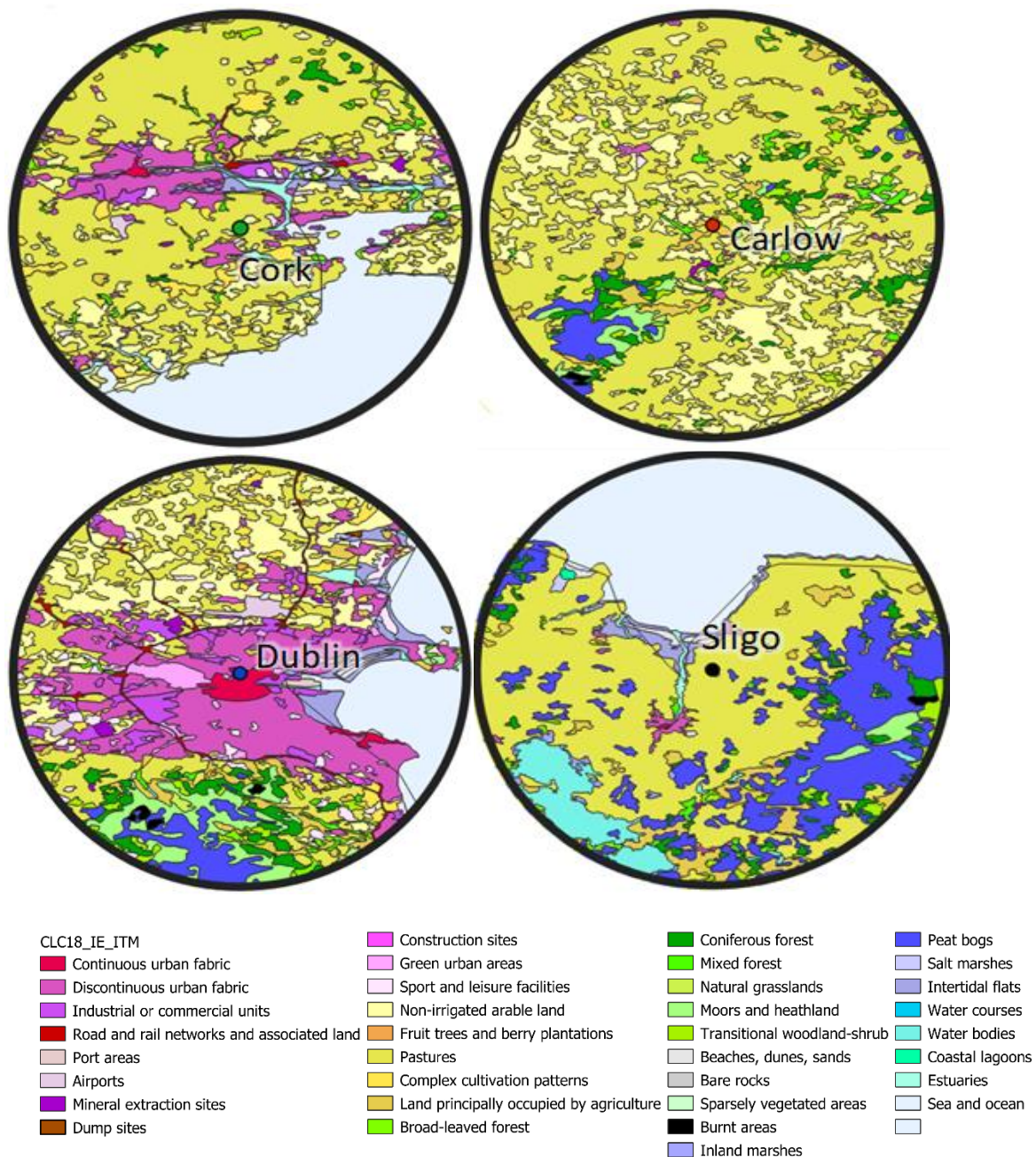


Figure 3.9: CORINE landcover maps of the four locations where fungal spore sampling occurred.

The two locations that are closest together in distance are those of Dublin and Carlow. The two-sampling point are roughly 70km apart. Dublin is the urban site with the highest population. In Figure 2.9, the scale of the built-up area can be seen in purple, as can the blue of the sea. This contrasts with the Carlow landcover map. Of the two rural locations, Carlow is further inland, allowing for further climactic comparison (Figure 3.9). There are many differences between the urban and rural settings, despite the fact that the main fructification periods and the time of greatest fungal activity are near identical in Dublin and Carlow. The

most noticeable shift across all years is the ratio of *Cladosporium* to other fungal spores. In Carlow, almost 75% of all fungal spores were identified as *Cladosporium*, compared to about 50% of all fungal spores in Dublin.

This was not an unexpected finding, as the Carlow sampling site is surrounded by grassland, which is a vector for *Cladosporium* growth, while the Dublin sampling site, being in the centre of a metropolitan urban area, is surrounded by sterile buildings rather than grassland. Additionally, The Carlow sampling device is raised just above the ground on a wooden platform to allow its sampling inlet to be positioned above long grasses, whereas the Dublin sampler is positioned much higher, on top of a 5-story building, further enhancing the difference in distance required for *Cladosporium* spores to travel before being collected by the respective samplers.

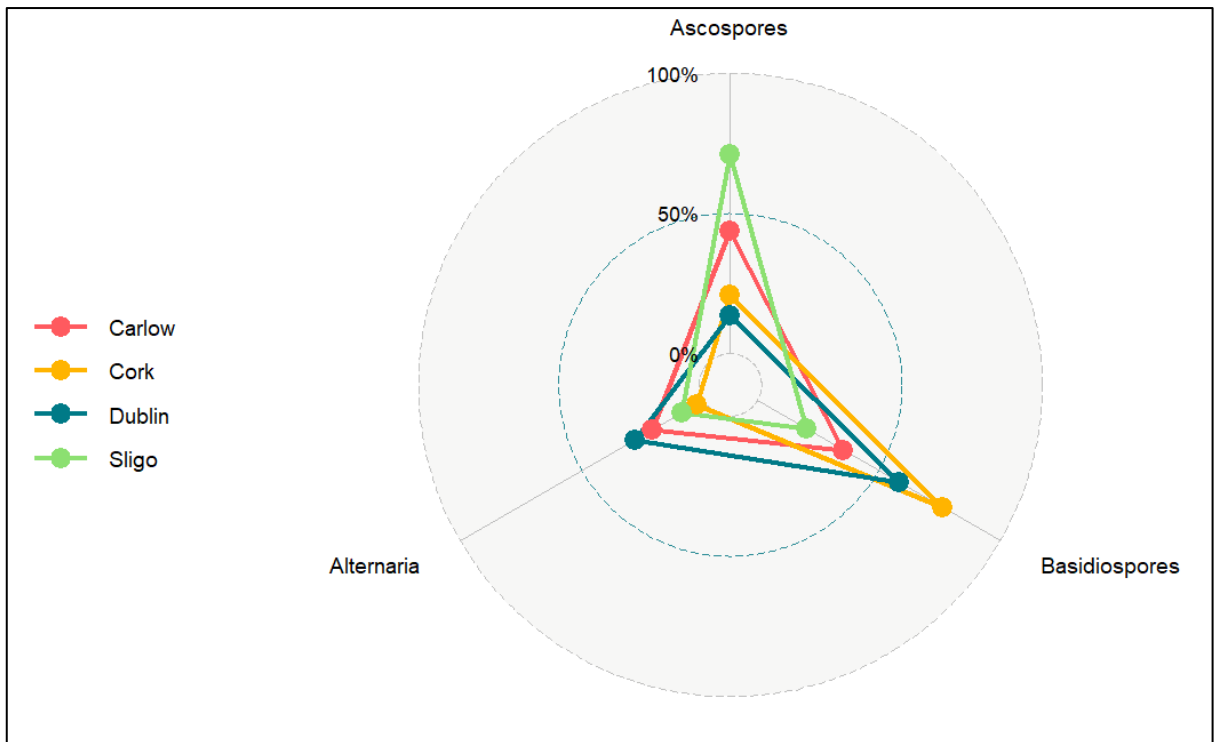


Figure 3.10: Spider Plot showing the compositional distribution of the major fungal spore types (less *Cladosporium*) at all four locations where sampling took place (Summer 2021).

Figure 3.10 (above) displays a spider plot of the relative ratios of Ascospores, Basidiospores, and *Alternaria* at each of the four locations—Carlow, Cork, Dublin, and Sligo—during the peak fructification period of June through August 2021. *Cladosporium* was not included as it made the graph unreadable and did not add any new information. The distance from the circle's centre indicates the proportion of the selected spore types in a particular area, and each

colour corresponds to a different county sampling site. The urban-rural division in terms of relative Ascospore and Basidiospore densities is the spider plot's most striking feature. The relative concentrations of Basidiospores are unmistakably higher than those of Ascospores in the two urban sampling sites of Dublin City and Cork City. This observation is contrasted with the rural sampling sites of Sligo and Carlow, where the relative concentrations of ascospores appear to be significantly higher than those of basidiospores.

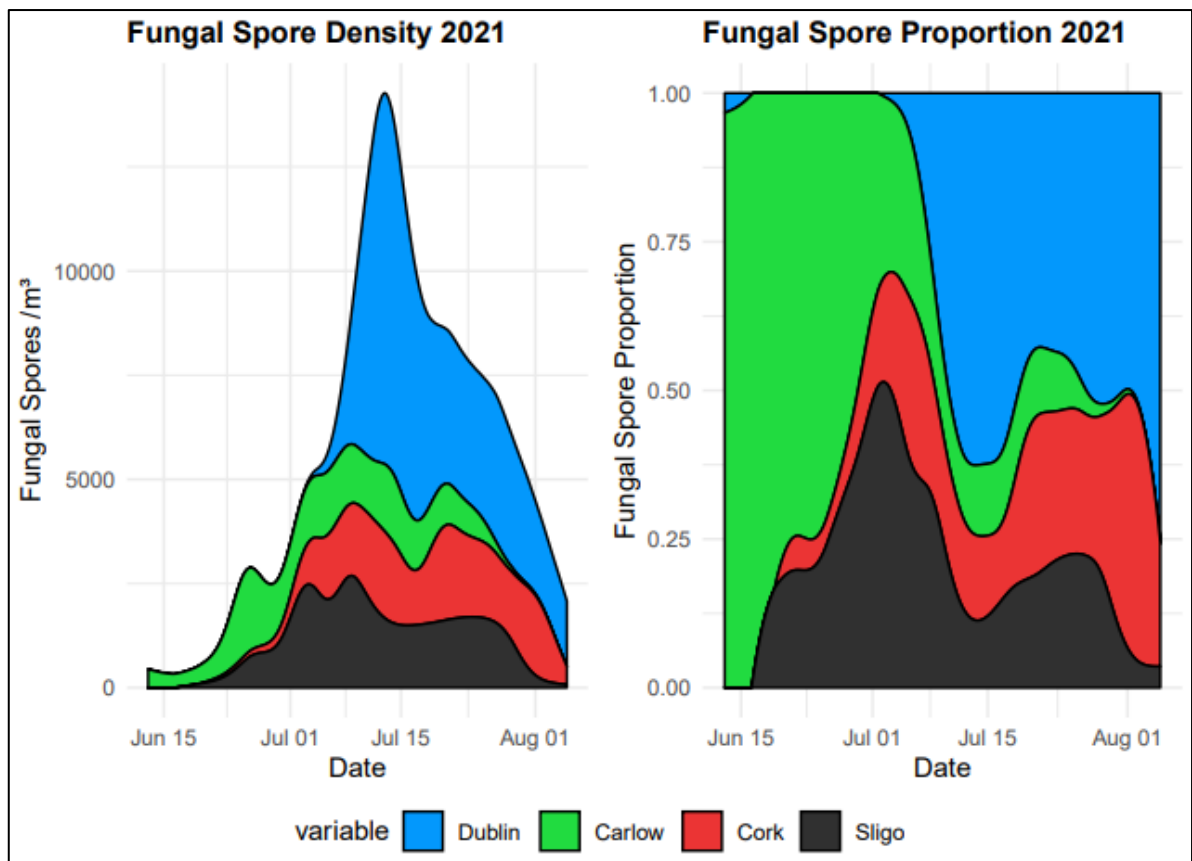


Figure 3.11: Fungal spore concentration and proportional density for Dublin, Carlow, Cork, and Sligo (Summer 2021).

A comparison of the four sampling sites throughout the course of the peak fructification period of 2021 is shown in Figure 3.11 (above). According to the data, the second week of July was the peak period for the island as a whole, when spore concentrations were relatively high at all four sample sites. Higher proportional Carlow concentrations at the start, and Dublin concentrations at the end of the summer, bookend the study, with a more balanced proportional during the middle of the sampling campaign. A bimodality is visible in the Carlow and Cork distributions, with both locations showing clear peaks, falls, and subsequent peaks within the month of July. Throughout the entire campaign, the patterns of Carlow and

Cork appear to follow each other closely, with Sligo concentration not appearing to differ greatly either.

However, the Dublin dataset does not exhibit this bimodal pattern whatsoever, while the Sligo time series shows it less clearly, with a sustained plateau throughout the month of July instead. Even while Dublin shows little to no fungal spores at the start of the sampling, there is a strong surge in concentration in mid-July. The fact that no other site replicated this peak to the same degree demonstrates the possible impact that localised climate/weather and anthropogenic sources may have on sites. This first nationwide comparative traditional sampler study emphasizes the necessity to establish a more comprehensive network of instruments and monitor bioaerosol seasonal patterns throughout the island. The peak in Dublin was not replicated in the other sampling sites, and the similar concentration patterns of Carlow and Cork, are both worthy of further investigation. Similarly, the fungal spore release pattern variations by spore or pollen type are deserving of a more in-depth analysis, as part of a collaborative research project.

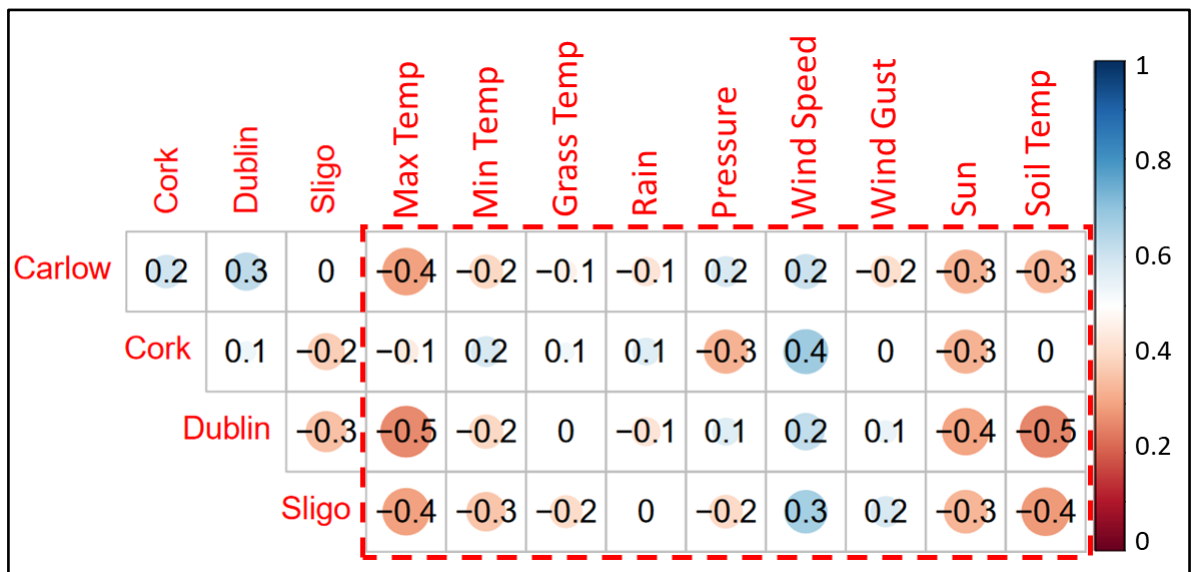


Figure 3.12: Correlation plot comparing fungal spore concentrations at each sampling site, with local meteorological conditions.

As part of an initial investigation, the locations and their respective meteorological conditions were investigated in Figure 3.12. The main objective was to see if fungal spores that develop in different regions of the country, react to the same meteorological conditions in the same way as each other. What was found was that some factors, such as wind speed, had much the same correlative value with spores no matter the location. For most factors there was little difference between locations. The one major exception was temperature.

When one compares the locations to each other, it is clearly apparent that the fungal spores in Cork are reacting differently to the temperature parameters than the other three sampling sites. The strong, negative correlation between temperature seen in Sligo, Dublin, and Carlow, is not clearly paralleled in Cork. Cork had the highest average annual temperature of the four locations during the sampling period of Summer 2021. Therefore, it could be hypothesised that in the Summer, there is a certain temperature, that when reached, diminishes fungal spore dispersal. As Cork was warmer, the temperature never decreased to the level that would allow a resulting concentration increase. Studies have found that temperature thresholds do exist for a variety of spore types, at multiple levels (Hollins et al., 2004; Martínez-Bracero et al., 2022; Oliveira et al., 2010).

Several studies have previously investigate the operation of multiple Hirst devices in various locations within the same state or nation simultaneously, over one year, peak season, or even week (Hollins et al., 2004; Lacey, 1962; Oliveira et al., 2010; Palmas and Cosentino, 1990; Patel et al., 2018; Rodríguez-Fernández et al., 2022). Repeatedly, studies find that when urban and rural sites are directly compared, the rural locations possess fungal spore concentrations that are higher by considerable quantities than those found in nearby urban centres (Oliveira et al., 2010) (Palmas and Cosentino, 1990). The only exception to this rule was that urban areas can sometimes possess much larger concentrations of basidiospores than the same country's rural areas (Oliveira et al., 2010). This pattern of increased basidiospore concentrations in urban areas is directly reflected in our own results (Figure 3.10).

Despite trends indicating that the majority of spore types are more common in rural areas, local effects can cause significant variances between locations within one urban centre. One study comparing the concentrations of fungal spores collected at 5 samplers from the same metropolitan area (La Vegas, USA) discovered significant heterogeneity between samplers even only a couple of city blocks apart (Patel et al., 2018). They argued for the greater use of bioaerosol samplers in "microenvironments" in order to better account for local factors such as the growth of younger plants in "newer developments" of the city. A comparative study in Malaga, Spain found similar results, with the outcome of their study being the increase of samplers in the urban centre from two samplers to three (Ruiz-Mata et al., 2023).

With regard to specific spore types, a Saudi Arabian study found that one city (Jizan) exhibited much larger concentrations of basidiospores than two other cities (Jeddah and Dammam) (Hasnain et al., 2005). Given that Jizan and Jeddah are the closer together cities in the study, and both sit on the Red Sea coast, while Dammam is located on the Persian Gulf coast, this

was an unexpected finding. The researchers in this project came to the conclusion that Jizan's proximity to the Yemeni border was having an impact on the basidiospore concentrations, thus indicating that local factors had a more acute impact upon bioaerosol concentrations than larger geographical and climatic characteristics. When brought back to an Irish context, this raises the possibility that cross-border monitoring between Ireland and Northern Ireland may be of great value to both researchers and citizens, as differences in environmental protection regulations or ecological standards could have inadvertent effects across the border. As well as reviewing bioaerosol impacts, attention on the impact of anthropogenic aerosols is important, as aerosolised particles tend to have little regard for political boundaries, and humans can influence concentration outputs of both particle types.

3.5. Conclusion

This chapter aimed to update knowledge on fungal spore seasonality and distribution in Ireland by analysing all available data as well as generating our own. The data includes daily collected and processed fungal spore samples from the seasons of 2017 to 2020, and recently unearthed daily fungal spore monitoring data from Trinity College, Dublin. The study analysed fungal spore composition from 1978-1980, identifying 23 unique types. Basidiospores (40%), *Cladosporium* (32%), Ascospores (24%), and Rusts (3%) were the predominant fungal spore types, accounting for 99% of the total concentration. The study found that seasonality played a role for all three major spore types, but ascospores had a less well-defined peak. The peak fructification periods for *Scopulariopsis* and yeasts were longer than four months, while *Venturia* had the shortest. Basidiospores had the highest seasonal spore integral, followed by *Cladosporium*, and Ascospores. The absence of sampling beyond September may have affected the overall spore values measured.

After this analysis, our own contemporary data was processed and analysed. In 2018, Ireland experienced a highly unusual year, with record snowfall and drought-like conditions affecting the phenological cycle across Europe. This resulted in drastically lower spore concentrations in relation to the years preceding and subsequent. Overall, the *Alternaria* spore type had the shortest phenological season, with the beginning occurring later than any other spore type. Ascospores had the longest phenological season, starting the season earliest by a large margin. The phenological season for total spores appears influenced most strongly by the high proportion of *Cladosporium* spores.

The data presented in this text provides an overview of the current state of the fungal spore season in Ireland, but only for a 4-year period. Climate change is the most significant factor in

this season-shifting, and it is unlikely that physical monitoring of bioaerosols will ever be completely replaced by advanced computer models and forecasts. As a result, we also investigated the impact of meteorological conditions on fungal spores in different regions of Ireland. Results showed that some factors, such as wind speed, positively correlated with spores, while temperature correlated negatively. Urban areas tend to have higher fungal spore concentrations than rural areas. In international studies, local factors, such as proximity to a national border, also often impact bioaerosol concentrations. This raises the possibility of requiring cross-border monitoring between Ireland and Northern Ireland, as differences in environmental protection regulations or ecological standards could have inadvertent effects across the border.

In conclusion, this work provides valuable insights into the seasonality and distribution of fungal spores in Ireland. The data from both historical and contemporary monitoring campaigns highlight the dominant fungal spore types and their concentrations. The study emphasizes the importance of seasonality in determining fungal spore concentrations and identifies the impact of meteorological conditions on spore numbers. It also highlights the need for a comprehensive network of monitoring instruments to understand the impact of localized climate and anthropogenic sources on fungal spore concentrations. Overall, this research contributes to the knowledge of fungal spore dynamics in Ireland and lays the foundation for future studies on bioaerosols. The amount of time it takes to collect and process all this data was restrictive, and resultantly, other, more efficient methods of fungal spore concentration determination we pursued and investigated, as will be described in the next chapter.

3.6. References

- Adams-Groom, B., Skjøth, C., Selby, K., Pashley, C., Satchwell, J., Head, K., Ramsay, G., 2020. Regional calendars and seasonal statistics for the United Kingdom's main pollen allergens. *Allergy Eur. J. Allergy Clin. Immunol.* 75, 1492–1494.
- Ajouray, N., Bouziane, H., Trigo Pérez, M.M., Kadiri, M., 2016. Variation interannuelle des spores fongiques de Tétouan (Nord-Ouest du Maroc) et calendrier sporal. *J. Mycol. Médicale* 26, 148–159. <https://doi.org/10.1016/j.mycmed.2016.02.018>
- Andrew, C., Heegaard, E., Gange, A.C., Senn-Irlet, B., Egli, S., Kirk, P.M., Büntgen, U., Kauserud, H., Boddy, L., 2018. Congruency in fungal phenology patterns across dataset sources and scales. *Fungal Ecol.* 32, 9–17. <https://doi.org/10.1016/j.funeco.2017.11.009>
- Anees-Hill, S., Douglas, P., Pashley, C.H., Hansell, A., Marczylo, E.L., 2022. A systematic review of outdoor airborne fungal spore seasonality across Europe and the implications for health. *Sci. Total Environ.* 818, 151716. <https://doi.org/10.1016/j.scitotenv.2021.151716>
- Arslan, O., 2017. INVESTIGATION OF TRENDS IN METEOROLOGICAL DROUGHTS IN NIĞDE PROVINCE. *ANADOLU Univ. J. Sci. Technol. - Appl. Sci. Eng.* 18, 919–928. <https://doi.org/10.18038/aubtda.293125>
- Beck, H.E., Zimmermann, N.E., McVicar, T.R., Vergopolan, N., Berg, A., Wood, E.F., 2018. Present and future Köppen-Geiger climate classification maps at 1-km resolution. *Sci. Data* 5, 180214. <https://doi.org/10.1038/sdata.2018.214>
- Bednarz, A., Pawłowska, S., 2016. fungal spore calendar for the atmosphere of Szczecin, Poland. *Acta Agrobot.*
- Burge, H.P., Boise, J.R., Rutherford, J.A., Solomon, W.R., 1977. Comparative recoveries of airborne fungus spores by viable and non-viable modes of volumetric collection. *Mycopathologia* 61, 27–33. <https://doi.org/10.1007/BF00440755>
- Buters, J.T.M., Antunes, C., Galveias, A., Bergmann, K.C., Thibaudon, M., Galán, C., Schmidt-Weber, C., Oteros, J., 2018. Pollen and spore monitoring in the world. *Clin. Transl. Allergy* 8, 9. <https://doi.org/10.1186/s13601-018-0197-8>
- Caloiero, T., Veltri, S., Caloiero, P., Frustaci, F., 2018. Drought Analysis in Europe and in the Mediterranean Basin Using the Standardized Precipitation Index. *Water* 10, 1043. <https://doi.org/10.3390/w10081043>

- Çeter, T., Bayar, E., Eltajouri, N.M.M., İşlek, C., 2020. INVESTIGATION OF FUNGI SPORES CONCENTRATION IN NIGDE ATMOSPHERE (TURKEY) 14.
- Cleveland, R.B., Cleveland, W.S., Terpenning, I., 1990. STL: A Seasonal-Trend Decomposition Procedure Based on Loess. *J. Off. Stat.* 6, 3.
- Corden, J.M., Millington, W.M., 2001. The long-term trends and seasonal variation of the aeroallergen *Alternaria* in Derby, UK. *Aerobiologia* 17, 127–136. <https://doi.org/10.1023/A:1010876917512>
- Etusivu - Ilmatieteen laitos [WWW Document], 2022. URL <https://www.ilmatieteenlaitos.fi/> (accessed 6.29.22).
- Falzoj, S., Gleeson, E., Lambkin, K., Zimmermann, J., Marwaha, R., O'Hara, R., Green, S., Fratianni, S., 2019. Analysis of the severe drought in Ireland in 2018. *Weather* 74, 368–373. <https://doi.org/10.1002/wea.3587>
- Galan, C., González, P.C., Teno, P.A., Vilches, E.D., Rodríguez, A., Jesús, M., Sánchez, A., Soler, B., Ramos, B., Artero, C., Fernández, C., González, C., González, F., Minero, G., Álvarez, I., Rodríguez, J., García, L., Andrés, M., Grau, M., Badía, P., Criado, R., Rajo, R., Javier, Francisco, Valenzuela, R., Pérez, S., Javier, F, Molina, T., Pérez, Tortajada, Pérez, Trigo, 2007. SPANISH AEROBIOLOGY NETWORK (REA): MANAGEMENT AND QUALITY MANUAL 36.
- Galán, C., Smith, M., Damialis, A., Frenguelli, G., Gehrig, R., Grinn-Gofroń, A., Kasprzyk, I., Magyar, D., Oteros, J., Šaulienė, I., Thibaudon, M., Sikoparija, B., EAS QC, W.G., 2021. Airborne fungal spore monitoring: between analyst proficiency testing. *Aerobiologia*. <https://doi.org/10.1007/s10453-021-09698-4>
- Gregory, P.H., 1978. Distribution of airborne pollen and spores and their long distance transport. *Pure Appl. Geophys.* 116, 309–315. <https://doi.org/10.1007/BF01636888>
- Grinn-Gofroń, A., Nowosad, J., Bosiacka, B., Camacho, I., Pashley, C., Belmonte, J., De Linares, C., Ianovici, N., Manzano, J.M.M., Sadyś, M., Skjøth, C., Rodinkova, V., Tormo-Molina, R., Vokou, D., Fernández-Rodríguez, S., Damialis, A., 2019. Airborne *Alternaria* and *Cladosporium* fungal spores in Europe: Forecasting possibilities and relationships with meteorological parameters. *Sci. Total Environ.* 653, 938–946. <https://doi.org/10.1016/j.scitotenv.2018.10.419>

- Hasnain, S.M., Fatima, K., Al-Frayh, A., Al-Sedairy, S.T., 2005. Prevalence of airborne basidiospores in three coastal cities of Saudi Arabia. *Aerobiologia* 21, 139–145. <https://doi.org/10.1007/s10453-005-4184-x>
- Hirst, J.M., 1952. An Automatic Volumetric Spore Trap. *Ann. Appl. Biol.* 39, 257–265. <https://doi.org/10.1111/j.1744-7348.1952.tb00904.x>
- Historical Data - Met Éireann - The Irish Meteorological Service [WWW Document], 2022. URL //climate/available-data/historical-data (accessed 11.22.21).
- Hollins, P.D., Kettlewell, P.S., Atkinson, M.D., Stephenson, D.B., Corden, J.M., Millington, W.M., Mullins, J., 2004. Relationships between airborne fungal spore concentration of *Cladosporium* and the summer climate at two sites in Britain. *Int. J. Biometeorol.* 48, 137–141. <https://doi.org/10.1007/s00484-003-0188-9>
- Jefferson, M., 1989. Why Geography? The Law of the Primate City. *Geogr. Rev.* 79, 226–232. <https://doi.org/10.2307/215528>
- Johnson, D.W., 1979. Eutypella Canker of Maple: Ascospore Discharge and Dissemination. *Phytopathology* 69, 130. <https://doi.org/10.1094/Phyto-69-130>
- Käpylä, M., Penttinen, A., 1981. An evaluation of the microscopical counting methods of the tape in hirst-burkard pollen and spore trap. *Grana* 20, 131–141. <https://doi.org/10.1080/00173138109427653>
- Lacey, M.E., 1962. The Summer Air-Spora of Two Contrasting Adjacent Rural Sites. *Microbiology* 29, 485–501. <https://doi.org/10.1099/00221287-29-3-485>
- Lagomarsino Oneto, D., Golan, J., Mazzino, A., Pringle, A., Seminara, A., 2020. Timing of fungal spore release dictates survival during atmospheric transport. *Proc. Natl. Acad. Sci.* 117, 5134–5143. <https://doi.org/10.1073/pnas.1913752117>
- Lo, F., Bitz, C.M., Battisti, D.S., Hess, J.J., 2019. Pollen calendars and maps of allergenic pollen in North America. *Aerobiologia* 35, 613–633.
- Lyon, F.L., Kramer, C.L., Eversmeyer, M.G., 1984. Vertical variation of airspora concentrations in the atmosphere. *Grana* 23, 123–125. <https://doi.org/10.1080/00173138409428887>
- Mandrioli, P., Negrini, M.G., Zanotti, A.L., 1982. Airborne pollen from the yugoslavian coast to the po valley (italy). *Grana* 21, 121–128. <https://doi.org/10.1080/00173138209427688>

- Marçais, B., Kavkova, M., Desprez-Loustau, M.-L., 2009. Phenotypic variation in the phenology of ascospore production between European populations of oak powdery mildew. *Ann. For. Sci.* 66, 814. <https://doi.org/10.1051/forest/2009077>
- Markey, E., Hourihane Clancy, J., Martínez-Bracero, M., Neeson, F., Sarda-Estève, R., Baisnée, D., McGillicuddy, E.J., Sewell, G., O'Connor, D.J., 2022. A Modified Spectroscopic Approach for the Real-Time Detection of Pollen and Fungal Spores at a Semi-Urban Site Using the WIBS-4+, Part I. *Sensors* 22, 8747. <https://doi.org/10.3390/s22228747>
- Martínez-Bracero, M., Alcázar, P., Díaz de la Guardia, C., González-Minero, F.J., Ruiz, L., Trigo Pérez, M.M., Galán, C., 2015. Pollen calendars: a guide to common airborne pollen in Andalusia. *Aerobiologia* 31, 549–557. <https://doi.org/10.1007/s10453-015-9385-3>
- Martínez-Bracero, M., Markey, E., Clancy, J.H., Sodeau, J., O'Connor, D.J., 2022. First Long-Time Airborne Fungal Spores Study in Dublin, Ireland (1978–1980). *Atmosphere* 13, 313. <https://doi.org/10.3390/atmos13020313>
- Maya-Manzano, J.M., Smith, M., Markey, E., Hourihane Clancy, J., Sodeau, J., O'Connor, D.J., 2021. Recent developments in monitoring and modelling airborne pollen, a review. *Grana* 60, 1–19. <https://doi.org/10.1080/00173134.2020.1769176>
- McDonald, M.S., O'Driscoll, B.J., 1980. Aerobiological studies based in Galway. A comparison of pollen and spore counts over two seasons of widely differing weather conditions. *Clin. Immunol. Allergy* 10, 211–215. <https://doi.org/10.1016/j.clim.1980.06.009>
- Moore, P., 2020. Summer 2018: An Analysis of the heatwaves and droughts that affected Ireland and Europe in the summer of 2018.
- Mullins, J., Warnock, D.W., Powell, J., Jones, I., Harvey, R., 1977. Grass pollen content of the air in the Bristol Channel region in 1976. *Clin. Exp. Allergy* 7, 391–395. <https://doi.org/10.1111/j.1365-2222.1977.tb01468.x>
- O'Connor, D.J., Sadyś, M., Skjøth, C.A., Healy, D.A., Kennedy, R., Sodeau, J.R., 2014. Atmospheric concentrations of *Alternaria*, *Cladosporium*, *Ganoderma* and *Didymella* spores monitored in Cork (Ireland) and Worcester (England) during the summer of 2010. *Aerobiologia* 30, 397–411. <https://doi.org/10.1007/s10453-014-9337-3>

- O'Dwyer, J., Chique, C., Weatherill, J., Hynds, P., ODwyer, J., 2020. 10 – REPEATED MEASURES RISK ASSESSMENT OF THE 2018 EUROPEAN DROUGHT ON MICROBIAL GROUNDWATER QUALITY IN SOUTHERN IRELAND 13.
- Oliveira, M., Ribeiro, H., Delgado, L., Fonseca, J., Castel-Branco, M., Abreu, I., 2010. Outdoor Allergenic Fungal Spores: Comparison Between an Urban and a Rural Area in Northern Portugal. *J Investig Allergol Clin Immunol* 20, 12.
- Palmas, F., Cosentino, S., 1990. Comparison between fungal airspore concentration at two different sites in the South of Sardinia. *Grana* 29, 87–95. <https://doi.org/10.1080/001731390009429979>
- Patel, T.Y., Buttner, M., Rivas, D., Cross, C., Bazylinski, D.A., Seggev, J., 2018. Variation in airborne fungal spore concentrations among five monitoring locations in a desert urban environment. *Environ. Monit. Assess.* 190, 634. <https://doi.org/10.1007/s10661-018-7008-5>
- Pecero-Casimiro, R., Maya-Manzano, J.M., Fernández-Rodríguez, S., Tormo-Molina, R., Silva-Palacios, I., Monroy-Colín, A., Gonzalo-Garijo, Á., 2020. Pollen calendars and regional gradients as information tools in the Extremadura pollen monitoring network (SW Spain). *Aerobiologia* 36, 731–748. <https://doi.org/10.1007/s10453-020-09667-3>
- Perrin, P.W., 1977. Spore Trapping Under Hot and Humid Conditions. *Mycologia* 69, 1214–1218. <https://doi.org/10.1080/00275514.1977.12020185>
- Rantio-Lehtimäki, A., 1977. Research on Airborne Fungus Spores in Finland. *Grana* 16, 163–165. <https://doi.org/10.1080/00173134.1977.11864655>
- Reyes, E.S., de la Cruz, D.R., Sánchez, J.S., 2016. First fungal spore calendar of the middle-west of the Iberian Peninsula. *Aerobiologia* 32, 529–539. <https://doi.org/10.1007/s10453-016-9430-x>
- Rivera-Mariani, F.E., Bolaños-Rosero, B., 2012. Allergenicity of airborne basidiospores and ascospores: need for further studies. *Aerobiologia* 28, 83–97. <https://doi.org/10.1007/s10453-011-9234-y>
- Rodríguez-Fernández, A., Oteros, J., Vega-Maray, A.M., Valencia-Barrera, R.M., Galán, C., Fernández-González, D., 2022. How to select the optimal monitoring locations for an aerobiological network: A case of study in central northwest of Spain. *Sci. Total Environ.* 827, 154370. <https://doi.org/10.1016/j.scitotenv.2022.154370>

- Rodríguez-Rajo, F.J., Iglesias, I., Jato, V., 2005. Variation assessment of airborne *Alternaria* and *Cladosporium* spores at different bioclimatical conditions. *Mycol. Res.* 109, 497–507. <https://doi.org/10.1017/s0953756204001777>
- Rojo, J., Picornell, A., Oteros, J., 2019. AeRobiology: A Computational Tool for Aerobiological Data.
- Ruiz-Mata, R., Trigo, M.M., Recio, M., de Gálvez-Montañez, E., Picornell, A., 2023. Comparative aerobiological study between two stations located at different points in a coastal city in Southern Spain. *Aerobiologia* 39, 195–212. <https://doi.org/10.1007/s10453-023-09786-7>
- Ščevková, J., Kováč, J., 2019. First fungal spore calendar for the atmosphere of Bratislava, Slovakia. *Aerobiologia* 2, 343–356. <https://doi.org/10.1007/s10453-019-09564-4>
- Sindt, C., Besancenot, J.-P., Thibaudon, M., 2016. Airborne *Cladosporium* fungal spores and climate change in France. *Aerobiologia* 32, 53–68. <https://doi.org/10.1007/s10453-016-9422-x>
- Stępańska, D., Wołek, J., 2005. Variation in fungal spore concentrations of selected taxa associated to weather conditions in Cracow, Poland, in 1997. *Aerobiologia* 21, 43–52. <https://doi.org/10.1007/s10453-004-5877-2>
- Viander, M., Koivikko, A., 1978. The seasonal symptoms of hyposensitized and untreated hay fever patients in relation to birch pollen counts: correlations with nasal sensitivity, prick tests and RAST. *Clin. Exp. Allergy* 8, 387–396. <https://doi.org/10.1111/j.1365-2222.1978.tb00474.x>

Chapter 4. Real-Time Monitoring

4.1. Introduction

Traditional methods used for fungal spore monitoring were developed decades ago. Various technologies and measurement methods have been developed in the interim with the aims of complimenting traditional sampling methods or directly replacing them. Real time methods can offer a suitable alternative to traditional sampling, which has drawbacks with regards to the sheer volume of personnel hours required. (Kubera et al., 2021; Tormo Molina et al., 2013).

Methods traditionally used for the detection and quantification of bioaerosols have tended to be impactors such as the Hirst volumetric trap (Hirst, 1952). This is the recommended sampling method by the EAN and the European Aeroallergen Society (EAS) (Oteros et al., 2015). The device collects bioaerosol samples onto an adhesive surface. Samples are then analysed manually via optical microscopy. Such methods are incredibly labour-intensive and require a high level of expertise for instrument operation, sample preparation, and optical discernment of a large variety of different fungal spores and pollen grains. Due to the slow process only a sample of the slides are analysed with the overall count determined by extrapolation (Maya-Manzano et al., 2021), resulting in a higher degree of uncertainty (Clot et al., 2020; Galán et al., 2014). The arduous and time-consuming process has also prevented the formations of nationwide and continentwide bioaerosol monitoring networks, that could greatly assist in the monitoring and tracking of possibly allergenic PBAPs (Martínez-Bracero et al., 2022).

The first real-time methods developed, were focussed mainly on the development of early warning systems for identification of bio-toxins that could harm the military or citizens. One of the samplers described in this chapter, the IBAC, was developed for this purpose specifically (Huffman et al., 2020; Paziienza, 2013; Santarpia et al., 2013). Because of this, the majority of real time monitoring methods currently rely on rapid identification of the physical characteristics of particles, such as their size, shape, and fluorescence, and a range of techniques also investigate the potential use of chemical properties to differentiate between bioaerosols (Fennelly et al., 2018; Huffman et al., 2020).

In recent years, more affordable and accessible newer techniques for locating and measuring PBAPs in the localised atmosphere have emerged (Martinez-Bracero et al., 2022). Though the general working concepts of each instrument, such as light induced fluorescence (LIF), light scatter, and holographic imaging, might differ significantly, the bulk of these devices can be characterized as utilising air-flow cytometry. The KH-3000-01, the WIBS, the IBAC, the Plair Rapid-E, and the Swinsens Poleno are some of these instruments. The WIBS-NEO and IBAC-

2 devices are both included in this study and are compared (Matsuda and Kawashima, 2018; Niederberger et al., 2018; O'Connor et al., 2013; Santarpia et al., 2013; Šauliene et al., 2019).

4.2. Instrumentation

The primary comparative device for this campaign was the WIBS-Neo real-time fluorescence sampler. The WIBS is a three-channel fluorescence detector for individual aerosol particles. It uses light-induced fluorescence (LIF) to detect fluorescent aerosol particles (FAP) in real time. By monitoring the forward and side optical scatter as well as the spectrally unresolved fluorescence intensity of individual particles at a temporal resolution of one millisecond, it is possible to determine the shape and size of both fluorescent and non-fluorescent particles. The WIBS instrument has been implemented in various iterations throughout the literature. These include models 3 and 4 (prototype instruments), as well as the commercially marketed Models WIBS-4A and WIBS-Neo, which was the model used in this study (Fennelly et al., 2017).

The WIBS has been deployed in several locations to track changes in ambient bioaerosol, including Ireland. Types of locations include urban, bio-waste, green-waste, coastal, and indoor environments (Daly et al., 2019a; Feeney et al., 2018; Gabey et al., 2010, 2011; D. A. Healy et al., 2012a, 2012b; Healy et al., 2014; Li et al., 2020; O'Connor et al., 2013, 2015a; Whitehead et al., 2010). When compared to conventional volumetric sampling techniques, field investigations have demonstrated the WIBS' superior ability to detect ambient bioaerosols ($R^2 > 0.9$) (O'Connor et al., 2014a).

Another device, the IBAC-2, was examined for its real-time monitoring capabilities as an UV-LIF continuous air monitoring device originally developed by ICx Biodefense for the purpose of detecting potential threats related to biological aerosols, the Instantaneous Bioaerosol Analysis and Collection (IBAC) was later commercialized by FLIR Systems. It was previously known as the FIDO B2 and the Instantaneous Biological Analyzer and Collector (IBAC).

Homeland security and defence customers were the target consumer of the first IBAC model and were the primary clients. Through the use of elastic scattering (photomultiplier tubes) and particle fluorescence using a 405nm laser as the excitation source, it can distinguish between fluorescent and non-fluorescent particles. While individual sizes for particles are determined the instrument simply labels them as “Small” (between 0.7-1.5 μm) and “Big” (between 1.5-10 μm) particle. Thus, based on size and fluorescence, there are four distinct particle groups, named as follows: “Small Biological” “Large Biological”, “Small Non-Biological”, and “Large

Non-Biological". In this instance, "Biological" represents particles that express fluorescence. While it is not a given that all fluorescent particles are in fact biological, that is the naming convention chosen by the manufacturer for ease of communication. The IBAC was built to be modular so that other features and capabilities, including aerosol samplers, may subsequently be installed into the system. It can detect particles as small as 0.7 microns and has a reaction time of between 30s and 1 min. (P. Anchlia, 2015; DeFreez, 2009a; Jonsson and Kullander, 2014a; Paziienza et al., 2014; Santarpia et al., 2013). Studies have tested cutting-edge particle analysis techniques using the IBAC device as a control. In a study by Choi et al. (Choi et al., 2018), the FIDO B2 IBAC was employed as a comparison and validation tool along with their proposed usage of a correlation value for categorization of airborne particles based on these particles' optical features.

The Hirst, WIBS, and IBAC were all co-located on a rooftop in an urban area for the campaign described in this chapter. Results from the conventional approach and both cutting-edge real-time monitoring techniques were contrasted and compared. Identification of the WIBS and IBAC particle outputs that strongly linked with ambient fungal spore and pollen concentrations was prioritised.

4.3. Materials and Methods

Bioaerosol monitoring was conducted at the sampling site located at the former TU Dublin Kevin Street site as shown in Figure 4.1 below.

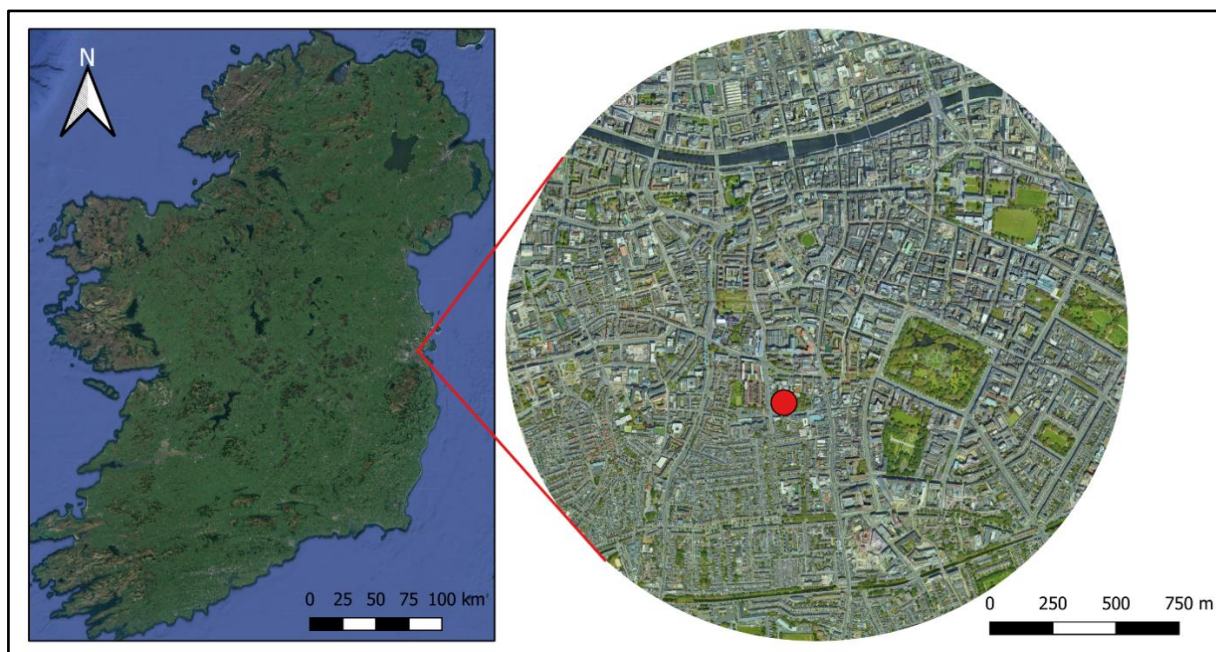


Figure 4.1: Real time monitoring sample site location in Dublin city centre, on the roof of the TU Dublin Kevin Street building.]

In this campaign, the Hirst-Lanzoni method of PBAP monitoring was contrasted with more recent spectrometric techniques of the WIBS-NEO and the IBAC in an effort to evaluate the potential of real-time monitoring. From the 7th of August, 12:00, until the 16th of September, 12:00, the monitoring program was continuously run, lasting for 41 days in total. The Hirst-Lanzoni volumetric trap was placed near the spectrometric equipment (WIBS-NEO and IBAC) on the roof of TU Dublin, Kevin Street, to enable parallel monitoring.

Only one brief period of inactivity was recorded throughout the nearly continuous operation of the WIBS-NEO (07/08/2019 12:00 – 16/09/2019 12:00). Therefore, before the comparison, pollen/fungal spore values recorded by the Hirst during these hours were eliminated, with these times listed as possessing no valid, rather than a value of zero. In order to verify that there were no significant fluctuations in fluorescence readings during the campaign and that the data could be utilized to later establish daily fluorescent thresholds, the WIBS was also put into force trigger mode at the beginning of each day. The IBAC-2 also ran nearly continuously from 07/08/2019 to 15/09/2019, however it wasn't operational on the 28th of August. As a result, to maintain data homogeneity for IBAC comparisons, pollen/fungal spores captured by the Hirst, and the data received from the WIBS during this time period were excluded.

In accordance with the standardized methods for airborne pollen monitoring counting and analysis recommended by the Spanish Aerobiology Network (REA) and EAN, bioaerosol ambient concentrations were sampled using a Hirst-Lanzoni sampler and manually counted using an optical microscope at 400x magnification. The sample device consists of an

electrically driven motor that draws air into it at a rate of 10L/min such that it flows over an adhesive surface that is kept within, allowing impaction of the bioaerosol sample onto the medium and enabling collection. Then the adhesive surface is removed from the device, containing the sample, and is analysed manually in a lab with an optical microscope. Because of its standardised operation, maintenance, and results analysis processes, this bioaerosol sampler is the most widely utilized.

4.4. WIBS Real-Time Monitoring Campaign

4.4.1. Campaign Overview

The city centre study had aims to both compare the real time and the traditional methods, as well as to collect the real-time data to increase the pool of information that could be used in the development of a bioaerosol prediction algorithm. Daily and diurnal hourly data obtained from the manual counting of fungal spore particles via the traditional microscopy method was compared with the each of the different fluorescence channel outputs observed using a WIBS-NEO over the same date range (August 7th to September 15th, 2019). The sampling took place on the roof of the TU Dublin Kevin Street site, a building that has since been demolished.

4.4.2. Fungal Monitoring Data

During the monitoring period, the most commonly identified single spore type throughout the study period was *Cladosporium*, which comprised 66.3% of all fungal spores counted during the study period.

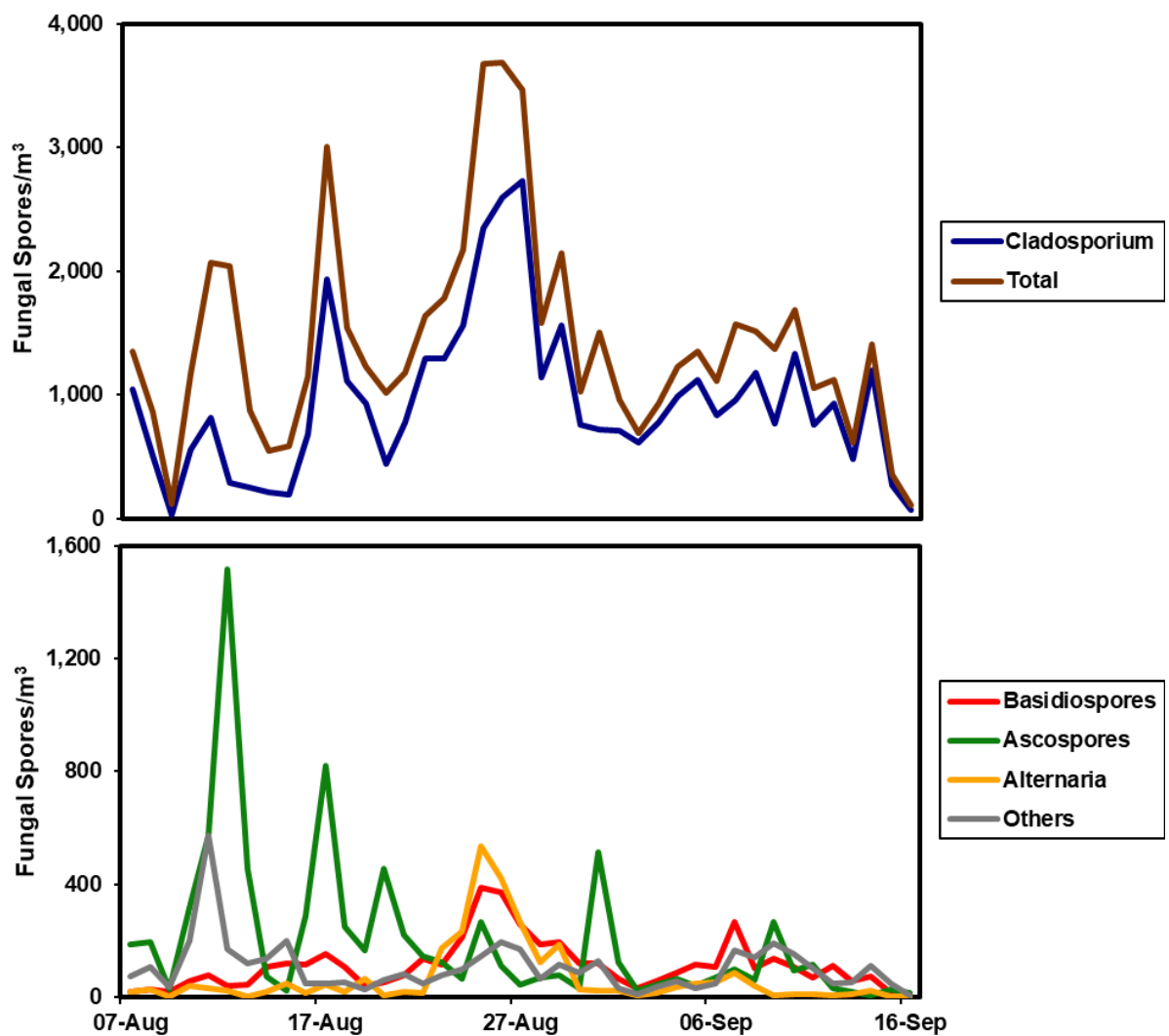


Figure 4.2: Daily concentrations of each major fungal spore identified during the study period, along with “other” fungal spores. Hourly measured Hirst data was used.

Of the identified fungal spores, ascospores made up 13.9%, basidiospores 7.8%, *Alternaria* 4.7%, and "other spores" made up 7.3%. Over a three-day period, a single, significant peak in the number of spores was seen, with two distinct "troughs" in low concentrations occurring five days before and five days following the peak. Since it made up the vast majority of all fungal spores, as shown in Figure 4.2, *Cladosporium* drove the concentration of total spores throughout the duration of the campaign. The first week of the research was a notable exception to this since there was some increase in the overall fungal spore concentrations at a period when *Cladosporium* concentrations themselves remained low. This rise in spore concentrations occurred as a result of substantial ascospore concentration increases at this time, as well as increases in the overall number of "other" spores.

4.4.3. WIBS Monitoring Data

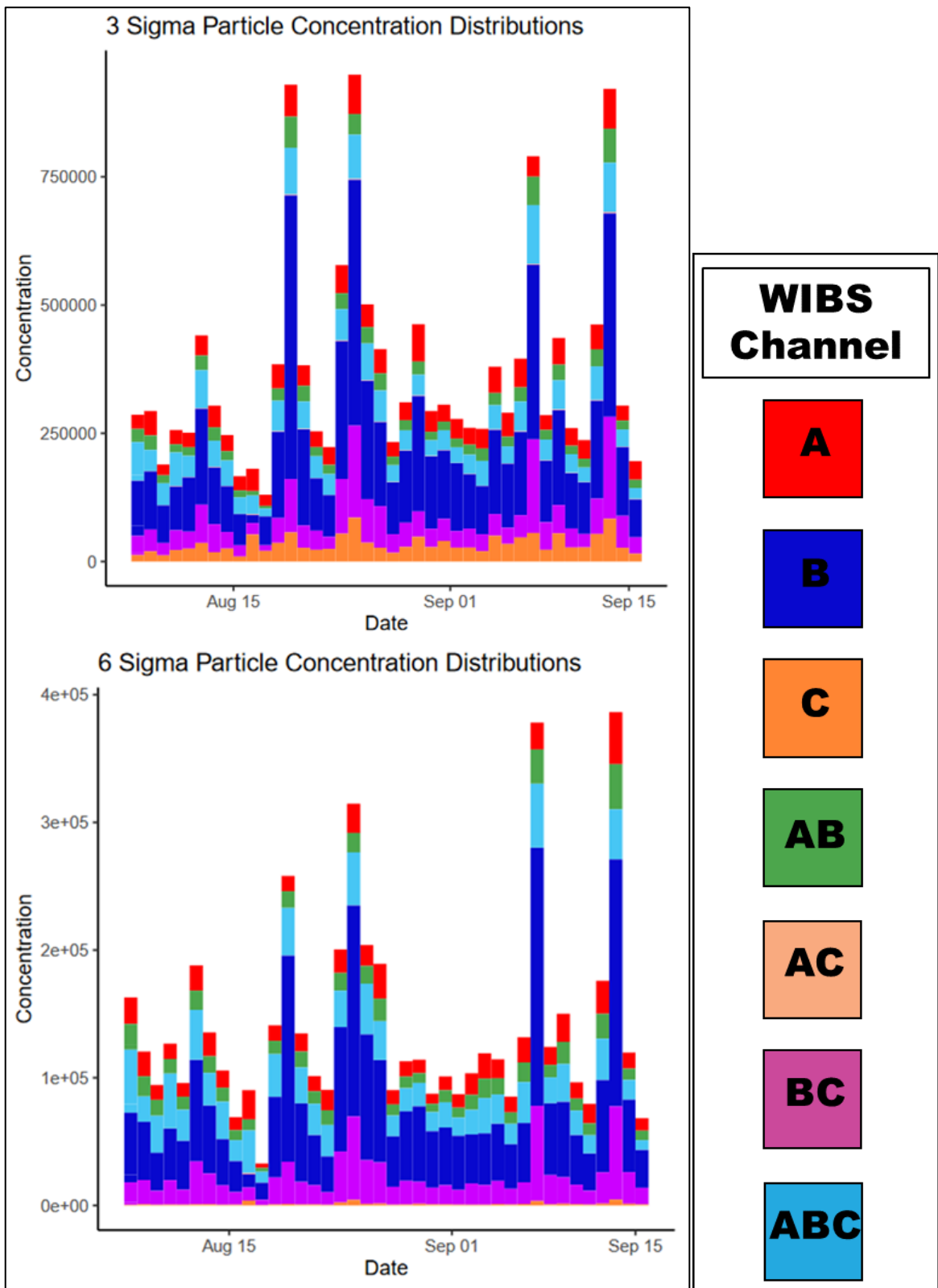
In parallel to the traditional sampling, the WIBS-NEO device sampled particles and determined their fluorescence characteristics. During the 41-day campaign, a total of 56,818,969 particles were detected and categorised by the WIBS -NEO device (Perring et al., 2015). Before analysis could be conducted a baseline fluorescence intensity of each FL channel was determined to be as follows.

The force trigger mode in the WIBS instrument was initiated. This effectively causes the Xenon flash lamps within the device to fire on empty space (within the optical chamber). This background measurement was allowed to continue for 5 minutes until sufficient data was collected and hence a baseline threshold for each fluorescence channel to be calculated. These baselines were determined to be the average value of the measured force trigger intensities (in each channel FL1, FL2 and FL3), plus three times the standard deviation of the obtained values. This will be hence known as the 3 Sigma (3σ) value and is described as such throughout this document. Similarly, a value of 6 Sigma would represent the average value of the force trigger fluorescence intensity measurement, plus six times the standard deviation.

For 3 Sigma, 6 Sigma, and 9 Sigma filters, Figure 28 shows the daily concentrations and overall breakdown of all fluorescence categories (as listed in Table 1) throughout the course of the study. One of the first things that stands out is that the AC category (pink) has so few particles that it does not effectively register on any of the charts in this Figure. At the 3-sigma level, 19,716 AC particles in total were found throughout the research period, however this is negligible compared to the other bands. For instance, throughout the same time period, almost 2.7 million B particles were found when counted at the same sigma level. Another finding in Figure 28 is that while the C grouping (Orange colour) makes up a relatively small portion of the particles identified at the 3-sigma level, C particle concentrations fall dramatically in comparison to all other particles once the fluorescence baseline is raised to a 6-sigma level (from 9% to 1% percent of the fluorescent particle total).

Apart from this one example, all other particle and band ratios seem to be stable. When comparing the bar charts at different sigma levels, the four "peak" days that occur at the 3-sigma level stand out the most. When using a 6-sigma filter level, the two peaks that appeared earlier in the study period start to appear less prominently, but the two peaks that appeared later in the study period increase more noticeably in comparison to the other days around. The 9-sigma level exhibits this phenomenon once more, and there now seem to be two peak dates.

The two peak days emerge in the second week of September, whereas the high concentration period arrives in the third week of August.



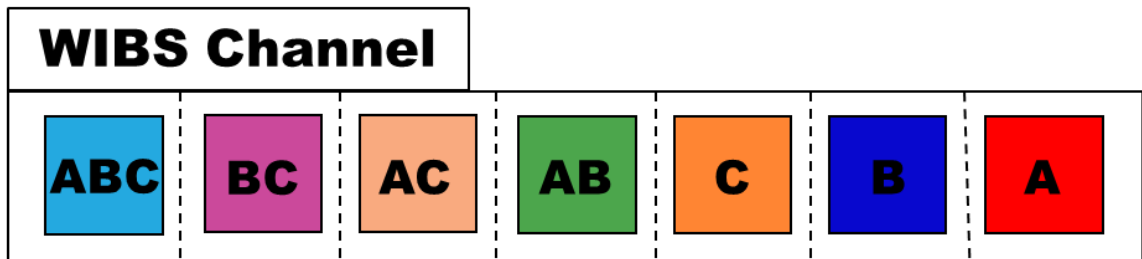
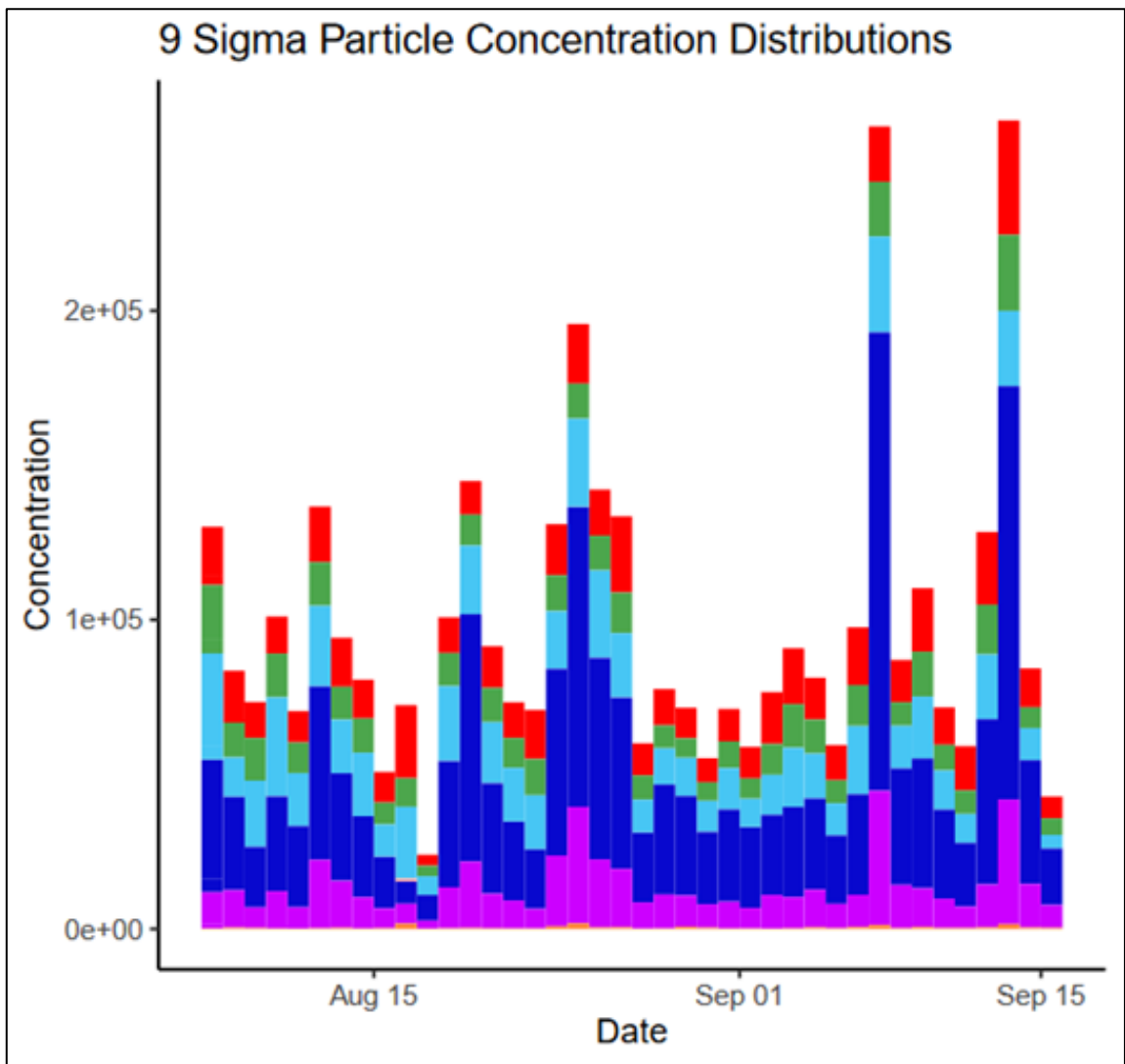


Figure 4.3: Concentrations of the WIBS fluorescent particle types at 3, 6, and 9 sigma during the real-time study period.

4.4.4. Comparison of Hirst and WIBS Fungal Data

Analyses were applied to various fungal spore groups when comparing them to detected FBAPs. Increasing the fluorescent threshold from 3σ to 6σ , and from 6σ to 9σ , was required to reduce the impact of interfering particles (anthropogenic fluorescent particles) (Figure 4.3), and to extract representative fungal fractions. BC type particles were determined to be the most representative FAP fraction for total fungal spore concentrations. Although several studies have highlighted the importance of the B and C fluorescence channels (FL2 and FL3)

for certain fungal spore fractions (Healy et al., 2014), the majority of studies have linked FL1 fluorescence to fungal spores, or the A channel (D. A. Healy et al., 2012a; Hernandez et al., 2016; O'Connor et al., 2015b; Savage et al., 2017).

In our own study, very little, or no correlation was observed for the majority of FL1 type particles. There are several potential reasons for this. Firstly, a range of different WIBS models (WIBS-3, WIBS-4 etc.) have been used previously, and this study is employing yet another variation of the WIBS technology – the WIBS-NEO. Any possible differences in fluorescence sensitivity between previous WIBS models, and the WIBS-NEO, even very minute ones such as a slight increase in FL2 or FL3 channel sensitivity (compared to other channels), could result in a shift towards particles with B and C-type fluorescence (Ila Gosselin et al., 2016).

Secondly, FBAPs detected by the WIBS in more complex urban environments, show that anthropogenic/combustion particles favour the FL1 channel over the FL2 or FL3 channels (Savage et al., 2017; Yu et al., 2016). A study by (Yu et al., 2016) illustrated these findings using the WIBS-4, where anthropogenic such as black carbon almost exclusively possessed FL1 type fluorescence, inhibiting the differentiation of PBAP from such anthropogenic pollution. A recent study by (Forde et al., 2019b) compared the WIBS-NEO to its predecessor the WIBS-4. A notable difference in fluorescent intensity was observed when examining various PBAP samples. This deviation was driven by higher fluorescent intensities being detected in FL1. It is therefore possible that due to the high fluorescent sensitivity of the FL1 channel and the urban environment of the sampling site, that any potential detection of PBAP in the FL1 channel could be masked by the fluorescence of anthropogenic aerosols.

BC particles between 2-30 μm at 9σ showed the relatively good correlation with total fungal spore concentrations, yielding a Pearson correlation coefficient of 0.54. Although the instruments track well for fungal spore peaks observed on the 25th of August and 14th of September, there are notable periods where BC particles failed to account for high concentrations of fungal spores. Notable periods where there are large peaks in total fungal spore concentration that are not reflected in the WIBS – NEO data correspond to periods in which ascospores concentrations are high. This illustrated that some spore types are not being detected within the BC fraction.

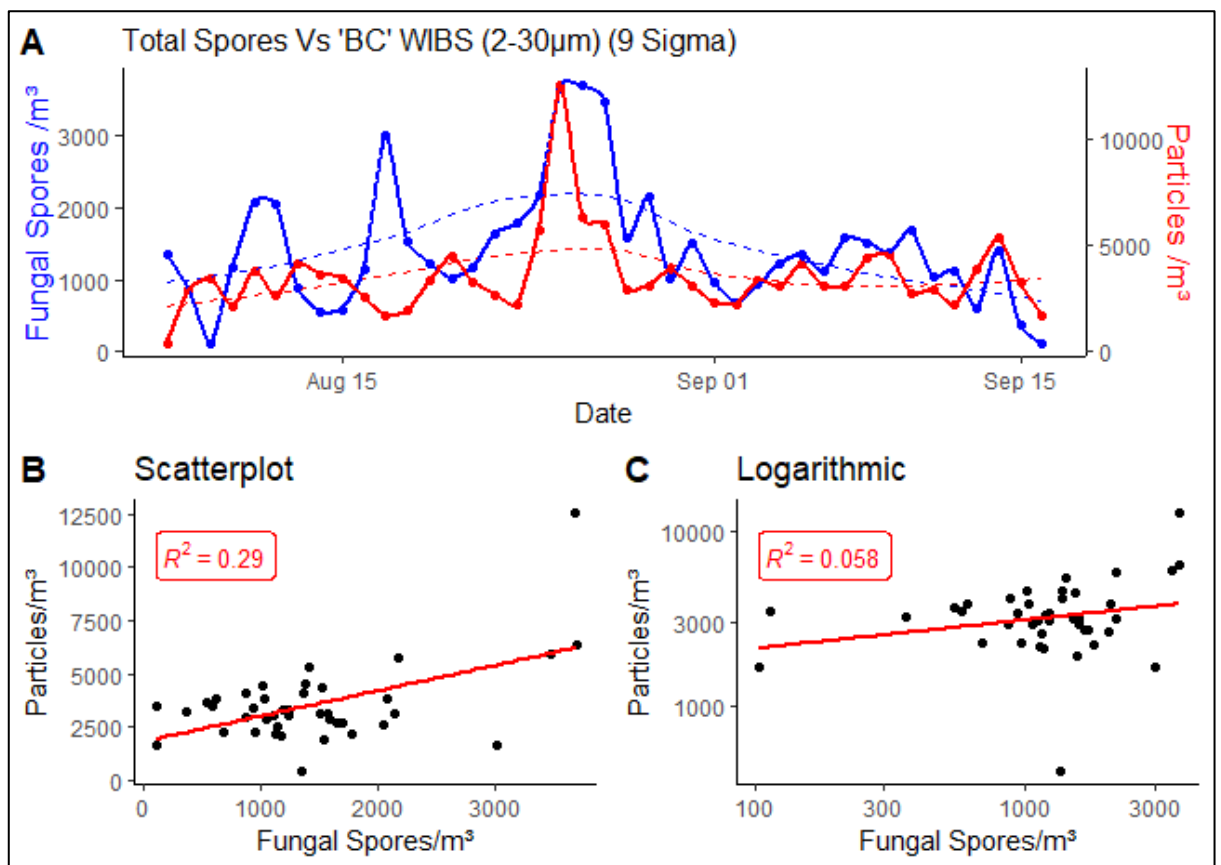


Figure 4.4: (A) Time series of Hirst fungal spore counts and BC WIBS particles (daily), with (B) linear scatterplot ($R^2 = 0.29$), and (C) logarithmic scatterplot of daily values ($R^2 = 0.058$). (All WIBS channels were analysed, BC was the most promising).

As a result, a second subset of data was created using a new variable “Dry Spores” that did not include ascospores. This increased the correlation of total spores with BC particles from $R=0.54$ to $R=0.60$. Notable correlation was also observed for C type particles and “Dry spores” yielding an $R=0.50$. Further analysis was attempted to correlate prevalent fungal spore types with FAP fractions. Both Basidiospores and *Alternaria* exhibited notable correlation with BC type particles when compared exclusively. Basidiospores correlated well with BC particles in the size range of 2-30µm ($R=0.66$) as illustrated in Figure 4.5, below.

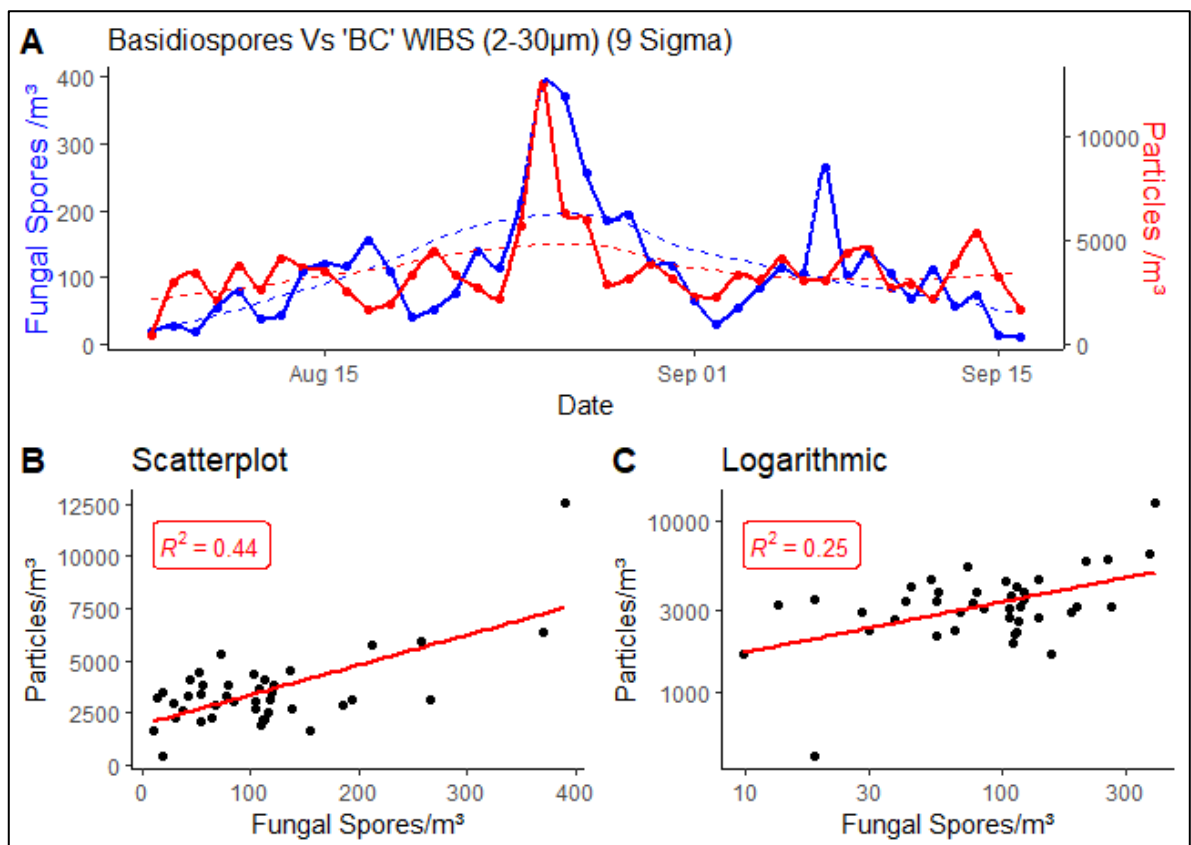


Figure 4.5: (A) Time series of Hirst basidiospore counts and BC WBS particles (daily), with (B) linear scatterplot ($R^2 = 0.44$), and (C) logarithmic scatterplot of daily values ($R^2 = 0.25$).

Although good correlation between the 2 devices was observed for basidiospores, there are periods where the WBS does not correlate with peaks in spores. Similarly, there are periods where peaks in BC particles do not correspond to increase in spores. Since it's known that BC particles also correlate well for other PBAP types, albeit at lower fluorescent thresholds, these peaks that do not equate to Basidiospore concentrations could be indicative of other PBAPs, or potential interferences that are not removed using fluorescent filtering.

With regards to other fungal spore types, *Alternaria* correlated well with BC particles greater than $8\mu\text{m}$ at 6σ ($R=0.6$). Poor correlation was observed for *Cladosporium* spores even though they were the most prevalent spore type sampled. Several reasons for this have been discussed previously in literature. *Cladosporium* spores have been shown in previous studies to be commonly miscounted by multiple variations of the WBS instrumentation (Fernández-Rodríguez et al., 2018; Healy et al., 2014; O'Connor et al., 2015a). In particular, the WBS has shown an inability to fully characterize sharp increases and decreases in *Cladosporium* concentrations. Several reasons have been discussed, including the physical characteristics of *Cladosporium*, and that it can be released in clusters which can lead to increased wall loss, as

well as photophysical properties of the spore which could inhibit the absorption of light by bio fluorophores within the cell (O'Connor et al., 2015b).

This spore type has typically also shown an association with FL1 (A) fluorescence. The likely contamination of FL1 type particles with anthropogenic interferences led to the WIBS being unable to differentiate *Cladosporium* like particles from other FL1 particles (O'Connor et al., 2015b). In similar campaigns conducted in less diverse ambient environments, *Cladosporium* has shown considerable affinity to FL1 or A type particles. Similarly, in a study by (Healy et al., 2014) Basidiospores showed considerably higher percentage contributions to total spore concentrations than *Cladosporium*. The findings of this study highlighted, in this case, fungal spores showed stronger correlation with FL2 and FL3 channel, corroborating the link observed for basidiospores and BC particles seen during the current study. This could explain why significant correlation was observed for certain spore types and not for others.

4.4.5. Meteorological Influence on Fluorescent particles and Fungal Spores

The Impact of meteorological parameters upon fungal spore and WIBS particles was also investigated. Figure 4.6 below shows the trend of Fluorescent Aerosols Particles (FAPs) over the campaign (i.e. any particle deemed fluorescent) versus a number of weather parameters (Pressure, Ground minimum temperature, minimum temperature and Wind speed).

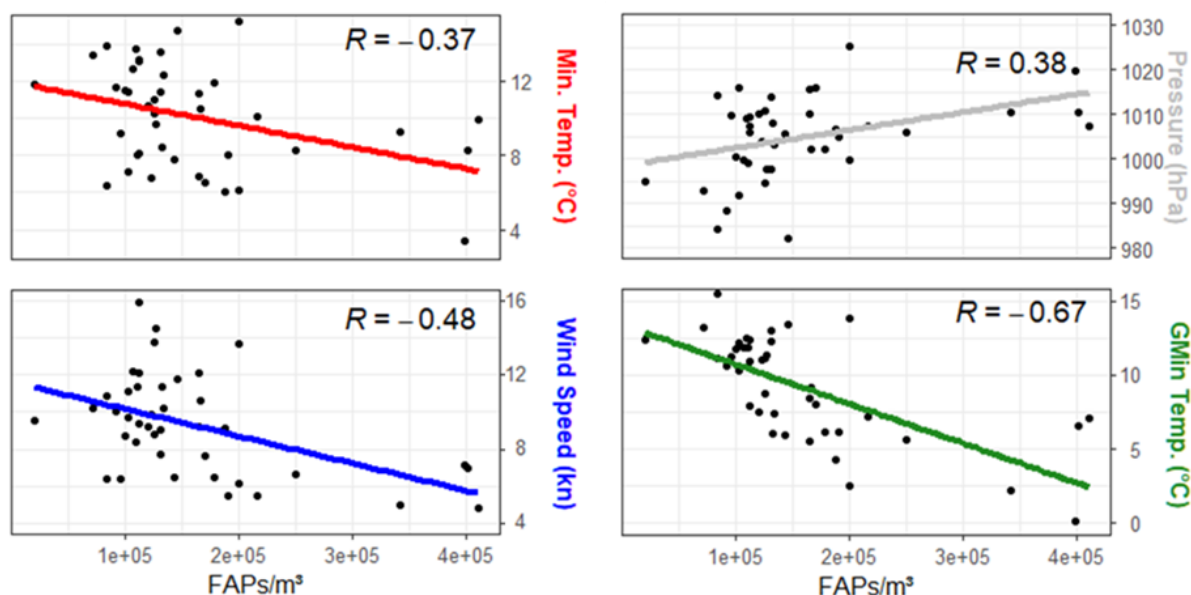


Figure 4.6: Fluorescent aerosols particles concentrations vs pressure (grey), ground minimum temperature (green), minimum temperature (red) and wind speed (blue).

It was observed that the majority of fluorescent WIBS particle classes exhibited significant negative correlation with minimum temperature, grass minimum temperature and wind speed. Daily trends and regression of such parameters are shown in Figure 4.6. This negative association with both temperature parameters during late-summer/early-Autumn months could be indicative of ambient bacterial activity. This is due to the increased bacterial population in the warmer summer months (Forde et al., 2019a). Although removing WIBS particles below 2 μm likely removes a large fraction of FAPs associated with the presence of bacteria, ambient bacterial concentrations have been shown to peak at size ranges of up to 4-5 μm (Bragoszewska and Pastuszka, 2018; Gong et al., 2020). The main reason for this decline in FAPs could also be related to the significant correlation seen between grass minimum temperature, rain and wind speed which are drivers for the transport and deposition of certain bioaerosols (Bragoszewska and Pastuszka, 2018; Davies and Smith, 1974; Hart et al., 1994; Oliveira et al., 2009). A notable positive correlation was also observed for FAPs detected by the WIBS with pressure. Such trends with pressure have been well documented in past literature for a myriad of pollen and fungal spore types (Kruczek et al., 2017; O'Connor et al., 2014b), potentially indicating a degree of contribution by bioaerosols to the FAP fraction.

An initial investigation into the correlation of fungal spores and different meteorological parameters was also undertaken. This resulted in unexpected results for Ascospores. Traditionally, Ascospores are considered “wet” spores (released in association with rain).

However, the R^2 Correlation between Ascospores and Rainfall over the WIBS campaign period was noted to be 0.01.

To further investigate this apparent anomaly, plots comparing Ascospores and Rainfall were constructed and can be seen below in Figure 4.7. Plot (A) Shows a time series plot, in which it becomes apparent, that while the two factors may not correlate using the current coefficient formulas being applied, as is seen in the linear regression line and scatterplot in Figure B, there is an apparent, strong relationship between rainfall and Ascospore concentrations. Visually, it appears that there is a delay, or lag between increases in rainfall, and increases in Ascospore concentrations. To test this hypothesis, a cross-correlation test was performed. Cross-correlation measures similarity between two datasets, as a function of the displacement of one relative to the other, such as a time lag. An example of its use would be investigation of the correlation between river pollution and aquatic fauna population crashes, as these events, if related, will not occur simultaneously (Croke et al., 2015).

The cross correlation of Ascospores and rainfall can be seen in part (C) of Figure 4.7 below. It can be seen that while the cross-correlation coefficient at a lag of 0 days was around 0.1, once this lag is adjusted, this value increases for each day the lag of rainfall is increased, up until 3 days, at this point, the correlation between the two parameters begins to decrease again. The peak point appeared to have a lag of 3 days and a peak cross-correlation coefficient of approximately 0.64. This was hard to ascertain on the graph provided. To further investigate exact values, a grid of scatterplots, each lagged by one more day than the scatterplot previous, was constructed. It can be seen in Figure 4.7 below.

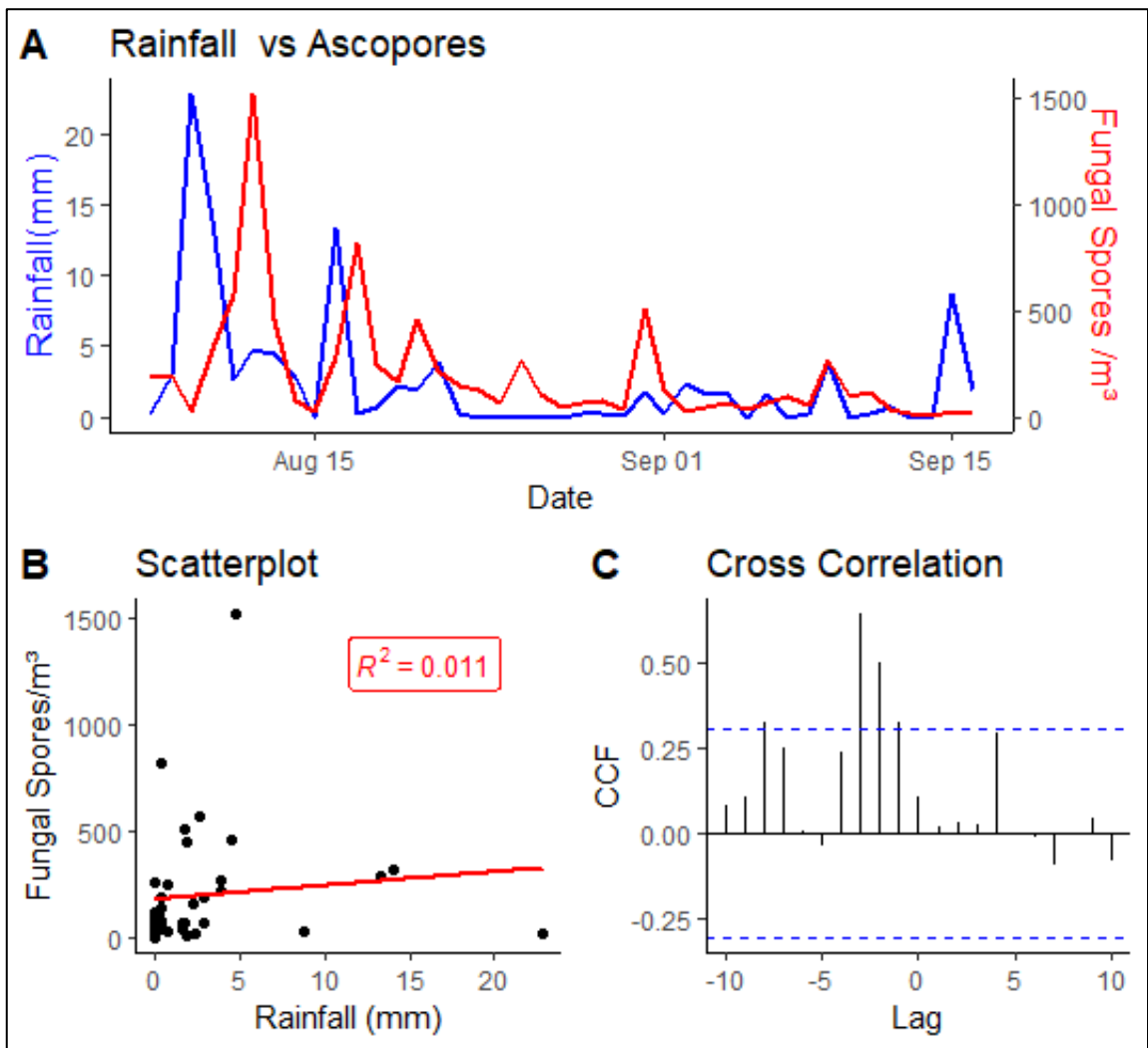


Figure 4.7: (A) Time series of Hirst ascospore counts and rainfall (daily), with (B) linear scatterplot ($R^2 = 0.011$), and (C) cross correlation lag regression plot.

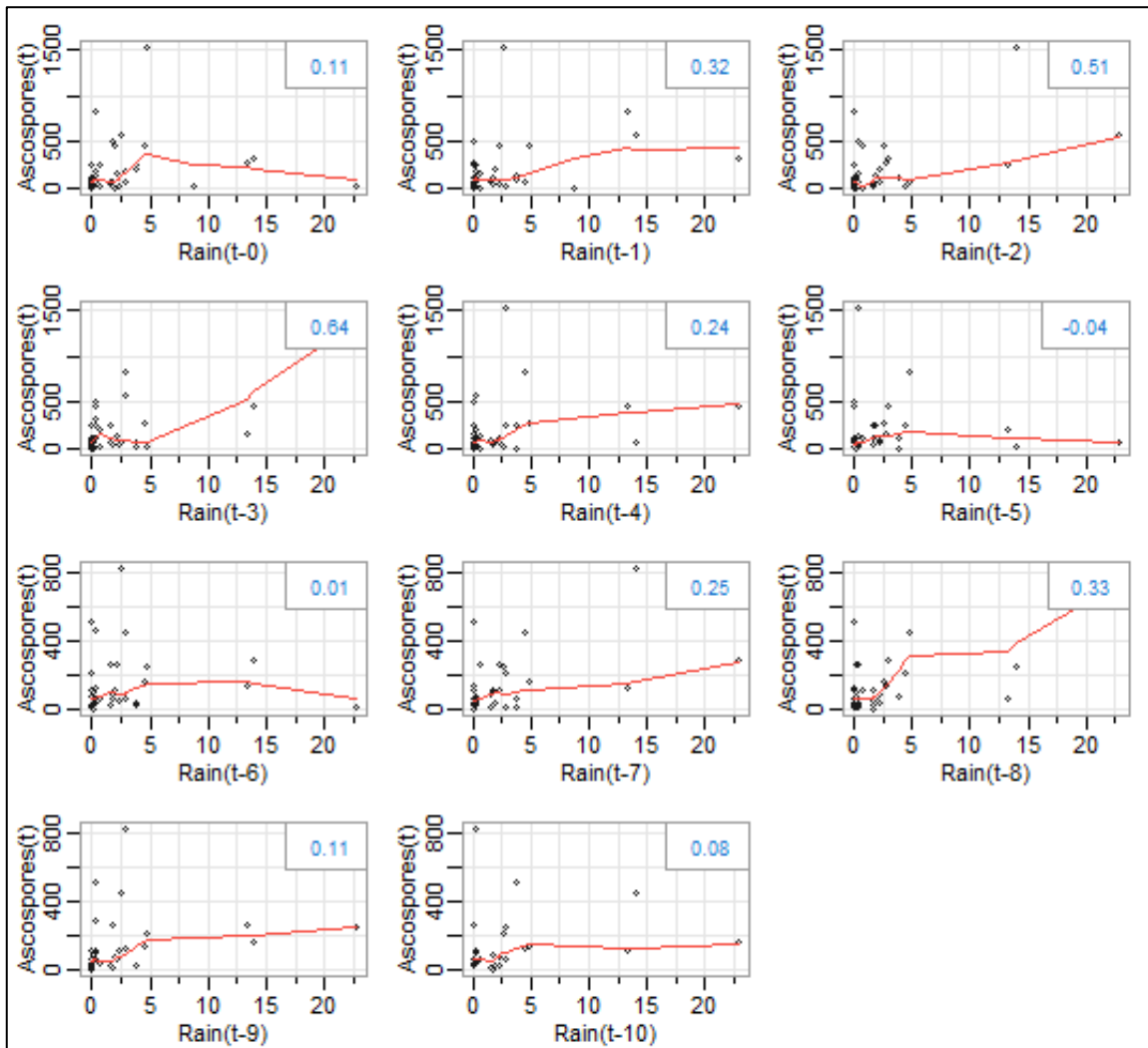


Figure 4.8: Grid of scatterplots of increasing rain data lag.

It becomes clear in the scatterplot grid, that significant cross-correlation is present when a 2-day lag (0.51) and 3-day lag (0.64) are applied to the rainfall data. The apparent increase in correlation at an 8-day lag is a result of Ascospore concentrations from the first major concentration peak aligning with Rainfall values from the second major concentration peak.

This pattern indicates a relationship between ascospores, and rainfall does exist, even if not evident after statistical analysis, and gives scope for development of new, and more comprehensive statistical tests in the future, relating to lagged data, variable lag, and directly for the application of fungal spore concentration forecasting and modelling. An ascospore and rainfall lagged positive correlative relationship has been observed in previous studies, with researchers similarly finding that the intensity of rainfall or wetness has an influence on the delay period before Ascospore concentrations increase as a response to this change in environmental conditions (Fourie et al., 2013; Stensvand et al., 2005).

This analysis was then applied in relation to the WIBS-NEO monitoring device, to identify whether different meteorological parameters had an impact upon the levels of correlation between Fungal spore concentrations and WIBS-NEO particle outputs. After a comprehensive analysis of various parameters and concentration thresholds, one strong pattern identified was the relationship between ascospores, and “AC” particles. At a 9 Sigma filtration, and size resolution of between 2 and 30 μm . This relationship was previously noted, with a relatively high Pearson correlation ($R=0.68$). But when meteorological parameters were taken into account, much higher levels of correlation were identified (Figure 4.9).

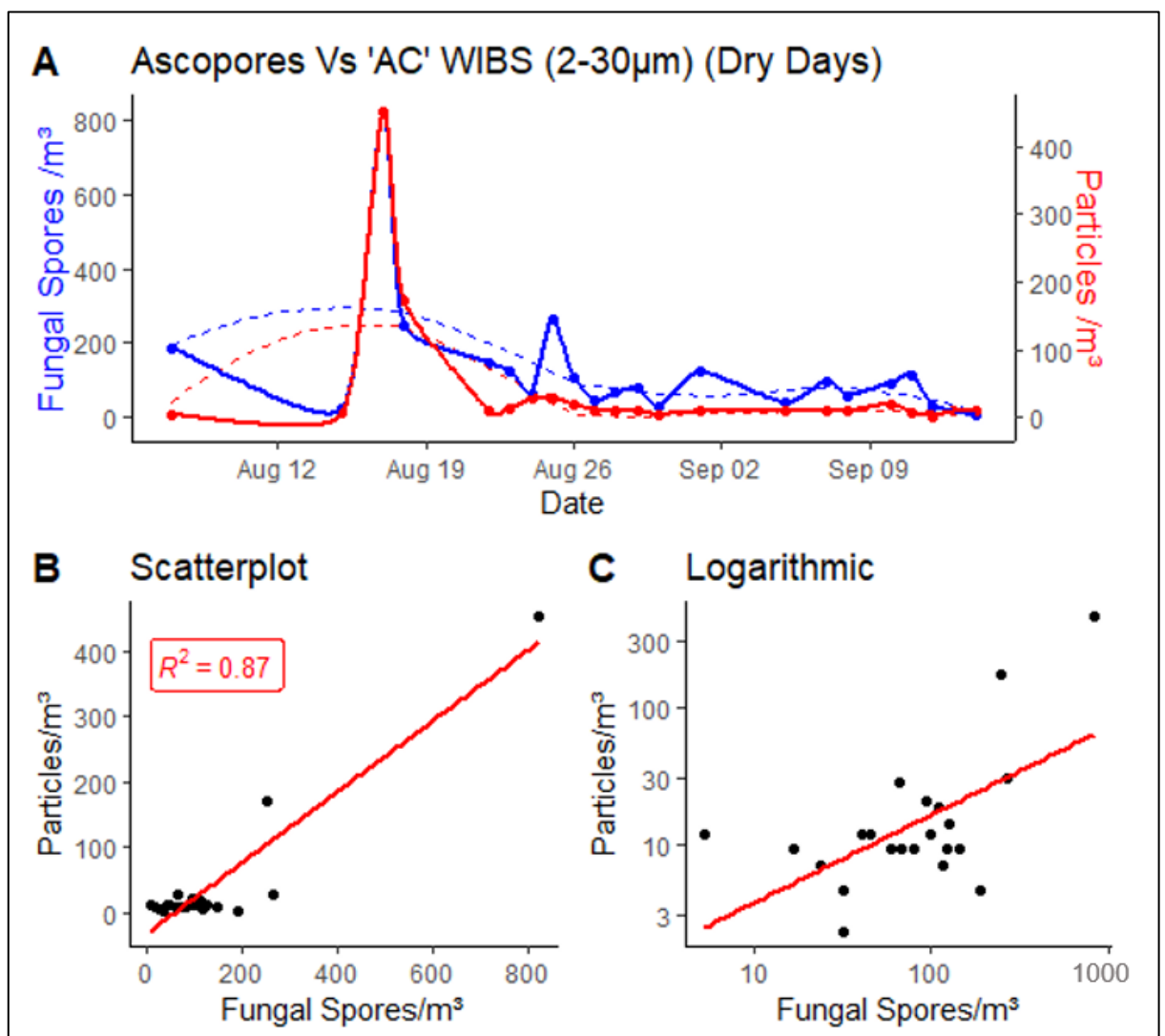


Figure 4.9: (A) Time series of Hirst ascospores counts and AC WIBS particles (days with 1mm of rainfall or less), with (B) linear scatterplot ($R^2 = 0.87$), and (C) logarithmic scatterplot of daily values.

In Figure 4.9 (above) the result of plotting ascospores against “AC” WIBS particles can be seen, when “days of rainfall” (>1mm in a day) were removed from the dataset. By removing these

days, the Pearson correlation rose to ($R=0.93$). The very strong, positive correlation, only present when rainfall days are removed, shows both the relationship between ascospores and rainfall, and the possible impact that rainfall may have upon the sensors within the WIBS-NEO sampling device.

4.4.6. Diurnal Comparisons

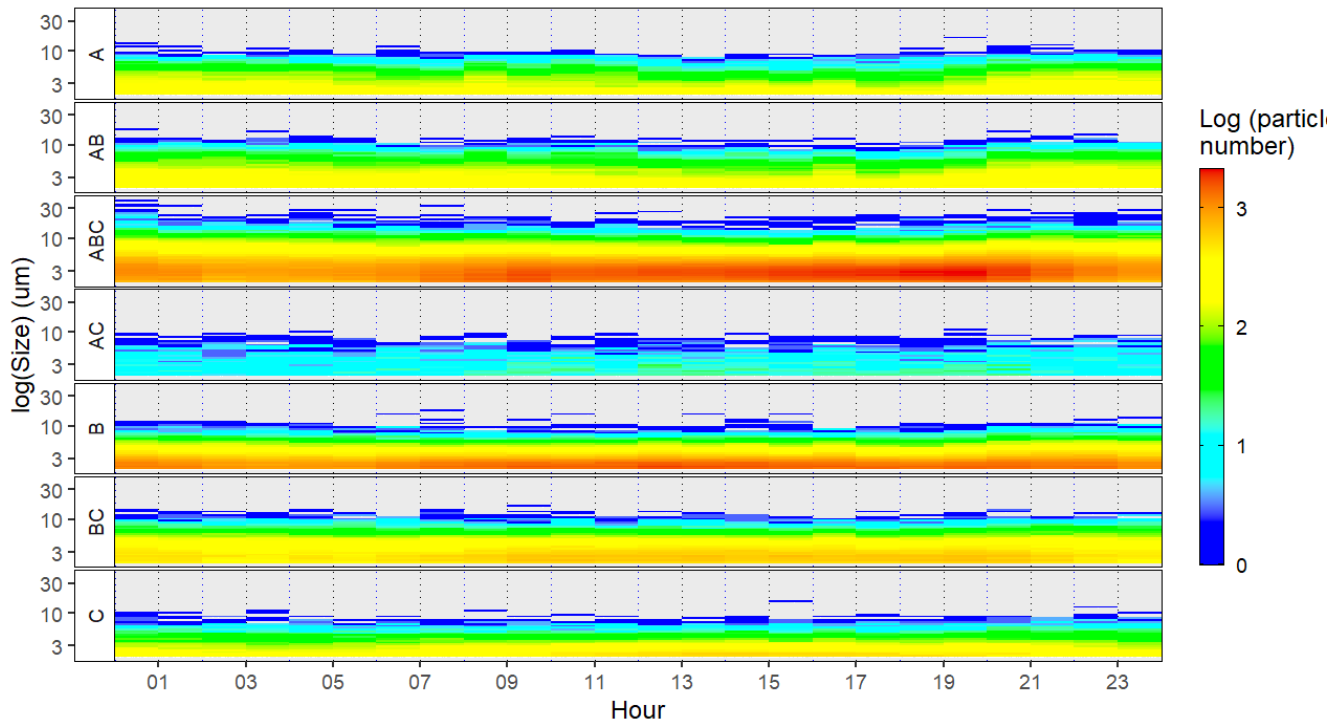


Figure 4.10: Log of diurnal WIBS particle distributions.

When exhibiting diurnal data (average daily cycle of particles) for the WIBS-NEO and fungal spores at the site in Dublin, a clear pattern is visible with regards to the WIBS-NEO data. When all fluorescent WIBS particle types are included (3-sigma level of filtration), the majority of WIBS categories follow the same trend as each other (Figure 4.10). This does not follow the expected diurnal trends seen in previous studies. Whereas other studies have seen increases in fluorescent particle concentrations in the night, reaching a peak in the early morning before the dawn, around 2 to 6 am, the data from the Dublin shows the exact opposite trend. As the sun sets, the concentrations begin to decrease, reaching a minimum concentration between 2am and 6am. While other studies have seen the concentration decrease as the sun comes out, with minimum values reached in the mid-afternoon, the Dublin data appears to rise in concentration with the sunrise, reaching a peak at 9am, and then dropping in concentration into the afternoon, before continuing the decrease at 7pm.

To note in the graph above, is the size distribution on the Y-axis. The particle log size in μm shows that while most WIBS channels are comprised of particles of $10\mu\text{m}$ and below, in the ABC channels, there is a considerable quantity of larger particles. As most larger particles are less likely to be anthropogenic in nature, further investigation into the ABC channel is warranted, and will be outlined further below (Lazaridis, 2011).

A clearer view of the overall size distributions can be seen in Figure 4.11 below. It highlights further the larger average size of the ABC particles, as well as the relatively large AB and AC particle sizes. This indicates further that the FLI channel may be a good indicator for bioaerosols, given their average size being greater than other airborne particles.

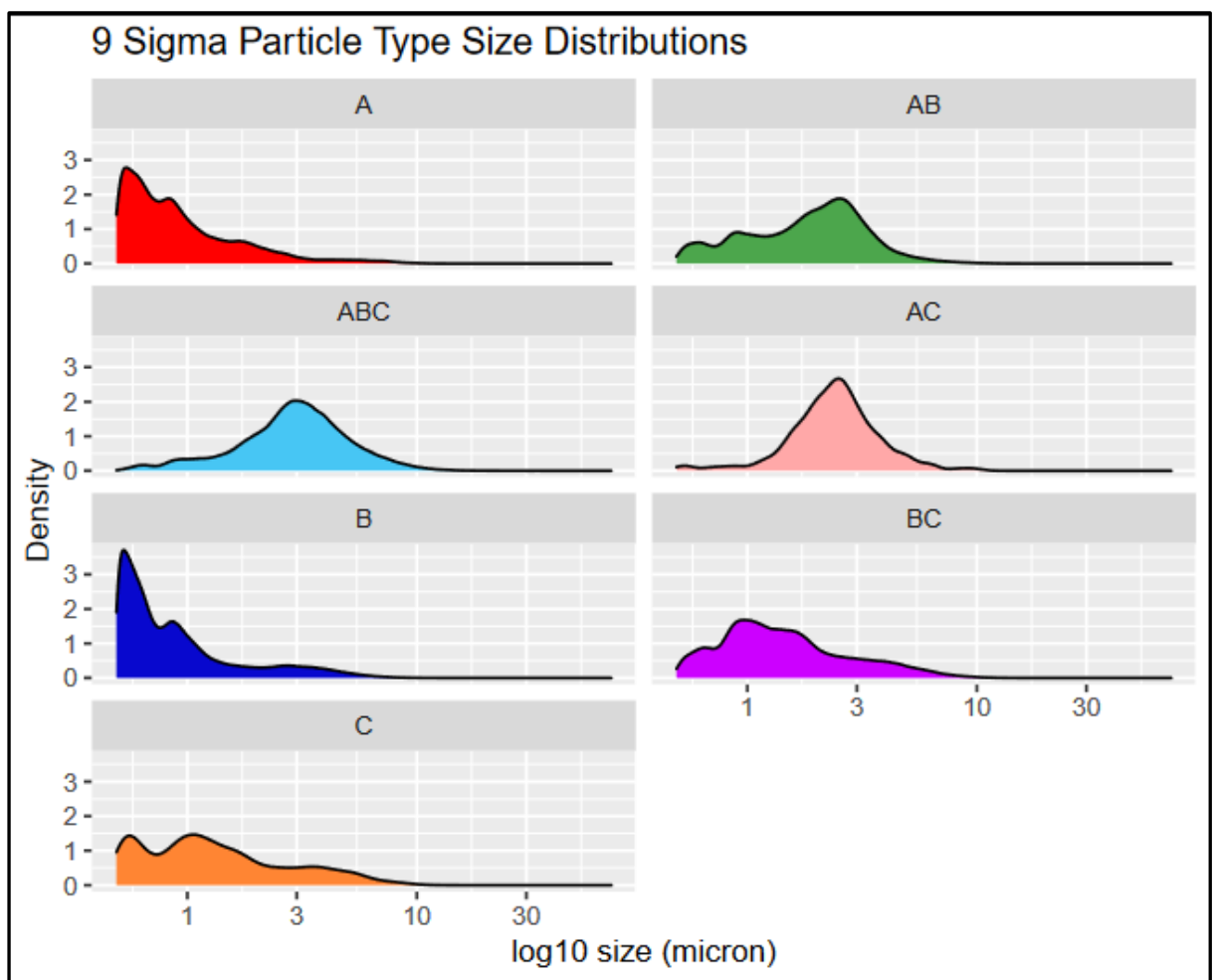


Figure 4.11: 9 Sigma, Log10 size distributions of WIBS particles.

The potential impact of anthropogenic pollution was considered, and a second dataset was created, in which only particles with a size of $2\mu\text{m}$ or above were included, as this would have the dual purpose of removing the majority of the anthropogenic pollution and is the minimum

size for visible optical analysis of fungal spores in the laboratory. In this dataset, we see diurnal patterns that are far more reflective of expected WIBS particle outputs, and ones that reflect those seen in numerous studies (Abdel Hameed et al., 2009; Calderon et al., 1995; Garland et al., 2009; Huffman et al., 2012; Khan et al., 2016; Saari et al., 2015).

To examine the possible diurnal correlations between individual WIBS bands and fungal spore types, and to account for possible discrepancies in sampling volume between methods, normalised WIBS particle concentration curves were created (Figure 4.12). Each graph shows all seven categories, and each separate band is highlighted and coloured in each successive chart, so as the relative positions of each band can be easily distinguished. Two clear “pairs” of WIBS bands become visible when viewing the data in this way. First are the B and BC bands, which see highest seasonal correlation with Basidiospores and other “dry weather spores”. These spores both fluoresce in the FL2 channel. Both follow the same pattern of rising to a sharp peak in the early morning, and slowly decreasing in concentration over the course of the day, before reaching their lowest concentrations in the middle of the night before dawn.

The second “pair” of WIBS bands are A and AB spores (and to a lesser extent, AC). These bands all share the FL1 channel of fluorescence and see highest seasonal correlation with the “wet weather” Ascospores. A very clear bimodal pattern is visible with these particles. A first peak in the early morning, similar to that seen in the B and BC bands, is followed by a drop-in concentration throughout the day. The difference is that in the evening, at around 6pm, concentrations begin to rise once again, and reach a second peak of equal concentration around 7pm. This bimodal distribution was noted for comparison with diurnal fungal spore concentrations, which were also determined over the same study period.

Additionally, a short, small, sharp peak in fluorescent particles is seen in all seven bands at 3pm. This is the only diurnal trend that is identifiable in every single band, (even though the pattern is very weak in the C band). A possible anthropogenic source at the same time every day could be responsible for this reading.

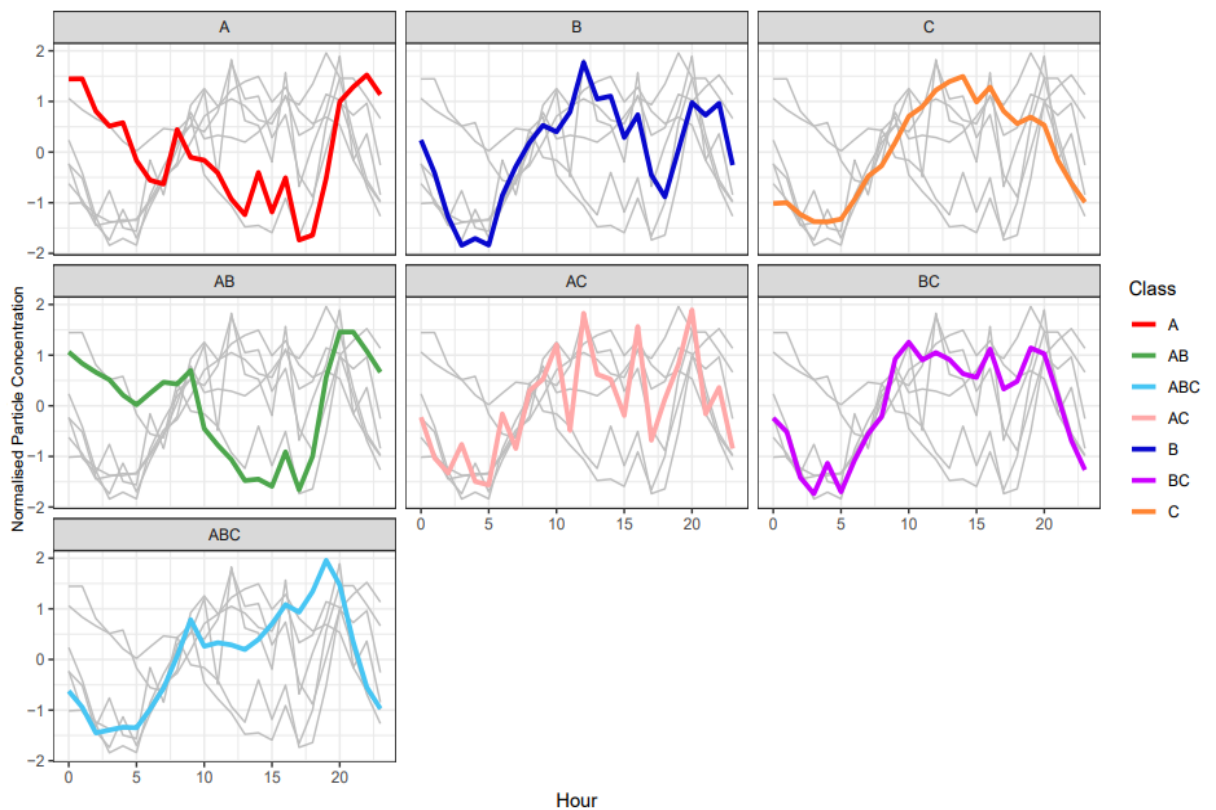


Figure 4.12: WIBS-NEO diurnal charts of each band (>2 μm , 3-Sigma). Each graph highlights one of the bands, with the remaining 6 in the background, to better highlight how each individual and fits within the overall fluorescent particle trend diurnally.

As fungal spores are counted using a Hirst-Lanzoni device, they can be analysed at a time resolution as short as one hour. This allows the creation of diurnal plots, the outputs of which are seen below in Figure 38. The normalised concentration diurnal curves of *Alternaria*, Ascospores, Basidiospores, and *Cladosporium*, show very different diurnal trends between spores. Basidiospore diurnal trends did not follow the expected early peak, and concentration decline throughout the day, as was seen with B and BC particles. Ascospores, however, did appear to have a bimodal distribution, similar to that of the A and AB bands.

In fact, the presence of two daily peaks in the data, seen in the A and AB bands, is particularly reflective of the shape of the diurnal Ascospore curve. Both the WIBS-NEO bands (>2 μm), and the ascospore diurnal charts, see similar drops in average concentrations around 8-9pm. This period of analysis took place during August and September, meaning these decreases in particles and fungal spores align with the setting of the sun in the evening. At the start of August, the sun sets from 21:20, and by the middle of September, the sun sets at 19:40, aligning with predicted particle concentration decreases. This could be one explanation for the decrease in concentrations around this time, with “wet spores” able to proliferate at the start

and end of the day, where sunlight is present along with damp and dew, but not in the heat of the day when it is too dry, and devoid of moisture (Almaguer et al., 2014).

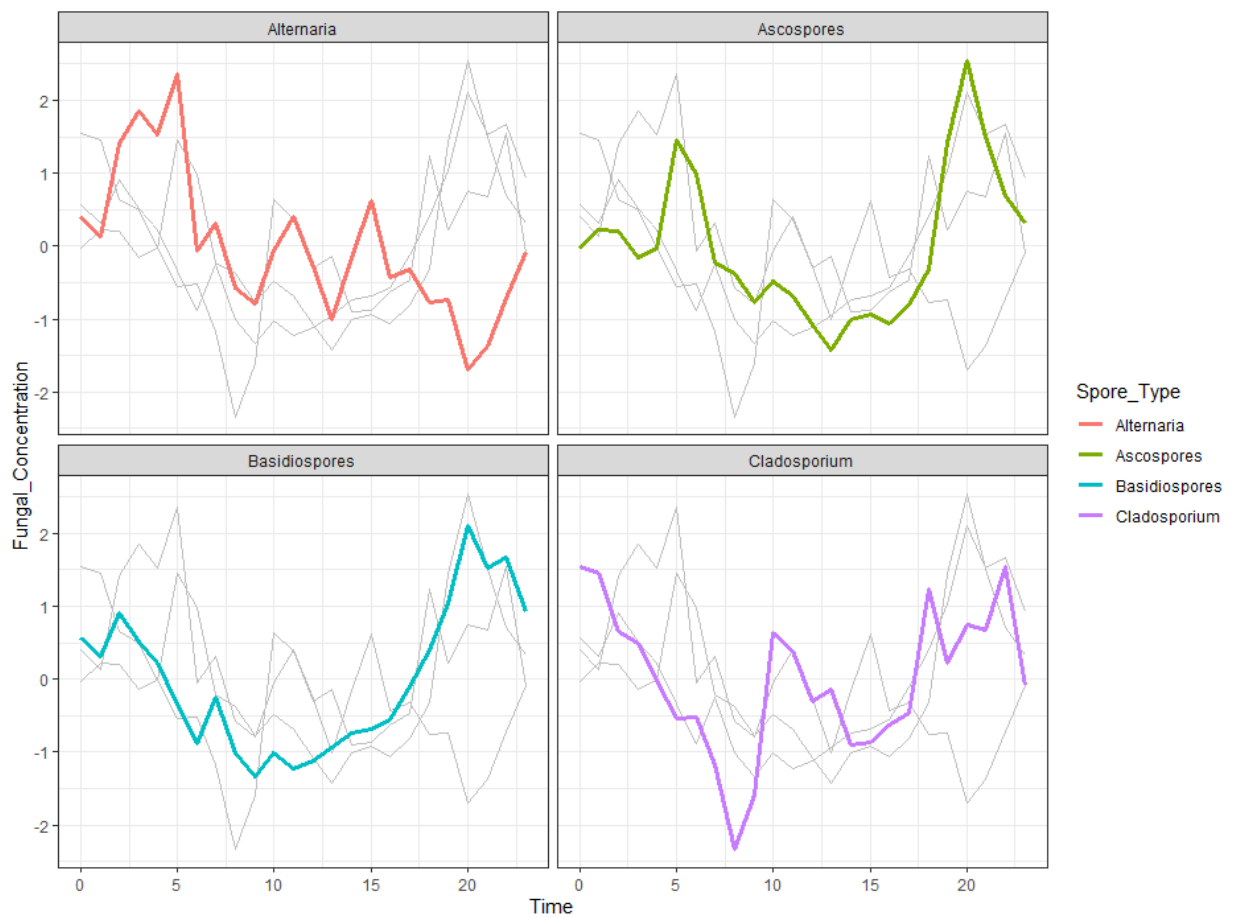


Figure 4.13: Diurnal charts of major fungal spore types, similar to the previous WIBS diurnal chart for direct comparison.

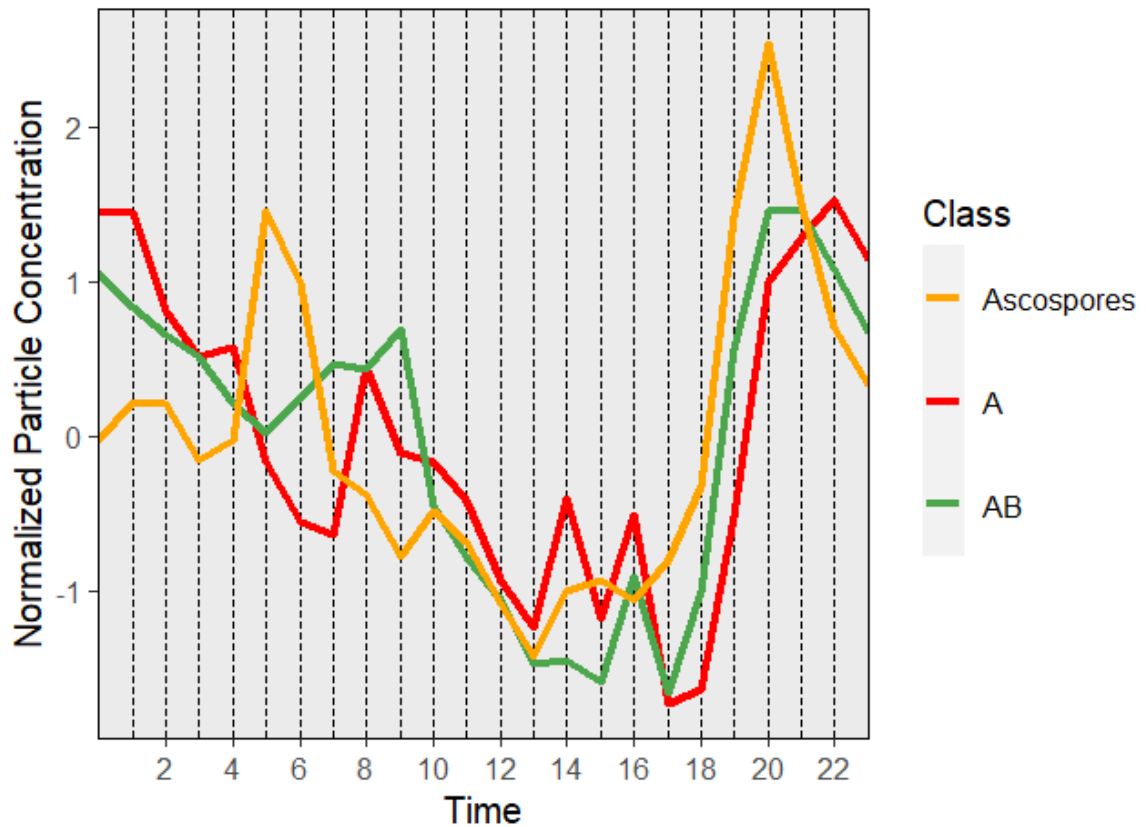


Figure 4.14: Combined normalized diurnal concentrations of A and AB WIBS bands, and ascospores. This is to highlight the correlation diurnally between WIBS particles and fungal spores.

In order to further investigate the apparent relationship between Ascospores, and the A and AB particles, a normalized distribution curve (Figure 4.14) was constructed. This shows that the evening peak does coincide precisely between the spores and particles, with ascospore concentrations rising much higher relative the WIBS particles during the morning peak, as well as “leading” the WIBS particles by about three hours. Many factors could account for the apparent 3-hour delay in the morning, not least the dramatically differing sampling methods used between the devices, and that as the Hirst device has an inlets width of 2mm, and rotates at a rate of 2mm per hour, accuracy is diminished at this smaller time resolution (Apangu et al., 2018; Orlandi et al., 2014).

4.4.7. WIBS Channel potential Bimodal distribution

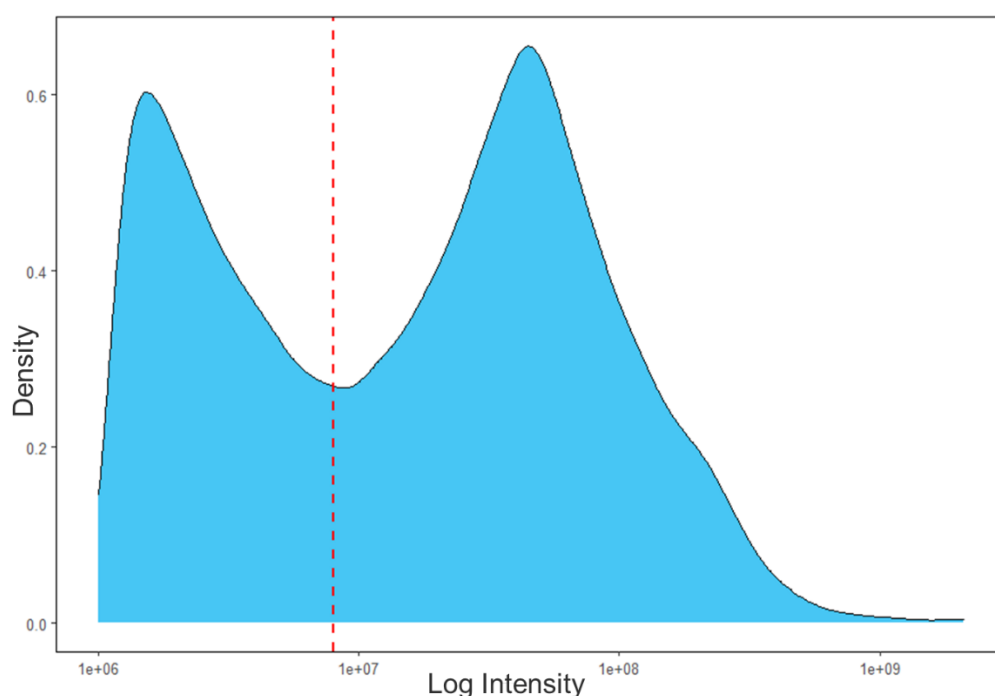


Figure 4.15: Graph showing the level of FLI intensity expressed by every ABC particle. This shows a clear bimodality between the more and less intense particles.

One of the more interesting discoveries during the WIBS particle analysis was revealed upon looking at the particle densities of each WIBS particle type at various fluorescence intensities. Throughout several previous campaigns and studies, no WIBS device has previously shown any bimodal distribution. (Daly et al., 2019b; Fernández-Rodríguez et al., 2018; David A. Healy et al., 2012; Markey et al., 2022; O'Connor et al., 2014b, 2013).

The above bimodal distribution is obvious in the FLI channel of the WIBS-Neo, but not so in the FL2 and FL3 channels, when looking at ABC classified particles. To further investigate the possibility of significant results, the bimodal distribution was divided into two separate datasets, as seen in Figure 4.15. They were categorised as ABC_1, and ABC_2” for the first and second mode respectfully. It was subsequently found that when both parameters were used for correlation analysis, each grouping was significantly correlated with a completely different type of bioaerosol (Figure 41). As a result, in the modelling campaign, the two modes were kept as separate parameters within the creation of different bioaerosol models. When combined as one parameter, the ABC channel was not very useful as a correlative factor or as a predictor for any spore type, but each mode, separately, has very different relationships with fungal spores, pollution concentrations, and meteorological factors, as will be expanded upon in the next section.

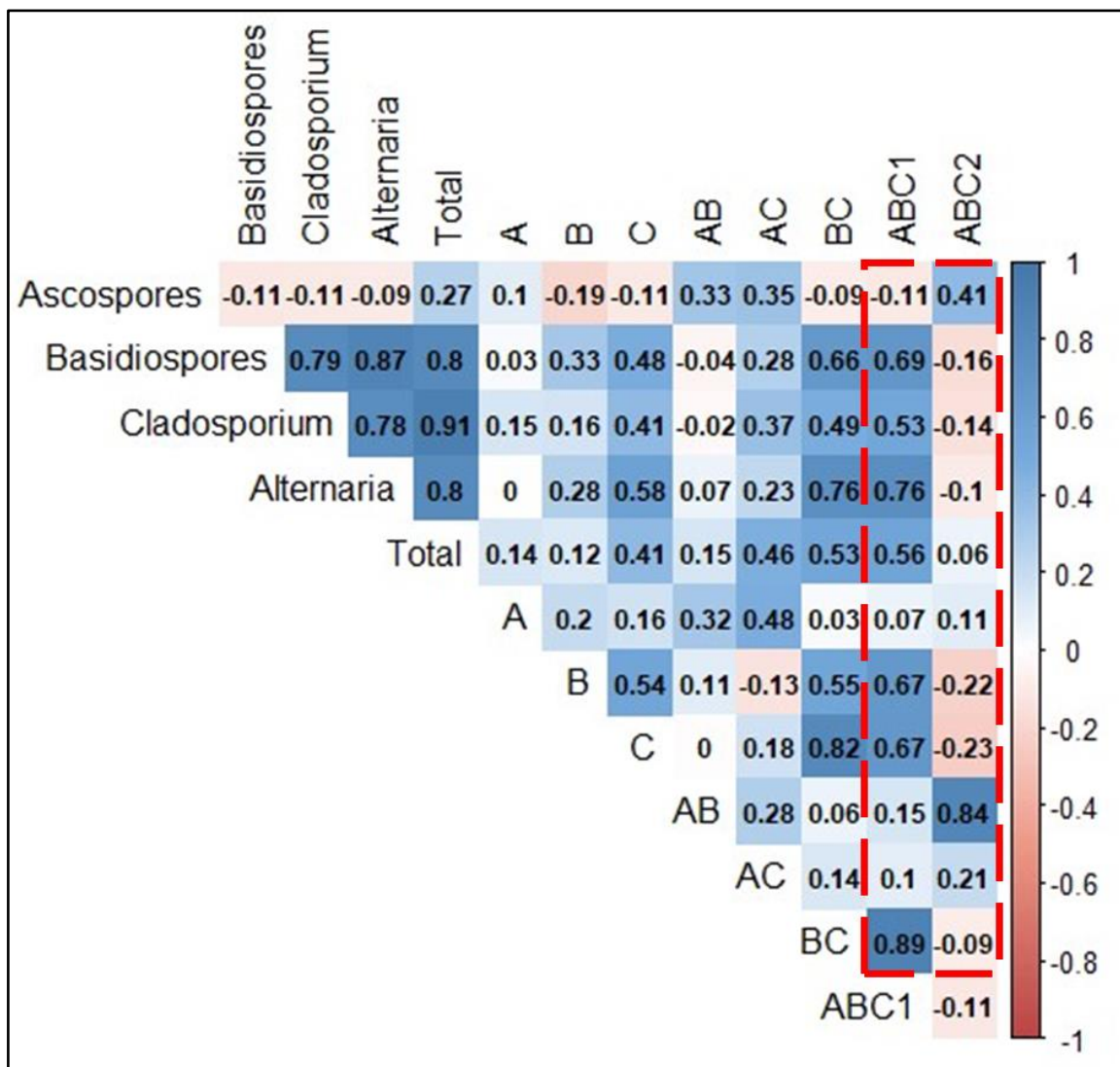


Figure 4.16: Corrplot highlighting the difference in correlative characteristics of the two ABC modes.

4.5. IBAC-2 Real-Time Monitoring Campaign

4.5.1. Campaign Overview

Another device being tested for suitability for fungal spores as part of the project is the Instantaneous Bioaerosol Analysis and Collection 2 (IBAC-2) (a successor to FIDO B2, and the Instantaneous Biological Analyzer and Collector (IBAC)). While the IBAC device was initially developed for the purpose of detecting potential threats. We focused on relating its output to biological aerosols and did not investigate its capabilities as an early warning system. Similar to the WIBS it can differentiate between biological and non-biological particles via elastic scattering (photomultiplier tubes) and particle fluorescence utilizing a 405nm laser as an excitation source. Particles are drawn into the device at a rate of 3.8 litres per minute. They

pass through an optical illumination region, where the 405nm laser excites the particles. Size and concentration of particles are measured from the light scatter. If the integrated fluorescence emitted by a particle falls between 450-600nm, and exceeds a pre-set threshold, it is determined to be fluorescent/biological. Individual particles analysis is capable at up to 400,000 particles per litre, and a count rate maximum of 25,000 particles per second.

Due to the size and fluorescence measurement abilities of the IBAC, the device can potentially detect spores, and bacteria, among other bioaerosols. Primary customers of the first IBAC have included homeland security and defence customers. (P. 1987- Anclia, 2015; DeFreez, 2009b; Jonsson and Kullander, 2014b; Paziienza, 2013; Santarpia et al., 2013)

Advantages of the IBAC over other biological particle sensors and detectors include its ability to work more efficiently and to run continually for long periods. A disadvantage that the IBAC possesses is possible confusion when detecting particles from anthropogenic sources, with the device occasionally struggling to correctly identify whether some particles from these sources are biological in origin. ("FLIR IBAC 2 Bio-Threat Detection & Collection | Teledyne FLIR," 2021)

4.5.2. IBAC-2 Monitoring Results.

Fungal spore concentrations were compared to IBAC-2 biological particles over the campaign period, however poor correlation was observed between the two methods, which are seen in Table 4.1. No significant correlations were found with the IBAC-2 device and any of the fungal spore types. The highest correlation, of 0.2 between *Alternaria* and small biological particles (0.7-1.5 μ m) is not of use given that small particles are categorised as below 1.5 μ m, whereas *Alternaria* is the largest of the studied spore types, with sizes ranging from 2 μ m and above (generally far larger). All other Pearson correlation values were below 0.2, (A correlation of 0.11 between Basidiospores and Small Biological particles being the next highest), showing that at least in this study, the instrument was not a strong indicator of fungal spore fructification values.

Table 3: Pearson correlation table of IBAC particles and fungal spores

Pearson Correlation Table	Small IBAC	Big IBAC	Small IBAC	Bio Large Bio IBAC
<i>Cladosporium</i>	0.01	-0.15	0.06	-0.07
<i>Alternaria</i>	0.09	-0.08	0.2	0.1
Ascospores	-0.08	-0.04	-0.1	0
Basidiospores	0.02	-0.18	0.11	-0.04
Other Spores	-0.24	-0.2	-0.18	-0.12
Total Spores	-0.03	-0.18	0.03	-0.06

*. Correlation is significant at the 0.05 level.

In Figures 4.17 and 4.18, below, boxplots of daily IBAC particle concentrations, over the course of the monitoring campaign can be seen. Each boxplot is made up of 24 points, one representing the average value for each hour of the day, so as to reduce the massive number of outliers seen when plotted at the maximum temporal resolution.

The peak point in IBAC concentrations was seen on the 9th of August. This occurred during a period of extremely heavy rainfall, and when looking at data from other sources such as the WIBS, and fungal spore concentrations at the time, it can be concluded that while the rainfall suppressed fungal spore release, the IBAC observed the rainfall to be an increase in “particulate number”. During the main fungal spore peak in the last week of August, the IBAC does not noticeably track, or predict this peak, resulting in the lower correlation values seen in Table 3.

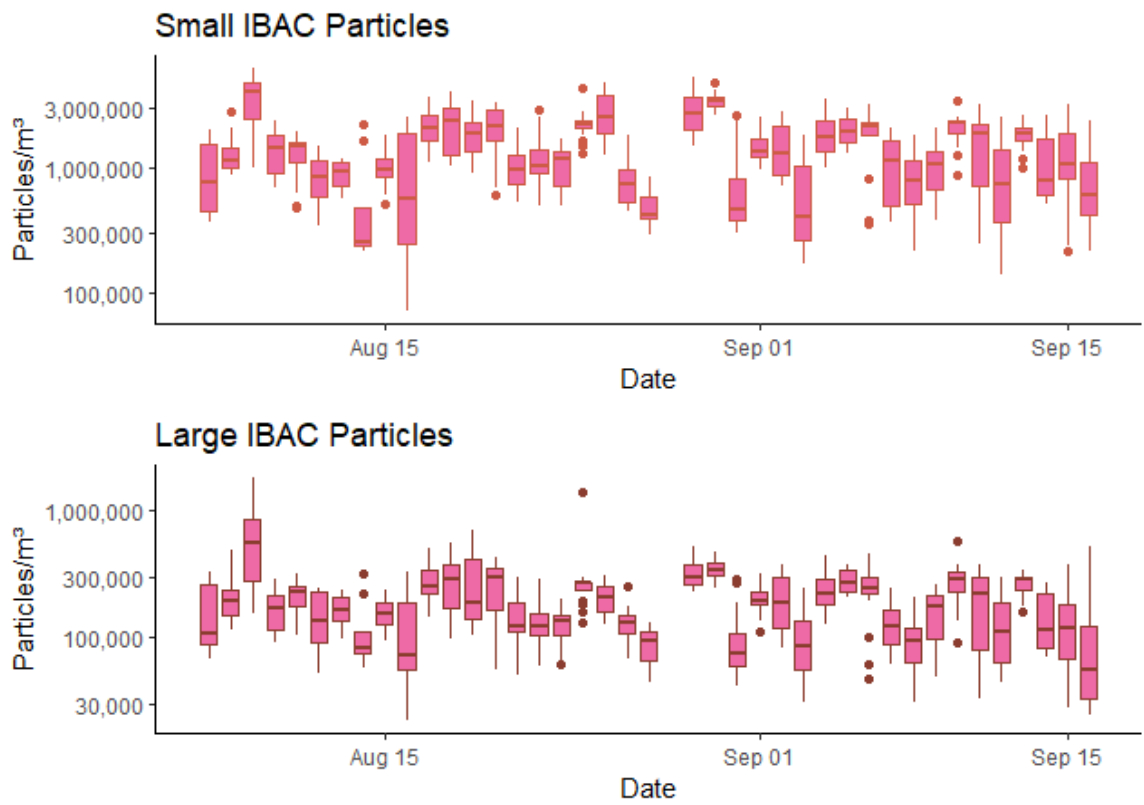


Figure 4.17: Daily boxplots of all small (0.7-1.5 μm) and large (1.5-10 μm) IBAC particles.

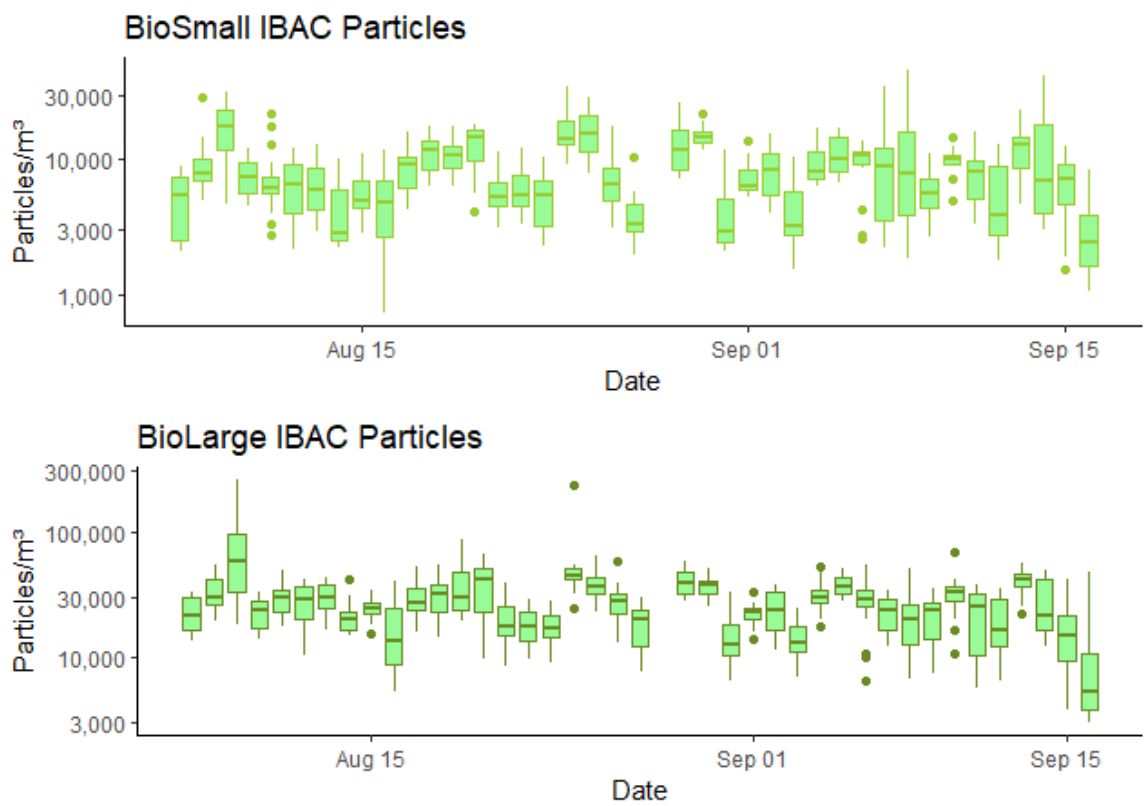


Figure 4.18: Daily boxplots of biological small (0.7-1.5 μm) and large (1.5-10 μm) IBAC particles.

Above show the daily boxplots of IBAC particles for all four categories. Each boxplot represents all measurements for that day, data was taken directly from the device and processed in R. Of note are that for “Total IBAC” particles, there are three times as many “small” particles as there are “Large”. This is reversed when looking at the fluorescent, or “biological” particles. There are ten times as many “Large” particles as there are “Small”. This indicates that the majority of anthropogenic particles are below 1.5 μm in size, as only one percent of “Small” particles are fluorescent, whereas approximately 30% of “Large” particles are fluorescent. Other studies into biological particle sizes with different instrumentation have seen that when size filtering is applied, usually the proportion of particles that are significantly correlated to biological aerosols increases dramatically (Huffman et al., 2012; Li et al., 2020).

4.6. Comparison Between Real Time Devices

The WIBS-NEO and IBAC particle sensor were both run across the same period in Summer 2019, allowing for a direct comparison between the two sensors. While both devices use similar technology, there is a significant difference in the quantity of information outputted by the devices. This is due to the WIBS monitoring a wider range of particle sizes (0.5-30 micron) and outputting it as single particle data. The IBAC has two defined particle size bands 0.7-1.5 and 1.5-10 micron. Thus, the IBAC data is far more agglomerated. Equally, individual particle fluorescence intensities are determined by the WIBS (with two excitation wavelengths and emission bands) while the IBAC-2 utilizes only one excitation source.

A correlation table for the two instruments was constructed, with values seen below in Table 4.2, while the WIBS instrument is capable of monitoring a different range compared to that of the IBAC-2. Its data was size filtered for this comparison thus the size ranges and groups exhibited by the IBAC-2 remain true for the WIBS in this analysis. There is a relatively good level of correlation between the two machines, particularly when comparing the “Small Biological Particle” output of the IBAC device with the different outputs of the WIBS apparatus.

Table 4: Pearson correlation table of IBAC particles and WIBS-Neo particles.

Pearson Correlation	Small IBAC	Big IBAC	Small Bio IBAC	Big Bio IBAC
Small WIBS	0.6*	0.49*	0.6*	0.44*
Big WIBS	0.67*	0.63*	0.7*	0.6*
Small Fluorescent WIBS	0.21	0.07	0.46*	0.26
Big Fluorescent WIBS	0.21	0.11	0.51*	0.32

*. Correlation is significant at the 0.05 level.

Correlation between approximately 0.5 and 0.7 can be seen for Small Bio IBAC groups compared with that of the WIBS. It should be noted that fluorescent particles in the WIBS groups reflect any particle with fluorescence.

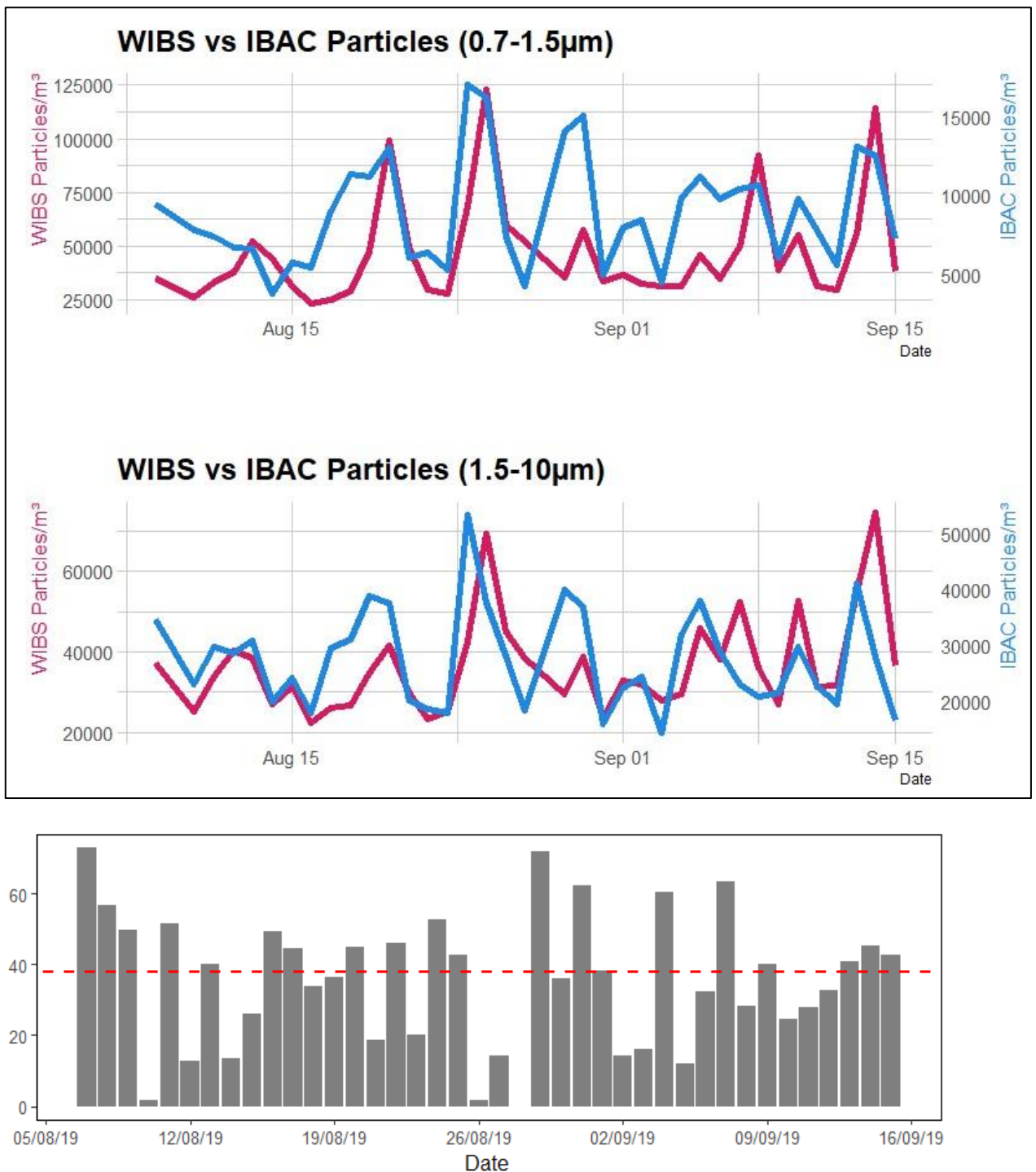


Figure 4.19: Comparison between the WIBS NEO, and the IBAC particle sensor for all particle type and size ranges, highlighting the points of agreement between the two devices (0.7-10 µm).

As summarized in Figure 4.19, a direct comparison of the two size bands for total particles, fluorescent particles, and non-fluorescent particles was also conducted. Overall, the IBAC-2 sampled more particles than the WIBS due to the WIBS-NEO's lower flow rate (0.3 L/min) in

comparison to the IBAC-2's higher flow rate (3.8 L/min). Additionally, the IBAC-2 derives both size and fluorescence information from a single 405nm laser, as opposed to the WIBS-NEO, which interrogates each particle under analysis using both the sizing laser and two separate Xenon flash lamps. Thus, the potential for missed particles in the IBAC is far lower than that of the WIBS, given the sequence of analysis involves less variables, instrumentation, etc. Similarly, taking into account the fact that the IBAC was created for bio-weapon detection, its counting efficiency for smaller particles maybe greater than that of the WIBS. While counting efficiency estimation of the WIBS has been conducted (David A Healy et al., 2012; Lieberherr et al., 2021), this has been not been carried out for the IBAC-2.

So, this is simply a possible reason for the differences between the two devices that have been noticed. It is interesting to note that the WIBS-neo reported a higher concentration of particles in the larger size range (1.5–10 μm). This could be because of the WIBS's ability to identify considerably larger particles, which makes it more effective in sampling particles at the IBAC-2's 10 μm size limit. Similar to this, the WIBS recorded more fluorescent particles whereas the IBAC-2 recorded more non-fluorescent particles. This is because the WIBS has more excitation and emission channels than the IBAC-2, which enables it to identify fluorescent particles that the IBAC-2 is not able to see.

The range of non-fluorescent particles between 1.5 and 10 μm ($R=0.67$) and the range of fluorescent particles between 0.7 and 1.5 μm ($R=0.60$) showed the best agreement between the two devices. A direct comparison between the IBAC-2 and each FL channel of the WIBS was made in an effort to identify increased correlation between the two devices. The FL1 channel showed the strongest correlation ($R=0.4$), particularly for fluorescent particles between 0.7 and 1.5 μm ($r=0.6$). The enhanced sensitivity of the FL1 channel in the WIBS-NEO seems to be more indicative of the ambient FAPs seen by both instruments, even if the FL3 channel is more similar to the IBAC-2 in terms of excitation and emission wavelengths.

4.6.1. Comparison of IBAC and WIBS with pollutant interferents

Common anthropogenic contaminants in the region were linked against the device outputs during the course of the monitoring experiment in an effort to identify other possible uses for the IBAC device. Most pollutants showed little to no association ($\text{NO}_x R^2 = 0.009$, $\text{PM}_{2.5} R^2 = 0.19$) but PM_{10} and the IBAC device showed a decent correlation (Figure 4.20). This suggests that a weaker connection between the IBAC device and fungal spores may be caused by the

interference of particles from anthropogenic sources. It also suggests that the IBAC could be used to measure these pollutants.

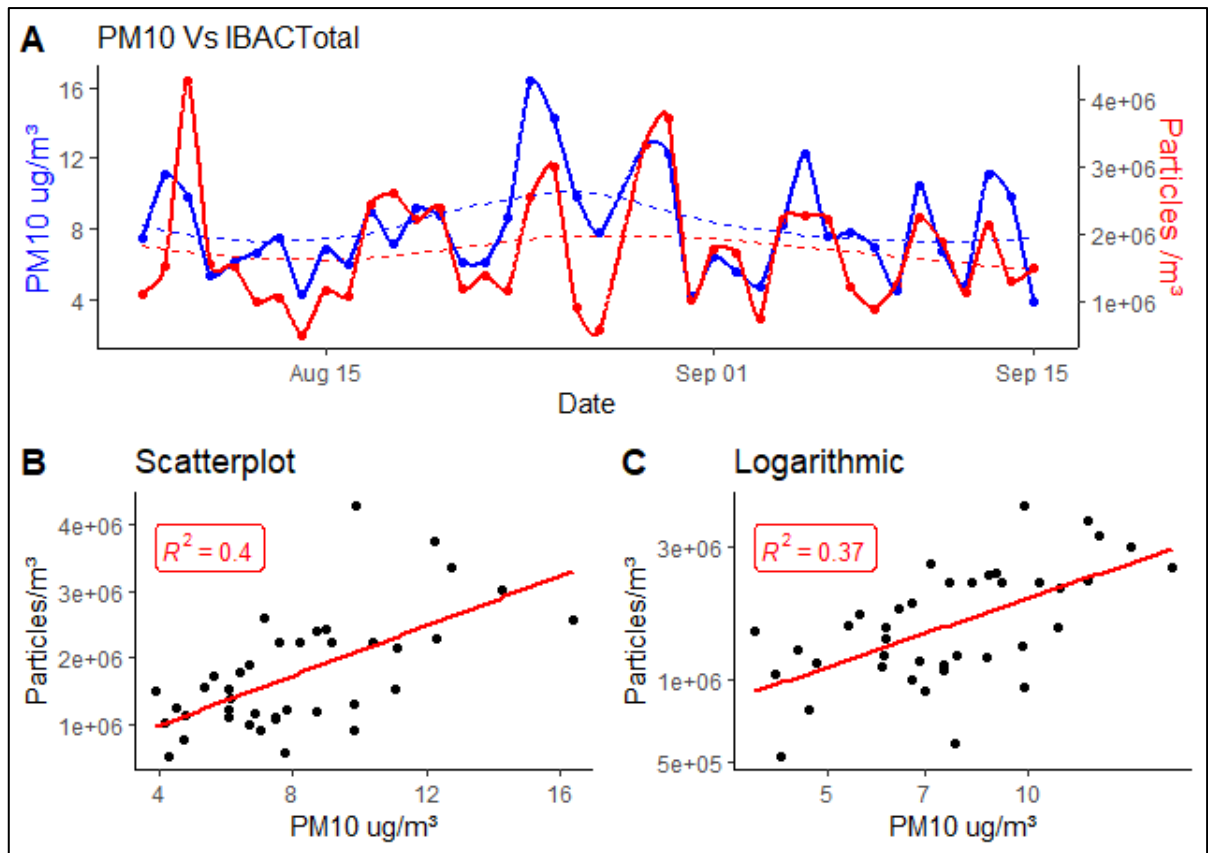


Figure 4.20: Comparison between IBAC particles and PM₁₀ emissions during the monitoring campaign.

One point of note is the location of the pollution monitoring device. This device was not specifically run as part of the project, but rather is publicly available data obtained from the Irish Environmental Protection Agency (EPA). As the data was simply taken from online data output by the nearby EPA monitoring station, some aspects relating to the running and operation of the instrument are outside of our control. Conversely, as the resources for yet another monitoring instrument were not available, this additional dataset is a great added asset for this project as it can potentially elucidate the contribution of anthropogenic pollution. As the device is located less than 1km away, but is not directly adjacent to the other devices, the resulting data will be more influenced by localised sources than that of the IBAC or the WIBS. Co-deployment of the IBAC-2 and the EPA particulate measurements at the same location could lead to a greater understanding of how the IBAC compares and how its fluorescence measurements could be used in terms of Air Quality and the AQI (Air Quality

Index). Recommendations would be for this to be completed as its own instrumentation validation campaign rather than as smaller part of this project.

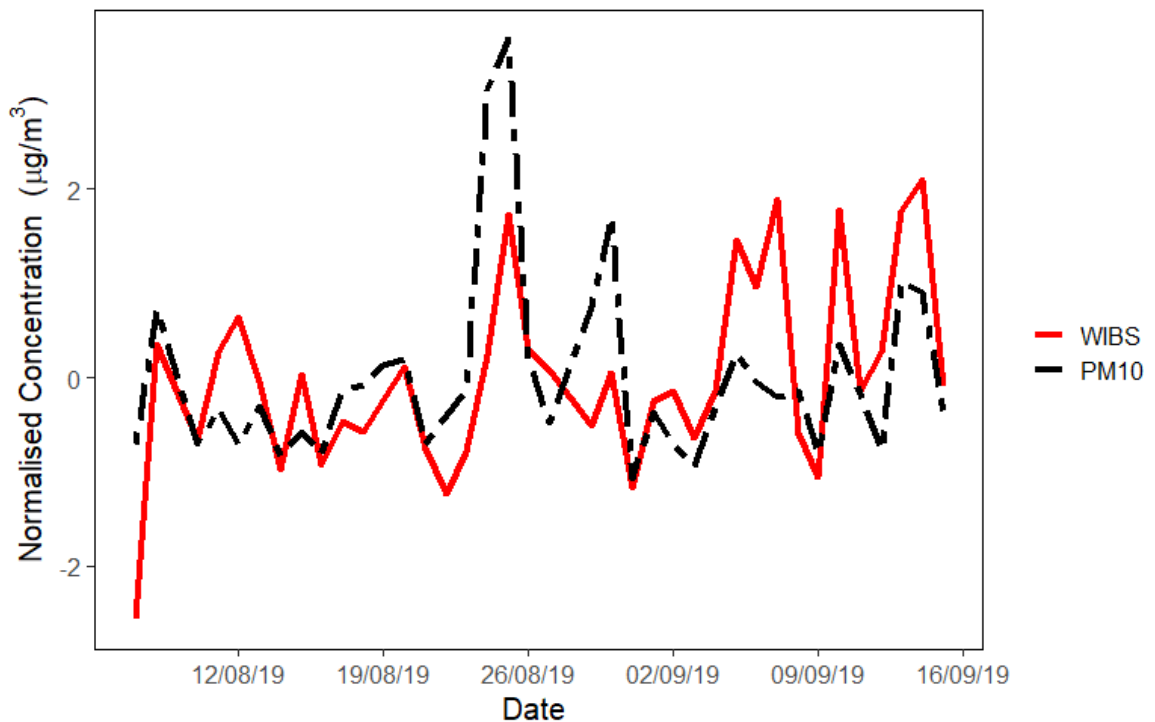


Figure 4.21: Normalised direct comparison of particles observed by the WIBS vs PM₁₀.

Equally, the WIBS showed similar trends when compared with PM₁₀, with a normalised time series shown between the WIBS and the PM₁₀ values above (Figure 4.21) and again it would be of interest to evaluate its potential as an Air Quality instrument, particularly as several anthropogenic aerosol particles do in fact fluoresce (PAHs and SOA) and could be potentially distinguished from biological particles by the WIBS.

The interactions that can, and do exist between fungal spores, pollen grains, meteorological parameters, and anthropogenic influences, are too complex to be analysed through a simple correlation analysis, and thus require their own dedicated analysis campaign, which will be outlined in the subsequent chapter.

4.7. Conclusion

Traditional methods for fungal spore monitoring have evolved over time, with real-time methods emerging as an alternative due to their rapid output and reduced workload. The Hirst volumetric trap is the standard sampling method worldwide, but it is labour-intensive and time-consuming. Real-time monitoring methods have been developed for early warning systems, such as the IBAC, which focuses on identifying bio-toxins. This is not possible with a traditional sampler. Newer techniques, such as the WIBS-NEO and IBAC-2, utilize air-flow cytometry to detect ambient fungal spore and pollen concentrations.

This study aimed to compare real-time bioaerosol monitoring methods and collect real-time data for the development of a bioaerosol prediction algorithm. The Hirst-Lanzoni method of PBAP monitoring was compared with the WIBS-NEO and IBAC spectrometric techniques. The monitoring program was continuously run from August 7th to September 16th, 2019 on the roof of the former TU Dublin Kevin Street site. The most commonly identified single spore type was *Cladosporium*, which comprised 66.3% of all fungal spores counted during the campaign. We found little correlation between FL1 type particles and fungal spores, possibly due to differences in fluorescence sensitivity between previous WIBS models and the WIBS-NEO. Previously it's been seen that anthropogenic/combustion particles favour the FL1 channel over the FL2 or FL3 channels in complex urban environments. BC particles between 2-30 μm at 9σ had a high correlation with total fungal spore concentrations, but there were periods where BC particles failed to account for high concentrations of fungal spores, indicating that some spore types are not being detected within the BC fraction. Basidiospores and *Alternaria* exhibited notable correlation with BC type particles, while *Cladosporium* spores showed poor correlation. We also investigated the impact of meteorological parameters on fungal spore and fluorescent aerosol particles (FAPs). Fluorescent WIBS particles showed a significant negative correlation with minimum temperature, grass minimum temperature, and wind speed. The decline in FAPs could be related to the correlation between grass minimum temperature, rain, and wind speed, which are drivers for the transport and deposition of certain bioaerosols. A notable positive correlation was also observed for FAPs detected by the WIBS with air pressure, potentially indicating a degree of contribution by bioaerosols to the FAP fraction.

The IBAC-2 real-time monitoring campaign focuses on the detection of fungal spores using a device that differentiates between biological and non-biological particles using a 405nm laser. The IBAC-2 has advantages such as efficiency and long-term remote operation, but it struggles to accurately identify particles from anthropogenic sources. Despite the monitoring campaign,

no significant correlations were found between the IBAC-2 device and fungal spore types. The WIBS-NEO and IBAC particle sensors were compared in Summer 2019, showing significant differences in their readings. The WIBS instrument has an overall higher correlation with Hirst values, particularly when comparing the "Small Biological Particle" output of the IBAC device with the different outputs of the WIBS apparatus. The WIBS showed good correlation when compared to PM10, and its potential as an air quality instrument was noted.

In conclusion, traditional methods for fungal spore monitoring, such as the Hirst volumetric trap, are labour-intensive and time-consuming. Real-time monitoring methods, such as the WIBS-NEO and IBAC, promise a fast alternative. The WIBS-NEO is effective in detecting ambient fungal spore and pollen concentrations, while the IBAC-2 is useful for detecting potential threats related to biological aerosols. Our research found correlations between certain types of fungal spores and WIBS-NEO particle outputs, but also identified limitations in detecting specific spore types. The IBAC-2 device struggled to accurately identify fungal spore types and track peak concentrations. WIBS instrument having a better level of correlation with all aerosols. Both devices showed potential for measuring anthropogenic contaminants and air quality. Overall, further research and analyses are needed to fully understand the complex interactions between fungal spores, pollen grains, meteorological parameters, and anthropogenic influences. Manual analysis alone is itself a time-consuming task, so investigations were made into the state of the art of bioaerosol analysis, and the next chapter outlines this process.

4.8. References

- Abdel Hameed, A.A., Khoder, M.I., Yuosra, S., Osman, A.M., Ghanem, S., 2009. Diurnal distribution of airborne bacteria and fungi in the atmosphere of Helwan area, Egypt. *Sci. Total Environ.* 407, 6217–6222. <https://doi.org/10.1016/j.scitotenv.2009.08.028>
- Almaguer, M., Aira, M.-J., Rodríguez-Rajo, F.J., Rojas, T.I., 2014. Temporal dynamics of airborne fungi in Havana (Cuba) during dry and rainy seasons: influence of meteorological parameters. *Int. J. Biometeorol.* 58, 1459–1470. <https://doi.org/10.1007/s00484-013-0748-6>
- Anchlia, P., 2015. *Aerosol Data Modeling & Similarity Assessment – a Probabilistic Approach (Thesis)*.
- Anchlia, P. 1987-, 2015. *Aerosol Data Modeling & Similarity Assessment – a Probabilistic Approach (Thesis)*.
- Apangu, G., Frisk, C.A., Adams-Groom, B., Petch, G., Skjøth, C., 2018. Spatial Bi-hourly Variation of *Alternaria* Spore Concentration in Worcester, UK. Presented at the 11th International Congress on Aerobiology, Parma, Italy, pp. 1-1.
- Bragoszewska, E., Pastuszka, J.S., 2018. Influence of meteorological factors on the level and characteristics of culturable bacteria in the air in Gliwice, Upper Silesia (Poland). *Aerobiologia* 34, 241–255. <https://doi.org/10.1007/s10453-018-9510-1>
- Calderon, C., Lacey, J., McCartney, H.A., Rosas, I., 1995. Seasonal and Diurnal Variation of Airborne Basidiomycete Spore Concentrations in Mexico City. *Grana* 34, 260–268. <https://doi.org/10.1080/00173139509429055>
- Choi, K., Koh, Y.J., Jeong, Y.S., Chong, E., 2018. Experimental studies on the classification of airborne particles based on their optical properties. *Bull. Korean Chem. Soc.* 39, 369–374. <https://doi.org/10.1002/bkcs.11396>
- Clot, B., Gilge, S., Hajkova, L., Magyar, D., Scheifinger, H., Sofiev, M., Büttler, F., Tummon, F., 2020. The EUMETNET AutoPollen programme: establishing a prototype automatic pollen monitoring network in Europe. *Aerobiologia* 4. <https://doi.org/10.1007/s10453-020-09666-4>
- Croke, B., Cornish, P., Islam, A., 2015. Chapter 5 - Modeling the Impact of Watershed Development on Water Resources in India, in: Reddy, V.R., Syme, G.J. (Eds.), *Integrated Assessment of Scale Impacts of Watershed Intervention*. Elsevier, Boston, pp. 99–148. <https://doi.org/10.1016/B978-0-12-800067-0.00005-0>

- Daly, S.M., O'Connor, D.J., Healy, D.A., Hellebust, S., Arndt, J., McGillicuddy, E., Feeney, P., Quirke, M., Wenger, J., Sodeau, J., 2019a. Investigation of coastal sea-fog formation using the WIBS (wideband integrated bioaerosol sensor) technique. *Atmospheric Chem. Phys.* 19, 5737–5751. <https://doi.org/10.5194/acp-19-5737-2019>
- Daly, S.M., O'Connor, D.J., Healy, D.A., Hellebust, S., Arndt, J., McGillicuddy, E.J., Feeney, P., Quirke, M., Wenger, J.C., Sodeau, J.R., 2019b. Investigation of coastal sea-fog formation using the WIBS (wideband integrated bioaerosol sensor) technique. *Atmospheric Chem. Phys.* 19, 5737–5751. <https://doi.org/10.5194/acp-19-5737-2019>
- Davies, R.R., Smith, L.P., 1974. Weather and the grass pollen content of the air. *Clin. Exp. Allergy* 4, 95–108. <https://doi.org/10.1111/j.1365-2222.1974.tb01367.x>
- DeFreez, R., 2009a. LIF bio-aerosol threat triggers: then and now. *Opt. Based Biol. Chem. Detect. Def.* V 7484, 74840H. <https://doi.org/10.1117/12.835088>
- DeFreez, R., 2009b. LIF Bio-Aerosol Threat Triggers: then and now. *Proc. SPIE - Int. Soc. Opt. Eng.* 7484. <https://doi.org/10.1117/12.835088>
- Feeney, P., Rodríguez, S.F., Molina, R., McGillicuddy, E., Hellebust, S., Quirke, M., Daly, S., O'Connor, D., Sodeau, J., 2018. A comparison of on-line and off-line bioaerosol measurements at a biowaste site. *Waste Manag.* 76, 323–338. <https://doi.org/10.1016/j.wasman.2018.02.035>
- Fennelly, M., Sewell, G., Prentice, M., O'Connor, D., Sodeau, J., 2017. Review: The Use of Real-Time Fluorescence Instrumentation to Monitor Ambient Primary Biological Aerosol Particles (PBAP). *Atmosphere* 9, 1. <https://doi.org/10.3390/atmos9010001>
- Fennelly, M.J., Sewell, G., Prentice, M.B., O'Connor, D.J., Sodeau, J.R., 2018. Review: The Use of Real-Time Fluorescence Instrumentation to Monitor Ambient Primary Biological Aerosol Particles (PBAP). *Atmosphere* 9, 1. <https://doi.org/10.3390/atmos9010001>
- Fernández-Rodríguez, S., Tormo-Molina, R., Lemonis, N., Clot, B., O'Connor, D.J., Sodeau, J.R., 2018. Comparison of fungal spores concentrations measured with wideband integrated bioaerosol sensor and Hirst methodology. *Atmos. Environ.* 175, 1–14. <https://doi.org/10.1016/j.atmosenv.2017.11.038>
- FLIR IBAC 2 Bio-Threat Detection & Collection | Teledyne FLIR [WWW Document], 2021. URL <https://www.flir.com/products/ibac-2/> (accessed 7.22.21).
- Forde, E., Gallagher, M., Foot, V., Sarda-Esteve, R., Crawford, I., Kaye, P., Stanley, W., Topping, D., 2019a. Characterisation and source identification of biofluorescent aerosol emissions over

- winter and summer periods in the United Kingdom. *Atmospheric Chem. Phys.* 19, 1665–1684. <https://doi.org/10.5194/acp-19-1665-2019>
- Forde, E., Gallagher, M., Walker, M., Foot, V., Attwood, A., Granger, G., Sarda-Estève, R., Stanley, W., Kaye, P., Topping, D., 2019b. Intercomparison of multiple UV-LIF spectrometers using the aerosol challenge simulator. *Atmosphere* 10, 1–29. <https://doi.org/10.3390/ATMOS10120797>
- Fourie, P., Schutte, T., Serfontein, S., Swart, F., 2013. Modeling the Effect of Temperature and Wetness on *Guignardia Pseudothecium* Maturation and Ascospore Release in Citrus Orchards. *Phytopathology*® 103, 281–292. <https://doi.org/10.1094/PHYTO-07-11-0194>
- Gabey, A.M., Gallagher, M.W., Whitehead, J., Dorsey, J.R., Kaye, P.H., Stanley, W.R., 2010. Measurements and comparison of primary biological aerosol above and below a tropical forest canopy using a dual channel fluorescence spectrometer. *Atmospheric Chem. Phys.* 10, 4453–4466. <https://doi.org/10.5194/acp-10-4453-2010>
- Gabey, A.M., Stanley, W.R., Gallagher, M.W., Kaye, P.H., 2011. The fluorescence properties of aerosol larger than 0.8 μ in urban and tropical rainforest locations. *Atmospheric Chem. Phys.* 11, 5491–5504. <https://doi.org/10.5194/acp-11-5491-2011>
- Galán, C., Smith, M., Thibaudon, M., Frenguelli, G., Oteros, J., Gehrig, R., Berger, U., Clot, B., Brandao, R., 2014. Pollen monitoring: minimum requirements and reproducibility of analysis. *Aerobiologia* 30, 385–395. <https://doi.org/10.1007/s10453-014-9335-5>
- Garland, R.M., Schmid, O., Nowak, A., Achtert, P., Wiedensohler, A., Gunthe, S.S., Takegawa, N., Kita, K., Kondo, Y., Hu, M., Shao, M., Zeng, L.M., Zhu, T., Andreae, M.O., Pöschl, U., 2009. Aerosol optical properties observed during Campaign of Air Quality Research in Beijing 2006 (CAREBeijing-2006): Characteristic differences between the inflow and outflow of Beijing city air. *J. Geophys. Res. Atmospheres* 114, D00G04. <https://doi.org/10.1029/2008JD010780>
- Gong, J., Qi, J., E, B., Yin, Y., Gao, D., 2020. Concentration, viability and size distribution of bacteria in atmospheric bioaerosols under different types of pollution. *Environ. Pollut.* 257, 113485. <https://doi.org/10.1016/j.envpol.2019.113485>
- Hart, M.L., Wentworth, J.E., Bailey, J.P., 1994. The effects of trap height and weather variables on recorded pollen concentration at leicester. *Grana* 33, 100–103. <https://doi.org/10.1080/00173139409427840>

- Healy, D.A., Huffman, J.A., O'Connor, D.J., Pöhlker, C., Pöschl, U., Sodeau, J.R., 2014. Ambient measurements of biological aerosol particles near Killarney, Ireland: A comparison between real-time fluorescence and microscopy techniques. *Atmospheric Chem. Phys.* 14, 8055–8069. <https://doi.org/10.5194/acp-14-8055-2014>
- Healy, D. A., O'Connor, D.J., Burke, A.M., Sodeau, J.R., 2012a. A laboratory assessment of the Waveband Integrated Bioaerosol Sensor (WIBS-4) using individual samples of pollen and fungal spore material. *Atmos. Environ.* 60, 534–543. <https://doi.org/10.1016/j.atmosenv.2012.06.052>
- Healy, David A., O'Connor, D.J., Burke, A.M., Sodeau, J.R., 2012. A laboratory assessment of the Waveband Integrated Bioaerosol Sensor (WIBS-4) using individual samples of pollen and fungal spore material. *Atmos. Environ.* 60, 534–543. <https://doi.org/10.1016/j.atmosenv.2012.06.052>
- Healy, D. A., O'Connor, D.J., Sodeau, J.R., 2012b. Measurement of the particle counting efficiency of the “Waveband Integrated Bioaerosol Sensor” model number 4 (WIBS-4). *J. Aerosol Sci.* 47, 94–99. <https://doi.org/10.1016/j.jaerosci.2012.01.003>
- Healy, David A, O'Connor, D.J., Sodeau, J.R., 2012. Measurement of the particle counting efficiency of the “Waveband Integrated Bioaerosol Sensor” model number 4 (WIBS-4). *J. Aerosol Sci.* 47, 94–99.
- Hernandez, M., Perring, A.E., McCabe, K., Kok, G., Granger, G., Baumgardner, D., 2016. Chamber catalogues of optical and fluorescent signatures distinguish bioaerosol classes. *Atmospheric Meas. Tech.* 9, 3283–3292. <https://doi.org/10.5194/amt-9-3283-2016>
- Hirst, J.M., 1952. AN AUTOMATIC VOLUMETRIC SPORE TRAP. *Ann. Appl. Biol.* 39, 257–265. <https://doi.org/10.1111/j.1744-7348.1952.tb00904.x>
- Huffman, J.A., Perring, A.E., Savage, N.J., Clot, B., Crouzy, B., Tummon, F., Shoshanim, O., Damit, B., Schneider, J., Sivaprakasam, V., Zawadowicz, M.A., Crawford, I., Gallagher, M., Topping, D., Doughty, D.C., Hill, S.C., Pan, Y., 2020. Real-time sensing of bioaerosols: Review and current perspectives. *Aerosol Sci. Technol.* 54, 465–495. <https://doi.org/10.1080/02786826.2019.1664724>
- Huffman, J.A., Sinha, B., Garland, R.M., Snee-Pollmann, A., Gunthe, S.S., Artaxo, P., Martin, S.T., Andreae, M.O., Pöschl, U., 2012. Size distributions and temporal variations of biological aerosol particles in the Amazon rainforest characterized by microscopy and real-time UV-APS

fluorescence techniques during AMAZE-08. *Atmospheric Chem. Phys.* 12, 11997–12019. <https://doi.org/10.5194/acp-12-11997-2012>

Ila Gosselin, M., Rathnayake, C.M., Crawford, I., Pöhlker, C., Fröhlich-Nowoisky, J., Schmer, B., Després, V.R., Engling, G., Gallagher, M., Stone, E., Pöschl, U., Alex Huffman, J., 2016. Fluorescent bioaerosol particle, molecular tracer, and fungal spore concentrations during dry and rainy periods in a semi-arid forest. *Atmospheric Chem. Phys.* 16, 15165–15184. <https://doi.org/10.5194/acp-16-15165-2016>

Jonsson, P., Kullander, F., 2014a. Bioaerosol Detection with Fluorescence Spectroscopy, in: *Bioaerosol Detection Technologies*. pp. 111–141. https://doi.org/10.1007/978-1-4419-5582-1_7

Jonsson, P., Kullander, F., 2014b. Bioaerosol Detection with Fluorescence Spectroscopy, in: Jonsson, P., Olofsson, G., Tjärnhage, T. (Eds.), *Bioaerosol Detection Technologies, Integrated Analytical Systems*. Springer New York, New York, NY, pp. 111–141. https://doi.org/10.1007/978-1-4419-5582-1_7

Khan, M., Perveen, A., Qaiser, M., 2016. SEASONAL AND DIURNAL VARIATION OF ATMOSPHERIC FUNGAL SPORE CONCENTRATIONS IN HYDERABAD; TANDOJAM-SINDH AND THE EFFECTS OF CLIMATIC CONDITIONS 7.

Kruczek, A., Puc, M., Wolski, T., 2017. Airborne pollen from allergenic herbaceous plants in urban and rural areas of Western Pomerania, NW Poland. *Grana* 56, 71–80. <https://doi.org/10.1080/00173134.2016.1145251>

Kubera, E., Kubik-Komar, A., Piotrowska-Weryszko, K., Skrzypiec, M., 2021. Deep Learning Methods for Improving Pollen Monitoring. *Sensors* 21, 3526. <https://doi.org/10.3390/s21103526>

Lazaridis, M., 2011. Atmospheric Aerosols, in: Lazaridis, M. (Ed.), *First Principles of Meteorology and Air Pollution, Environmental Pollution*. Springer Netherlands, Dordrecht, pp. 169–199. https://doi.org/10.1007/978-94-007-0162-5_5

Li, J., Wan, M.P., Schiavon, S., Tham, K.W., Zuraimi, S., Xiong, J., Fang, M., Gall, E., 2020. Size-resolved dynamics of indoor and outdoor fluorescent biological aerosol particles in a bedroom: A one-month case study in Singapore. *Indoor Air* 30, 942–954. <https://doi.org/10.1111/ina.12678>

Lieberherr, G., Auderset, K., Calpini, B., Clot, B., Crouzy, B., Gysel-Beer, M., Konzelmann, T., Manzano, J., Mihajlovic, A., Moallemi, A., O'Connor, D., Sikoparija, B., Sauvageat, E.,

- Tummon, F., Vasilatou, K., 2021. Assessment of real-time bioaerosol particle counters using reference chamber experiments. *Atmospheric Meas. Tech.* 14, 7693–7706. <https://doi.org/10.5194/amt-14-7693-2021>
- Markey, E., Hourihane Clancy, J., Martínez-Bracero, M., Neeson, F., Sarda-Estève, R., Baisnée, D., McGillicuddy, E.J., Sewell, G., O'Connor, D.J., 2022. A Modified Spectroscopic Approach for the Real-Time Detection of Pollen and Fungal Spores at a Semi-Urban Site Using the WIBS-4+, Part I. *Sensors* 22, 8747. <https://doi.org/10.3390/s22228747>
- Martinez-Bracero, M., Markey, E., Clancy, J.H., McGillicuddy, E.J., Sewell, G., O'Connor, D.J., 2022. Airborne Fungal Spore Review, New Advances and Automatisation. *Atmosphere* 13, 308. <https://doi.org/10.3390/atmos13020308>
- Martínez-Bracero, M., Markey, E., Clancy, J.H., Sodeau, J., O'Connor, D.J., 2022. First Long-Time Airborne Fungal Spores Study in Dublin, Ireland (1978–1980). *Atmosphere* 13, 313. <https://doi.org/10.3390/atmos13020313>
- Matsuda, S., Kawashima, S., 2018. Relationship between laser light scattering and physical properties of airborne pollen. *J. Aerosol Sci.* 124, 122–132. <https://doi.org/10.1016/j.jaerosci.2018.07.009>
- Maya-Manzano, J.M., Smith, M., Markey, E., Hourihane Clancy, J., Sodeau, J., O'Connor, D.J., 2021. Recent developments in monitoring and modelling airborne pollen, a review. *Grana* 60, 1–19. <https://doi.org/10.1080/00173134.2020.1769176>
- Niederberger, E., Abt, R., Burch, P., Zeder, Y., 2018. First experiences with the newly-developed Swisens Pollen Monitor 9.
- O'Connor, D.J., Daly, S.M., Sodeau, J.R., 2015a. On-line monitoring of airborne bioaerosols released from a composting/green waste site. *Waste Manag.* 42, 23–30. <https://doi.org/10.1016/j.wasman.2015.04.015>
- O'Connor, D.J., Healy, D.A., Hellebust, S., Buters, J.T.M., Sodeau, J.R., 2014a. Using the WIBS-4 (Waveband Integrated Bioaerosol Sensor) technique for the on-line detection of pollen grains. *Aerosol Sci. Technol.* 48, 341–349. <https://doi.org/10.1080/02786826.2013.872768>
- O'Connor, D.J., Healy, D.A., Sodeau, J.R., 2015b. A 1-month online monitoring campaign of ambient fungal spore concentrations in the harbour region of Cork, Ireland. *Aerobiologia* 31, 295–314. <https://doi.org/10.1007/s10453-015-9365-7>

- O'Connor, D.J., Healy, D.A., Sodeau, J.R., 2013. The on-line detection of biological particle emissions from selected agricultural materials using the WIBS-4 (Waveband Integrated Bioaerosol Sensor) technique. *Atmos. Environ.* **80**, 415–425. <https://doi.org/10.1016/j.atmosenv.2013.07.051>
- O'Connor, D.J., Sadyś, M., Skjøth, C.A., Healy, D.A., Kennedy, R., Sodeau, J.R., 2014b. Atmospheric concentrations of *Alternaria*, *Cladosporium*, *Ganoderma* and *Didymella* spores monitored in Cork (Ireland) and Worcester (England) during the summer of 2010. *Aerobiologia* **30**, 397–411. <https://doi.org/10.1007/s10453-014-9337-3>
- Oliveira, M., Ribeiro, H., Delgado, J.L., Abreu, I., 2009. The effects of meteorological factors on airborne fungal spore concentration in two areas differing in urbanisation level. *Int. J. Biometeorol.* **53**, 61–73. <https://doi.org/10.1007/s00484-008-0191-2>
- Orlandi, F., Oteros, J., Aguilera, F., Dhiab, A.B., Msallem, M., Fornaciari, M., 2014. Design of a downscaling method to estimate continuous data from discrete pollen monitoring in Tunisia. *Environ. Sci. Process. Impacts* **16**, 1716–1725. <https://doi.org/10.1039/C4EM00153B>
- Oteros, J., Pusch, G., Weichenmeier, I., Heimann, U., Möller, R., Röseler, S., Traidl-Hoffmann, C., Schmidt-Weber, C., Buters, J.T.M., 2015. Automatic and online pollen monitoring. *Int. Arch. Allergy Immunol.* **167**, 158–166. <https://doi.org/10.1159/000436968>
- Pazienza, M., 2013. Use of Particle Counter System for the Optimization of Sampling, Identification and Decontamination Procedures for Biological Aerosols Dispersion in Confined Environment. *J. Microb. Biochem. Technol.* **06**. <https://doi.org/10.4172/1948-5948.1000120>
- Pazienza, M., Britti, M.S., Carestia, M., Cenciarelli, O., D'Amico, F., Malizia, A., Bellecci, C., Fiorito, R., Gucciardino, A., Bellino, M., Lancia, C., Tamburrini, A., Gaudio, P., 2014. Use of particle counter system for the optimization of sampling, identification and decontamination procedures for biological aerosols dispersion in confined environment. *J. Microb. Biochem. Technol.* **6**, 043–048. <https://doi.org/10.4172/1948-5948.1000120>
- Perring, A.E., Schwarz, J.P., Baumgardner, D., Hernandez, M.T., Spracklen, D.V., Heald, C.L., Gao, R.S., Kok, G., McMeeking, G.R., McQuaid, J.B., Fahey, D.W., 2015. Airborne observations of regional variation in fluorescent aerosol across the United States. *J. Geophys. Res. Atmospheres* **120**, 1153–1170. <https://doi.org/10.1002/2014JD022495>

- Saari, S., Niemi, J., Rönkkö, T., Kuuluvainen, H., Jaärvinen, A., Pirjola, L., Aurela, M., Hillamo, R., Keskinen, J., 2015. Seasonal and Diurnal Variations of Fluorescent Bioaerosol Concentration and Size Distribution in the Urban Environment. *Aerosol Air Qual. Res.* 15, 572–581. <https://doi.org/10.4209/aaqr.2014.10.0258>
- Santarpia, J.L., Ratnesar-Shumate, S., Gilberry, J.U., Quizon, J.J., 2013. Relationship Between Biologically Fluorescent Aerosol and Local Meteorological Conditions. *Aerosol Sci. Technol.* 47, 655–661. <https://doi.org/10.1080/02786826.2013.781263>
- Šauliene, I., Šukiene, L., Daunys, G., Valiulis, G., Vaitkevičius, L., Matavulj, P., Brdar, S., Panic, M., Sikoparija, B., Clot, B., Crouzy, B., Sofiev, M., 2019. Automatic pollen recognition with the Rapid-E particle counter: The first-level procedure, experience and next steps. *Atmospheric Meas. Tech.* 12, 3435–3452. <https://doi.org/10.5194/amt-12-3435-2019>
- Savage, N.J., Krentz, C.E., Könemann, T., Han, T.T., Mainelis, G., Pöhlker, C., Alex Huffman, J., 2017. Systematic characterization and fluorescence threshold strategies for the wideband integrated bioaerosol sensor (WIBS) using size-resolved biological and interfering particles. *Atmospheric Meas. Tech.* 10, 4279–4302. <https://doi.org/10.5194/amt-10-4279-2017>
- Stensvand, A., Eikemo, H., Gadoury, D.M., Seem, R.C., 2005. Use of a Rainfall Frequency Threshold to Adjust a Degree-Day Model of Ascospore Maturity of *Venturia inaequalis*. *Plant Dis.* 89, 198–202. <https://doi.org/10.1094/PD-89-0198>
- Tormo Molina, R., Maya Manzano, J.M., Fernández Rodríguez, S., Gonzalo Garijo, Á., Silva Palacios, I., 2013. Influence of environmental factors on measurements with Hirst spore traps. *Grana* 52, 59–70. <https://doi.org/10.1080/00173134.2012.718359>
- Whitehead, J.D., Gallagher, M.W., Dorsey, J.R., Robinson, N., Gabey, A.M., Coe, H., McFiggans, G., Flynn, M.J., Ryder, J., Nemitz, E., Davies, F., 2010. Aerosol fluxes and dynamics within and above a tropical rainforest in South-East Asia. *Atmospheric Chem. Phys.* 10, 9369–9382. <https://doi.org/10.5194/acp-10-9369-2010>
- Yu, X., Wang, Z., Zhang, M., Kuhn, U., Xie, Z., Cheng, Y., Pöschl, U., Su, H., 2016. Ambient measurement of fluorescent aerosol particles with a WIBS in the Yangtze River Delta of China: potential impacts of combustion-related aerosol particles. *Atmospheric Chem. Phys.* 16, 11337–11348. <https://doi.org/10.5194/acp-16-11337-2016>

Chapter 5. Data Analysis of Modelling and Forecasting of Fungal Spores

5.1. Introduction

The development of various observational predictive and forecasting models for fungal spores has been the focus of an increasing volume of research in recent years (Grinn-Gofroń et al., 2019; Martinez-Bracero et al., 2022). Recently, there has been a growing awareness around the acute and severe health impacts, and agricultural impacts that fungal spores can have. This has meant that the previously accepted fungal spore calendars are no longer sufficient, particular for those whose reaction to phytopathogenic fungal spores can be particularly rapid or severe (Bush and Yunginger, 1987; Carlile and Watkinson, 2021; Elbert et al., 2007; Kainz et al.).

With a comprehensive fungal spore forecasting programme, or accurate early warning system, vulnerable members of society will be able to self-manage exposure. This could be achieved through the use of premedication or PPE (Personal Protective Equipment) applications which can in turn decrease the number of severe allergic reactions and the subsequent expenses incurred by healthcare systems as a result of both mild and more severe allergic reactions (Dales et al., 2000; Iwen et al., 1994). In regard to the agricultural industry, forecasts would help to improve understanding around fungal spore release and dispersal and enable implementation of early warning systems and defence mechanisms right at the onset of phytopathogenic fungal infections or spore release. Reducing or completely eliminating crops losses and again saving money for the industry (Kapadi and Patel, 2019; O'Connor et al., 2013). In addition, fungal spore forecasts could be used in the ecological field, focussing on environmental protection not for financial gain, but to assist in climate trend, and biodiversity loss or growth analysis (Crandall et al., 2020; Fröhlich-Nowoisky et al., 2016).

5.2. Modelling and Forecasting Developments as they Relate to Bioaerosols

The process of developing predictive models can be a difficult task to carry out. There are numerous elements that must be carefully considered. These include the inclusion and exclusion criteria of data at hand, and the types of transformations required to make the data appropriate for analysis (Bańbura and Rünstler, 2011; Barredo-Arrieta et al., 2019).

A recent development in the world of model construction and development is the rapid growth of the use of machine learning algorithms (MLA), artificial neural networks (ANN) and artificial intelligence based prediction, with each new algorithm promising better accuracy and less effort than the one that came before (Grinn-Gofroń and Strzelczak, 2008; Kleine Deters et al., 2017; Lee et al., 2023; Li et al., 2020; Liu et al., 2023). These new methods

promise to provide us with approaches that can perform the clustering, numerical prediction, and show the ability to learn and grow, improving over time.

One issue with all of these advanced modelling techniques is the lack of data transparency. As we reach a point where a set of parameters are selected, placed into a set of “black boxes”, resulting in accurate output, without a full understanding of what happened in the steps in between, some are concerned that the impact of these advanced systems could lead ultimately to a form of mathematical illiteracy (Bańbura and Rünstler, 2011; Barredo-Arrieta et al., 2019).

Thankfully some previous concerns have been allayed over the years. The advent of cloud computing has allowed those with less financial resources to run models as complex and advanced as those with state-of-the-art equipment, leading to further scientific democratisation. Researchers can now, from home, design and run a model to predict the workload impact upon a cloud computer server. They can send the model to the server under investigation, and subsequently have that computer teach itself through machine learning how to run the model and improve upon it, so as to get better at investigating its own resource limits (Kumar et al., 2021). Automatic analysis and management tools such as these are continuously freeing up more time for researchers. More time can now be devoted to the traditional scientific pursuits of exploration and discovery, without needing to spend weeks or months behind a computer screen afterwards (“Computer-Assisted Research Design and Analysis,” 2000).

With regard to bioaerosol modelling and its applications, the advent of logistic regression for forecasting, is granting some researchers the ability to simultaneously forecast hourly and daily concentrations, while determining annual fungal spore or pollen integrals, in one workload, thus saving time and energy expended (Martinez-Bracero et al., 2022; Vélez-Pereira et al., 2019).

5.3. Model Parameters

5.3.1. Parameter Sourcing Methods

Due to the short duration of the real-time monitoring campaign and the known effect of anthropogenic pollution and weather parameters on real-time bio/aerosols monitoring, additional data from suitably close air quality stations and meteorological were sourced as to aid in the determination of the influences on our monitoring site. As a result, data from three bioaerosol monitoring instruments (the WIBS, the IBAC, and the Lanzoni Hirst type sampler) was combined with 17 different meteorological parameters from the Meteorological Agency, Met Éireann, along with data on five different anthropogenic pollutants, sourced from the Irish Environmental Protection Agency (EPA)(Agency (EPA), 2023.; “Historical Data - Met Éireann - The Irish Meteorological Service,” 2023). This wealth of data was processed and used for the construction of Multiple Linear Regression plots and equations. In addition, the wind data provided by Met Éireann was sufficiently comprehensive for us to construct Windrose models, highlighting both the prevailing winds during the monitoring campaign, as well as predominant wind sources for each bioaerosol species, as well as each WIBS particle category. The ZeFir wind and air mass origin software package was used to construct these Wind roses (“ZeFir - Tracking Pollution Back to the Origin | Igor Pro by WaveMetrics,” 2023).

5.3.2. Bioaerosol Instrumentation

The bioaerosol devices used during this campaign were the WIBS-Neo, the IBAC bio-threat detector, and the Lanzoni 7-day volumetric spore sampler. The Hirst traditional sampler ran continuously for the entire 4-year campaign, from 2017 to 2020 allowing for the construction of a comprehensive picture of the state of the fungal fructification season in Dublin. The WIBS and IBAC real-time online sensors ran simultaneously with the Hirst for a 40-day high intensity monitoring campaign in the Summer and Autumn of 2019. They output data relating to particle size shape, and fluorescent characteristics in vast detail, and are also being investigated for their potential use as continuously running bioaerosol sensors that update databases and alert the public in real-time of changes in bioaerosol concentrations.

5.3.3. Geographical origin of ambient bioaerosol and FAP (Fluorescent Aerosol Particle) concentrations

The influence of wind plays a significant role in the process of pollen dispersion and transportation for a vast array of pollen types (Dowding, 1987). The ZeFir source receptor models were utilised in order to accomplish the goal of determining the potential geographic location of the detected pollen taxa that were tracked throughout the campaign. The wind-rose plots that were generated as a result provide valuable information on the spatial origins of the pollen, fungal spores, and FAPs (Fluorescent Aerosol Particles) that were studied. This modelling approach has been applied in the past to a variety of bioaerosols, most notably pollen (Sarda-Estève et al., 2020, 2019, 2018), but it has only recently been applied to FAPs that are identified by the WIBS, and only by our research group specifically (Markey et al., 2022a; Martinez-Bracero et al., 2022).

Figure 5.1 below illustrates the predominant winds that were recorded in Dublin throughout the sampling period. The heatmap displays the combined average wind direction data from the entire campaign. The data was collected at an hourly temporal resolution. Each hour's average wind direction was expressed in polar coordinates (values between 0° and 360°, or one revolution of a circle, with both the 0° and the 360° values representing North). Distance from the centre of the circle represents windspeed. Near the centre of the circle are the lowest windspeeds, and at the edge are the highest. Areas with higher concentration on the chart (in red), had more hours of the campaign where wind originated from that direction, at that windspeed ("ZeFir - Tracking Pollution Back to the Origin | Igor Pro by WaveMetrics," 2023).

The prevailing winds throughout the campaign came almost exclusively from the West-Southwest sector at faster wind speeds, mainly greater than 12 kilometres per hour. The fact that a large degree of the prevailing winds came from the same location, at the same speed for the entirety of the campaign can be helpful for biological aerosol analysis. Any deviations from this primary wind direction should see more immediate and obvious changes in bioaerosol or fluorescent particle concentrations than would be identifiable in highly volatile or changeable conditions.

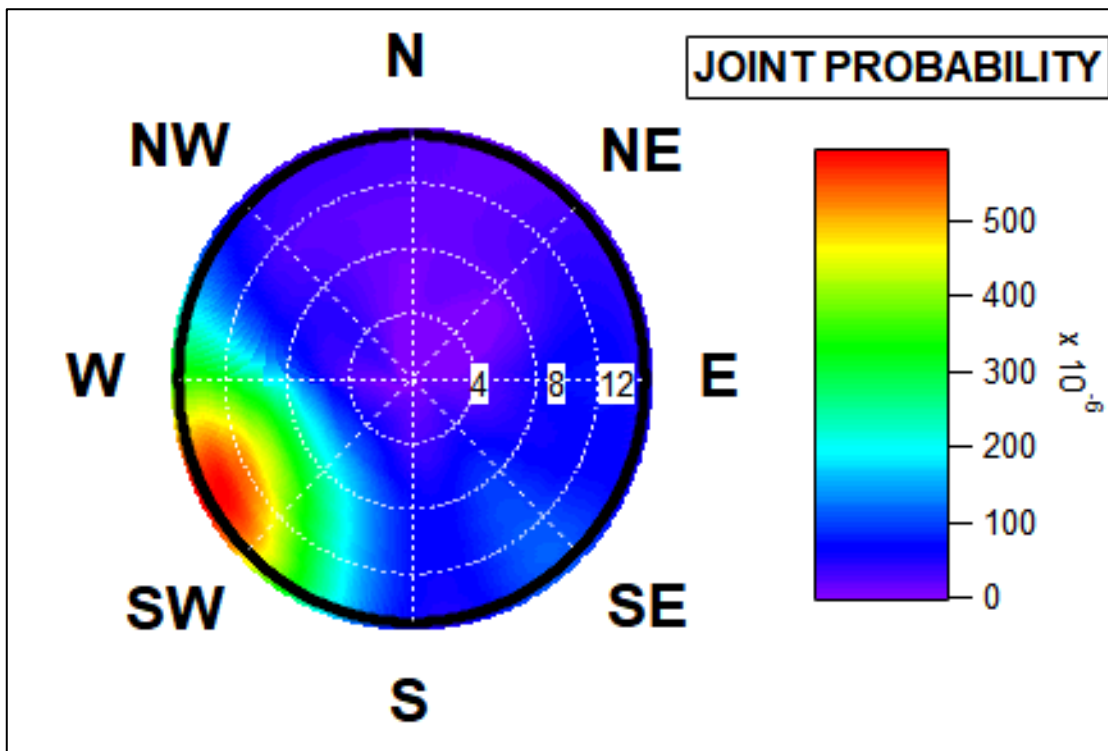


Figure 5.1: NWR generated wind rose for WIBS sampling period. White circles represent a wind speed scale in kilometres per hour. The colour grid represents the estimated concentration (Particles/m³) at each wind speed and wind direction.

The NWR model was applied to all the bioaerosol data. This data included the pollen types of *Urticaceae* and *Poaceae*, as well as the fungal types of Basidiospores, *Cladosporium*, *Alternaria*, and Ascospores. The wind analysis was carried out with the goal of gaining a greater insight into the factors that led to the formation of important (allergenic or pathogenic) pollen and fungal spore types. Using the NWR method, we were able to determine the geographical origins of these PBAPs over Dublin for the entire campaign period (Figure 5.1).

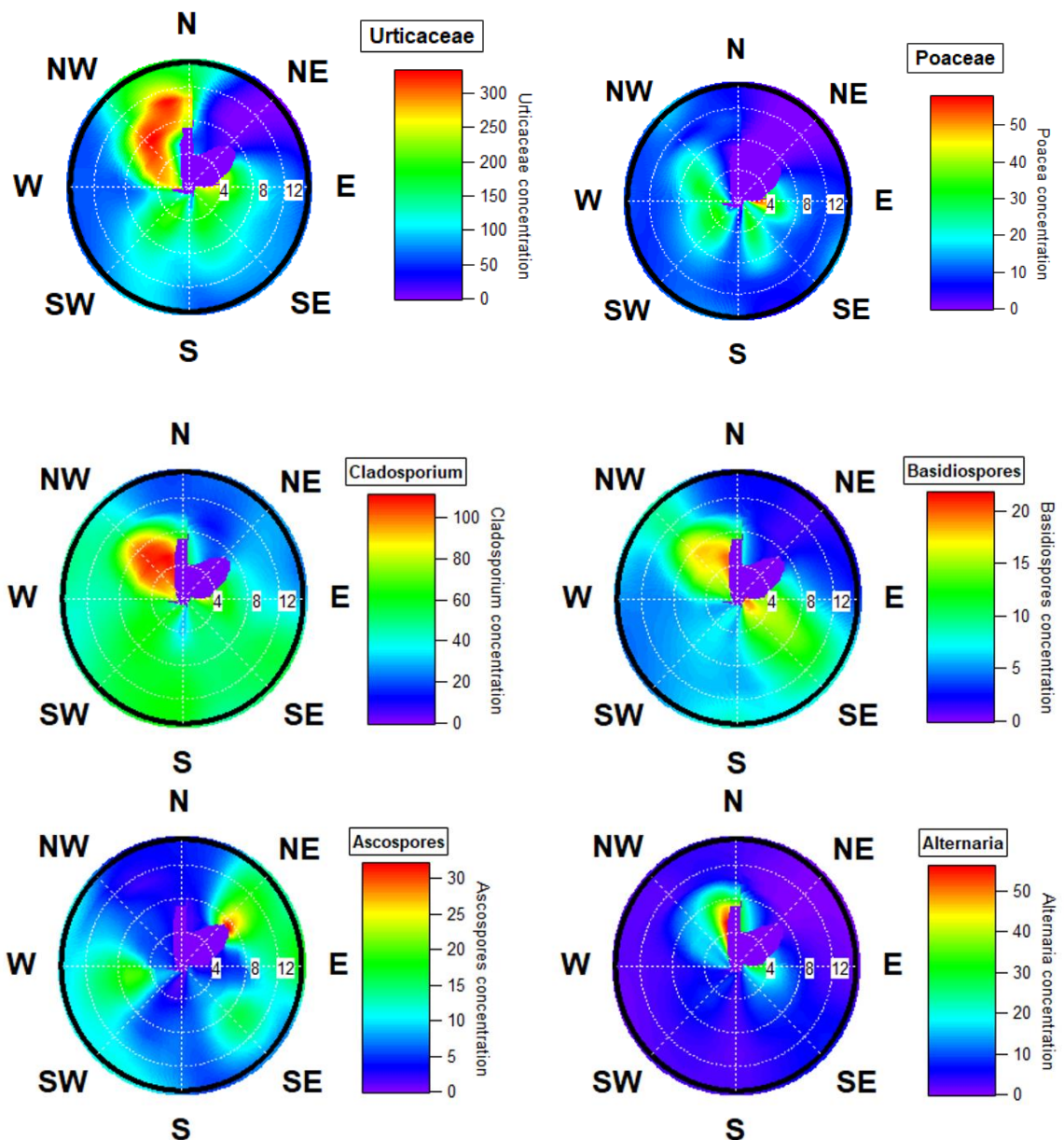


Figure 5.2: Origin of (A) *Urticaceae* and (B) *Poaceae* pollen, and (C) *Cladosporium*, (D) *Basidiospore*, (E) *Ascospore*, and (F) *Alternaria* fungal spores at Dublin. The colour grid represents the estimated concentration (Particles/m³) at each wind speed and wind direction.

In Figure 5.2, above, the origin of various biological aerosols are outlined. The prevailing wind direction did not coincide with the geographical origin of the *Urticaceae* pollen, which accounted for the bulk of all pollen that was collected (around 80 percent). Pollen from *Urticaceae* plants often travelled at speeds up to and exceeding 12 kilometres per hour and originated in the North-Northwest direction. Pollen from *Poaceae* came from a number of different directions, most likely because it comes from such a large variety of sources (Rojo

et al., 2015; Silva Palacios et al., 2000). The easterly winds, which had average speeds of less than 8 kilometres per hour, were responsible for the greatest densities of *Poaceae*. Several weaker source points, coming from the South, South West, and Northwest Easterly/Southeasterly directions also contributed to lower *Poaceae* density.

Because there was no strong relationship between prevailing wind direction, and bioaerosol origin wind direction, a map of Dublin was constructed (Figure 5.3) It shows a 5km radius around the bioaerosol sampling point, with “green areas” of interest in red. The objective, to investigate possible sources of biological aerosols, immediately identified multiple points of interest. In the North-north east direction, which is one of the primary *Poaceae* source directions, is the largest urban park in Europe, the Phoenix park (“Nature and Biodiversity | Phoenix Park,” 2023). This 7km² park is comprised primarily of open grassland, which explains the likely source of the *Poaceae* pollen grains collected at the sampler.

The other major source direction for *Poaceae*, the East and South East, contains one of the parts of Dublin city centre with the highest density of green spaces (“Green Spaces | Dublin City Council,” 2018). Immediately to the east of the bioaerosol sampling point are Stephens Green, Merrion Square, Iveagh Gardens, and Trinity College green, among other spaces. This helps complete the image of where *Poaceae* pollen grains are coming from, when they are collected by the city centre sampler.

Although it may be reasonable to anticipate that pollen from *Urticaceae* would also display similar multidirectional behaviour, the high wind speeds associated with *Urticaceae* pollen coming from the North sector imply that longer distance pollen transport is possibly occurring here. Higher wind speeds have historically correlated with longer distance pollen transport (Damialis et al., 2005). It is likely that high concentrations of *Urticaceae* pollen were being transported from the grasslands located to the north of the city centre such as the various public parks, specifically including the Phoenix Park .. Figure 49, below supports this conclusion, as the Phoenix Park is the one large green space in the path of the main *Urticaceae* concentration originations. Conversely, It is possible that high concentrations of *Poaceae* pollen originated from much closer local sources located in the East such as St. Stephen's Green, which is an urban greenspace located to the immediate east of the sampling site But because of the presence of the wind rose, and the source map, it appears highly unlikely that this is the case

Basidiospores, *Cladosporium*, and *Alternaria* all follow similar patterns of having a north-westerly dominant origin, with a bias towards originating from lower wind speeds of 4 to 8 km/h, and a smaller concentration originating from the southeast, at very low wind speeds.

As these spores comprise the majority of all spores counted, their similar geographical origins will influence any results from a total combined fungal spore chart. Ascospores have a different primary geographical origin to the other common spores identified, with no or very low concentrations of spores originating from the northwest, and the majority of spores originating from the northeast. Another ascospore concentration originates from the west/southwest. This correlates with the joint probability, indicating that some ascospores originate in the same direction as the prevailing wind, or directly opposite to the prevailing wind, whereas Basidiospores, *Cladosporium*, and *Alternaria* have a separate, distinct predominant geographical source. Given the size ranges of fungal spores (with some as small as one micrometre), they have the ability to travel much further than pollen spores in the same weather conditions. Additionally, fungal spores such as ascospores and *Cladosporium*, have shown the ability to travel long distances at windspeeds that would not allow for wind dispersal for the larger, denser pollen grains. Their small size and light weight allow other factors such as heat from intense sunlight or smoke from biomass burning to assist in airborne dispersal (Mims and Mims, 2004).

These factors align to result in the possibility that while wind roses are extremely valuable tools for bioaerosol analysis, they cannot explain 100% of the data. Some fungal spores can rise high enough in the atmosphere to form clouds, and cross seas before settling and deposition (Hirst et al., 1967; Olsen et al., 2020)

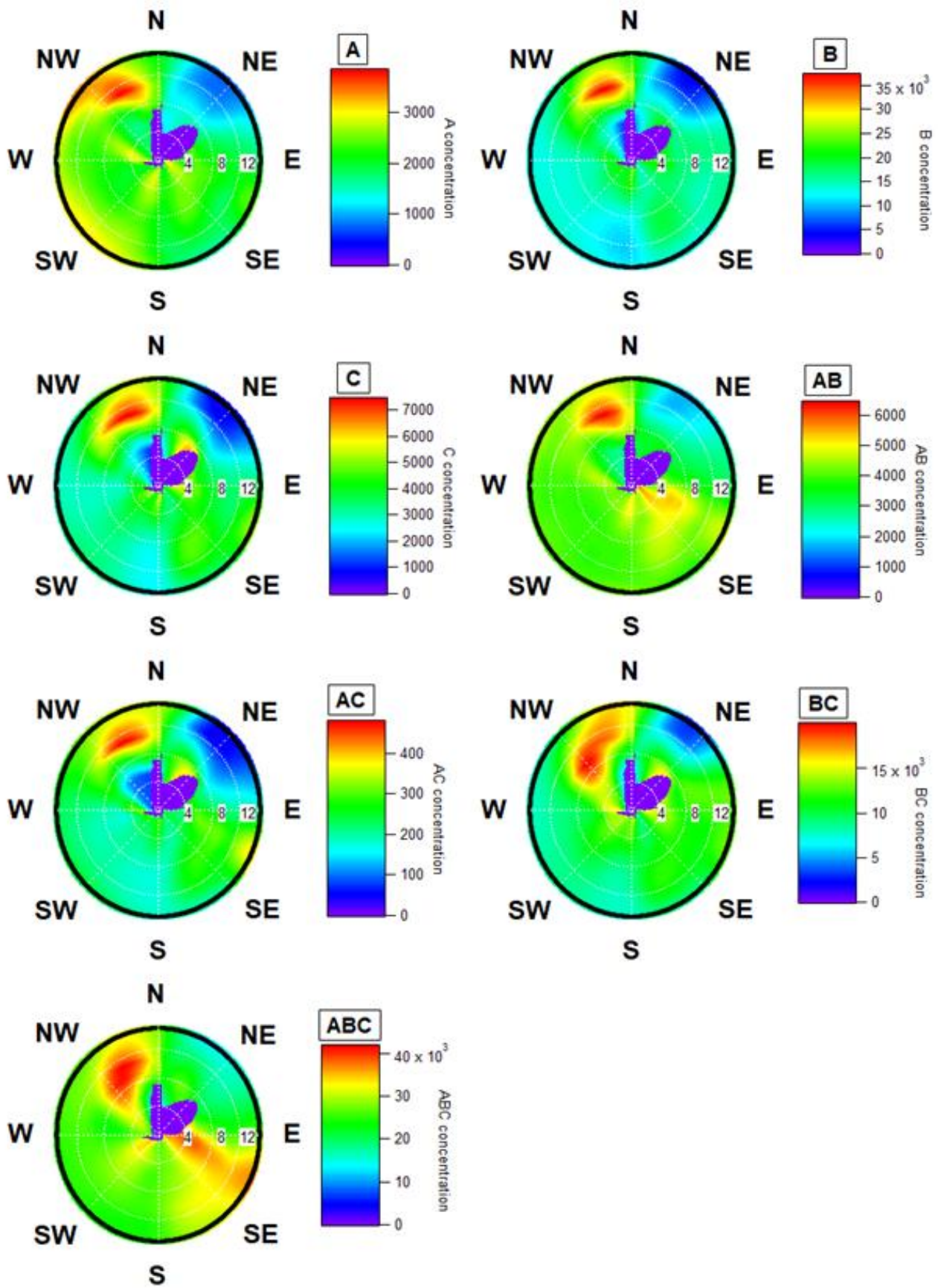


Figure 5.4: Origin of WIBS Particles at Dublin. The colour grid represents the estimated concentration (Particles/m³) for any wind speed and wind direction.

The origin of the different FAP classes was seen to be more multidirectional due to likelihood of multiple sources for each fraction. Previous studies involving the WIBS have often found that anthropogenic particles can act as an interferent to the WIBS fluorescent bands (Daly et al., 2019; Markey et al., 2022b; O'Connor et al., 2014a; Su et al., 2015). Most of the WIBS channels showed a considerable association with the Northwest sector and a poor association with the Northeast sector. High concentrations of A, AB and ABC particles originated from a range of multidirectional sources, the strongest being from the Northwest at higher windspeeds. Although AB and ABC also showed strong associations with wind originating from the Southeast sector at wind speeds of up to and exceeding 15 km/hr. There was not much meaningful correlation observed for A, AB and ABC channels with pollen and fungal spore concentrations. This made it more difficult to link their sampling with bioaerosol activity. This could be due to their previously seen link to combustion particles, in which studies have found that FII band particles in particular, tend to positively correlate with particles such as black carbon (Toprak and Schnaiter, 2013; Yu et al., 2016). Similarly, both C and AC particles had high concentrations originating from the North at winds greater than 10 km/h with a second A weaker regime originating from the Southeast can also be seen. B type particles also showcased this strong Northern origin, however these particles were shown to have little correlation to pollen grains/spores and could indicate anthropogenic origin or in the case of AC particles – had relatively poor ambient concentrations (Gabey et al., 2011; Toprak and Schnaiter, 2013; Twohy et al., 2016). However, BC particles originated mostly from the north, almost perfectly mirroring the strong behavior witnessed for *Urticaceae* pollen. This further corroborates the suspected link between BC particles and *Urticaceae* pollen. A second weaker regime was observed from the East sector. This deviated from the *Urticaceae* wind-rose plot, but could account for other aerosols within the BC fraction that do not follow the expected pollen trend. Although, major wind directions and possible sources of long- and short-range transport varied by pollen/spore and WIBS particle type, similarities were observed for BC particles and *Urticaceae* pollen.

5.3.4. Anthropogenic Pollutants

Despite the fact that the WIBS emission channels have been designed for the selective detection of biomarkers that may be found in bioaerosols, a number of investigations have brought to light the impacts of possible interferents that may potentially contribute to the fluorescence signals in these channels. (Savage et al., 2017). In most cases, these interferences are caused by anthropogenic sources, and would not be unexpected at the urban sampling

location, which was situated in the middle of the Dublin city centre. Polycyclic aromatic hydrocarbons, also known as PAH, humic-like compounds, also known as HULIS, mineral dust, secondary organic aerosols, and black carbon are examples of interferents expected to be found in a region with these characteristics (Savage et al., 2017; Yue et al., 2016). The impacts of possibly interfering aerosols may be mitigated by raising the initial fluorescence threshold, which can be done by going from 3σ (Three Sigma) to 6σ and 9σ respectively. It has been demonstrated that by increasing the fluorescence threshold in this manner, interference from non-biological aerosols may be greatly reduced, without having any effect on the relative fraction of bioaerosols that can be detected by the WIBS. (Savage et al., 2017).

While the IBAC was also not designed specifically for the purpose of anthropogenic particle detection, it possesses fluorescent categories of “biological” and “non-biological”, and the unused potential of these secondary fluorescence outputs could be of interest (“FLIR IBAC 2 Bio-Threat Detection & Collection | Teledyne FLIR,” 2021). The so called biological categorisation could also encounter interference from anthropogenic pollutants, given the generous ranges in both fluorescence signature and particle size, allowing for particle detection down to $0.7\mu\text{m}$ in size (Pazienza, 2013).

Both the IBAC-2 and WIBS-NEO were compared to a range of potential anthropogenic pollutants, obtained from the publicly accessible EPA SAFER database (Agency (EPA), 2023). The publicly available SAFER dataset had an adjacent sampling site located in the same area of the city, about 700 metres from the bioaerosol sampling site. While it is not a massive distance, there were reasonable arguments that reducing the potential impact that local factors could have on the three datasets should be a high priority if possible. Bioaerosol studies in the past have on occasion found considerable degrees of local differences in composition of the air (Patel et al., 2018; Saari et al., 2014) After analysis, both instruments found significant levels of correlation with just one interferent, ambient PM₁₀ data monitored at a near-by sampling site. Comparisons are illustrated in Figures 5.5 and 5.6 below.

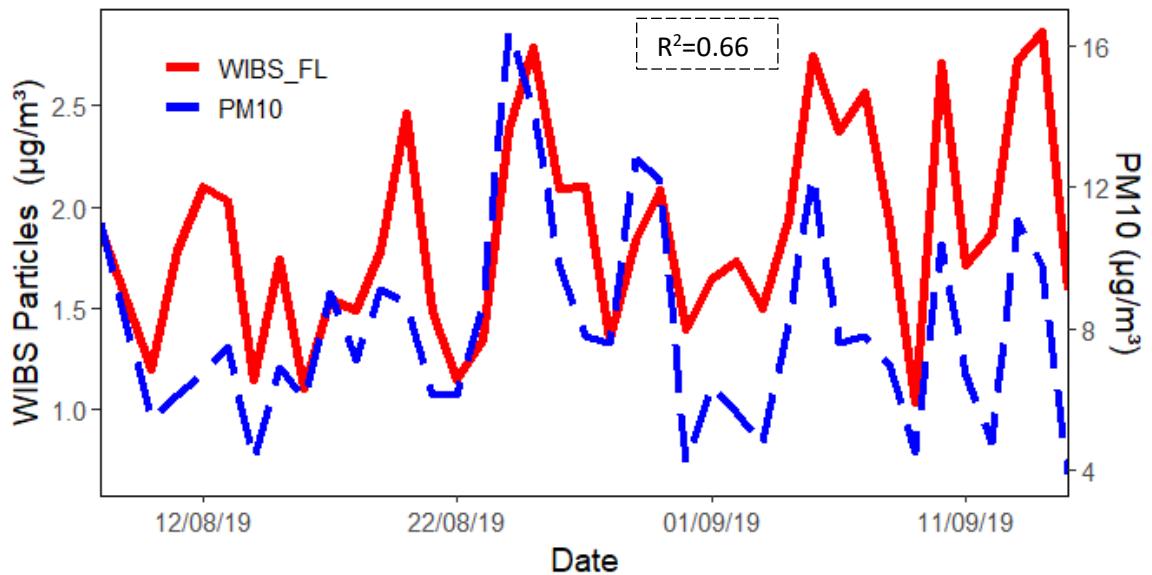


Figure 5.5: Comparison between WIBS fluorescent particles and PM10 particles.

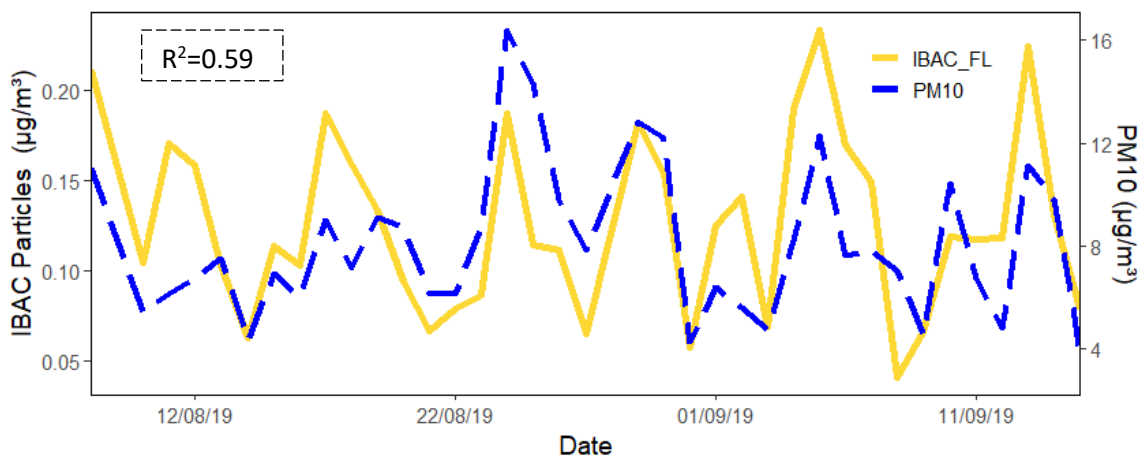


Figure 5.6: Comparison between IBAC fluorescent particles and PM10 particles.

Ambient PM10 concentrations corresponded most significantly with Fluorescent WIBS particles of 10µm or smaller ($R^2=0.66$). This at least highlights that the sizing of particles by the WIBS device is relatively accurate and provides some reassurance for the project. The IBAC particles that correlated most significantly with ambient PM10 concentrations were Fluorescent IBAC particles of all sizes ($R^2=0.59$).

Most peak PM10 days are identified by both instruments however, deviations are observed between the concentrations. This is mostly due to a range of factors including, but not limited to; differing sampling methodologies of each device, the geographical distance between the

PM₁₀ sampler and the WIBS and IBAC-2 instruments. While this distance was not excessively large, but could result in a disproportionately strong influence of very local interferents, relative to more widespread pollution events or circumstances. (Markey et al., 2022b; Santarpia et al., 2013). Most significantly the heights at which the sampling was done differed with the air pollution monitoring seen at ground level while the bioaerosol measurements done on a roof top. For subsequent studies a primary objective, and recommendation relates specifically to the measurement of anthropogenic particles. This will help to eliminate any uncertainties we have relating to local factors and allow a more direct particle type correlation analysis. This initial investigation provided the project with an invaluable first look into the potential influence that these interferents can have on real-time fluorescent instruments and helped us to greatly expand the data used to design and construct our Multiple Linear Regression algorithms. Future projects will include more active involvement of these chemical interferents, given the rising concerns around possible secondary and tertiary impacts of air pollution on our ecosystem and citizens.

5.3.5. Meteorological parameters

Met Éireann made its meteorological data for the dates of the campaigns accessible for use in the creation of the MLR outputs and the prediction models as part of both the real-time monitoring campaign and the long-term monitoring campaign (“Historical Data - Met Éireann - The Irish Meteorological Service,” 2023). Some weather circumstances, such as high wind speeds, might make it more difficult for the WIBS to properly collect samples of bioaerosols. This is in part due to the fact that larger particles at higher wind speeds have significantly more momentum than at lower wind speeds. Thus, the ability of the WIBS to alter the direction of these particles and allow for subsequent analysis is far more limited than that of the Hirst (O’Connor et al., 2014a). The inlet of the Hirst traditional volumetric sampler is oriented in such a way that it always faces the prevailing wind direction, whereas the inlet of the WIBS remains stationary during the sampling process. As a consequence of this, the Hirst at high wind speeds actually over samples particles be them smaller or larger in size when oriented into a wind that is greater than its own flow rate. Orientating into the wind also mean the flow of the Hirst does not need to alter the direction of the particle flow when sampling. To investigate the association and significance between daily WIBS particle concentrations and individual meteorological parameters, Spearman's rank correlation coefficients were

calculated using meteorological data recorded by Met Éireann. These coefficients were used to investigate the association between the two sets of parameters. This is seen in Table 5 below.

Table 5: Spearman's rank correlation coefficients between daily hourly Dublin WIBS channel data and meteorological parameters.

	A	B	C	AB	AC	BC	ABC	Total FAPs
Max Temperature	-0.06	-0.16	-0.13	0.02	-0.1	-0.07	0.04	-0.11
Mean Temp	-0.23	-0.29	-0.36*	-0.19	-0.37*	-0.23	-0.2	-0.27
Min Temp	-0.29	-0.33*	-0.43**	-0.29*	-0.48**	-0.28*	-0.32*	-0.33*
Grass Min Temp	-0.48**	-0.66**	-0.67**	-0.61**	-0.62**	-0.57**	-0.57**	-0.66**
Rain	-0.42	-0.33	-0.49	-0.032	-0.4	-0.22	-0.22	-0.33
CBL	0.32	0.4*	0.45**	0.39*	0.41**	0.28*	0.16	0.36*
Wind Speed	-0.19	-0.39**	-0.24*	-0.48**	-0.4**	-0.51**	-0.48**	-0.4**
Wind Direction	-0.12	-0.1	-0.05	-0.2	-0.09	-0.14	-0.1	-0.11
Gust	-0.14	-0.33**	-0.03*	-0.3*	-0.39*	-0.39**	-0.38**	-0.33**
Sun	0.24	0.2	0.25	0.18	0.19	0.1	0.3	0.19
Radiation	0.04	0	0.06	0	0.05	-0.03	0.24	0.03
Soil Temp	-0.26	-0.24	-0.33	-0.14	-0.28	-0.09	-0.03	-0.19
Evapotranspiration	-0.1	-0.22	-0.2	-0.19	-0.16	-0.22	-0.02	-0.19
Evaporation	-0.1	-0.23	-0.18	-0.23	-0.18	-0.26	-0.03	-0.2
Humidity	-0.09	-0.02	-0.16	0.12	-0.03	0.14	0.1	0.02

*Significance at the 95% level, **significance at the 99% level

With regard to certain WIBS bands, previous studies have warned that any air sampling in which B type particles dominate the fluorescence fraction should be checked closely for probable interferences (Hernandez et al., 2016). This caution is warranted as a consequence of the fact that B type particles contribute only very marginally to PBAP fractions (Hernandez et al., 2016). Given the urban location of the sample site in the centre of Dublin City and the declining bioaerosol concentrations at this stage in the season, the presence of potentially anthropogenic or interfering particles should not come as a surprise.

It was observed that the majority of fluorescent WIBS particle classes exhibited significant negative correlation with minimum temperature, grass minimum temperature and wind speed. This inverse relationship between both temperature parameters in the late summer

and early autumn months is suggestive of the presence of bacterial activity in the surrounding environment. While removing WIBS particles below 2 μm is likely to remove a significant fraction of FAPs associated with the presence of bacteria, ambient concentrations have been shown to peak at size ranges of up to 4-5 μm , which completely overlaps with the modal particle sizes of the most common fungal spore types (Bragoszewska and Pastuszka, 2018; Gong et al., 2020). The main reason for this decline in FAPs may be related to the significant correlation seen between grass minimum temperature, rain, and wind speed which are drivers for the transport and deposition of certain bioaerosols (Bragoszewska and Pastuszka, 2018; Davies and Smith, 1974; Hart et al., 1994; Oliveira et al., 2009). A notable positive correlation was observed between cbl (pressure) and WIBS FAPs. This is a well-studied observation and has been seen in a range of bioaerosol types, which indicates that bioaerosols do make a large contribution to the FAP totals (Kruczek et al., 2017; O'Connor et al., 2014b).

5.4. Real-Time Campaign Investigations

5.4.1. Multiple Linear Regression

For the real-time instrumentation campaign, a single 40-day period of monitoring data was carried out. After the data underwent the required tests and processes to ensure validity and eliminate the possibility of covariance or autocorrelation (Sadyś et al., 2015), the optimal data filtration conditions were obtained. These included setting a 9 σ level of filtration, and particle size filtration to include only particles greater than 2 μm in diameter, to minimise anthropogenic interference. Additional size filtering was also utilized as to only include particles less than or equal to 8 μm in diameter. This was done to allow particles larger (most likely pollen grains) to be removed and to not influence fungal spore totals, thus confusing the analysis and reducing significance. Particularly as fungal spores were of particular interest in this campaign.

Below are the statistically most significant results of the MLR analysis (Figure 5.7). All fungal spores apart from *Alternaria* were combined into a “fungal spore” parameter, seen as the “Observed” variable on the graph. The reason for the exclusion of *Alternaria* is due to its much larger average particle size that meant its inclusion would result in changing size filtering to a point that interference from pollen grains was beginning to occur. The “Calculated” variable on the graph is a line constructed via multiple linear stepwise backwards regression, with the equations as follows:

$$- 1278.43 + 28.58 \times \textit{AC particles (WIBS-NEO)} + 0.93 \times \textit{BC particles (WIBS-NEO)}$$

$$- 8427.46 \times \textit{Carbon Monoxide (CO)} - 71.06 \times \textit{Grass Minimum Temperature}$$

$$- 1650.75 \times \textit{Easterly Wind} + 435.52 \times \textit{Soil Temperature}$$

$$- 432.22 \times \textit{Potential Evapotranspiration} - 177.23 \times \textit{Cloud Cover}$$

The presence of two bands from the WIBS-Neo is encouraging, as it indicates that these are in fact influenced by fungal spore particles. As the dataset is comprised of four different fungal spores, each with their own unique characteristics and spore release mechanisms, it was expected that a range of meteorological parameters would need to be involved. All involved parameters appear related to temperature, or related factors, such as cloud cover. This again highlights one of the few parameters that all spores have in common, and that is temperature sensitivity (Hollins et al., 2004; Sabariego et al., 2000; Sarda-Estève et al., 2019)

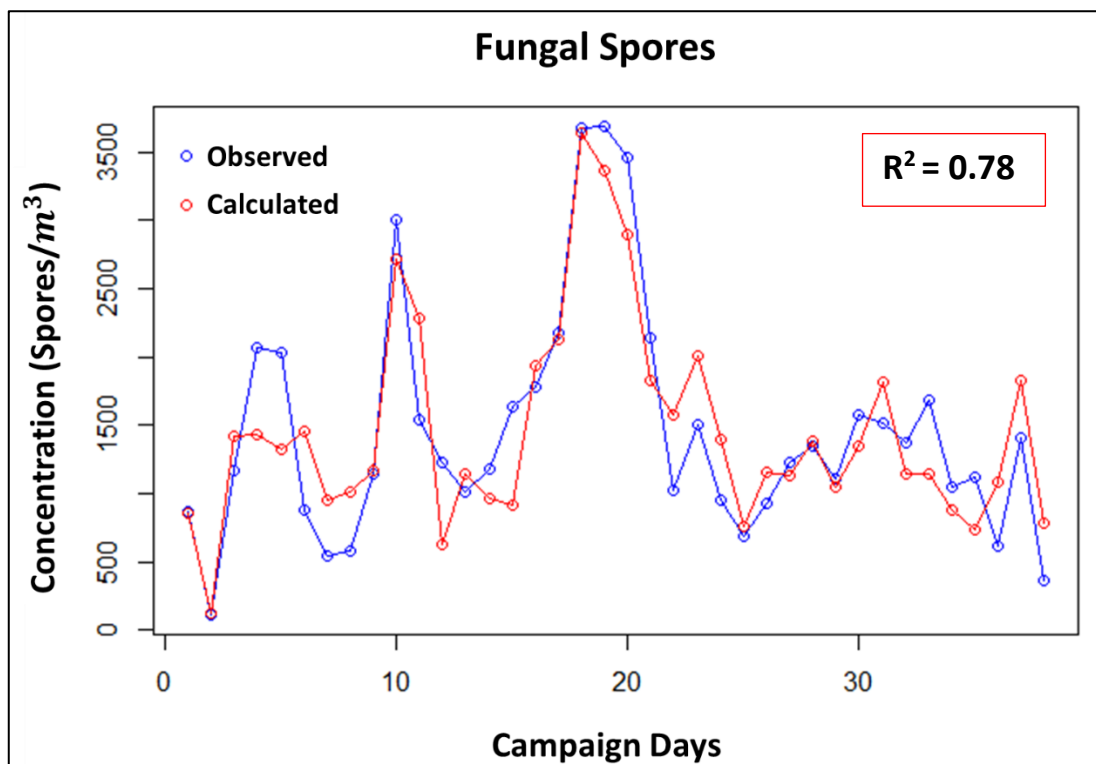


Figure 5.7: Multiple Linear Regression plot of fungal spores for the real-time monitoring campaign.

The calculated fungal spore concentration, based upon a combination of meteorological parameters including wind trajectory models, pollution values, and real-time instrumentation outputs, possessed an R^2 of 0.78, which is a very strong positive correlation. This shows that the selected MLR parameters are in fact significant, meaning AC, BC, CO, Grass Minimum Temperature, easterly wind, soil temperature, potential evapotranspiration, and cloud cover, can indeed be combined for use as a predictive tool for fungal spores. This indicates that potentially with a long enough campaign, and a large enough pool of valid WIBS data, along with meteorological and pollution data, accurate models and forecasts could be envisaged (Filho et al., 2011).

When looking at individual species of fungal spores, one parameter that stood out as being highly significant predictor on its own, was the first mode of ABC particles. Below (Figure 5.8) is a Multiple Linear Regression analysis of Basidiospore concentrations throughout the campaign. The ABC first mode had a significance value of <0.0001 , indicating that it's an extremely significant predictor of basidiospore concentrations. It also possessed a standard error of 0.01, which is a great indicator that this result will be repeatable with new datasets

in the future, given it indicates the likelihood that a sample accurately represents a full population.

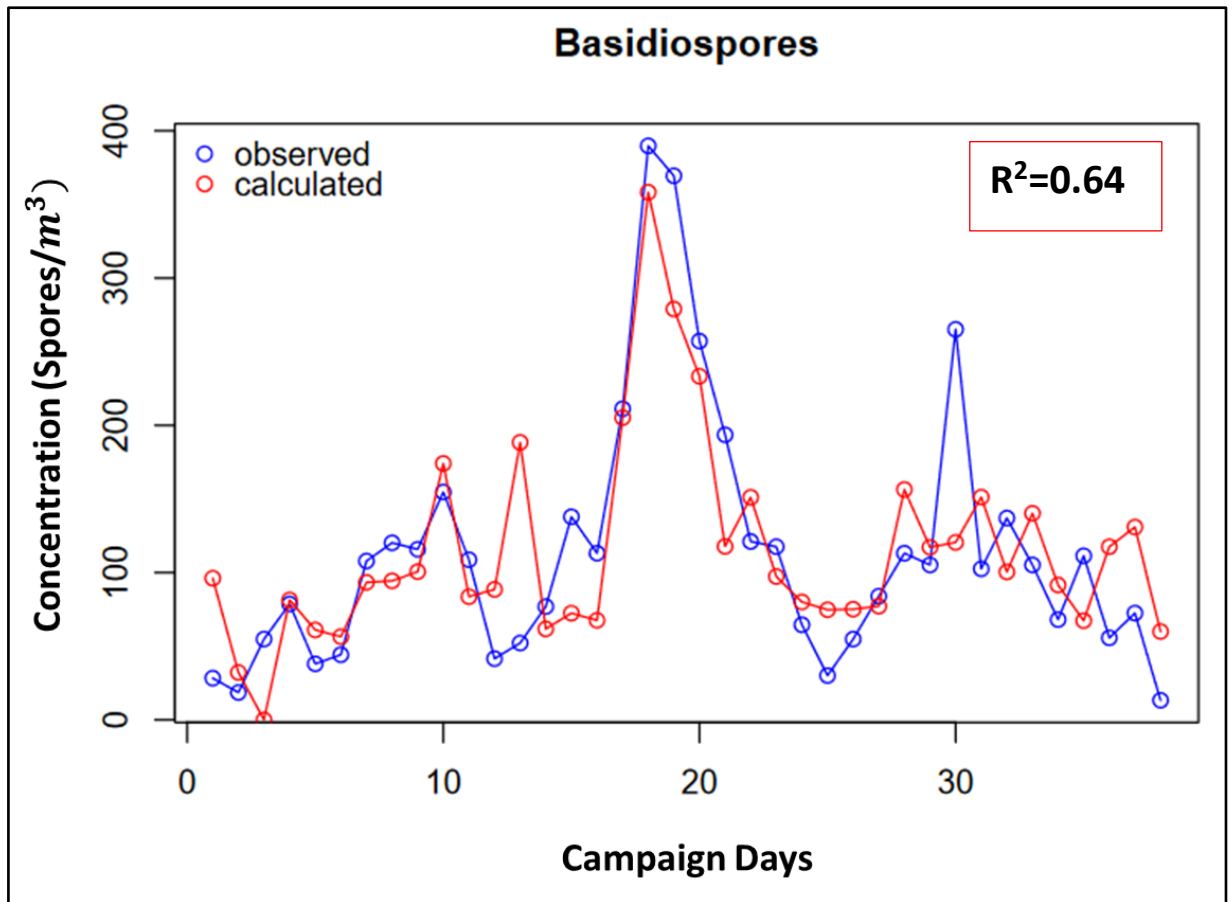


Figure 5.8: Multiple Linear Regression plot of Basidiospores for the real-time monitoring campaign.

MLR Results:

$$37.17 + 8.08 \times \text{ABC First Mode particles (WIBS-NEO)}$$

$$- 0.02 \times \text{AB particles (WIBS-NEO)}$$

$$+ 4.76 \times \text{AC particles (WIBS-NEO)}$$

$$- 4.94 \times \text{Rainfall}$$

The results above are even more encouraging due to the number of parameters that were kicked out by the analysis. The only remaining parameters are three WIBS bands that excite in the FLI channel, along with rainfall. Recommendations for the future are to carry out another WIBS monitoring campaign, to further investigate the potential of these MLR results,

which have not been replicated in other studies (Markey et al., 2022b; O'Connor et al., 2014a; Toprak and Schnaiter, 2013; Yu et al., 2016)

5.4.2. Other investigated methods

During this project, the appropriateness, or lack thereof, of various other modelling techniques was investigated for implementation on the 40-day dataset. The ultimate recommendation is that either a higher temporal resolution or a longer campaign period is recommended various methods such as the use of regression trees and subsequent evolution in Random Forest analysis were carried out, and work was completed into attempting to construct a valid linear ARIMA (autoregressive integrated moving average) or a non-linear model with the data at hand, as these methods have been successfully implemented in past studies (Babu and Reddy, 2014; Grinn-Gofroń et al., 2021; Grinn-Gofroń and Strzelczak, 2008; Kihoro et al., 2004; Martinez-Bracero et al., 2022; Philibert et al., 2011).

Results from these investigations either came to the conclusion stated above, that larger datasets are needed for valid results, or just did not obtain the high quality of outputs obtained from the MLR campaign. Subsequently, it was decided to use the longest dataset available, the Hirst-Lanzoni fungal spore counts, which cover four entire fungal spore fructification seasons, and combine them with the Met Éireann meteorological data to attempt to construct valid and high performing bioaerosol forecasting models.

5.5. Development of an Irish Fungal Spore Model

For the forecasting model development, the fungal spore data from the Hirst-Lanzoni instrument for the years 2017, 2018, 2019, and 2020 were utilized. The two most studied fungal spore types, *Cladosporium* and *Alternaria* were the fungal spores of choice when undertaking the creation Irish fungal models (Corden and Millington, 2001; Martinez-Bracero et al., 2022; O'Connor et al., 2014c; Rodríguez-Rajo et al., 2005; Tariq et al., 1996; Vélez-Pereira et al., 2019). A large variety of regression-based forecast models were studied to determine their appropriateness for the dataset at hand, and a selection were chosen, with the results of this comparative study shown below. Given the slight differences in start and end time of each season of counting, and some truncation to fungal spore tape sample collection in 2020 due both to the impacts of the Coronavirus pandemic, and the impact of the shutting down of our university building, which was scheduled for demolition that Winter, the calibration data (80% of the dataset) was made up of the entirety of the 2017, 2018, and 2019 fungal spore seasons, and the validation data (20% of the dataset) was made

up of the 2020 fungal spore season. This in essence means that these forecasts were attempting to predict the daily concentrations of the 2020 fungal spore season.

5.5.1. Forecast Input Variables

All long-term forecasts outlined in this section used the same set of input variables. These included fungal spore data from the Hirst volumetric sampler at the Dublin sampling site, and meteorological data provided by Met Éireann.

Table 6: Input variable characteristics, for Cladosporium and Alternaria regression models. Two variables with data quality issues had to be removed due to the quantity of missing data.

Variable Class	Input Variables	Individual Parameters
Fungal spore inputs	Fungal spore concentration of the day listed (spores/m ³)	<i>Alternaria</i> <i>Cladosporium</i>
Meteorological Inputs	Maximum Air Temperature (°C)	MaxTemp
	Minimum Air Temperature (°C)	MinTemp
	09 UTC Grass Minimum Temperature (°C)	GrassMin
	Precipitation Amount (mm)	Rain
	Mean CBL Pressure (hPa)	cbl
	Highest Gust (Knots)	Gust
	Wind direction similarity to 0° polar coordinate (%)	Northerly
	Wind direction similarity to 270° polar coordinate (%)	Westerly
	Wind speed (Knots)	WindSp
	Sunshine duration (hours)	Sun
	Global Radiation (J/cm ²)	Radiation
	Mean soil temperature (°C)	SoilTemp
	Potential evapotranspiration (mm)	PtEvt
	Evaporation (mm)	Evap
	Soil moisture deficits (mm)	
	Poorly drained	smd_pd
	Moderately drained	smd_md
	Well drained	smd_wd

5.5.2. Cladosporium forecasting

Cladosporium is the most abundant fungal spore in every year of our campaign, making up between 30 and 40 percent of total fungal spores counted, and by only monitoring this one species, inferences about fungal spores as a bioaerosol group can often be made (Kurkela, 1997; Sindt et al., 2016). There are two primary species of *Cladosporium*, namely *Cladosporium Cladosporioides* and *Cladosporium herbarum*. *Cladosporium* is particularly suited to modelling and forecasting, due to the high levels of homogeneity and uniformity between individual spores, allowing for easier and more accurate identification and aggregation. The majority of research groups do not even bother to distinguish between the two main species, due to their visual similarities (the *herbarum* variant appears slightly larger, more hyaline, and lighter in colour). The ability to forecast *Cladosporium* would allow resources to be redistributed to focussing on fungal spores that are found in lower concentrations but have a much larger variety of size and shape characteristics, like ascomycetes and basidiomycetes.

5.5.2.1. *Cladosporium* Regression Forecast Models

Subsequent to the classification analysis, a set of regression forecast models using the 2017-2019 calibration data and associated meteorological data was completed. Each forecast was plotted together against the observed *Cladosporium* concentrations obtained from the traditional Hirst Sampler in 2020. These forecasts were all run together at a monthly temporal resolution, to analyse seasonal forecasting capabilities. Subsequently each model was separately run at a daily temporal resolution, for more short-term forecasting analysis. The models with a valid output, and thus included in this comparison were the K-Nearest Neighbours algorithm, the Random Forest Regression algorithm, and the Support Vector Machine Regression algorithm (Figure 5.9). Each of these methods has been used in previous studies for the forecasting of fungal spore concentrations, including *Cladosporium* (Picornell et al., 2022; Truong et al., 2017; Wang et al., 2022).

After analysis and comparison to look at model accuracy and correlation with observed values, the three models possessed monthly R^2 values of 0.6, 0.58 and 0.96 as well as daily R^2 values of 0.13, 0.23, and 0.53 for the K-Nearest Neighbours, Random Forest Regression, and the Support Vector Machine Regression algorithm respectfully. As can be seen in Figure 55, all three models were able to reliably predict the timing of the central main peak fructification period, as well as the early season and late season fructification peaks, with some predicting the intensity either more accurately or less accurately than others.

Because it was the most accurate algorithm by a significant margin, both with regard to monthly and daily temporal resolutions, the Support Vector Machine Regression (SVMR) algorithm was shown in greater detail with the observed *Cladosporium* concentrations in Figure 5.9 below.

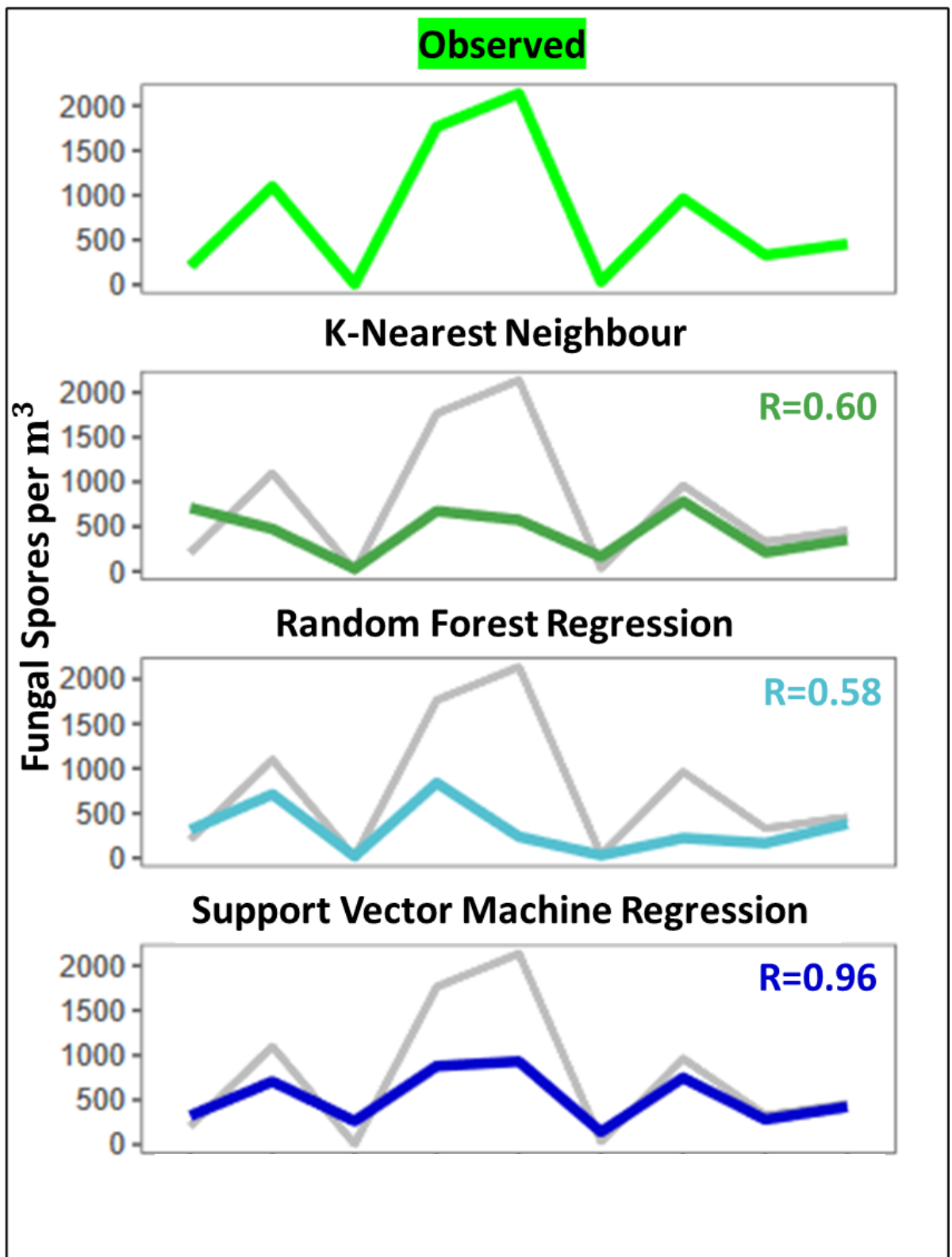


Figure 5.9: Comparison of selected regression forecast models based on previous studies, contrasted with observed *Cladosporium* concentrations.

5.5.2.2. Cladosporium SVMR Analysis

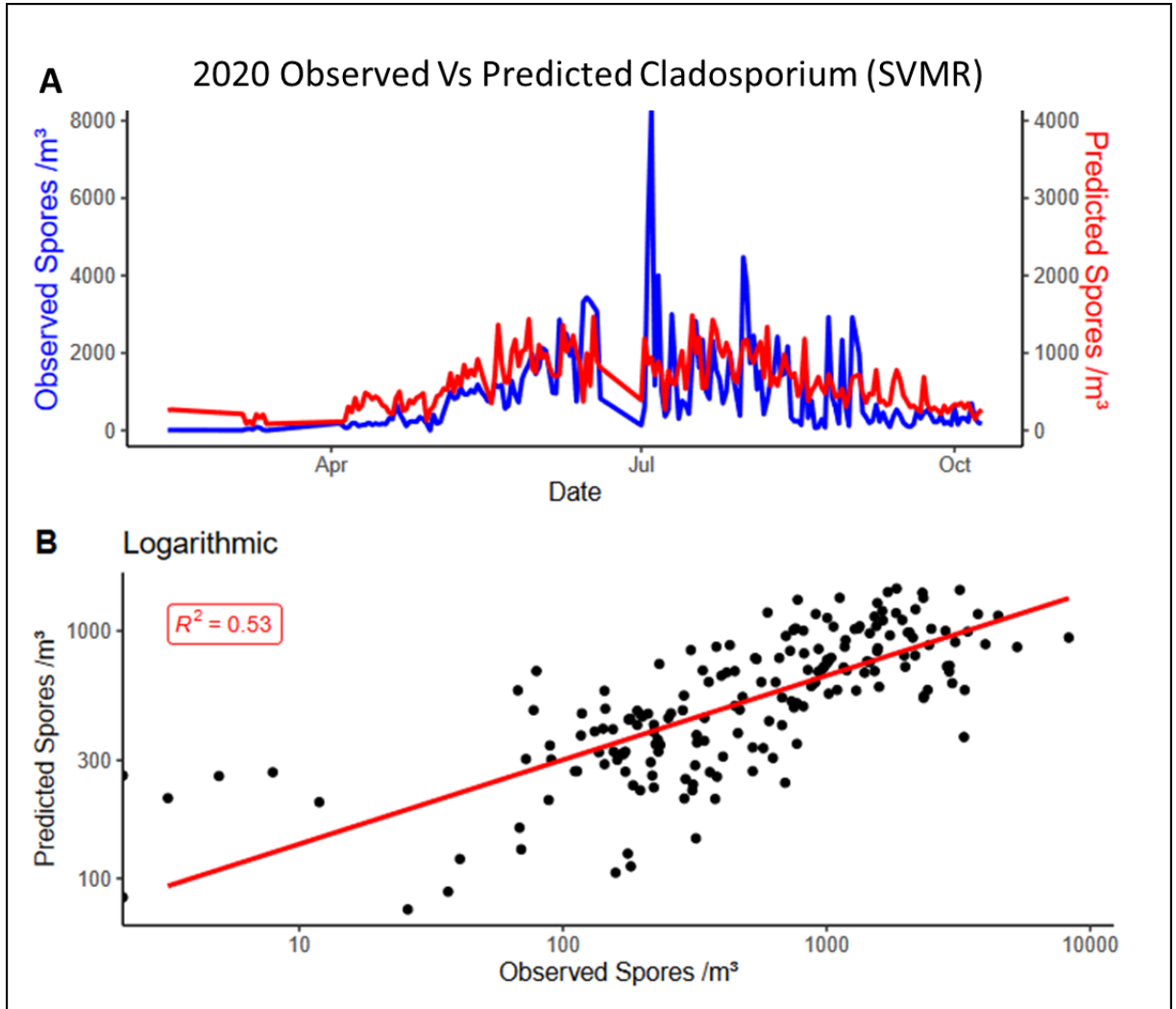


Figure 5.10: A: Time series comparison of counted 2020 *Cladosporium* fungal concentrations with forecast support vector machine regression values. B: Logarithmic regression line of the data.

Figure 5.10 shows the comparison between the predicted and the observed *Cladosporium* concentrations for the 2020 fungal fructification season, using the SVMR algorithm. The high levels of correlation at both high and low concentrations highlight the ability of the SVMR to accurately predict the *Cladosporium* concentrations. Similar results have been found previously (Tianxing and Hong, 2021; Zheng et al., 2021), with other studies following a similar approach of combining traditionally counted *Cladosporium* data with a range of meteorological parameters. The study by Tianxing and Hong (2021) have now commenced implementation of their developed SVMR as a crop defence mechanism, providing local farmers with crucial, and accurate predicted days when their grain may be vulnerable. Similarly, et al., Zheng (2021) found that the SVMR performed 10% better than other forest

models and are investigating its potential for monitoring wheat affecting pathogenic spores across the region. As counting into the subsequent years has continued, it will be of great interest to see if this process can be further refined, and if it maintains its relatively high level of predictive success. This can be aided by the addition of anthropogenic air concentration information, which will be available to us for future implementation and forecast expansion. Studies have found that the addition of these manmade pollutant interferences does in fact increase forecast accuracy and reliability (Grewling et al., 2019)

On further analysis, the SVMR model has a Root Mean Square Error value of 1,022. With peak values lying at around 8,000 for *Cladosporium*. As this is a preliminary model, an RMSE of 1/8th of the peak value, and an R^2 of 0.53 can be considered sufficient at this point in the data collation process.

5.5.3. *Alternaria* Forecasting

Alternaria is the largest species of fungal spores monitored as part of this campaign, and for many bioaerosol studies, it is analysed alongside pollen grains rather than other fungal spores, due to its large size, and due to the sensitisation it can cause in the sinuses of those who suffer from allergic rhinitis (González-Alonso et al., 2023; Hernandez-Ramirez et al., 2021). This reaction in hay fever sufferers is part of the reason why forecasting *Alternaria* concentrations in advance is so important. Additionally, while the majority of *Alternaria* species are saprophytic, several species have developed pathogenic capabilities. These can be very harmful for crops, leading to diseases such as black rot, which can occur in many fruits such as tomatoes, olives, and citrus, and *Alternaria* disease and black point rot can destroy apple and cereal crops respectfully (Logrieco et al., 2009; Thomma, 2003; Tsuge et al., 2013).

5.5.3.1. *Alternaria* Regression Forecast Models

Following the same process as was carried out in the *Cladosporium* model comparative study, a set of regression forecast models using the 2017-2019 meteorological and calibration data were constructed, with each of the models being plotted together against the observed *Alternaria* concentrations, obtained from the traditional Hirst Sampler in 2020.

This time, the models included in this comparison due to possessing a valid output, were the K-Nearest Neighbours algorithm, the Random Forest Regression algorithm, and the

Support Vector Machine Regression algorithms with the addition of a standard regression and a Generalised Additive Model (GAM) algorithm (Figure 5.II). There were more models in this section compared to *Cladosporium*, as some models completed for the *Cladosporium* regression analysis were extremely unreliable, and not at all correlatives. Again, these models have both previously implemented for the forecasting of fungal spore concentrations (Saar, 2007; Vélez-Pereira et al., 2019).

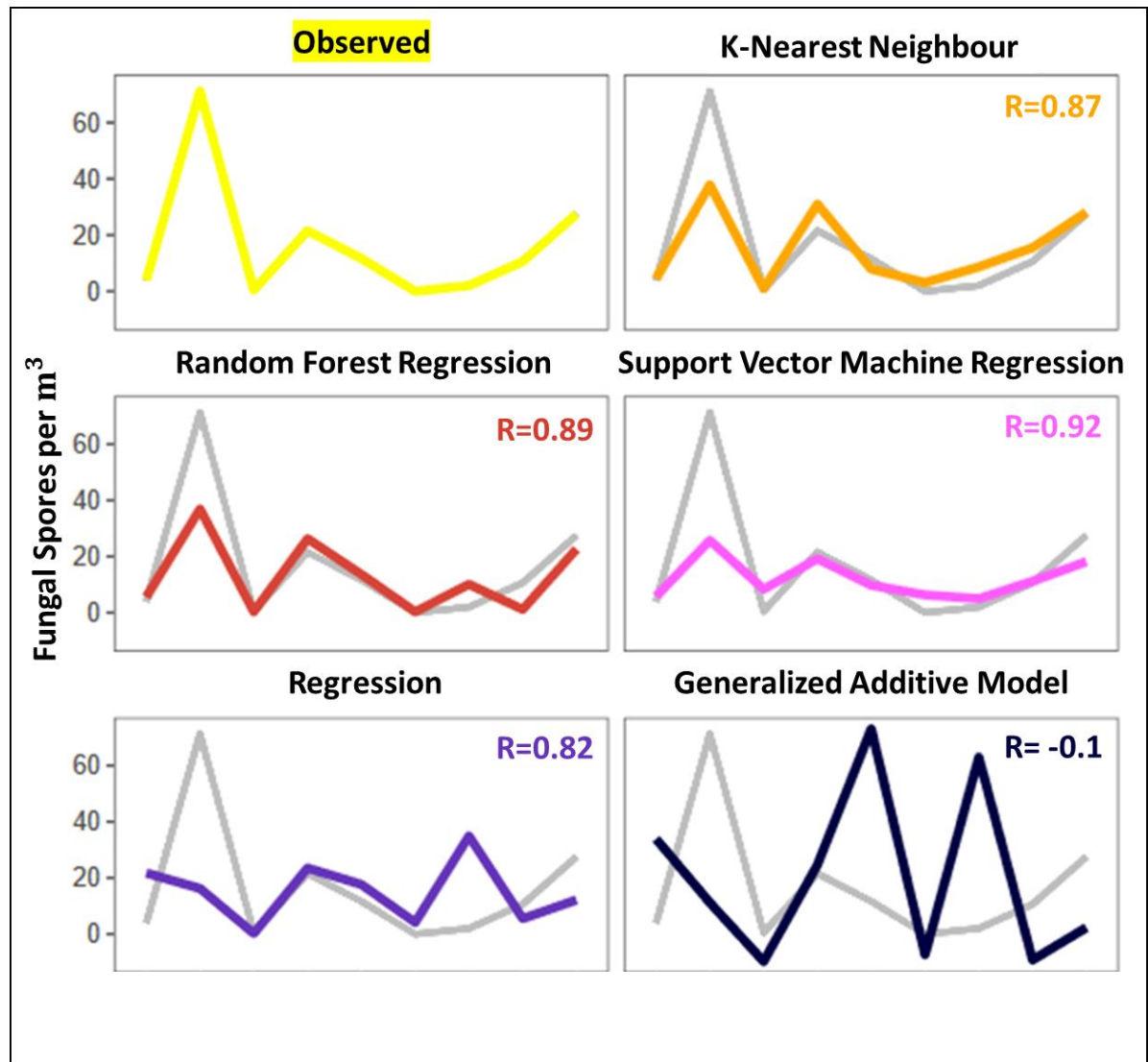


Figure 5.II: Comparison of selected regression forecast models with observed *Alternaria* concentrations.

The five models were analysed and compared with the observed *Alternaria* fungal spore counts at two temporal resolutions, with the monthly temporal resolution, for seasonal forecasting, are shown in Figure 5.II. The resulting monthly correlative strengths are also displayed in Figure 5.II above. The daily R^2 values for the same time period were as follows;

K-Nearest Neighbour had an R^2 of <0.01 , GAM had $R^2 = 0.04$, the Random Forest and Regression algorithms possessed values of $R^2 = 0.24$ and $R^2 = 0.26$, and the Support Vector Machine Learning algorithm had a final value of $R^2 = 0.42$, once again making it the most accurate forecast model by a considerable margin. Of note is that when one can make the visual observation that the K-Nearest Neighbour looks to be highly correlated with the observed values over the season. It must be noted that at lower temporal resolution, this is the case, but the models were assessed at their ability to predict fungal spore concentrations at daily intervals. As a result, it may be of value to later investigate the potential use of the K-Nearest Neighbour algorithm as a predictive tool for longer time periods, rather than daily or weekly concentrations.

Because it was the most accurate algorithm by a significant margin yet again, the Support Vector Machine Regression (SVMR) algorithm was compared in greater detail with the observed *Alternaria* concentrations below in Figure 5.12.

5.5.3.2. *Alternaria* SVMR Analysis

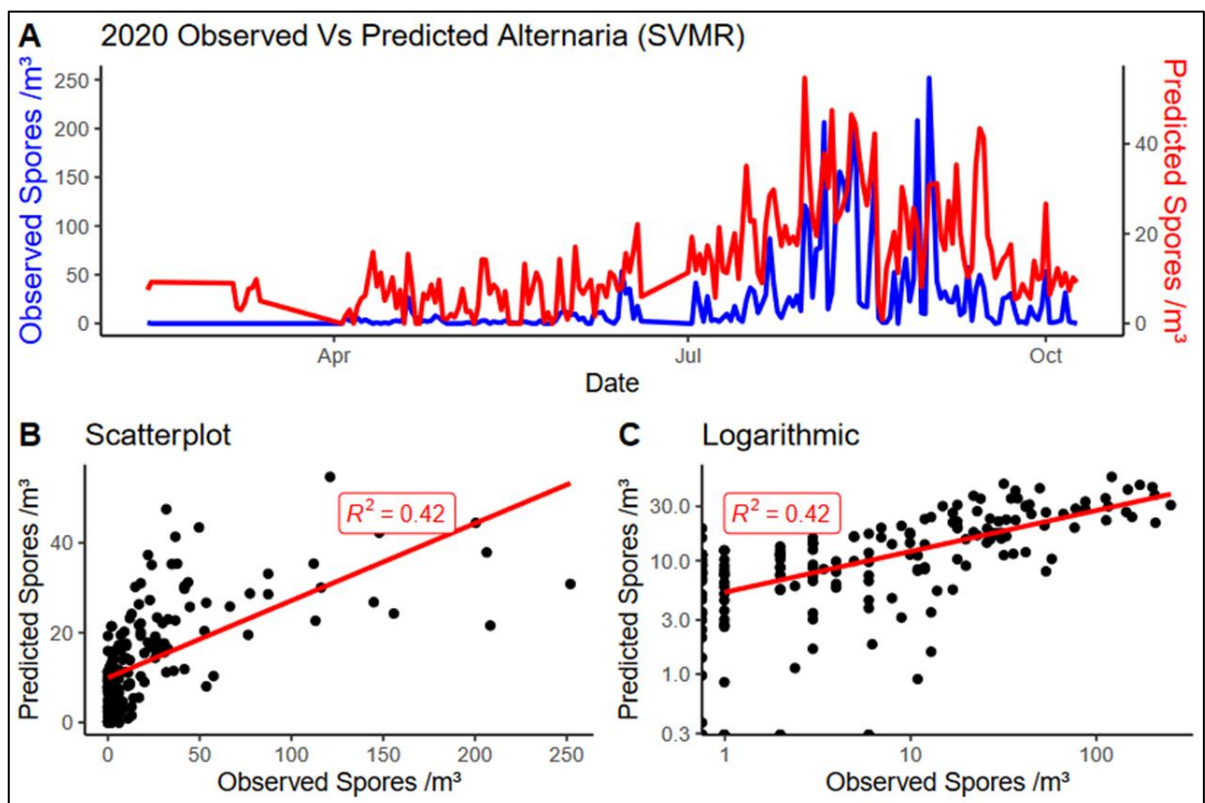


Figure 5.12: Comparison of counted 2020 *Alternaria* fungal concentrations with forecast support vector machine regression values.

As with the *Cladosporium* comparison, SVMR predicted spore concentrations are more easily identifiable when the dataset is shown as a logarithmic, rather than a linear regression scatterplot. This is due to the small number of days with extremely high fungal spore concentrations, meaning the majority of fungal spore campaigns are logarithmically distributed datasets. Again, the SVMR predicted concentrations are generally accurate at both higher and lower *Alternaria* concentrations.

The RMSE value of the forecast was 36 for *Alternaria*, when the peak concentrations lie around 250 for *Alternaria* spores. With the RMSE value being 19th of the peak, and the R² value being 0.42, again this is a sufficiently high-quality result for this preliminary forecast.

Given that both fungal spore types investigated as part of this campaign were found to correlate most highly with the support vector machine regression algorithm, there is scope for investigating the potential use of SVMR models to predict more spore types, or to predict fungal spores as a whole with this model. Several other studies have also successfully implemented the use of SVMR algorithms for the prediction of *Alternaria* concentrations, with high degrees of success (Aquino et al., 2021; Omrani et al., 2014; Van De Vijver et al., 2020). If subsequent investigations into the use of support vector machine regression for the forecasting of fungal spores are as successful, this could potentially lead to improved health outcomes for citizens, and improved crops yields across the Island, dramatically reducing government expenditure in these sectors, and improving the lives of countless people as a result.

5.6. Conclusion

The development of predictive and forecasting models for fungal spores has gained attention due to the growing awareness of their health and agricultural impacts. A comprehensive fungal spore forecasting program could help vulnerable individuals self-manage exposure, potentially reducing allergic reactions and healthcare costs. Forecasts could also help in the agricultural industry by enabling early warning systems and defence mechanisms at the onset of fungal infections or spore release. Fungal spore forecasts could also be used in the ecological field for environmental protection. Developing predictive models can be challenging due to the inclusion and exclusion criteria of data and the transformations required for analysis. However, the advent of cloud computing has allowed researchers to run models more efficiently, leading to further scientific democratization. Additionally, logistic regression for forecasting allows researchers to forecast hourly and daily concentrations while determining annual fungal spore or pollen integrals in one workload, saving time and energy.

The influence of wind on pollen and spore dispersion and transportation is significant. ZeFir source receptor models were used to determine the potential geographic location of detected pollen taxa tracked throughout a campaign in Dublin. Wind-rose plots provided valuable information on the spatial origins of pollen, fungal spores, and FAPs. The prevailing winds throughout the campaign came almost exclusively from the West-Southwest sector at faster wind speeds, mainly greater than 12 kilometres per hour. Fungal spores like Basidiospores, *Cladosporium*, and *Alternaria* have a north-westerly dominant origin, with a bias towards lower wind speeds. Ascospores have a different primary geographical origin, with no or very low concentrations originating from the northwest. Fungal spores can travel much further than pollen grains in the same weather conditions, and their small size and light weight allow for airborne dispersal. The WIBS emission channels are designed for selective detection of biomarkers in bioaerosols, but potential interferents such as anthropogenic sources and non-biological aerosols can impact the fluorescence signals. Raising the initial fluorescence threshold can mitigate these impacts without affecting the relative fraction of bioaerosols detected by the WIBS. The real-time instrumentation campaign used a 40-day period of monitoring data to analyse fungal spores. The MLR analysis calculated a fungal spore concentration that had a correlative R^2 of 0.78, indicating that the selected parameters can be combined for use as a predictive tool for fungal spores.

This project investigated various modelling techniques for implementing bioaerosol forecasting models on a 40-day dataset. The recommendation was to use larger datasets or longer campaigns for more appropriate results. *Cladosporium*, the most abundant fungal spore species, makes up 30-40% of total fungal spores in the campaign and was the first species investigated. Three regression forecast models were used, including the K-Nearest Neighbours algorithm, Random Forest Regression algorithm, and Support Vector Machine Regression algorithm. All three models reliably predicted the timing of the central main peak fructification period and early and late season fructification peaks. *Alternaria*, the largest fungal spore species, is monitored in bioaerosol studies due to its large size and potential sensitization to allergic rhinitis sufferers. Forecasting *Alternaria* concentrations is crucial for crop health, as it can cause diseases like black rot and destroy apple and cereal crops. Similarly positive results were obtained from its algorithm analysis.

In conclusion, the development of predictive and forecasting models for fungal spores has the potential to have significant impacts on health, agriculture, and environmental protection. These models can help individuals manage their exposure to fungal spores, reducing allergic reactions and healthcare costs. They can also aid in early warning system and defence implementation programmes for fungal infections in the agricultural industry. The use of cloud computing has made running these models more efficient, leading to further scientific democratization. Wind patterns play a significant role in the dispersion of fungal spores and pollen, and wind rose plots provide valuable information on their spatial origins. The WIBS instrument and MLR analysis have shown promise in predicting fungal spore concentrations. Additionally, forecasting models for specific fungal spore species like *Cladosporium* and *Alternaria* have been developed and found to be accurate, which can have implications for crop health and overall well-being. Ultimately, the use of predictive and forecasting models for fungal spores has the potential to improve health outcomes, reduce costs, and protect the environment.

5.7. References

- Agency (EPA), E.P., n.d. Reports & SAFER-Data [WWW Document]. Environ. Prot. Agency EPA. URL <https://eparesearch.epa.ie/safer/> (accessed 10.9.23).
- Aquino, H., Concepcion, R., Dadios, E., Mendigoria, C.H., Alajas, O.J., Sybingco, E., 2021. Severity Assessment of Potato Leaf Disease Induced by *Alternaria solani* Fungus Using Hybrid Decision Tree and Support Vector Machine Regression, in: 2021 IEEE 9th Region 10 Humanitarian Technology Conference (R10-HTC). Presented at the 2021 IEEE 9th Region 10 Humanitarian Technology Conference (R10-HTC), IEEE, Bangalore, India, pp. 1–6. <https://doi.org/10.1109/R10-HTC53172.2021.9641616>
- Babu, C.N., Reddy, B.E., 2014. A moving-average filter based hybrid ARIMA–ANN model for forecasting time series data. *Appl. Soft Comput.* 23, 27–38. <https://doi.org/10.1016/j.asoc.2014.05.028>
- Bañbura, M., Rünstler, G., 2011. A look into the factor model black box: Publication lags and the role of hard and soft data in forecasting GDP. *Int. J. Forecast.* 27, 333–346. <https://doi.org/10.1016/j.ijforecast.2010.01.011>
- Barredo-Arrieta, A., Laña, I., Del Ser, J., 2019. What Lies Beneath: A Note on the Explainability of Black-box Machine Learning Models for Road Traffic Forecasting, in: 2019 IEEE Intelligent Transportation Systems Conference (ITSC). Presented at the 2019 IEEE Intelligent Transportation Systems Conference (ITSC), pp. 2232–2237. <https://doi.org/10.1109/ITSC.2019.8916985>
- Braęoszewska, E., Pastuszka, J.S., 2018. Influence of meteorological factors on the level and characteristics of culturable bacteria in the air in Gliwice, Upper Silesia (Poland). *Aerobiologia* 34, 241–255. <https://doi.org/10.1007/s10453-018-9510-1>
- Bush, R.K., Yunginger, J.W., 1987. Standardization of fungal allergens. *Clin. Rev. Allergy* 5, 3–21. <https://doi.org/10.1007/BF02802254>
- Carlile, M., Watkinson, S., 2021. *The Fungi* - 2nd Edition.
- Computer-Assisted Research Design and Analysis [WWW Document], n.d. . Guide Books. <https://doi.org/10.5555/556711>
- Corden, J.M., Millington, W.M., 2001. The long-term trends and seasonal variation of the aeroallergen *Alternaria* in Derby, UK. *Aerobiologia* 17, 127–136. <https://doi.org/10.1023/A:1010876917512>
- Crandall, S.G., Saarman, N., Gilbert, G.S., 2020. Fungal spore diversity, community structure, and traits across a vegetation mosaic. *Fungal Ecol.* 45, 100920. <https://doi.org/10.1016/j.funeco.2020.100920>

- Dales, R.E., Cakmak, S., Burnett, R.T., Judek, S., Coates, F., Brook, J.R., 2000. Influence of Ambient Fungal Spores on Emergency Visits for Asthma to a Regional Children's Hospital. *Am. J. Respir. Crit. Care Med.* 162, 2087–2090. <https://doi.org/10.1164/ajrccm.162.6.2001020>
- Daly, S.M., O'Connor, D.J., Healy, D.A., Hellebust, S., Arndt, J., McGillicuddy, E.J., Feeney, P., Quirke, M., Wenger, J.C., Sodeau, J.R., 2019. Investigation of coastal sea-fog formation using the WIBS (wideband integrated bioaerosol sensor) technique. *Atmospheric Chem. Phys.* 19, 5737–5751. <https://doi.org/10.5194/acp-19-5737-2019>
- Damialis, A., Gioulekas, D., Lazopoulou, C., Balafoutis, C., Vokou, D., 2005. Transport of airborne pollen into the city of Thessaloniki: the effects of wind direction, speed and persistence. *Int. J. Biometeorol.* 49, 139–145. <https://doi.org/10.1007/s00484-004-0229-z>
- Davies, R.R., Smith, L.P., 1974. Weather and the grass pollen content of the air. *Clin. Exp. Allergy* 4, 95–108. <https://doi.org/10.1111/j.1365-2222.1974.tb01367.x>
- Donnelly, A., Misstear, B., Broderick, B., 2015. Realtime air quality forecasting using integrated parametric and non-parametric regression techniques. *Atmos. Environ.* 103, 53–65. <https://doi.org/10.1016/j.atmosenv.2014.12.011>
- Dowding, P., 1987. Wind Pollination Mechanisms and Aerobiology. *Int. Rev. Cytol.* 107, 421–437. [https://doi.org/10.1016/S0074-7696\(08\)61084-0](https://doi.org/10.1016/S0074-7696(08)61084-0)
- Elbert, W., Taylor, P.E., Andreae, M.O., Pöschl, U., 2007. Contribution of fungi to primary biogenic aerosols in the atmosphere: wet and dry discharged spores, carbohydrates, and inorganic ions. *Atmospheric Chem. Phys.* 7, 4569–4588. <https://doi.org/10.5194/acp-7-4569-2007>
- Filho, D.B.F., Júnior, J.A.S., Rocha, E.C., 2011. What is R2 all about? *Leviathan São Paulo* 60–68. <https://doi.org/10.11606/issn.2237-4485.lev.2011.132282>
- FLIR IBAC 2 Bio-Threat Detection & Collection | Teledyne FLIR [WWW Document], 2021. URL <https://www.flir.com/products/ibac-2/> (accessed 7.22.21).
- Fröhlich-Nowoisky, J., Kampf, C.J., Weber, B., Huffman, J.A., Pöhlker, C., Andreae, M.O., Lang-Yona, N., Burrows, S.M., Gunthe, S.S., Elbert, W., Su, H., Hoor, P., Thines, E., Hoffmann, T., Després, V.R., Pöschl, U., 2016. Bioaerosols in the Earth system: Climate, health, and ecosystem interactions. *Atmospheric Res.* 182, 346–376. <https://doi.org/10.1016/j.atmosres.2016.07.018>
- Gabey, A.M., Stanley, W.R., Gallagher, M.W., Kaye, P.H., 2011. The fluorescence properties of aerosol larger than 0.8 μ in urban and tropical rainforest locations. *Atmospheric Chem. Phys.* 11, 5491–5504. <https://doi.org/10.5194/acp-11-5491-2011>

- Gong, J., Qi, J., E, B., Yin, Y., Gao, D., 2020. Concentration, viability and size distribution of bacteria in atmospheric bioaerosols under different types of pollution. *Environ. Pollut.* 257, 113485. <https://doi.org/10.1016/j.envpol.2019.113485>
- González-Alonso, M., Boldeanu, M., Koritnik, T., Gonçalves, J., Belzner, L., Stemmler, T., Gebauer, R., Grewling, Ł., Tummon, F., Maya-Manzano, J.M., Ariño, A.H., Schmidt-Weber, C., Buters, J., 2023. *Alternaria* spore exposure in Bavaria, Germany, measured using artificial intelligence algorithms in a network of BAA500 automatic pollen monitors. *Sci. Total Environ.* 861, 160180. <https://doi.org/10.1016/j.scitotenv.2022.160180>
- Green Spaces | Dublin City Council [WWW Document], 2018. URL <https://www.dublincity.ie/residential/parks/dublin-city-parks/green-spaces> (accessed 10.12.23).
- Grewling, Ł., Nowak, M., Szymańska, A., Kostecki, Ł., Bogawski, P., 2019. Temporal variability in the allergenicity of airborne *Alternaria* spores. *Med. Mycol.* 57, 403–411. <https://doi.org/10.1093/mmy/myy069>
- Grinn-Gofroń, A., Bogawski, P., Bosiacka, B., Nowosad, J., Camacho, I., Sadyś, M., Skjøth, C.A., Pashley, C.H., Rodinkova, V., Çeter, T., Traidl-Hoffmann, C., Damialis, A., 2021. Abundance of *Ganoderma* sp. in Europe and SW Asia: modelling the pathogen infection levels in local trees using the proxy of airborne fungal spore concentrations. *Sci. Total Environ.* 793, 148509. <https://doi.org/10.1016/j.scitotenv.2021.148509>
- Grinn-Gofroń, A., Nowosad, J., Bosiacka, B., Camacho, I., Pashley, C., Belmonte, J., De Linares, C., Ianovici, N., Manzano, J.M.M., Sadyś, M., Skjøth, C., Rodinkova, V., Tormo-Molina, R., Vokou, D., Fernández-Rodríguez, S., Damialis, A., 2019. Airborne *Alternaria* and *Cladosporium* fungal spores in Europe: Forecasting possibilities and relationships with meteorological parameters. *Sci. Total Environ.* 653, 938–946. <https://doi.org/10.1016/j.scitotenv.2018.10.419>
- Grinn-Gofroń, A., Strzelczak, A., 2009. Hourly predictive artificial neural network and multivariate regression tree models of *Alternaria* and *Cladosporium* spore concentrations in Szczecin (Poland). *Int. J. Biometeorol.* 53, 555–562. <https://doi.org/10.1007/s00484-009-0243-2>
- Grinn-Gofroń, A., Strzelczak, A., 2008. Artificial neural network models of relationships between *Alternaria* spores and meteorological factors in Szczecin (Poland). *Int. J. Biometeorol.* 52, 859–868. <https://doi.org/10.1007/s00484-008-0182-3>

- Grinn-Gofroń, A., Strzelczak, A., 2008. Artificial neural network models of relationships between *Cladosporium* spores and meteorological factors in Szczecin (Poland). *Grana* 47, 305–315. <https://doi.org/10.1080/00173130802513784>
- Han, Q., Meng, F., Hu, T., Chu, F., 2017. Non-parametric hybrid models for wind speed forecasting. *Energy Convers. Manag.* 148, 554–568. <https://doi.org/10.1016/j.enconman.2017.06.021>
- Hart, M.L., Wentworth, J.E., Bailey, J.P., 1994. The effects of trap height and weather variables on recorded pollen concentration at leicester. *Grana* 33, 100–103. <https://doi.org/10.1080/00173139409427840>
- Henry, R., Norris, G.A., Vedantham, R., Turner, J.R., 2009. Source region identification using kernel smoothing. *Environ. Sci. Technol.* 43, 4090–4097. <https://doi.org/10.1021/es8011723>
- Hernandez, M., Perring, A.E., McCabe, K., Kok, G., Granger, G., Baumgardner, D., 2016. Chamber catalogues of optical and fluorescent signatures distinguish bioaerosol classes. *Atmospheric Meas. Tech.* 9, 3283–3292. <https://doi.org/10.5194/amt-9-3283-2016>
- Hernandez-Ramirez, G., Barber, D., Tome-Amat, J., Garrido-Arandia, M., Diaz-Perales, A., 2021. *Alternaria* as an Inducer of Allergic Sensitization. *J. Fungi* 7, 838. <https://doi.org/10.3390/jof7100838>
- Hirst, J.M., Stedman, O.J., Hurst, G.W., 1967. Long-distance Spore Transport: Vertical Sections of Spore Clouds over the Sea. *Microbiology* 48, 357–377. <https://doi.org/10.1099/00221287-48-3-357>
- Historical Data - Met Éireann - The Irish Meteorological Service [WWW Document], n.d. URL <https://www.met.ie/climate/available-data/historical-data> (accessed 10.7.23).
- Hollins, P.D., Kettlewell, P.S., Atkinson, M.D., Stephenson, D.B., Corden, J.M., Millington, W.M., Mullins, J., 2004. Relationships between airborne fungal spore concentration of *Cladosporium* and the summer climate at two sites in Britain. *Int. J. Biometeorol.* 48, 137–141. <https://doi.org/10.1007/s00484-003-0188-9>
- Iwen, P.C., Davis, J.C., Reed, E.C., Winfield, B.A., Hinrichs, S.H., 1994. Airborne Fungal Spore Monitoring in a Protective Environment During Hospital Construction, and Correlation with an Outbreak of Invasive Aspergillosis. *Infect. Control Hosp. Epidemiol.* 15, 303–306. <https://doi.org/10.2307/30146558>
- Kainz, K., Bauer, M.A., Madeo, F., Carmona-Gutierrez, D., n.d. Fungal infections in humans: the silent crisis. *Microb. Cell* 7, 143–145. <https://doi.org/10.15698/mic2020.06.718>

- Kapadi, M.R., Patel, S.I., 2019. Aeromycological approach of some fungal diseases on Tomato Crop (*Lycopersicon esculentum* Mill.) at Nashik, India 422007. *J. Drug Deliv. Ther.* 9, 329–331. <https://doi.org/10.22270/jddt.v9i3.2666>
- Kasprzyk, I., Rodinkova, V., Šaulienė, I., Ritenberga, O., Grinn-Gofron, A., Nowak, M., Sulborska, A., Kaczmarek, J., Weryszko-Chmielewska, E., Bilous, E., Jedryczka, M., 2015. Air pollution by allergenic spores of the genus *Alternaria* in the air of central and eastern Europe. *Environ. Sci. Pollut. Res. Int.* 22, 9260–9274. <https://doi.org/10.1007/s11356-014-4070-6>
- Kihoro, J., Otieno, R.O., Wafula, C., 2004. Seasonal time series forecasting: A comparative study of ARIMA and ANN models.
- Kleine Deters, J., Zalakeviciute, R., Gonzalez, M., Rybarczyk, Y., 2017. Modeling PM2.5 Urban Pollution Using Machine Learning and Selected Meteorological Parameters. *J. Electr. Comput. Eng.* 2017, e5106045. <https://doi.org/10.1155/2017/5106045>
- Kruczek, A., Puc, M., Wolski, T., 2017. Airborne pollen from allergenic herbaceous plants in urban and rural areas of Western Pomerania, NW Poland. *Grana* 56, 71–80. <https://doi.org/10.1080/00173134.2016.1145251>
- Kumar, J., Singh, A.K., Buyya, R., 2021. Self directed learning based workload forecasting model for cloud resource management. *Inf. Sci.* 543, 345–366. <https://doi.org/10.1016/j.ins.2020.07.012>
- Kurkela, T., 1997. The number of *Cladosporium* conidia in the air in different weather conditions. *Grana* 36, 54–61. <https://doi.org/10.1080/00173139709362591>
- Lee, J.Y.Y., Miao, Y., Chau, R.L.T., Hernandez, M., Lee, P.K.H., 2023. Artificial intelligence-based prediction of indoor bioaerosol concentrations from indoor air quality sensor data. *Environ. Int.* 174, 107900. <https://doi.org/10.1016/j.envint.2023.107900>
- Li, X., Cheng, X., Wu, W., Wang, Q., Tong, Z., Zhang, X., Deng, D., Li, Y., Gao, X., 2020. An improved wavelet de-noising-based back propagation neural network model to forecast the bioaerosol concentration. *Aerosol Sci. Technol.* 55, 352–360. <https://doi.org/10.1080/02786826.2020.1846678>
- Liu, Z., Chu, J., Huang, Z., Li, H., Xiao, X., He, J., Yang, W., Shao, X., Liu, H., 2023. Machine learning predicts bioaerosol trajectories in enclosed environments: Introducing a novel method. *Aerosol Sci. Technol.* 57, 998–1012. <https://doi.org/10.1080/02786826.2023.2230240>
- Logrieco, A., Moretti, A., Solfrizzo, M., 2009. *Alternaria* toxins and plant diseases: an overview of origin, occurrence and risks. *World Mycotoxin J.* 2, 129–140. <https://doi.org/10.3920/WMJ2009.1145>

- Markey, E., Clancy, J.H., Martínez-Bracero, M., Maya-Manzano, J.M., Smith, M., Skjøth, C., Dowding, P., Sarda-Estève, R., Baisnée, D., Donnelly, A., McGillicuddy, E., Sewell, G., O'Connor, D.J., 2022a. A comprehensive aerobiological study of the airborne pollen in the Irish environment. *Aerobiologia* 38, 343–366. <https://doi.org/10.1007/s10453-022-09751-w>
- Markey, E., Hourihane Clancy, J., Martínez-Bracero, M., Neeson, F., Sarda-Estève, R., Baisnée, D., McGillicuddy, E.J., Sewell, G., O'Connor, D.J., 2022b. A Modified Spectroscopic Approach for the Real-Time Detection of Pollen and Fungal Spores at a Semi-Urban Site Using the WIBS-4+, Part I. *Sensors* 22, 8747. <https://doi.org/10.3390/s22228747>
- Martinez-Bracero, M., Markey, E., Clancy, J.H., McGillicuddy, E.J., Sewell, G., O'Connor, D.J., 2022. Airborne Fungal Spore Review, New Advances and Automatisation. *Atmosphere* 13, 308. <https://doi.org/10.3390/atmos13020308>
- Mims, S.A., Mims, F.M., 2004. Fungal spores are transported long distances in smoke from biomass fires. *Atmos. Environ.* 38, 651–655. <https://doi.org/10.1016/j.atmosenv.2003.10.043>
- Nature and Biodiversity | Phoenix Park, n.d. URL <https://www.phoenixpark.ie/nature-and-biodiversity/> (accessed 10.12.23).
- O'Connor, D.J., Healy, D.A., Hellebust, S., Buters, J.T.M., Sodeau, J.R., 2014a. Using the WIBS-4 (Waveband Integrated Bioaerosol Sensor) Technique for the On-Line Detection of Pollen Grains. *Aerosol Sci. Technol.* 48, 341–349. <https://doi.org/10.1080/02786826.2013.872768>
- O'Connor, D.J., Healy, D.A., Sodeau, J.R., 2013. The on-line detection of biological particle emissions from selected agricultural materials using the WIBS-4 (Waveband Integrated Bioaerosol Sensor) technique. *Atmos. Environ.* 80, 415–425. <https://doi.org/10.1016/j.atmosenv.2013.07.051>
- O'Connor, D.J., Sadyś, M., Skjøth, C.A., Healy, D.A., Kennedy, R., Sodeau, J.R., 2014b. Atmospheric concentrations of *Alternaria*, *Cladosporium*, *Ganoderma* and *Didymella* spores monitored in Cork (Ireland) and Worcester (England) during the summer of 2010. *Aerobiologia* 30, 397–411. <https://doi.org/10.1007/s10453-014-9337-3>
- O'Connor, D.J., Sadyś, M., Skjøth, C.A., Healy, D.A., Kennedy, R., Sodeau, J.R., 2014c. Atmospheric concentrations of *Alternaria*, *Cladosporium*, *Ganoderma* and *Didymella* spores monitored in Cork (Ireland) and Worcester (England) during the summer of 2010. *Aerobiologia* 30, 397–411. <https://doi.org/10.1007/s10453-014-9337-3>

- Oliveira, M., Ribeiro, H., Delgado, J.L., Abreu, I., 2009. The effects of meteorological factors on airborne fungal spore concentration in two areas differing in urbanisation level. *Int. J. Biometeorol.* 53, 61–73. <https://doi.org/10.1007/s00484-008-0191-2>
- Olsen, Y., Skjøth, C.A., Hertel, O., Rasmussen, K., Sigsgaard, T., Gosewinkel, U., 2020. Airborne *Cladosporium* and *Alternaria* spore concentrations through 26 years in Copenhagen, Denmark. *Aerobiologia* 36, 141–157. <https://doi.org/10.1007/s10453-019-09618-7>
- Omrani, E., Khoshnevisan, B., Shamshirband, S., Saboohi, H., Anuar, N.B., Nasir, M.H.N.M., 2014. Potential of radial basis function-based support vector regression for apple disease detection. *Measurement* 55, 512–519. <https://doi.org/10.1016/j.measurement.2014.05.033>
- Patel, T.Y., Buttner, M., Rivas, D., Cross, C., Bazylnski, D.A., Seggev, J., 2018. Variation in airborne fungal spore concentrations among five monitoring locations in a desert urban environment. *Environ. Monit. Assess.* 190, 634. <https://doi.org/10.1007/s10661-018-7008-5>
- Pazienza, M., 2013. Use of Particle Counter System for the Optimization of Sampling, Identification and Decontamination Procedures for Biological Aerosols Dispersion in Confined Environment. *J. Microb. Biochem. Technol.* 06. <https://doi.org/10.4172/1948-5948.1000120>
- Petit, J.E., Favez, O., Albinet, A., Canonaco, F., 2017. A user-friendly tool for comprehensive evaluation of the geographical origins of atmospheric pollution: Wind and trajectory analyses. *Environ. Model. Softw.* 88, 183–187. <https://doi.org/10.1016/j.envsoft.2016.11.022>
- Philibert, A., Desprez-Loustau, M.-L., Fabre, B., Frey, P., Halkett, F., Husson, C., Lung-Escarmant, B., Marçais, B., Robin, C., Vacher, C., Makowski, D., 2011. Predicting invasion success of forest pathogenic fungi from species traits. *J. Appl. Ecol.* 48, 1381–1390. <https://doi.org/10.1111/j.1365-2664.2011.02039.x>
- Picornell, A., Rojo, J., Trigo, M.M., Ruiz-Mata, R., Lara, B., Romero-Morte, J., Serrano-García, A., Pérez-Badia, R., Gutiérrez-Bustillo, M., Cervigón-Morales, P., Ferencova, Z., Morales-González, J., Sánchez-Reyes, E., Fuentes-Antón, S., Sánchez-Sánchez, J., Dávila, I., Oteros, J., Martínez-Bracero, M., Galán, C., García-Mozo, H., Alcázar, P., Fernández, S., González-Alonso, M., Robles, E., de Zabalza, A.P., Ariño, A.H., Recio, M., 2022. Environmental drivers of the seasonal exposure to airborne *Alternaria* spores in Spain. *Sci. Total Environ.* 823, 153596. <https://doi.org/10.1016/j.scitotenv.2022.153596>

- Recio, M., del Mar Trigo, M., Docampo, S., Melgar, M., García-Sánchez, J., Bootello, L., Cabezudo, B., 2012. Analysis of the predicting variables for daily and weekly fluctuations of two airborne fungal spores: *Alternaria* and *Cladosporium*. *Int. J. Biometeorol.* 56, 983–991. <https://doi.org/10.1007/s00484-011-0509-3>
- Rodríguez-Rajo, F.J., Iglesias, I., Jato, V., 2005. Variation assessment of airborne *Alternaria* and *Cladosporium* spores at different bioclimatical conditions. *Mycol. Res.* 109, 497–507. <https://doi.org/10.1017/S0953756204001777>
- Rojo, J., Rapp, A., Lara, B., Fernández-González, F., Pérez-Badia, R., 2015. Effect of land uses and wind direction on the contribution of local sources to airborne pollen. *Sci. Total Environ.* 538, 672–682. <https://doi.org/10.1016/j.scitotenv.2015.08.074>
- Saar, M., 2007. Seasonality in quantity of atmospheric fungal aerosol in Tartu (Estonia). *Folia Cryptogam. Est.* 43, 57–67.
- Saari, S., Reponen, T., Keskinen, J., 2014. Performance of Two Fluorescence-Based Real-Time Bioaerosol Detectors: BioScout vs. UVAPS. *Aerosol Sci. Technol.* 48, 371–378. <https://doi.org/10.1080/02786826.2013.877579>
- Sabariego, S., Díaz de la Guardia, C., Alba, F., 2000. The effect of meteorological factors on the daily variation of airborne fungal spores in Granada (southern Spain). *Int. J. Biometeorol.* 44, 1–5. <https://doi.org/10.1007/s004840050131>
- Sadyś, M., Strzelczak, A., Grinn-Gofroń, A., Kennedy, R., 2015. Application of redundancy analysis for aerobiological data. *Int. J. Biometeorol.* 59, 25–36. <https://doi.org/10.1007/s00484-014-0818-4>
- Santarpia, J.L., Ratnesar-Shumate, S., Gilberry, J.U., Quizon, J.J., 2013. Relationship Between Biologically Fluorescent Aerosol and Local Meteorological Conditions. *Aerosol Sci. Technol.* 47, 655–661. <https://doi.org/10.1080/02786826.2013.781263>
- Sarda-Estève, R., Baisnée, D., Guinot, B., Mainelis, G., Sodeau, J., O'connor, D., Besancenot, J.P., Thibaudon, M., Monteiro, S., Petit, J.E., Gros, V., 2020. Atmospheric biodetection part i: Study of airborne bacterial concentrations from january 2018 to may 2020 at saclay, france. *Int. J. Environ. Res. Public Health* 17, 1–25. <https://doi.org/10.3390/ijerph17176292>
- Sarda-Estève, R., Baisnée, D., Guinot, B., Petit, J.E., Sodeau, J., O'Connor, D., Besancenot, J.P., Thibaudon, M., Gros, V., 2018. Temporal variability and geographical origins of airborne pollen grains concentrations from 2015 to 2018 at Saclay, France. *Remote Sens.* 10. <https://doi.org/10.3390/rs10121932>
- Sarda-Estève, R., Baisnée, D., Guinot, B., Sodeau, J., O'Connor, D., Belmonte, J., Besancenot, J.-P., Petit, J.-E., Thibaudon, M., Oliver, G., Sindt, C., Gros, V., 2019. Variability and

- Geographical Origin of Five Years Airborne Fungal Spore Concentrations Measured at Saclay, France from 2014 to 2018. *Remote Sens.* 11, 1671. <https://doi.org/10.3390/rs11141671>
- Savage, N.J., Krentz, C.E., Könemann, T., Han, T.T., Mainelis, G., Pöhlker, C., Alex Huffman, J., 2017. Systematic characterization and fluorescence threshold strategies for the wideband integrated bioaerosol sensor (WIBS) using size-resolved biological and interfering particles. *Atmospheric Meas. Tech.* 10, 4279–4302. <https://doi.org/10.5194/amt-10-4279-2017>
- Silva Palacios, I., Tormo Molina, R., Muñoz Rodríguez, A.F., 2000. Influence of wind direction on pollen concentration in the atmosphere. *Int. J. Biometeorol.* 44, 128–133. <https://doi.org/10.1007/s004840000059>
- Sindt, C., Besancenot, J.-P., Thibaudon, M., 2016. Airborne *Cladosporium* fungal spores and climate change in France. *Aerobiologia* 32, 53–68. <https://doi.org/10.1007/s10453-016-9422-x>
- Su, H., Wang, Z., Cheng, Y., Xie, Z., Kecorius, S., McMeeking, G.R., Yu, X., Pöhlker, C., Zhang, M., Wiedensohler, A., Kuhn, U., Poeschl, U., Huffman, J.A., 2015. Online measurements of ambient fluorescent aerosol particles by WIBS at a polluted regional site in the North China Plain: potential impact of burning activities 2015, A54A-08.
- Tariq, S.M., Matthews, S.M., Stevens, M., Hakim, E.A., 1996. Sensitization to *Alternaria* and *Cladosporium* by the age of 4 years. *Clin. Exp. Allergy J. Br. Soc. Allergy Clin. Immunol.* 26, 794–798.
- Thomma, B.P.H.J., 2003. *Alternaria* spp.: from general saprophyte to specific parasite. *Mol. Plant Pathol.* 4, 225–236. <https://doi.org/10.1046/j.1364-3703.2003.00173.x>
- Tianxing, X., Hong, G., 2021. Design of Agricultural Environmental Data Collection System Based on Internet of Things, in: 2021 IEEE International Conference on Power, Intelligent Computing and Systems (ICPICS). Presented at the 2021 IEEE International Conference on Power, Intelligent Computing and Systems (ICPICS), pp. 150–152. <https://doi.org/10.1109/ICPICS52425.2021.9524091>
- Toprak, E., Schnaiter, M., 2013. Fluorescent biological aerosol particles measured with the Waveband Integrated Bioaerosol Sensor WIBS-4: Laboratory tests combined with a one year field study. *Atmospheric Chem. Phys.* 13, 225–243. <https://doi.org/10.5194/acp-13-225-2013>
- Truong, T., Dinh, A., Wahid, K., 2017. An IoT environmental data collection system for fungal detection in crop fields, in: 2017 IEEE 30th Canadian Conference on Electrical and Computer Engineering (CCECE). Presented at the 2017 IEEE 30th Canadian

- Conference on Electrical and Computer Engineering (CCECE), pp. 1–4.
<https://doi.org/10.1109/CCECE.2017.7946787>
- Tsuge, T., Harimoto, Y., Akimitsu, K., Ohtani, K., Kodama, M., Akagi, Y., Egusa, M., Yamamoto, M., Otani, H., 2013. Host-selective toxins produced by the plant pathogenic fungus *Alternaria alternata*. *FEMS Microbiol. Rev.* 37, 44–66.
<https://doi.org/10.1111/j.1574-6976.2012.00350.x>
- Twohy, C.H., McMeeking, G.R., DeMott, P.J., McCluskey, C.S., Hill, T.C.J., Burrows, S.M., Kulkarni, G.R., Tanarhte, M., Kafle, D.N., Toohey, D.W., 2016. Abundance of fluorescent biological aerosol particles at temperatures conducive to the formation of mixed-phase and cirrus clouds. *Atmospheric Chem. Phys.* 16, 8205–8225.
<https://doi.org/10.5194/acp-16-8205-2016>
- Van De Vijver, R., Mertens, K., Heungens, K., Somers, B., Nuyttens, D., Borra-Serrano, I., Lootens, P., Roldán-Ruiz, I., Vangeyte, J., Saeys, W., 2020. In-field detection of *Alternaria solani* in potato crops using hyperspectral imaging. *Comput. Electron. Agric.* 168, 105106. <https://doi.org/10.1016/j.compag.2019.105106>
- Vélez-Pereira, A.M., De Linares, C., Canela, M.-A., Belmonte, J., 2019. Logistic regression models for predicting daily airborne *Alternaria* and *Cladosporium* concentration levels in Catalonia (NE Spain). *Int. J. Biometeorol.* 63, 1541–1553.
<https://doi.org/10.1007/s00484-019-01767-1>
- Wang, H., Reponen, T., Adhikari, A., Grinshpun, S.A., 2013. Contribution of Fungal Spores to Organic Carbon Aerosol in Indoor and Outdoor Environments in the Greater Cincinnati Area. *Aerosol Air Qual. Res.* 13, 1348–1355.
<https://doi.org/10.4209/aaqr.2012.10.0291>
- Wang, Y., Mao, H., Xu, G., Zhang, X., Zhang, Y., 2022. A Rapid Detection Method for Fungal Spores from Greenhouse Crops Based on CMOS Image Sensors and Diffraction Fingerprint Feature Processing. *J. Fungi* 8, 374. <https://doi.org/10.3390/jof8040374>
- Yu, X., Wang, Z., Zhang, M., Kuhn, U., Xie, Z., Cheng, Y., Pöschl, U., Su, H., 2016. Ambient measurement of fluorescent aerosol particles with a WIBS in the Yangtze River Delta of China: potential impacts of combustion-related aerosol particles. *Atmospheric Chem. Phys.* 16, 11337–11348. <https://doi.org/10.5194/acp-16-11337-2016>
- Yue, S., Ren, H., Fan, S., Sun, Y., Wang, Z., Fu, P., 2016. Springtime precipitation effects on the abundance of fluorescent biological aerosol particles and HULIS in Beijing. *Sci. Rep.* 6, 1–10. <https://doi.org/10.1038/srep29618>

ZeFir - Tracking Pollution Back to the Origin | Igor Pro by WaveMetrics [WWW Document], n.d. URL <https://www.wavemetrics.com/case-study/zefir-tracking-pollution-back-origin> (accessed 10.9.23).

Zheng, Q., Ye, H., Huang, W., Dong, Y., Jiang, H., Wang, C., Li, D., Wang, L., Chen, S., 2021. Integrating Spectral Information and Meteorological Data to Monitor Wheat Yellow Rust at a Regional Scale: A Case Study. *Remote Sens.* 13, 278. <https://doi.org/10.3390/rs13020278>

Chapter 6. Future Work and Recommendations

6.1. Traditional Monitoring

Given the variability in spore types and their distribution, it is important to continue monitoring fungal spore concentrations in Dublin. This will help track any changes in spore types and their abundance over time. To get a more comprehensive understanding of fungal spore seasons in Ireland, permanently expanding the study to the other regions rather than just isolated campaigns. This will help identify any regional variations in spore types and their seasonality. To detect any long-term trends in fungal spore seasons, it is important that we continue monitoring over an extended period of time. Long-term data will provide insights into changes in spore season start and end dates, peak concentrations, and duration.

Climate change is likely to have an impact on fungal spore seasons and their characteristics. We plan to conduct further research to understand how climate change is affecting fungal spore concentrations and phenological patterns in Dublin. This will become clearer as our database grows. External factors such as meteorological conditions can significantly influence fungal spore concentrations. Taking these into account at the earliest point in our analysis is essential. The impact of factors like drought, rainfall, and wind speed when analysing spore data needs further precedence. While computer models and forecasts can provide valuable insights, real-world sampling of bioaerosols is essential to fully understand the impact of climate change on fungal spore seasons. Continuing the use of physical monitoring alongside modeling approaches will help maintain that.

6.2. Real-time monitoring

We will look into refining the method for determining the baseline fluorescence intensity of each FL channel. This could involve exploring alternative techniques or technologies to ensure accurate and consistent baseline values. A more thorough analysis into the effectiveness of different sigma filter levels (3 Sigma, 6 Sigma, and 9 Sigma) in capturing and categorizing particles is recommended. Determining the most appropriate filter level for different types of particles and adjusting accordingly will help our analysis.

Possibly conducting further research to understand the fluorescence sensitivity of different WIBS models, including the WIBS-NEO could be of value. Comparing the sensitivity of different fluorescence channels (FL1, FL2, FL3) and assessing their impact on particle detection and categorization is also under consideration. Development of strategies to minimize the interference of anthropogenic particles in fluorescence analysis would be beneficial also. This could involve refining the fluorescence filtering process or exploring alternative methods to differentiate between natural and anthropogenic particles by using the Mie scattering values. Continued studying the impact of meteorological parameters on both fluorescent particles and fungal spores. Exploration of additional weather parameters that may influence particle concentrations and develop a comprehensive understanding of their relationship, through our partnership with Met Eireann.

Overall, these recommendations aim to improve the accuracy, sensitivity, and reliability of the WIBS technology in detecting and categorizing particles, particularly fungal spores. By addressing the limitations and challenges identified in this study, future research can enhance the capabilities and applications of the WIBS technology in various fields, such as environmental monitoring and air quality assessment.

6.3. IBAC

Here is an outline of our objectives for future work relating to the IBAC device.

1. Further investigate the capabilities of the IBAC-2 device as an early warning system for detecting biological aerosols. This will involve conducting additional research and testing to determine its effectiveness in identifying and differentiating between biological and non-biological particles. Longer campaigns will provide us with more robust datasets.
2. Address the issue of confusion when detecting particles from anthropogenic sources. Develop algorithms or methods that can improve the device's ability to correctly identify whether particles from these sources are of biological origin. Our work in the development of models will assist in this process.
3. Explore the possibility of using the IBAC-2 device for monitoring other types of bioaerosols, such as smaller pollen or bacteria, in addition to fungal spores. This could expand its potential applications and possibly find a more suited particle type.
4. Conduct more comparative studies with other biological particle sensors and detectors to assess the advantages and disadvantages of the IBAC-2 device in different scenarios. This would help identify its unique strengths and areas for improvement, much like what we saw in our WIBS comparative.
5. Further investigate the correlation between IBAC-2 particle concentrations and other environmental factors, such as rainfall and fungal spore release timing. This could provide insights into the device's ability to track and predict peaks in biological aerosol concentrations, especially as the rainfall-spore lag can significantly alter results.

Overall, these recommendations aim to enhance the capabilities and effectiveness of the IBAC-2 device for real-time monitoring of biological aerosols, as the current campaign found little beyond possible anthropogenic source monitoring applications.

6.4. Forecasts

Here are a set of recommendations relating to future work around forecasts and bioaerosol monitoring and modelling.

1. Continue using the *Cladosporium* and *Alternaria* fungal spores as the primary focus for forecasting models, as they are the most abundant and have significant implications for bioaerosol studies and crop defence.
2. Further refine the forecasting models by incorporating more anthropogenic air concentration information, possibly co-located with the device. This additional data can enhance the accuracy and reliability of the forecasts.
3. Explore the potential of the K-Nearest Neighbours algorithm for longer time periods, as it showed high correlation with observed values over the season. This algorithm may be suitable for predicting fungal spore concentrations at weekly or monthly intervals.
4. Investigate the use of the Support Vector Machine Regression (SVMR) algorithm for predicting other types of fungal spores or fungal spores as a whole. Since both *Cladosporium* and *Alternaria* showed high correlation with SVMR, it may be effective for predicting other spore types as well.
5. Continuously monitor and evaluate the performance of the forecasting models as more data becomes available. This will help identify areas for improvement and ensure the models maintain their predictive success.
6. Consider expanding the forecast models to include other relevant fungal spore types that are found in lower concentrations but have a larger variety of size and shape characteristics. This will provide a more comprehensive understanding of fungal spore relationships with various external factors.
7. Collaborate with other research groups and studies that have implemented similar forecasting models for fungal spore concentrations. Sharing of our own experiences can assist them and visa-versa.
9. Further explore the practical applications of the forecasting models, such as using them as crop defence mechanisms or monitoring pathogenic spores affecting crops. This can provide valuable information to farmers and help mitigate potential crop diseases.

10. Continuously collect data and refine the forecasting models to improve their accuracy and reliability over time. As more data is accumulated, it will be important to update and enhance the models to ensure they remain effective in predicting fungal spore concentrations.

END

